

University of Strathclyde

Department of Civil and Environmental Engineering

Faulting, Sedimentation and Fluid Flow at the
Basin Margin: The North Solway Fault

By

Stewart Beattie

A thesis presented in fulfilment of the requirements for the degree of Doctor of Philosophy

2018

This thesis is the result of the author's original research. It has been composed by the author and has not been previously submitted for examination which has led to the award of a degree.

The copyright of this thesis belongs to the author under the terms of the United Kingdom Copyright Act as qualified by the University of Strathclyde Regulation 3.50. Due acknowledgement must always be made of the use of any material contained in, or derived from, this thesis.

Signed:

Date:

Dedication

For my parents.

Acknowledgements

The first thank you has to go to Zoe and Becky. They have been everything that supervisors should be and have supported me through some tough times that were beyond anyone's control. Countless hours of supervision have led to this point, which at times seemed like it may never come.

Thank you to Dr Alan Gibbs who provided excellent field maps which informed this project from its inception.

To my friends, family and colleagues I can only apologise. There is no hiding from it; this has taken a long time. I look forward to answering "yes" to the question "Are you finished that PhD yet?" Compared to geological timescales, it has been pretty quick though.

Special thanks go to Cheryl; you have been so supportive of me over the years that I can never thank you enough. Our unborn non-gender-specific child will be very lucky to have you as a mum.

Abstract

Faults exert control over the formation of basins and are geometrically complex 3D structures. Several industries rely on characterisation of the subsurface and faults are an important component of subsurface models. Faults are poorly constrained in subsurface data sets and by necessity are approximated to planar membranes. To adequately characterise faults in 3D it is necessary to study exhumed faults in the field.

The architecture of basin margin faults has received relatively little attention in the literature (Caine et al 2010 and Kristensen et al 2016 are notable exceptions). The North Solway fault is a basin margin fault exposed at the boundary of the Southern Uplands and the Solway-Northumberland trough. The fault offsets Lower Palaeozoic lithologies (basement) against Lower Carboniferous sediments. The North Solway fault is a rare example of an onshore fault with a basement footwall and sedimentary hanging wall. The fault is exposed in extensive along-strike and limited down-dip direction in a number of localities which are accessed at low tide.

Field data is used to interpret the internal architecture and fault scale geometry of the North Solway fault. Sketches, descriptions and detailed mapping have been carried out and are complemented by quantitative data from scanlines, image analysis and orientation data.

This study shows that the North Solway fault has a complex zig-zag plan-view geometry which has been offset by major cross faults. Simple segment linkage models are not adequate to describe the plan-view geometry of the fault. Fault throw can only be constrained to between 100m and 1500m, demonstrating the difficulty in characterising large faults. The internal architecture of the fault is shown to be a product of host lithology,

deformation style, depth and fluid flow. The coupling of sedimentary processes and tectonic activity is demonstrated at the basin margin. Predictive algorithms which are used for faults within basins are not applicable in faults with a basement footwall. The textures within fault rocks such as gouge and breccias are shown to give an indication of the mechanical state of the fault at the time of deformation. Contrasting fault zone internal structures are observed where the fault is interpreted to be the result of either basement-basement faulting or basement-sedimentary faulting. The results of this study show that large basin bounding faults are highly variable in both down-dip and along-strike directions.

Table of Contents

1. Introduction	1
2. Literature Review	4
2.1 Definition of Terms	4
2.1.1 Basin and Basin margin fault.....	4
2.1.2 Fault Architecture (fault internal structure)	5
2.1.3 Footwall and Hanging wall	5
2.1.4 Fault Gouge and Breccia	6
2.2 Faults and Fluid Flow	7
2.2.1 Fault and Fluid Flow Models	7
2.3 Basin Margin Faults.....	9
2.4 Fault Rocks	12
2.4.1 Breccia.....	12
2.4.2 Tectonic Breccia	13
2.4.3 Breccia Forming Mechanisms	14
2.4.4 Breccia in Voids	16
2.4.5 Reworking of breccias	17
2.4.6 Sedimentation in fractures and voids	19
2.4.7 Non-destructive particulate flow	20
2.4.8 Continuum of Processes	21
2.5 Classifying Breccias	22

2.6 Fault Gouge	24
2.6.1 Continuum of processes in gouge.....	25
2.7 Mineralisation of fault rocks	26
2.8 Fault Scarp sedimentation	27
2.9 Sediments at the Tip of Upward Propagating fault	29
3. Regional Geological Setting	32
3.1 Introduction	32
3.2 Southern Uplands	33
3.2.1 Pre-Carboniferous.....	35
3.2.2 Carboniferous.....	38
3.2.3 Permo-Triassic.....	41
3.2.4 Jurassic onwards	41
3.2.5 Summary of Solway Basin	41
3.3 The North Solway Fault.....	42
4. North Solway Fault Field Exposures.....	44
4.1 General Description of fieldwork.....	44
4.2 Site Topography	46
4.3 Footwall.....	47
4.4 Hanging wall.....	51
4.4.1 Distinguishing Between Tectonic and Sedimentary Breccia.....	52
4.5 Deformation Elements	55

4.6 Site locations (from south west to north east)	56
4.6.1 Rascarrell Bay to Door of the Heugh.....	58
4.6.2 Castlehill Point to Lagmuck Sands.....	62
4.6.3 East of Lagmuck Sands to Bells Isle	65
4.6.4 Bell’s Isle to Sandyhills	67
4.6.5 East of Sandyhills.....	70
4.7 Evidence for the geometry of the main fault trace	70
4.8 Tectonic Breccia	72
4.8.1 Along strike variability at the outcrop scale	74
4.8.2 Re-worked breccias.....	75
4.8.3 Matrix.....	77
4.8.4 Summary of Tectonic Breccia.....	83
4.9 Fault Gouge	84
4.9.1 Fault Gouge Summary.....	88
5. Data from Multiple Sites at the North Solway Fault.....	90
5.1 Hanging Wall	90
5.1.1 Sedimentary Logs.....	90
5.1.2 Fine-grained Hanging Wall Sediments.....	94
5.1.3 Summary of Hanging Wall Textures.....	95
5.2 Clast Lithology and Shape	96
5.2.1 Clast Composition Count Scanlines.....	97

5.2.2 Results of Clast Composition Scanlines.....	97
5.3 Image Analysis.....	101
5.3.1 Clast Size Image Analysis Results	103
5.3.2 Clast Size and Shape All Data	104
5.3.3 Clast Orientation	106
5.3.4 Image Analysis Limitations.....	111
5.3.5 Source of Clasts	112
5.4 Discontinuities and Veins.....	115
5.4.1 Hanging wall.....	116
5.4.2 Tectonic Breccia	121
5.4.3 Footwall.....	124
5.4.4 Veins through clasts.....	129
5.4.5 Interpretation of Fracture and vein Data.....	130
5.4.6 Summary of discontinuities and veins	131
6. The North Solway fault Geometry	133
6.1.1 Fault Plan View Geometry	133
6.1.2 Interpretation of the North Solway fault plan-view geometry.....	140
6.1.3 Fault Throw	146
6.1.4 Summary of fault scale geometry.....	151
7. The North Solway Fault Internal Architecture	152
7.1.1 Breccia Formation	152

7.1.2 Breccia pods	155
7.1.3 Re-worked breccia textures	159
7.1.4 Tectonic Breccias Cut by Sedimentary Textures	161
7.1.5 Gouge at Door of the Heugh	165
7.1.6 Portling Bay	166
7.1.7 Evidence of Granular Behaviour in Faults	171
7.1.8 Sedimentation at Active Faults	177
7.1.9 Fault Proximal Sediments and Deformation Characteristics	181
7.2 Relative deformation depths of the NSF field sites	183
7.3 Fault Zone Fractures and Veins	186
8. Conclusions and Further Work	193
8.1 Further work	195

List of Figures

Figure 2-1 Conceptual sketch of three principal brecciation processes. After Sibson (1986)	14
Figure 2-2 Processes of attrition breccia. (a) Bulk crushing by compressive stress and (b) abrasion by clast rotation and fragmentation. After Billi (2005)	15
Figure 2-3 Brecciation in fault void space by (a) implosion into transient voids and (b) gravity driven collapse into persistent voids. After Woodcock et al (2006)	17
Figure 2-4 Conceptual sketch of the formation of multi-cycle breccias. After Hausegger et al (2010)	18
Figure 2-5 Sedimentation in voids (a) subterranean voids created by fault wall mismatch (other subterranean voids in Walker et al (2011) include lava tubes) filled and reworked by sediment laden fluids. (b) sub-vertical fractures filled by sub-horizontal laminated sediments. Sediments are subsequently displaced by small shear fractures (adapted from field photos and descriptions in Walker et al 2011).	20
Figure 2-6 Conceptual sketch of non-destructive particle flow. (a) Randomly oriented particles in an incohesive matrix. (b) Re-orientation of some particles (coloured red) into the direction of shear, yellow circle highlights low levels of cataclasis. After Balsamo et al (2008)	21
Figure 2-7 Some common features of gouge. After Rutter (1986)	24
Figure 2-8 Cross section view of the model for A) Frictional drag tilting, and B) Upward propagating fault tilting. After Ferrill et al (2012)	30
Figure 2-9 Figure from Ferrill et al (2012) showing photographs with and without annotation of layer parallel extension in competent limestone beds (blue shading).	31

Figure 3-1 Map showing the location of the Solway basin and the associated Carboniferous basins. After Floodpage et al (2001).	32
Figure 3-2 Map of the southern Uplands showing the main geological units and their ages. After Lintern and Floyd (2000) and Toghil (2009).....	35
Figure 3-3 Composite map after Chadwick et al (1995; top right of figure) and Newman (1999; bottom left of figure) showing the regional scale faulting of the Northumberland-Solway basin complex. 200m contours shown in the top right are of depth to top of basement (pre-Carboniferous). Major faults in the region are shown as black heave polygons with markers on the down-throw side in the Chadwick et al map and blacks lines in the Newman map. Most faults follow the ENE-WSW trend of the Iapetus Suture, with a sub-set trending NNW-SSE. Pink shading represents depth and the key for this is shown at the top of the figure.	37
Figure 3-4 Interpretation of seismic surveys from the Solway and Peel basins. From Floodpage et al (2001). Vertical exaggeration approx 2x.....	40
Figure 3-5 Map of the main fault trace. Includes observed and interpreted trends after Lintern and Floyd (2000), BGS 1:50,000 series (Sheet 5E and part 6W), Piper et al (2007) and the unpublished work of Alan Gibbs.	42
Figure 4-1 Exposures at the North Solway fault field site. Text shows the name of each location with the rock units found there. Shaded areas show where exposures were either; mapped as part of this project, or inferred from previous information (unpublished field map by Dr Alan Gibbs and published work). The interpreted trace of the main fault is shown as a thick red line. A solid red line indicates fault rocks are well exposed and a dashed red line indicates either no exposure or a single exposure of fault rocks. UTM coordinates at black dot	45
Figure 4-2 The North Solway fault basic elements (exposure from Castlehill Point to Lagmuck Sands). The scale bar in the top left represents approximate foreground scale. The main fault scarp is approximately 100m long and is	

oblique to the photograph. Isolated Hanging wall outliers are located just above the label “Hanging Wall”	47
Figure 4-3 Summary histograms of modal composition data of five thin section of the Ross Formation from Lintern and Floyd (2000). 1000 points were counted in each thin section.....	48
Figure 4-4 Poles to meta-sediment bedding exposed at the North Solway fault.....	49
Figure 4-5 Scans of thin sections of intrusions from the Lagmuck Sands location showing increasing levels of chloritisation from left to right.	50
Figure 4-6 Intrusions of granitic dykes into meta-sediments (a) planar dyke near Sandyhills Bay, and (b) complex geometry dyke near Bell's Isle.	50
Figure 4-7 Poles to planes plot of hanging wall beds. Squares represent exposures close to the fault scarp. Dots represent exposure at a distance of 20m or more from the fault scarp.	51
Figure 4-8 Steeply dipping hanging wall sediments	52
Figure 4-9 Rose diagram showing faults cutting footwall lithologies.....	55
Figure 4-10 Detailed map of Door of the Heugh. Map colours are described in Table 1 and in the figure key. Grey areas are obscured by vegetation and boulders. Cross section view for Figure 4-9 is marked on the right hand side of the figure. The location of a sedimentary log described in Section 5.1 is shown.	60
Figure 4-11 Cross-sectional view of the fault zone at Door of the Heugh. Photograph taken oblique to the main fault strike, main fault units digitised over the photograph. The key follows Table 1 and Figure 4-9.	60
Figure 4-12 Detailed map of Lagmuck Sands. The footwall has been mapped as a single unit as distinguishing between lithologies became impractical due to frequent changes in lithology in plan view. The field of view for the cross section in Figure 4-11 is shown in the centre of the map. The location for a sedimentary log described in Section 5.1 is shown.	64

Figure 4-13 Cross section view of area shown in Figure 4-10. Photograph taken roughly fault parallel.....	64
Figure 4-14 Detailed map of Gutcher's Isle. Much of the area is obscured by sand, boulders and vegetation. Location of sedimentary log is shown and described in Section 5.1.	66
Figure 4-15 Cross Section view of Gutcher's Isle. Photograph is taken roughly perpendicular to the fault.....	66
Figure 4-16 Portling Bay detailed map (a) map of gouge exposure. (b) interpreted cross section, and (c) photo of typical exposure showing clasts. The location for a sedimentary log is shown and is described in Section 5.1.	69
Figure 4-17 Breccia pods at Lagmuck Sands showing mixed clast lithology breccia adjacent to single lithology host rock. Breccia pods contain patches of single clast lithology breccia which appear to show little or no mixing of lithologies.....	73
Figure 4-18 Re-worked breccia clasts at Lagmuck Sands.....	76
Figure 4-19 Laminated matrix in tectonic breccias at Lagmuck Sands. Note the tilting of the laminations which is towards the basin (dipping to the SW). The dip was estimate to be 20° by eye as the laminations are difficult to reach (above head height on the underside of a breccia pod).....	79
Figure 4-20 Laminations in matrix at Gutcher's Isle (a) field photograph and (b) digitised field sketch of the same exposure. (c) Photograph of exposure showing blocky, fractured granitic host rock with planar fractures. Fracture is filled with laminated granular matrix. (d) Close up of planar fracture with laminated granular matrix. Lineations either deflect near clast boundaries or remain in the same orientation adjacent to clasts.	80
Figure 4-21 Thin Section photographs of laminations in breccia at A) Lagmuck Sands and B) Gutcher's Isle. Thin section in plane polarised light showing sub-angular to sub-rounded quartz grains in a fine grained matrix. Note the graded	

contact between layers of fine and coarse grained material. B) Thin section in plane polarized light showing grains with a granitic texture in a fine grained matrix. Section is approximately vertical and strikes NW-SE. Layers show coarsening upwards with a complete succession from coarse to fine grain size approximately 0.7mm thick. Transitions from coarse to fine grained layers are abrupt when compared with section A.	82
Figure 4-22 Field photograph of gouge exposure at Door of the Heugh (left), and annotated photograph showing principal gouge features: flow banding, Reidel shears and survivor clasts.	85
Figure 4-23 Portling Bay. Top right – whole exposure map with locations of detailed sketches and dextral Reidel shears.....	87
Figure 4-24	87
Figure 4-25 Sandstone beds adjacent to the gouge exposure at Portling Bay. Deformation of sandstone beds increases towards the fault (right to left). Sandstone beds become isolated lenses in a fine grained matrix closer to the fault zone.	88
Figure 5-1 Sedimentary log for Door of the Heugh. Sediments c. 100m from the main fault.	91
Figure 5-2 Sedimentary Log for Lagmuck Sands. Sediments c. 40m from the main fault.	92
Figure 5-3 Sedimentary Log for Gutcher's Isle. Key is the same as that used for figures 5-1 and 5-2. Sediments c. 20m from the main fault.....	93
Figure 5-4 Sedimentary Log for Portling Bay. Key is in the bottom right corner of the figure. Sediments c. 100m from the main fault.	94
Figure 5-5 Sedimentary rocks at Portling Bay c. 100m from the NSF. The distance to the fault is estimated at this location based on a projected fault geometry from adjacent exposures because the fault scarp is obscured by	

vegetation. (a) Beds of mudstone and sandstone, and (b) ripple marks in the same location.....	95
Figure 5-6 Scanline count tape on tectonic breccia.....	97
Figure 5-7. Clast count scanlines in sedimentary breccia. Histograms of number of clasts by lithology and location with cumulative line graphs of the same data below.	99
Figure 5-8. Clast count scanlines in tectonic breccia. Histograms of number of clasts by lithology and location with cumulative line graphs of the same data below.	100
Figure 5-9 (a) Square marked out for field photograph for image analysis. (b) metasediment clast outlines digitised and ortho-rectified.	102
Figure 5-10. Image analysis clast long axis length in tectonic breccia. Histograms of number of clasts by lithology and location with cumulative line graphs of the same data below.	104
Figure 5-11 Clast long axis orientation from image analysis of 2 breccia photographs at Door of the Heugh. The location of each field site along the whole fault is shown as is the location of the breccia faces analysed on the detailed maps at Door of the Heugh and Lagmuck Sands. The strike of the analysed faces are plotted onto a compass symbol along with the main fault trace at each location to show the relationship between the orientation of the faces analysed to the orientation of the main fault trace. Rose plots are used to present the number of clasts oriented in 10° bins to the horizontal. Rose plot colours as follows; Blue – metasediment clasts, pink – granitic clasts, and green Both lithologies plotted together.	108
Figure 5-12 Clast long axis orientation from image analysis of 2 breccia photographs at Lagmuck Sands. See Caption of figure 5-7 for explanation of the figure.	110

Figure 5-13 Three hypotheses for the lack of clasts derived from sedimentary lithologies within tectonic breccia deposits. A - hanging wall lithologies are not entrained in the fault zone. B - preferential grain size reduction in the hanging wall derived clasts. C – breccias are the result of basement against basement faulting.	114
Figure 5-14 Stereographic projection of poles to planes of hanging wall fractures, plotted by location along the fault.	117
Figure 5-15 Stereographic projection of poles to planes of hanging wall veins.	119
Figure 5-16 Quartz and carbonate minerals occupying the same vein in the hanging wall.	121
Figure 5-17 Stereographic projection of poles to planes of breccia fractures	122
Figure 5-18 Stereographic projection of poles to planes of veins in breccia.	123
Figure 5-19 Stereographic projection of poles to planes of fractures in granitic footwall	124
Figure 5-20 Stereographic projection of poles to planes of metasedimentary footwall	125
Figure 5-21 Stereographic projection of poles to planes of fractures in the footwall	126
Figure 5-22 Stereographic projection of poles to planes of veins in the footwall.	128
Figure 5-23 Poles to planes stereographic projection of Veins which cut through clasts.	129
Figure 5-24 Vein in tectonic breccia passing through clasts. The scale showing on the yellow pencil is 10mm intervals	130
Figure 6-1 Reproduction of Figure 4.1 showing the evidence of the main fault trace of the North Solway, with the addition of indicative cross faults in the large bays.	134

Figure 6-2 Three models for the formation of zig-zag plan view geometry. (a) Cartwright et al (1995) model of isolated segments which link kinematically and form a large fault as the segments become soft linked. (b) from Henstra et al (2015) where non coaxial extension results in fault segments being linked by later, oblique faults. (c) Gibbs (1984) model of transfer strike-slip faults forming at the same time as the normal fault segments. 135

Figure 6-3 Mechanisms for forming large segmented faults. (a) Isolated segments model, (b) coherent fault from segments parallel to an underlying structure, (c) variation of (b) where fault segments form oblique to an underlying structure. Red arrows show the direction of extension and the dashed lines in (b) and (c) represent the trend of the underlying structure. Figure from Fossen and Rotevatn (2016)..... 135

Figure 6-4 Map view of the Northumberland - Solway system showing normal faulting at the flanks of the Alston Block and Lake District Block. The North Solway fault is represented by straight line on the left hand side of the figure. From Chadwick et al (1993). 136

Figure 6-5 Isometric sketch of normal fault slip (S_n) and oblique fault slip (S_o) on a listric fault surface, connected to a shallow dipping sole detachment (S), from Gibbs (1984). 137

Figure 6-6 Gibbs (1984) cross section showing listric fault geometry in the North Sea. The hanging wall beds adjacent to synthetic faults dip away from the basin. The hanging wall beds adjacent to the antithetic faults dip towards the basin, similar to that at the NSF. 138

Figure 6-7 Formation of zig-zag plan view geometry at the North Traena Basin margin, Norway. The initial faults created in the stress field E1 are linked by subsequent faulting in the direction E2. From Henstra et al (2015). 139

Figure 6-8 Sketches of potential fault geometries in the obscured section of fault zone between Door of the Heugh and Castlehill Point. A thicker pink line is used to show interpretive fault segments to make it clear which segments speculative and which are mapped. The black circles highlight the locations

where segments overlap when segments are drawn parallel to the mapped segments.....	141
Figure 6-9 Model for reverse polarity of basin sedimentation which includes large transfer faults which cross the basin. After Barret (1988).....	143
Figure 6-10 reproduction of Figure 3-4. Interpretation of seismic lines in the Peel and Solway basins, from Floodpage et al (2001).	145
Figure 6-11 Cross sections and structural map of the Solway Basin (to the east of the NSF) and Northumberland Trough from Chadwick et al (1995).	147
Figure 6-12 the extents of the NSF from the present study (in red) superimposed on a close-up of a map of the Solway basin in Newman et al (1999). The NSF in the Newman et al map is shown as a straight black line.....	149
Figure 6-13 Fault length v displacement plot from Schlische et al (1996) annotated (brown lines) to highlight the values used in the present study. Maximum and minimum values for the length of the NSF (brown lines) are projected to estimate the possible range of throw for the NSF.....	150
Figure 7-1 Formation of dilation breccias (a) with a fitted fabric and (b) with a chaotic texture.	154
Figure 7-2 Breccia textures at (a) Dixie Valley, Nevada (from Caine et al 2010) showing quartz dominated matrix; and (b) the NSF showing a granular matrix.....	157
Figure 7-3 Model for the development of breccia pods at Lagmuck Sands and Door of the Heugh. Slip indicators shown with black arrows. Light blue indicates gouge formation.	158
Figure 7-4 model for the generation of reworked breccia textures in fault voids	160
Figure 7-5 Sedimentary textures within tectonic breccia at (a) Lagmuck Sands, and (b) Gutcher's Isle.	161
Figure 7-6 Model for sedimentation in breccias at Gutcher's Isle.....	164

Figure 7-7 Model for the development of layer parallel shear at Portling Bay	169
Figure 7-8 Four end member models for degree of mixing in ultracataclasite from Chester and Chester (1998). (a) single slip surface controls deformation – no mixing. (b) slip on multiple anastomosing surfaces leads to mixing. (c) laminar or streamlined flow occurs in the ultracataclasite but is distributed and the units remain juxtaposed. and (d) turbulent flow causes mixing of the fault rocks.	173
Figure 7-9 Fault rock units at the Copper Canyon fault. The thickness of zones I and II vary between 100mm and 1m. Note the descriptions of each zone mentioning footwall and hanging wall calsts are found in each. From Cowan et al (2003).	174
Figure 7-10 Entrainment of wall rock lithologies into gouge at the Copper Canyon fault in Death Valley, USA. From Cowan et al (2003)	175
Figure 7-11 Schematic cross section of typical alluvial fan structures and textures. A) Debris flow dominated fan, and B) Sheet flood dominated fan. Vertical exaggeration is 2x.	179
Figure 7-12 Schematic diagram of relative rates of fault scarp uplift versus geomorphic processes. From McCalpin (1996)	180
Figure 7-13 Schematic cross section of a basin bounding fault with syn-rift sediments. From Kristensen et al (2016).	182
Figure 7-14 Model for the variations in relative depth of faulting at the NSF, with a map to show the 4 key locations.	185
Figure 7-15 Basic scheme linking vein type and crystal morphology. After Bons et al (2012)	188
Figure 7-16 Reproduction of Figure 2-2. Processes of attrition of breccia clasts. (a) Bulk crushing by compressive stress and (b) abrasion by clast rotation and fragmentation. After Billi (2005).....	190

Figure 7-17 Processes at basin margin faults..... 192

1. Introduction

Fault zones are geometrically complex 3D structures which evolve through time.

Understanding the complex behaviour of fluid in the crust is vital to many industries, and the interaction between faulting and fluid flow is of particular interest to hydrocarbon exploration and production, geological sequestration of CO₂, mineral resources and geothermal energy. Where possible, geological models are built from various data sources and then analysed to enable predictions of flow characteristics at depth. Quantitative evaluation of the internal structure of fault zones is problematic. Current practice of using geological factors such as fault throw, clay content, burial depth, fault zone composition and mechanical factors to predict the flow properties of faults at depth (eg. Zhang et al. 2011) severely underestimates the complexity and variability of real world fault zones (Lunn et al. 2008).

Studies of fault architecture at surface exposures are necessary to augment industrial methods for detecting and characterising fault zones. For example, faults can be detected by seismic surveys but rely on offset of sub-horizontal reflectors in the host rock, and faults with a throw of less than 10 m cannot be imaged this way. The internal architecture of fault zones cannot be constrained in such surveys, with a best-case scenario containing information on fault shape (listric or planar), slip direction and throw. Faults which have no markers for throw, such as faults in basement lithologies, are poorly characterised by seismic surveys. The detailed architecture of faults can only be accurately studied in the field where outcrops provide opportunities to observe exhumed fault rocks.

Basin margin faults have long been recognised as significant to basin evolution (eg. Gibbs 1984) and the migration of economically significant fluids (eg. hydrocarbons - Boles et al 2004). Detailed studies of basin margin fault architecture where the fault has basement

footwall and sedimentary hanging wall are almost absent from the literature (Caine et al 2010; and Kristensen et al 2016 are rare examples). The internal structure of major basin bounding faults is often relatively poorly exposed compared to the size of the structure. The North Solway fault (NSF) provides a rare opportunity to study an on-shore basin margin fault. The fault offsets Carboniferous sediments against lower Palaeozoic basement (Lintern and Floyd 2000). The fault is exposed in extensive strike view (c. 10 km along-strike length) and relatively limited dip view (10s of metres).

The primary objectives of this thesis are as follows:

- To map the internal structure of a large basin bounding fault zone.
- Gain an understanding of the processes that shape such a fault.
- Describe the interaction between the internal structure of a basin bounding fault zone and the deposition of fault-scarp related sediments.

To achieve this, detailed mapping of the fault at 4 key locations along the NSF was carried out (Chapter 4). The main fault trace was also mapped and the results are compared to literature on both the Solway-Northumberland trough and faults in general to gain insight into the multi-segment nature of the North Solway fault.

The fault rock exposed at the North Solway fault contains clues as to the nature of deformation during fault slip. Breccias were studied in detail to determine the source of the fault rock (basement-basement or basement to sediment faulting) and to determine the mode of deformation. Gouge was also mapped in detail where encountered (2 locations). Sedimentary logs and orientation data of fractures and veins were collected. Hand samples and thin sections aided descriptions where appropriate.

Chapter 2 begins by defining some of the terms used in this thesis to provide clarity to the proceeding chapters then reviews the relevant literature in order to set up the research problem. Chapter 3 describes the regional geological setting of the North Solway fault in order to place the fault in the context of the surrounding basin complex. Chapter 4 describes the field site in detail including; descriptions of the whole fault from west to east, constraints on the location of main fault and detailed mapping of 4 key locations. Chapter 5 contains quantitative data collected at several sites and collates this data in order to investigate the along strike variability of the fault. Chapter 6 discusses the geometry of the North Solway fault and Chapter 7 discusses the implications for understanding processes that must occur in large basin margin faults. Chapter 8 summarises the main conclusions drawn from this thesis and recommends future work to compliment the present study and further the understanding of the internal architecture of basin margin faults.

2. Literature Review

This Chapter reviews the literature relevant to the present study in order to place the thesis in the context of current knowledge and understanding of; basin margin faults, fault architecture, brecciation mechanisms and sedimentary deposits at basin margins. The Chapter begins by defining the terms used in this thesis before moving on to review the relevant literature.

2.1 Definition of Terms

The following section defines the terms used in the thesis, to provide clarity for the reader of the terminology used in order to effectively convey the findings of this thesis. Peacock et al (2016) noted that increased interest in the 2D and 3D geometries and development of faults has led to increasingly bewildering terminology. For that reason, a clear basis for the terminology used in this thesis is required.

2.1.1 Basin and Basin margin fault

For the purposes of this project, a basin will refer to an area of depression of the crust at the regional scale (kms to 10's of km), subsequently filled with sediment and lithified sediment. This scale is suitable for the Solway basin as seismic reflection surveys and well data suggest that sediments within the basin are around 5km thick (Newman 1999) and include sandstones, conglomerates and mudstones (Brookfield 2008). A basin margin fault is defined here as a fault which forms the major structural boundary of a basin. In this case, the North Solway fault forms the boundary between the Solway basin and the topographic highs of the southern Uplands.

2.1.2 Fault Architecture (fault internal structure)

For the purposes of this thesis, the terms fault architecture and fault internal structure will be used interchangeably and will refer to the arrangement of structural elements of the fault zone. A widely cited model of fault zone architecture according to Caine et al (1996) refers to three distinct components of a fault zone. They are protolith, damage zone and fault core. Although there are no standard criteria for defining the damage zone and fault core (Shipton et al 2006), the fault core generally refers to the area where most of the displacement is accommodated and comprises highly altered or disaggregated rocks. The damage zone which surrounds the fault core refers to a zone of structures formed by fault-related processes which has accommodated less strain than the fault core and more than the background level of deformation in the protolith (Caine et al 1996).

Following this model of fault architecture at the North Solway fault is problematic as faulting at the site is structurally complex, meaning that identifying distinct units of protolith or “undeformed” country rock is difficult. Most of the exposures display features that could reasonably be expected to be fault related and large amounts of the exposures are so altered that they could be considered fault core. Therefore, the basic model of fault geometry used in this report will involve the following elements; footwall, hanging wall and fault rock. Hanging wall and footwall exposures are considered to be “in-situ” and attached to the country rock and so could be either damage zone or protolith. Fault rock will refer to completely disaggregated rock and could involve breccia or gouge. These components are described in more detail below.

2.1.3 Footwall and Hanging wall

The footwall and hanging wall of faults are terms applied to the units that are juxtaposed against each other and form the basis of the simplest models of fault movement. At the

North Solway fault, the footwall forms a fault scarp and contains granitic and meta-sedimentary lithologies of the Southern Uplands. The terms granitic and meta-sedimentary are simplification of the footwall lithologies. Defining subdivisions of these rock types is beyond the scope of this thesis and it is considered sufficient to separate these rock types into these basic terms. The term *basement* is also used to refer to the granitic and meta-sedimentary rocks at a larger scale which is not directly applicable to the fault scale.

The hanging wall contains the sandstones, conglomerates and mudstones of the Solway basin. These components are described in more detail in Chapters 3, 4 and 5.

2.1.4 Fault Gouge and Breccia

The term gouge refers to material that has been crushed to a fine powdery or slaty texture by processes of faulting. This is in contrast to fault breccia which refers to rock consisting of clasts (>30% of volume), fragmented from the host rock by either tectonic or sedimentary processes. Breccia can be described as either clast-supported or matrix-supported referring to the clast to matrix ratio of deposits. The definition of grains as clast or matrix follows Woodcock and Mort (2008) where 2mm is used as a threshold below which a grain is classified as matrix and above which, a grain is termed a clast. It is possible to make a further distinction of fine grained material within breccia as either matrix or cement which is based on cement being formed in-situ due to mineral growth and matrix being composed of grains transported from elsewhere. Distinguishing between matrix and cement is difficult in the field (Woodcock and Mort 2008) and therefore the term “matrix” is used to refer to all grains and crystals with a diameter less than 2mm regardless of genesis.

2.2 Faults and Fluid Flow

Fault zones exert a large influence on fluid flow in the crust and the relationship between fault zone structure and fluid flow is widely recognised as complex (eg. Knipe et al 1998; Cartwright et al 2007; Lunn et al 2008; Wibberley et al 2008). The structure and permeability of fault zones is highly heterogeneous and difficult to predict. Variations in structure and flow patterns occur spatially at a wide variety of scales (from millimetres to several kilometres) and the permeability of fault zones is transient and can vary over geological time and over timescales relevant to industrial applications (Faulkner et al 2010). Faults can act as conduits or barriers to flow in both fault parallel and cross-fault directions (Eichhubl et al 2009; Dockrill and Shipton 2010). Complex feedback mechanisms also operate between fluids and the structural behaviour of the crust because the mechanics of faulting are affected by the presence and flow of fluids (Sibson 2000; Caine et al 2010; Tenthorey et al 2003; Barnhoorn et al 2010). Under the right conditions, flow pathways can become sealed with precipitates which then restrict the flow and alter the permeability structure and strength of a fault zone through time (Woodcock et al 2007, Benedicto et al 2008). Alteration can also weaken fault rocks and which in turn affects the mechanical strength of the fault zone as a whole (Solum et al 2005).

2.2.1 Fault and Fluid Flow Models

A commonly used analysis of fault permeability in industrial applications involves evaluating across fault juxtapositions combined with algorithms such as shale gouge ratio. Shale gouge ratio (SGR) is defined as the fraction of clay within a fault sequence that has passed each point on a fault (Manzocchi et al 2010). However, these methods neglect the complexity of fault zone architecture (Faerseth et al 2007) which can have an adverse impact on the effectiveness of predictions (Lunn et al 2008). Models which represent the complexity and

variability of fluid flow in fault zones are elusive and there is a lack of truly quantitative data which relates the internal structure of fault zones to flow (Manzocchi et al 2010, Lunn et al 2008).

Flow models typically treat faults as approximated planar membranes or volumes which are assigned properties relating to deformation and fluid flow. Basin models tend to be 2 or 3-dimensional representations showing stratigraphic relationships between fault bounded blocks. Finite element models (eg. Boles et al 2004) assign values to cells which represent physical properties such as permeability, porosity and hydraulic conductivity. Faults are approximated to geometrically simple zones of fixed width (Bense et al 2013) or are represented as planes over which transmissibility multipliers are applied to retard flow (Manzocchi et al 1999; 2010). The latter approach cannot accommodate along-fault flow.

Lopez and Smith (1995 and 1996) examined fluid flow and heat transfer in fault zones by finite element modelling which represented a fault as a planar vertical column of fixed width. Two types of simulations were carried out. First, the fault zone was considered as having homogeneous but anisotropic permeability and second, the fluid flow and thermal regime were considered as heterogeneous. Homogeneous anisotropy was modelled by fixing vertical (down dip) permeability and varying horizontal (along strike) permeability. Heterogeneity was represented by assigning a permeability value to each finite element grid block based on a lognormal distribution. In the first case, varying horizontal permeability affected the aspect ratio (width/length) of convective cells within the fault zone. In the second case, heterogeneous permeability created complex flow patterns with channelization of flow and smaller convective cells. This shows how an idealised planar fault zone with a simple geometry can display variable flow and heat transfer regimes by manipulation of the hydraulic properties of the fault alone. There is no representation of

fault geometry such as juxtaposition or fault throw and the country rock is assumed to be homogeneous, yet the results show variable flow and heat transfer. The internal structure or architecture of a fault zone will always be approximated in geological models, the task for effective analysis is to find out which simplifications will adversely affect results and which are of little significance (Manzocchi et al 2010).

2.3 Basin Margin Faults

Faults at the basin margin, commonly referred to as basin-bounding faults exert a major control on basin development and basin flow conditions. Faults at the basin margin typically involves 2 groups of faults; faults parallel to the basin long axis, and transfer faults at high angles to the basin margin and display a zig-zag plan-view geometry. There are competing models for the development of this plan-view geometry (see Fossen and Rotevatn 2016 for a useful review). These models will be explored in Section 6.1, when discussing the North Solway fault plan-view geometry.

Several studies to date have focussed on basin scale processes such as the development of fault arrays (Gibbs 1984; Cartwright et al 1995; McLeod et al 2000; Henstra et al 2015), footwall uplift and erosion rates in offshore basin margins (McLeod et al 2000; Densmore et al 2004; Cowie et al 2006; Elliot et al 2012) and tectonic control of sedimentation at the basin scale (Kim et al 2003; Bell et al 2009; Ford et al 2013). Studies which document fault architecture at the basin margin are relatively rare.

Two published studies of fault internal structure with a crystalline footwall are Caine et al (2010) at the Stillwater fault, Dixie Valley, Nevada and Kristensen et al (2010) at the Dombjerg fault, NE Greenland.

The Stillwater fault is thought have originated as a basement to basement fault and currently offsets crystalline basement against quaternary sediments. There is an abrupt transition between the footwall damage zone and fault core. The fault core is between 1m and 5m thick. Breccia pods (tabular to curvilinear bodies of breccia) dominate the fault core with their edges delineated by slip surfaces. The breccia pods have been cemented with silica rich fluids (Caine et al 2010).

Caine et al (2010) used contrasting textures of clast and matrix supported breccias at the basin-bounding Stillwater fault, Nevada, to interpret a fault valve model where fluids build up and interact with fractures and the fault core. The build-up of fluid pressure during inter-seismic periods can open pathways for flow which in turn can seal fractures and breccia. Variations in fluid pressures may also cause a feedback mechanism where principal stresses in the fault zone are altered and may cause further fault slip. During co-seismic events, new hydraulic connections can be made through fracturing and faulting. Minerals can be precipitated and further alter the mechanical and fluid flow properties of the fault zone (Caine et al 2010). This model demonstrates the complex feedback mechanisms that can operate between faulting, fluid flow and mineralisation at a basin-bounding fault zone. The model also highlights the multiple episodes of faulting and fluid flow that combine to form fault rocks.

Whilst the Stillwater fault zone provides an opportunity to study basement to basement faulting which has become a basin margin fault, the current hanging wall deposits are quaternary sediments. By contrast, the North Solway fault provides an opportunity to study a basin margin fault zone juxtaposing basement rocks with sedimentary rocks which are lithified. This is more similar in setting to the Dombjerg fault, NE Greenland (Kristensen et al (2016).

The Dombjerg fault offsets a footwall of Caledonian migmatite gneisses, pegmatites and amphibolites against a hanging wall of Middle Jurassic to Early Cretaceous conglomerates and sandstones. Deformation in the footwall is characterised by several discrete slip surfaces which have accommodated a portion of the total throw. These slip surfaces contain breccia and gouge up to 500mm thick. The fault displays evidence of mineral rich fluid flow in the form of a Chemical Alteration Zone (CAZ) which is characterised by calcite precipitation of veins in the footwall and pore space in the hanging wall. Deformation within the near fault sediments which are part of the CAZ contrasts with the sediments outside the CAZ which are poorly lithified. Joints and minor faults are associated with the CAZ whilst sediments further from the fault are deformed by disaggregation deformation bands.

Kristensen et al (2016) interpret the Dombjerg fault zone to have a c. 1km wide damage zone. They state that the several individual slip surfaces represent multiple cores, so the authors prefer to use the terms damage zone and chemical alteration zone (instead of the fault core/damage zone/protolith terminology of Caine et al 1996) because this places emphasis on the influence of fluid flow on the Dombjerg fault.

There are studies of fluid flow and basin margin fault architecture in faults within sedimentary rocks. Boles et al (2004) constructed a model of hot basinal fluids “venting” through the basin-bounding Refugios-Carneros fault and mixing with meteoric water. Over a timescale of c. 100,000 years, fluid flow conditions evolved from rapid expulsion of fluids to buoyancy driven seepage of hydrocarbons.

Agosta (2008) and Agosta and Aydin (2006) used structural and petrophysical data to evaluate the internal structure of carbonate hosted basin-bounding faults of the Fucino Basin in the Apennines, Italy. Agosta (2008) demonstrated that faults with a carbonate

footwall and quaternary sediment hanging wall have the potential to act as a combined barrier-conduit to flow through spatial variability in porosity and permeability characteristics. Higher values of porosity and permeability as well as a more connected pore space in the damage zone and quaternary hanging wall compared to the protolith and fault core show the potential for barriers or baffles to flow to be flanked by conduits to flow (Agosta 2008). Agosta and Aydin (2006) also studied the fractures and faults within a basin bounding fault zone of the Fucino basin to create a conceptual model of normal fault growth. Structural elements inherited from earlier thrust movements were exploited in several subsequent stages of normal faulting. Pressure solution seams, joints, fractures and cataclasis recorded development of the fault zone through time (Agosta and Aydin 2006).

2.4 Fault Rocks

The geometry and spatial arrangement of fault rocks within a fault zone is usually heterogeneous, as are the mechanical and fluid flow properties of these fault rocks. These factors contribute to the complex relationship between fault internal structure and fluid flow. In order to adequately understand the interaction of faults and fluid, it is important to understand the processes of fault rock development inside a fault zone and the consequent implications for fault zone hydraulic properties.

2.4.1 Breccia

Breccias are a common product of several different rock deformation processes. Broadly, these processes can be grouped as breccias which have formed by; tectonic action (Sibson 1986), hydrothermal activity (Jebrak 1997), sedimentary processes (Sanders 2010), collisions and impacts (Reimold 1995) and volcanic activity (Fisher 1960). Within each of the above categories lie a number of sub-divisions of brecciation processes. The present study

focusses on tectonic and sedimentary breccia as the site is a large basin bounding fault where both these processes have operated (Ord et al 1988).

2.4.2 Tectonic Breccia

Tectonic breccia is recognised as an important component in fault and fluid interaction (Sibson 1986) and the nature and genesis of fault breccias has been the subject of much previous work (eg. Sibson 1977; Jebrak 1997; Cowan et al 2003; Boles et al 2004; Billi 2005; Woodcock et al 2006; Mair and Hazzard 2007; Caine et al 2010; Hausegger et al 2010; Woodcock et al 2014). The texture, geometry and composition of breccias yield evidence of the evolution of fault zones through time and also the spatial and temporal heterogeneity of a fault zone. Tectonic breccias can be formed by a number of different processes in the upper crustal brittle regime. Sibson (1986) splits tectonic breccia into three main divisions (Figure 2-1); attrition breccia from progressive frictional wear, distributed crush brecciation from compressional stresses at anti-dilational fault jogs, and implosion breccia from tensile stresses in voids at dilational jogs. Subsequent studies have suggested further breccia forming processes which are either sub-divisions of the three Sibson categories (ie. attrition by bulk fragmentation or grain abrasion, Billi et al 2005), a hybrid of processes (ie. attrition and dilation, Caine et al 2010) or additional processes not covered by the Sibson scheme (persistent voids with gravity collapse, Woodcock et al 2006; fluidization of breccia clasts Smith et al 2008; and sedimentation in subterranean voids, Walker et al 2011).

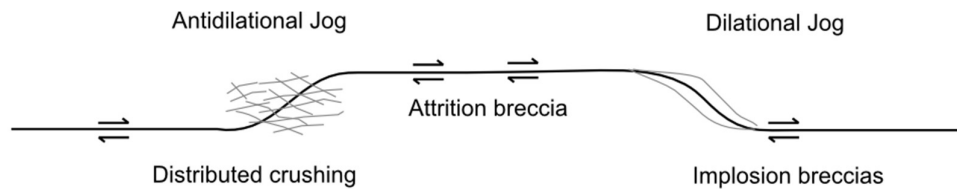


Figure 2-1 Conceptual sketch of three principal brecciation processes. After Sibson (1986)

2.4.3 Breccia Forming Mechanisms

Attrition

Attrition brecciation involves frictional wear and progressive fragmentation, rotation and entrainment of clasts (Sibson 1986). Clasts are formed by penetrative fracturing of fault walls, disaggregation from the host rock and entrainment into fault rocks. Two processes of fault rock attrition, abrasion and bulk crushing, are recognised by Billi (2005). Abrasion results from progressive rotation of clasts within a matrix and collisions with neighbouring clasts as they slide and rotate past one another (Blenkinsop 1991; Billi 2005). Bulk crushing (or grain splitting in Mair and Abe 2011) results from dense packing of clasts in shear that cluster together to form “bridges”. Resistance to shearing can form compressive stress concentration across these bridges which may cause clasts to fragment (Billi 2005; Rawling and Goodwin 2003).

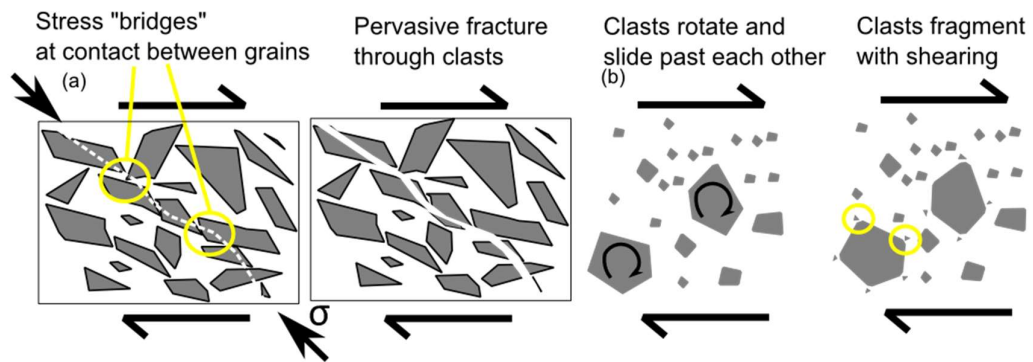


Figure 2-2 Processes of attrition breccia. (a) Bulk crushing by compressive stress and (b) abrasion by clast rotation and fragmentation. After Billi (2005)

Crush Breccia

Distributed crush breccia is formed on impediments to slip such as fault wall asperities or compressional “anti-dilational jogs”. This style of deformation is likely to lead to micro cracking with a minimal shearing component (Sibson 1986).

Numerical Simulations of Grain Fracture

Grain fracturing has been simulated in granular materials undergoing shear by Abe and Mair (2005;2009), Mair and Hazzard (2007) and Mair and Abe (2008;2011). 3D numerical models have been shown to produce grain size distribution profiles that are similar to natural gouges and laboratory sheared granular materials (Abe and Mair 2005). The way in which granular materials breakdown is governed by; particle size distributions and the contacts between particles (Mair and Hazzard 2007), particle shape (Abe and Mair 2009) and stress conditions (Mairs and Hazzard 2007; Mair and Abe 2011). Localisation of strain evolves with grain size reduction and this has been shown to have a feedback effect on the frictional strength of simulated faults (Mair and Abe 2008). The processes of comminution in simulated fault gouges provides insights into the behaviour of granular materials in faults and emphasises the significance of these processes to the strength and evolution of faults.

2.4.4 Breccia in Voids

Implosion breccia

Implosion breccia results from the creation of void space during fault slip events that is filled with a mass of dilated rock fragments (Figure 2-3a). Implosion of the wall rock may result from the contrast between the pressure in the void and the lithostatic pressure or hydraulic pressure exceeding the tensile strength of the rock (Sibson 1986). Clast rotation and evidence of attrition are frequently absent in these breccias reflecting the transient collapse of breccia into limited open space (Sibson 1986; Jebrak 1997).

Collapse into persistent fault voids

During slip events, geometric mismatch of opposing fault walls can create fault voids. These fault voids can be supported for longer timescales than those of the implosion model of Sibson (1986) and may subsequently be filled by breccia formed by gravity collapse (Figure 2-3 b) (Jebrak 1997; Woodcock et al 2006; Woodcock et al 2014). The process can be repeated over several fault slip events and create a chaotic breccia texture with complex geometries of crude bedding and cross cutting faults (Woodcock et al 2006; Woodcock et al 2014).

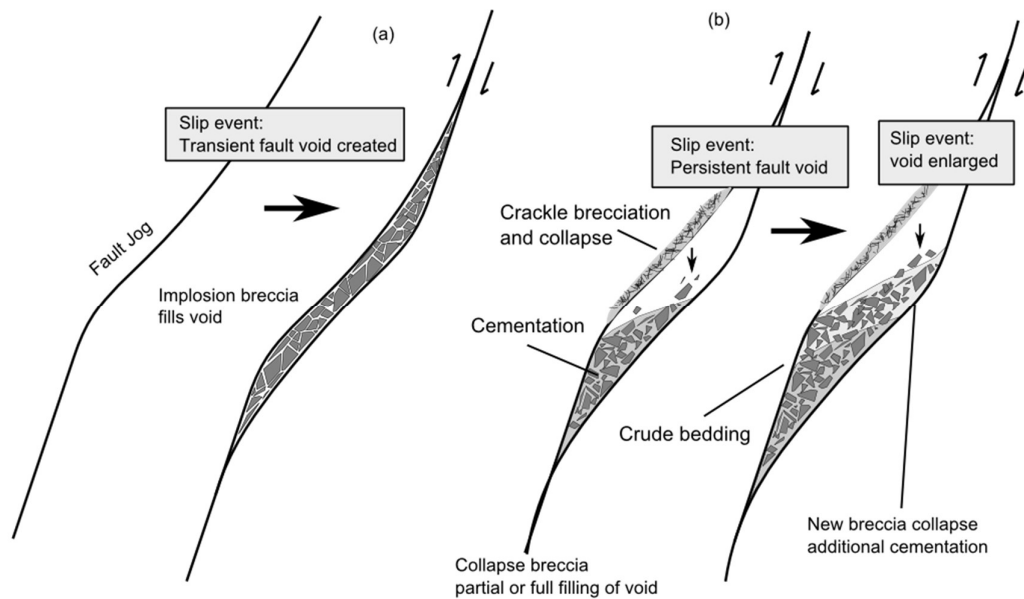


Figure 2-3 Brecciation in fault void space by (a) implosion into transient voids and (b) gravity driven collapse into persistent voids. After Woodcock et al (2006)

2.4.5 Reworking of breccias

Tectonic breccias may also be subjected to reworking processes. Repeated cycles of fault slip have long been recognised and it follows logically that subsequent deformation events will have an impact on pre-existing fault rocks.

Multi-cycle breccias have been documented in several studies (eg. Woodcock et al 2007; Caine et al 2010; Hausegger et al 2010; Motoki et al 2011; Woodcock et al 2014) which demonstrate repeated deformation of the same breccia mass. During inter-seismic periods, breccias may be cemented by mineral deposition from fluids. This changes the mechanical behaviour of the breccia from a granular material to a more cohesive unit by increasing tensile and cohesive strength (Balsamo et al 2008). Subsequent deformation may cause the formation of new joints and fractures which eventually result in “polyphase” or multi-cycle breccia formation (Figure 2-4) which are clasts of breccia consisting of individual breccia clasts from earlier phases of faulting (Woodcock et al 2007; Hausegger et al 2010).

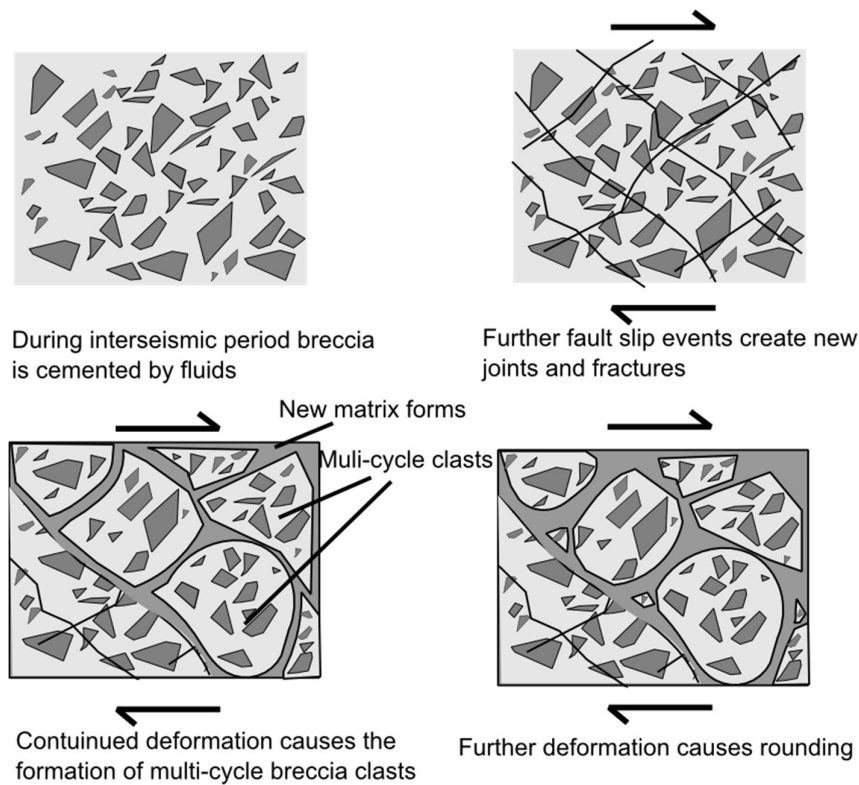


Figure 2-4 Conceptual sketch of the formation of multi-cycle breccias. After Hausegger et al (2010)

Fluidisation of breccias

Fluidisation of fault rocks has been defined by Monzawa and Otsuki (2003) as “the state in which grains fly around with a mean free path like gaseous molecules”. This definition allows for fluidisation to be brought on by shaking of granular material (eg. fault rupture) or by pressurised fluids remobilising pre-existing breccias. Smith et al (2008) interpreted the Shape Preferred Orientation (SPO) of clasts to have been caused by remobilisation of clasts by pressurised fluids at the Zuccale fault, Italy. Fluid pressure build up beneath an impermeable fault core caused pre-existing breccias to become fluidised during inter seismic periods. Acoustic fluidisation of granular materials mobilised by vibrations has long been recognised (Melosh 1979) may cause sorting phenomena related to particle shape

and density (Kudrolli 2004) and also develop SPO of clasts (Borzsonyi and Stannarius 2013). Re-organisation of granular materials due to shaking requires dilation of the material (Jaeger 1996) and the space to accommodate that dilation. The creation of void space in fault zones is well documented as is dilation of fault zones during slip (eg. Sibson 1986; Woodcock et al 2006; Caine et al 2010; Soden and Shipton 2013; Woodcock et al 2014) so void space and room to accommodate grain re-organisation could be expected.

2.4.6 Sedimentation in fractures and voids

Wright et al (2009) and Woodcock et al (2014) observed void filling sediments, breccias and cements to infer a multi-phase model of cyclic void formation and filling. Re-working of loose sediments in persistent subterranean void space and tectonic-related fractures has been inferred by Walker et al (2011) who observed well-developed fabrics in granular fill which occupies lava tubes and fault associated fractures (Figure 2-5). Inferred emplacement processes are; sediment laden water flow switching periodically between deposition and erosion, and transient over-pressure of fluids in pre-existing sediments causing localised remobilisation and injection of sediments into fractures (Walker et al 2011). Wall and Jenkyns (2004) recorded Jurassic surface sedimentation deposits in tectonic fractures hosted in Carboniferous Limestone. All of these deposits may not have strictly tectonic origin (consider a lava tube collapsing and fragmenting under gravity conditions) but they are associated with fault-based fluid pressures and fault-based fractures so the processes that affect these deposits are worthy of consideration.

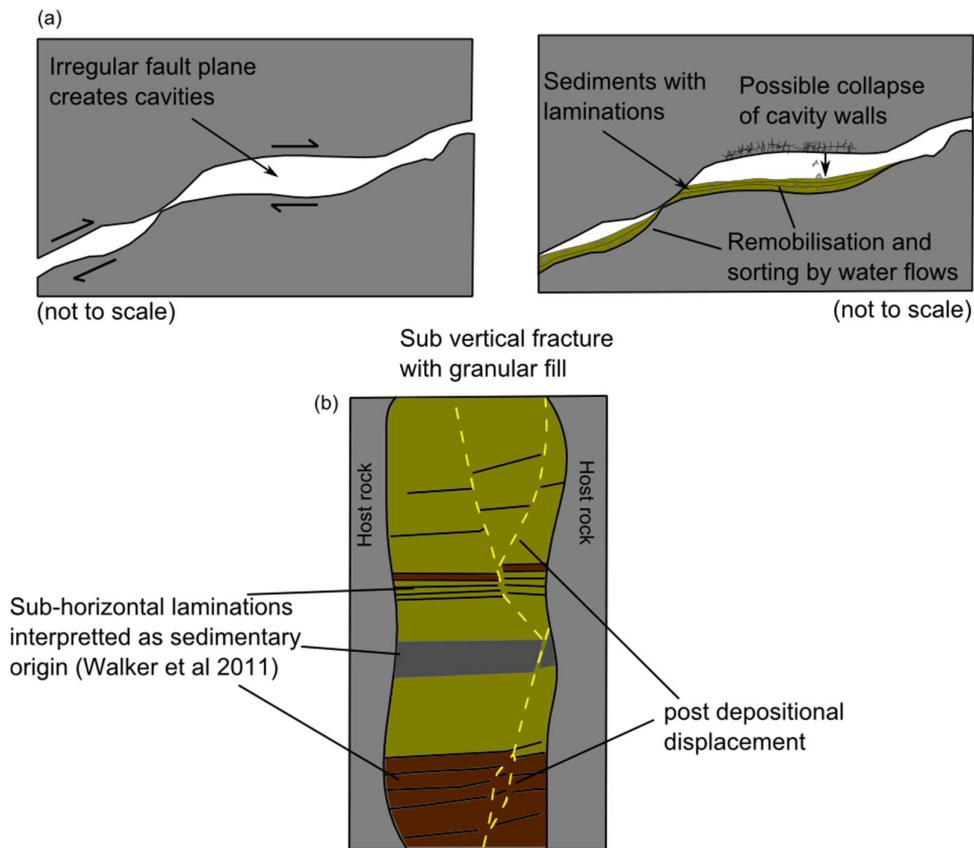


Figure 2-5 Sedimentation in voids (a) subterranean voids created by fault wall mismatch (other subterranean voids in Walker et al (2011) include lava tubes) filled and reworked by sediment laden fluids. (b) sub-vertical fractures filled by sub-horizontal laminated sediments. Sediments are subsequently displaced by small shear fractures (adapted from field photos and descriptions in Walker et al 2011).

2.4.7 Non-destructive particulate flow

Another process of reorganisation of granular materials is non-destructive particulate flow. This has been observed in unlithified and semi-lithified sediments (Cowan et al 2003; Balsamo et al 2008; Loveless et al 2011). When sheared, sediments under low confining stress with low cohesive strength (lack of significant burial and cementation) can undergo particulate flow and reorientation of clasts by particle rotation and grain boundary sliding (Balsamo et al 2008). Mechanical clast rotation during shearing has been shown to be another way of generating SPO of clasts in poorly lithified sediments either in the direction

of shear or at low angles to shear (Figure 2-6) (McCalpin 1995; Balsamo et al 2008; Loveless et al 2011).

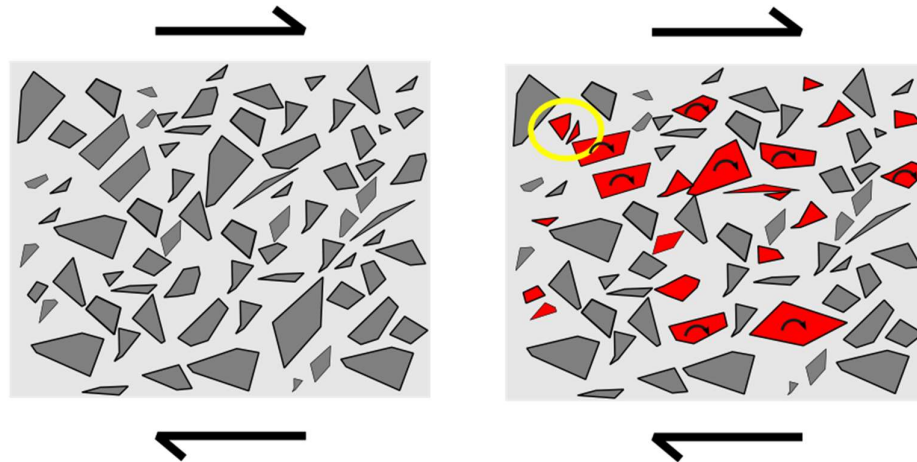


Figure 2-6 Conceptual sketch of non-destructive particle flow. (a) Randomly oriented particles in an incohesive matrix. (b) Re-orientation of some particles (coloured red) into the direction of shear, yellow circle highlights low levels of cataclasis. After Balsamo et al (2008).

Grain scale mixing has been observed in faulted poorly lithified sediments and the degree of mixing has been shown to increase with fault slip (Loveless et al 2011). An important aspect of the Balsamo et al (2008) model is that the style of deformation changes through time from soft sediment deformation to brittle deformation as the sediments increase in cohesive strength.

2.4.8 Continuum of Processes

The above review of tectonic breccia formation identifies some key breccia formation and breccia reworking processes. These processes should not be considered mutually exclusive. Multiple processes may operate on the same breccia (Caine et al 2010; Billi 2005; Balsamo et al 2008) and it is more realistic to think of these processes as a continuum with overlapping characteristics. For example, fluidisation is listed as a separate process above,

but fluidisation of breccias may be involved in other processes such as non-destructive particle flow of smaller clasts (Monzawa and Otsuki 2003) and granular fracture fill through fluid over pressure (Walker et al 2011). Multi-cycle brecciation involves the sealing of breccias by cementation but the actual processes involved in creating the original breccia, and subsequent reworking into multi-cycle breccia could feasibly be caused by friction, dilation or crushing. In poorly lithified sediments, a small degree of cataclasis is found to occur in tandem with non-destructive particulate flow, even at low confining pressures (Loveless et al 2011). Woodcock et al (2014) therefore argues that it is more applicable to think of breccia processes as a continuum where processes grade into each other without absolute distinction from one another.

2.5 Classifying Breccias

Distinguishing between different breccia formation processes is often problematic.

Multiple processes may operate on the same breccia and these processes may produce very similar textures. Breccia deposits may be subjected to several episodes of brecciation and alteration (eg. Blenkinsop 1991; Smith et al 2008; Hausegger et al 2010; Caine et al 2010; Motoki et al 2011) causing over-printing of previous textures.

Classifying breccias based on a system of purely non-genetic parameters has been suggested by Woodcock and Mort (2008). Previous systems used the inferred genetic classifications of Sibson (1977; 1986) and Jebrak (1997). Use of such systems requires an understanding of processes operating in a particular setting which result in breccia formation. This may lead to misinterpretations and user bias (Woodcock et al 2007). Woodcock and Mort (2008) suggested a classification scheme based on the ratio of clast to matrix and the rotation and goodness of fit of clasts. This system borrows terms used in

cave collapse literature that defines breccia textures with increasing levels of disaggregation as crackle, mosaic and chaotic. The textures are also defined based on the percentage of clasts and matrix in the rock volume, distinguished by a 2mm particle size cut off between clast and matrix. A benefit of this system over previous genetic classifications is the lack of need to identify primary cohesion (Woodcock and Mort 2008). The textural classification scheme of Sibson (1977), in which gouge and breccia are distinguished from other fault rocks based on a lack of cohesion, requires the identification of primary cohesion (Mort and Woodcock 2008). In Sibson's classification fault rock which is incohesive immediately after formation is described as either fault gouge or fault breccia depending on the percentage of "visible clasts". Fault rocks which retain some cohesion are classified as part of either the cataclasite or mylonitic series. It is widely known that fault rocks are often subjected to cementation or sealing in fault zones and numerous examples exist in the literature (eg. Woodcock et al 2007; Smith et al 2008; Caine et al 2010; Hausegger et al 2010; Motoki et al 2011). Identifying a fault rock which was previously incohesive but has now been subject to cementation and distinguishing this from fault rocks which retained primary cohesion is problematic in the field (Cladouhos 1999a; Mort and Woodcock 2008).

A scheme which identifies fault rocks based purely on observable characteristics has obvious advantages in terms of both application to individual studies and comparison between studies. Breccias may be formed at several different stages in the seismic cycle and distinguishing between these breccias based on observational data alone is not reliable (Woodcock et al 2007). The Woodcock and Mort (2008) scheme does however offer useful descriptive measures by which to classify the widely variable and inconsistent media of fault rocks without the need to prematurely infer formation and emplacement mechanisms.

2.6 Fault Gouge

Fault gouge studied in both natural (e.g. Cladouhos 1999a,b; Cowan et al 2003) and experimental settings (e.g. Haines et al 2013) have some typical features (Figure 2-7).

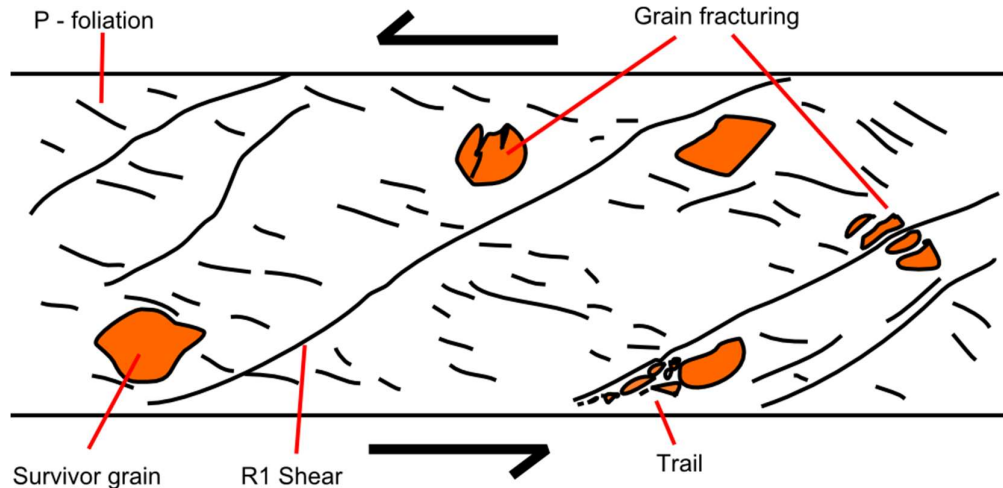


Figure 2-7 Some common features of gouge. After Rutter (1986)

P-foliation forms when shearing causes the alignment of particles in clay rich fault gouge at angles between 135° and 180° to the shear direction (Rutter et al 1986; Cowan et al 2003). R1 Riedel shear surfaces are minor shears that form in gouge material at an angle up to 45° to the principal shear surface and R2 Riedel shears are less common antithetic shears which form at high angles to the shear plane (Rutter et al 1986). Haines et al (2013) have shown that in experimental gouges that Riedel shears develop at the shear boundary and propagate through the gouge layer as the magnitude of displacement increases. The development of Riedel shears in gouge can change the mode of cataclastic flow: before Riedel formation particles slide past one another, after Riedel formation particles rotate and deform, causing significant grain size reduction (Haines et al 2013). “Y-surfaces” or “Y-shears” are shear zones within gouge material that form at or near the direction of shear

(Rutter et al 1986) and have the same shear sense as both R1 Reidel shears and the gouge boundary zone.

A feature commonly observed in granular fault gouges is termed flow banding (Cladouhos 1999b; Cowan et al 2003). Flow banding in gouges undulates but generally forms at low angles to the direction of shear and is defined by segregations in minerals, foliation and boudinaged clasts and layers (Cladouhos 1999a).

Survivor grains are isolated clasts in fault gouge that are free to rotate without interference from other similar sized clasts (Cladouhos 1999b). Survivor grains are formed by fracturing of larger clasts, and subsequent rolling and sliding against other particles causes rounding (Cowan et al 2003). These clasts typically display a strong Shape Preferred Orientation (SPO) either in the direction of shear (granular gouges) or inclined to the shear plane (clay rich gouges) (Cladouhos 1999b). Survivor grains may also exhibit “trails” which form when grains are fractured and fragmented by continued deformation (Rutter et al 1986). The fragments spread from the source grain and can be used to infer a sense of shear in the gouge.

2.6.1 Continuum of processes in gouge

Similar to the above discussion regarding breccia formation, processes which form the features observed in gouge should not be considered mutually exclusive. Flow banding develops with continued shearing in granular gouges (Cladouhos 1999a). Reidel shears, which only form after significant displacement, have been shown to rotate in experimental clay rich gouge to a similar orientation to “Y-shears” and undulating flow banding (Haines et al 2013).

In the Woodcock and Mort (2008) classification system fault gouge consists of >30% matrix (grains <2mm). Other authors have used different criteria to distinguish breccia and gouge which principally involve determining the percentage of “visible fragments” (Sibson 1977; Cladouhos 1999b; Cowan et al 2003). Although the 2mm cut off between clasts and matrix in the Woodcock and Mort (2008) scheme has no relation to tectonic process (the 2mm cut off follows sedimentary classification schemes), it removes the need for users to determine what constitutes a “visible” fragment and what does not.

Particle size reduction during continued brittle deformation is well documented (eg. Blenkinsop 1991; Cowan et al 2003; Billi 2005; Luther et al 2013). The development of fault gouge can be seen as a product of particle size reduction in fault rocks through continued shearing. Volumes of breccia have been observed as tongues, preserved and detached from the “host” breccia and partially mixed within fault gouge (Cowan et al 2003).

Breccia and gouge could also be considered a continuum, as opposed to definite contrasting fault rocks. The Woodcock and Mort (2008) criteria usefully separates gouge and breccia based on easily identified criteria but in reality they are both part of a continuum of fault rock formation.

2.7 Mineralisation of fault rocks

Veins and cements can hold clues to mechanical and fluid conditions in a fault zone (Bons et al 2012). Vein and cement textures such as crystal growth style and geometrical aspects such as dip and strike, thickness and relationship with other structures are used to reconstruct fault and fluid flow interaction (Woodcock et al 2006; Woodcock et al 2007; Eichhubl et al 2009; Caine et al 2010; Woodcock et al 2014). Conversely, lack of mineralisation has been previously used to suggest structures are formed later than the

most recent episodes of fluid flow (eg. Walker et al 2011). Four different fluid transportation and precipitation mechanisms can be defined: i) Stagnant fluid in pores; ii) Flow through pores; iii) flow through fractures and iv) hydraulic fracturing through fluid pressure (Bons et al 2012).

Crystal growth into open voids can be inferred from deposits which show the formation of large euhedral crystals (well defined faces and edges) (Woodcock et al 2014). Relationships between rate of mineralisation and void opening (fracture or otherwise) can be inferred from vein cement texture. Veins with elongate fibres suggest that precipitation and opening rates were similar. Granular textures suggest that veins were opening at higher rates than mineral precipitation (Woodcock et al 2007). Post-brecciation fracturing has been inferred from vein structures that cut clasts and matrix in dilational breccias (Woodcock et al 2006). Veins which contain brecciated mineral deposits can indicate post emplacement deformation.

The interaction of deep-sourced fluid and the seismic cycle (“fault valve” model discussed above) was inferred by Caine et al (2010) using the composition of mineral deposits contained in the breccia bodies. Boles et al (2004) described the interaction of meteoric water and basinal fluids along a basin margin fault where flow has evolved from rapid expulsion of over pressured fluids to steady buoyancy-driven seepage.

2.8 Fault Scarp sedimentation

Sedimentation along active fault scarps is a widely recognised process (eg. Leeder et al 1991; Wignall and Pickering 1993; McLeod et al 2000; Densmore et al 2004; Cowie et al 2006; Elliot et al 2012; McArthur et al 2013). However, slope deposits as marginal components of basin fill are rarely reported in the literature (Ventra et al 2013).

One example of marine fault scarp sedimentation is the Helmsdale fault at the margin of the Inner Moray Firth Basin (Wignall and Pickering 1993; McArthur et al 2013). “Boulder Beds” of up to 800m thick are exposed onshore and are characterised by large sedimentary clasts (typically <0.75m but as large as 45m), poor sorting and variable bed thickness (0.5m to 61m thick) (MacArthur et al 2013). The exposure represents an initially shallow marine sedimentary succession progressing to deep marine, that was deposited on steep slopes, resulting in slumping and sliding (Wignall and Pickering 1993). Sedimentation along active propagating normal faults is also found in the Gulf of Corinth, Greece (Leeder et al 1991). Footwall uplift relative to a subsiding hanging wall has caused the formation of a number of features such as raised coastal terraces, syn-tectonic talus cones and alluvial fans (Leeder et al 1991).

Fault displacement at the basin margin has been shown to exert control over sediment supply and deposition processes at the basin scale (eg Gawthrope and Leeder 2000; Allen and Densmore 2000; Ford et al 2013) but the deciphering the interaction of fault displacement and sedimentation using the detailed field surveys of the architecture of basin margin sediments has received much less attention. In one such study Mortimer et al (2005) used facies variations in progradational units to reconstruct fault displacement at the Loreto fault in the Gulf of California. Progradational units were mapped in detail showing shallow water facies grading into Gilbert type deltas. The authors propose that cycles of variable fault displacement rates have exerted a primary control on the deltas. Periods of low fault displacement are characterised by shallow water sediments being deposited. During periods of accelerated fault displacement, increased topographic relief has resulted in the deposition of coarser grained facies. Mortimer et al (2005) postulate that the variations in fault displacement rates are due to the evolving frictional properties of the basin bounding Loreto fault.

2.9 Sediments at the Tip of Upward Propagating fault

Sharp et al (2000) described steeply dipping normal faults which propagated upwards at the Suez Rift Egypt and caused beds above the fault to tilt towards the basin centre. Where the fault propagates upwards and ruptures the surface, the folded beds which were previously above the fault become monoclines adjacent to the fault surface (Figure 2-8). In some locations of the Suez Rift, older beds which are lower in the stratigraphic sequence are tilted to near vertical and the younger beds are dipping progressively shallower up sequence. Ferrill et al (2012) described deformation above an upward propagating fault in mechanically contrasting beds. As the fault propagates upwards a monocline forms above the fault tip. As displacement continues the monocline limb steepens and boudinage forms in mechanically stronger layers due to bedding parallel extension (Figure 2-9). Ferrill et al (2012) concluded that incompetent beds inhibit fault tip propagation as they accommodate pre failure strain rather than failing in a brittle way. As displacement continues in the incompetent beds monocline folding produces fault synthetic dips as steep as the fault plane. This is echoed in a review paper by Ferrill et al (2017) and references therein.

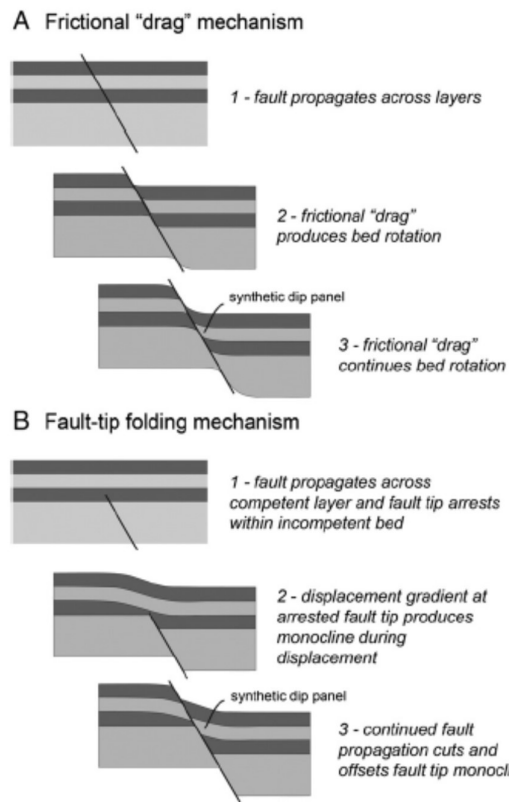


Figure 2-8 Cross section view of the model for A) Frictional drag tilting, and B) Upward propagating fault tilting. After Ferrill et al (2012).

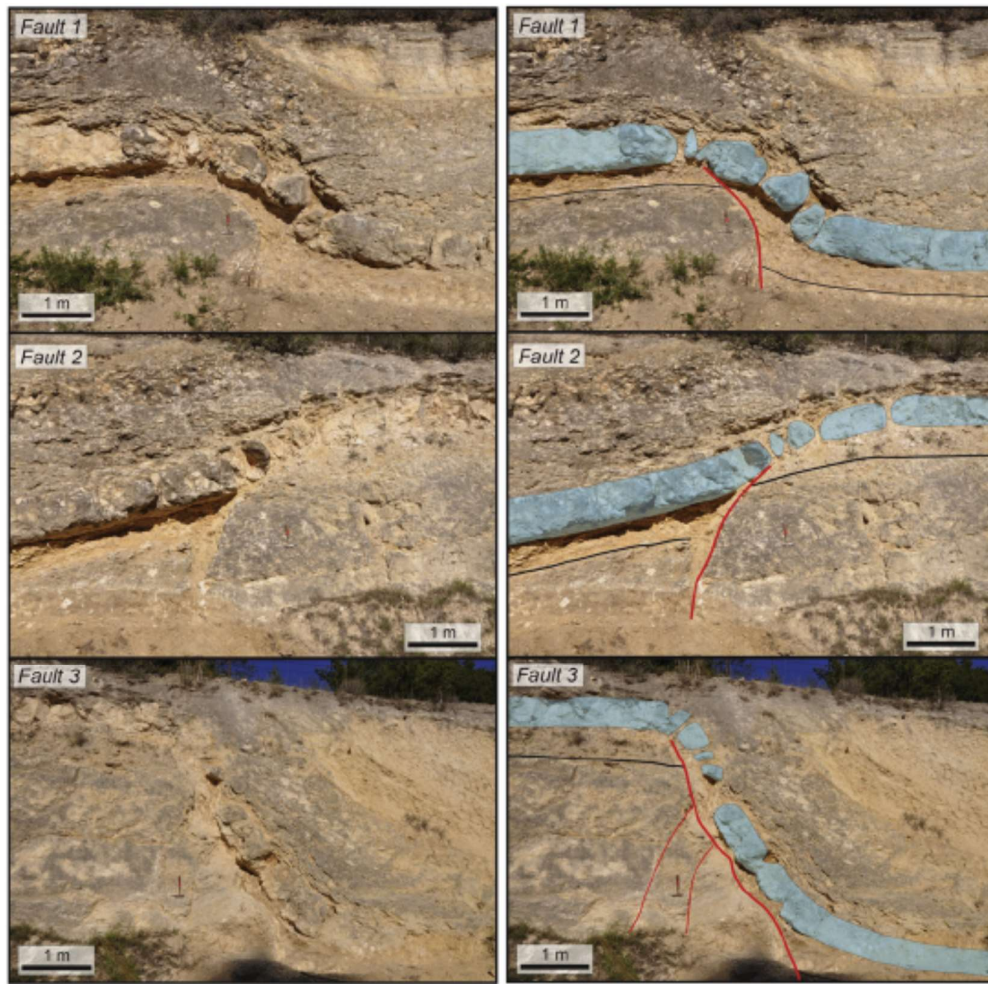


Figure 2-9 Figure from Ferrill et al (2012) showing photographs with and without annotation of layer parallel extension in competent limestone beds (blue shading).

The model of a tilted monocline above an upward propagating fault tip is often postulated as an alternative to the traditional frictional “drag” mechanism (Ferrill et al 2017).

The significance of these studies showing sediments at the tip of an upward propagating fault for the present study is discussed in Section 6.2.6.

3. Regional Geological Setting

3.1 Introduction

This Chapter describes the regional geology of the Solway basin and the North Solway fault.

This Chapter principally intends to put the field area into context with the regional geology but also serves as a general introduction to the field site. The detailed descriptions of the fault zone are covered in Chapters 4 and 5.

The North Solway fault sits at the boundary between the Southern Uplands and the Solway Basin. This basin margin fault zone roughly follows the regional ENE-WSW strike, which is thought to be inherited from Lower Palaeozoic basement rocks (Chadwick and Holliday 1991). This is similar to the axial trend of the Solway Basin itself (Lintern and Floyd 2000) which forms part of a suite of basins that extends from the Northumberland Trough through to the offshore Peel Basin (Figure 3-1).

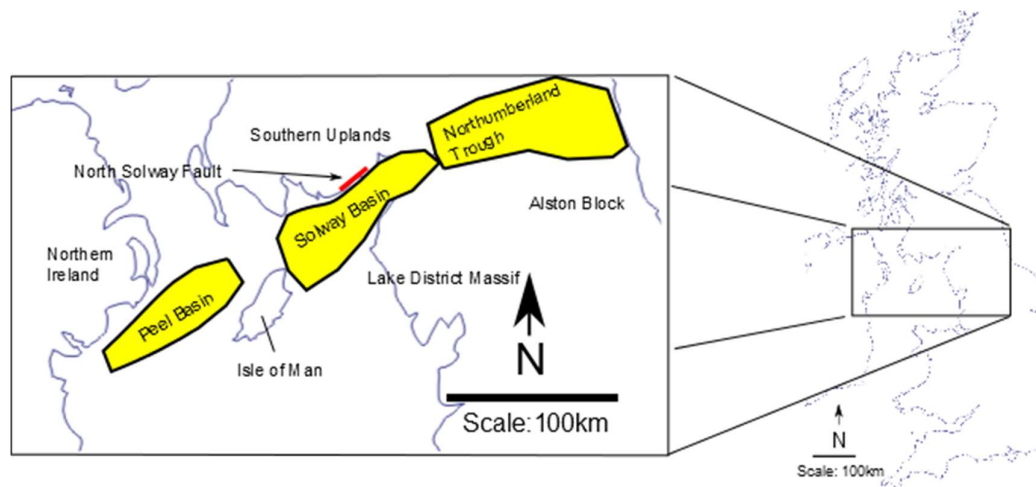


Figure 3-1 Map showing the location of the Solway basin and the associated Carboniferous basins. After Floodpage et al (2001).

The present day North Solway fault is exposed in extensive strike view (c. 10 km along-strike length) and relatively limited dip view (10s of metres). These exposures demonstrate variable fault zone architecture and variable strike. The fault downthrows Early Carboniferous (Dinantian) basin sediments (Ord et al 1988; Deegan 1973) against footwall rocks consisting of Silurian meta-sediments intruded by Devonian dykes and plutons (Piper et al 2007). The fault has been active since Dinantian times and syn-sedimentary faulting is evidenced by liquefaction features and soft sediment faults in the hanging wall rocks at several locations along strike (Ord et al 1988). Lintern and Floyd (2000) reported that the fault displays multiple shear surfaces and cemented angular breccia which contains clasts generated from the Lower Palaeozoic rocks of the Southern Uplands.

3.2 Southern Uplands

The Southern Uplands is a Lower Palaeozoic terrane of Ordovician and Silurian meta-sediments intruded by Devonian granitic rocks. The terrane is bounded to the north by the Southern Uplands fault, and to the South by unconformable and faulted contact with Dinantian sediments (Lintern and Floyd 2000).

It is widely accepted that the Southern Uplands Terrane formed as a result of the closure of the Iapetus Ocean when the continents of Laurentia and Avalonia collided. Three competing models have been put forward to explain the formation of the Southern Uplands, these are; an accretionary wedge model, a back arc thrust model, or a rifted continental margin (Trewin and Rollin 2002). Discussing the relative merits or otherwise of each model is beyond the scope of the present study. For the purposes of this study it is sufficient to understand that the closure of the Iapetus Ocean caused the Ordovician and Silurian turbidite sequences to be deformed into thrust stacks and isoclinal folds (Lintern

and Floyd 2000). The Southern Uplands has been divided into three strike-parallel, fault-bounded terranes and the present study area lies in the Southern belt (Figure 3-2).

The next significant phase in the development of the Southern Uplands is marked by the intrusion of igneous rocks from late Silurian to early Devonian (c. 430 to 390 Ma). The earliest intrusions are thought to be a series of porphyritic dykes, followed by emplacement of the quartz diorite and granodiorite Bengairn complex, which was in turn intruded by the Criffel-Dalbeattie granodiorite pluton (Lintern and Floyd 2000). The Criffel-Dalbeattie pluton (shown in Figure 3-2) was emplaced in the Early Devonian (Piper et al 2007) and by the late Devonian had been uplifted and eroded. All the plutons in the region are cut by microdiorite dykes (Lintern and Floyd 2000).

Extensional activity caused the formation of a Carboniferous basin system stretching from the Northumberland trough to the East Irish Sea (Figure 3-1) (Barrett 1988). A later period of extension occurred in the Permian. This caused the formation of north-west trending half-graben basins in the Permo-Triassic as shown in Figure 3-2.

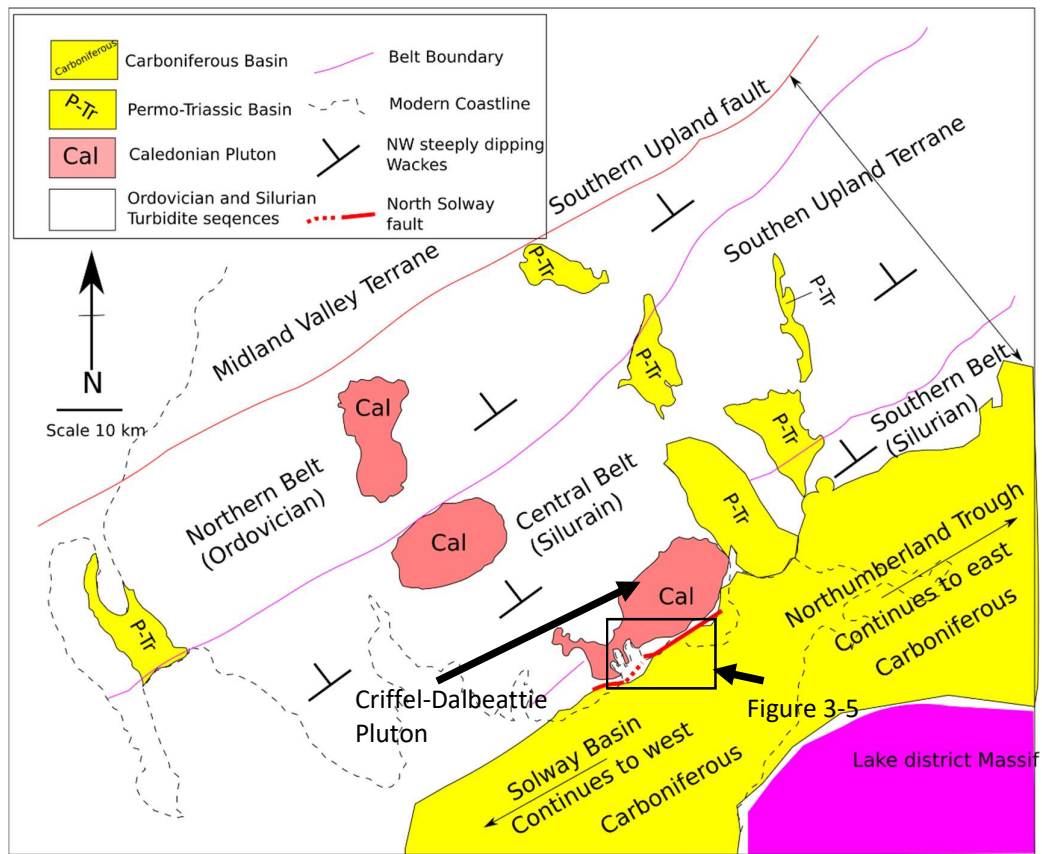


Figure 3-2 Map of the southern Uplands showing the main geological units and their ages. After Lintern and Floyd (2000) and Toghil (2009).

3.2.1 Pre-Carboniferous

The structural trend of the Solway basin is thought to be inherited from the Caledonian Orogeny when the closure of Iapetus Ocean brought together the Avalonian and Laurentian continents (Chadwick and Holliday 1991; Newman 1999). The collision of the two continents, as a result of subduction caused the formation of a 15-25° N-NW dipping structural lineament, the Iapetus suture (Beamish and Smythe 1986; Chadwick and Holliday 1991).

Figure 3-3 is a composite map after Chadwick et al (1995; top right of figure) and Newman et al (1999; bottom left of figure) which shows the dominant structural elements in the Northumberland Trough and Solway Basin.

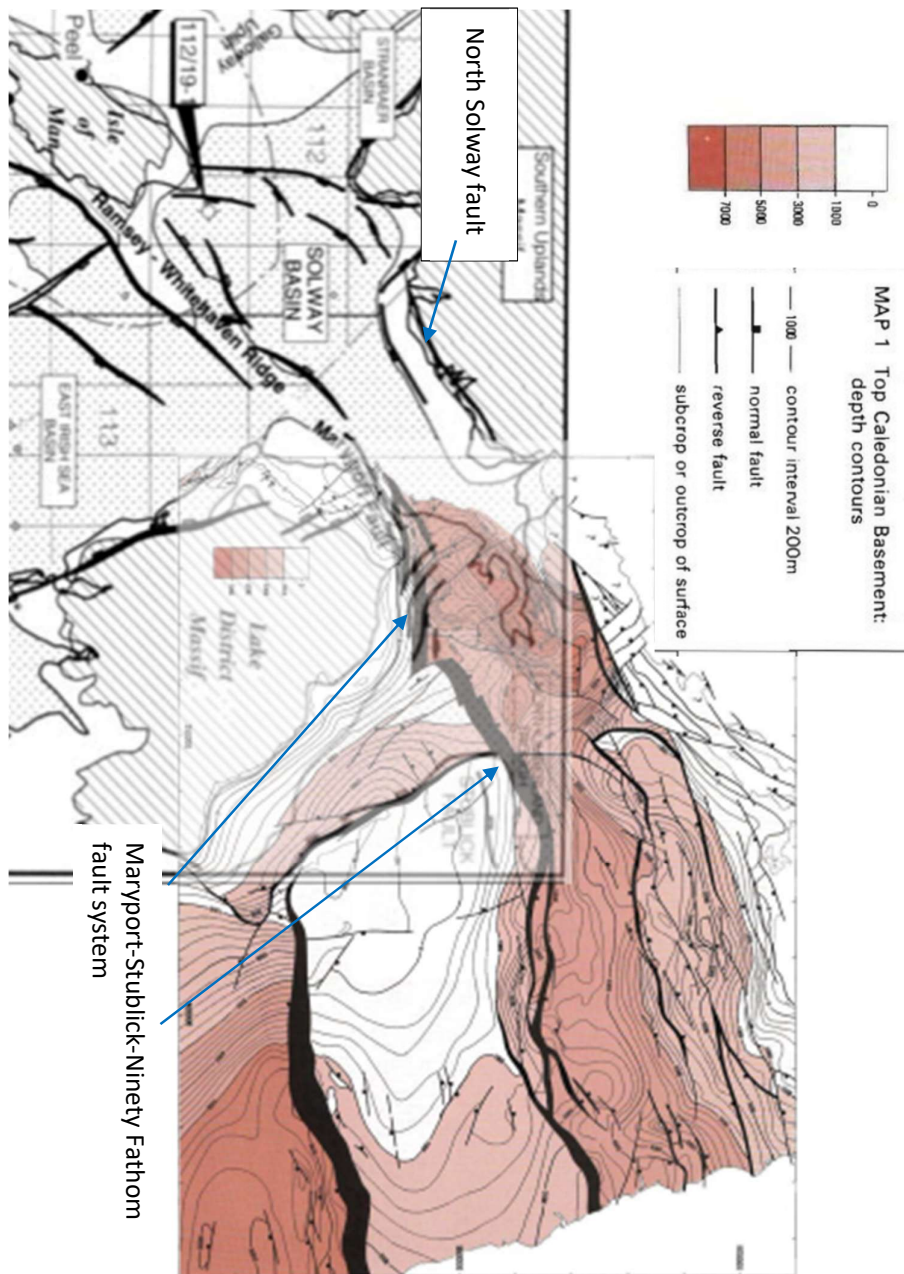


Figure 3-3 Composite map after Chadwick et al (1995; top right of figure) and Newman (1999; bottom left of figure) showing the regional scale faulting of the Northumberland-Solway basin complex. 200m contours shown in the top right are of depth to top of basement (pre-Carboniferous). Major faults in the region are shown as black heave polygons with markers on the down-throw side in the Chadwick et al map and blacks lines in the Newman map. Most faults follow the ENE-WSW trend of the Iapetus Suture, with a sub-set trending NNW-SSE. Pink shading represents depth and the key for this is shown at the top of the figure.

The major through-going normal fault system on the southern margin of the Northumberland trough is termed the Maryport-Stublick-Ninety Fathom system and is estimated to have a maximum throw of up to 5000m based on seismic surveys (Chadwick et al 1995). By contrast, the northern margin of the Northumberland-Solway basin complex is shown to consist of a number of partially parallel and discontinuous normal faults. The total throw on the northern margin of the Northumberland-Solway basin complex is therefore accommodated by more than one fault and throw on individual faults such as the NSF is much lower than the total thickness of the sediments on the Solway Basin. A discussion on fault throw is included in Chapter 6.

3.2.2 Carboniferous

The Solway basin was initiated around the Devonian/Carboniferous transition (Ord et al 1988). Early Carboniferous sedimentation in the Solway basin consisted of cyclical deltaic and shallow-water sandstones, shales, limestones and coals (Floodpage et al 2001; Newman 1999). The North Solway fault had become a major controlling element in basin growth by the early Carboniferous (Newman 1999). Newman (1999) suggests the maximum thickness of Carboniferous strata is up to 3000m, whereas Barrett (1988; and references therein) reports possible Carboniferous sedimentary thickness up to 5000m. By the late Carboniferous, basin shortening and inversion was taking place in the region (De Paola 2005), probably in response to Variscan-associated North-South compression (Chadwick et al 1995; Floodpage et al 2001). This has caused much of the Upper Carboniferous facies to be absent from the record in the Solway basin and has resulted in a strong angular unconformity with the overlying Permo-Triassic succession (Newman 1999; Brookfield 2004; Brookfield 2008).

Figure 3-4 shows the interpretation of seismic data within the Solway and Peel Basins after Floodpage et al (2001). The key seismic line for this thesis is line (a) in Figure 3-4, the location of which is shown in the top right corner of the figure (Floodpage et al (2001)'s 7a). The section cuts across the Solway basin perpendicular to the NSF and shows there are a number of faults within the sediments which are synthetic and antithetic to the NSF. These faults are developed within the Carboniferous sediments and if they are synsedimentary, the displacement along these faults is likely to have created accommodation space for basin development.

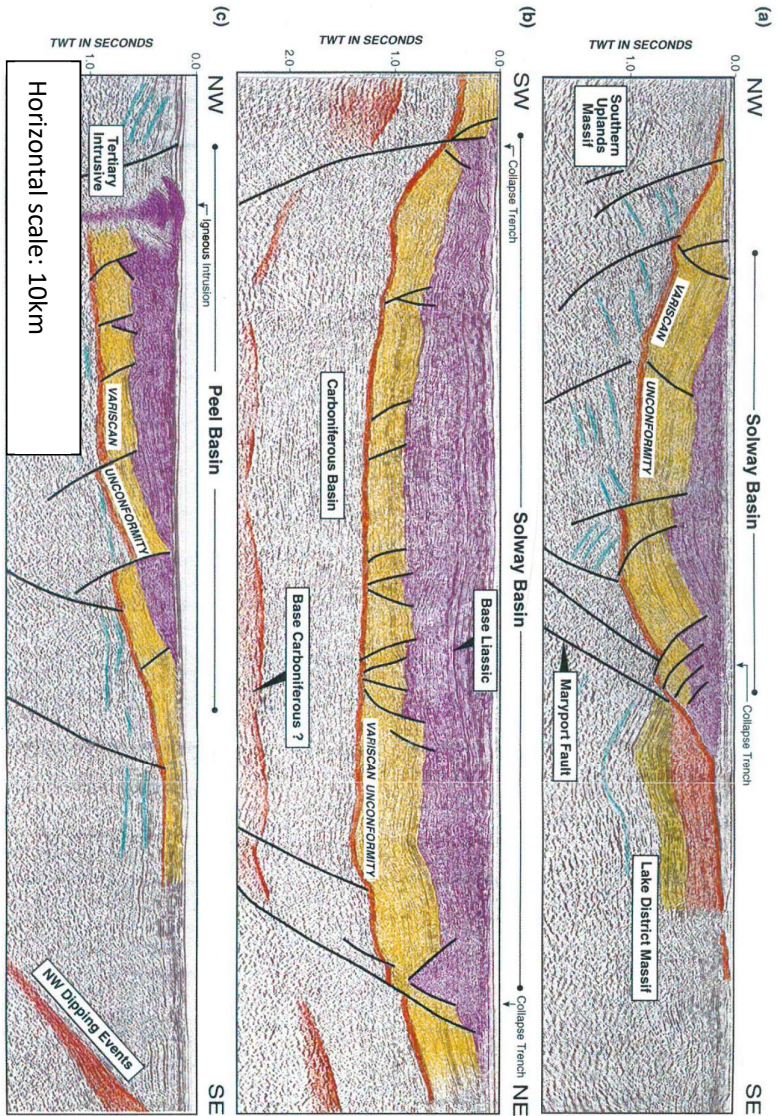


Figure 3-4 Interpretation of seismic surveys from the Solway and Peel basins. From Floodpage et al (2001). Vertical exaggeration approx 2x.

3.2.3 Permo-Triassic

The Permo-Triassic in the Solway basin is characterised by another period of basin extension (Ord et al 1988) in which E-W extension created approximately N-S trending faults (Newman 1999) and the Permian basins of the Southern Uplands (Figure 3-2). At this time, Scotland occupied a similar latitude to present day Sahara and was drifting slowly northward (Glennie 2002). Palaeoenvironmental conditions were semi-arid to hyper arid (Brookfield 2004; Brookfield 2008) and sediments deposited during this time are characterised by predominantly fine grained red clastics. Hydrocarbons are thought to have formed in the Solway basin from Carboniferous source rocks during the Permo-Triassic (Parnell 1995).

3.2.4 Jurassic onwards

The Jurassic age geological activity of this area is difficult to reconstruct due to a lack of post-Triassic preservation (Newman 1999). Parnell (1955) and Miller and Taylor (1966) have dated fluid migration of hydrocarbons along the North Solway fault to the Jurassic era using U-Th dating. Maximum burial depth was achieved during the Jurassic and is estimated to have been around 4-5km (Parnell 1995). This was followed by several phases of uplift and erosion which removed much of the Mesozoic cover in the area (Newman 1999).

3.2.5 Summary of Solway Basin

In summary, the Solway Basin is thought to have originated in early Carboniferous times. The basin has undergone 2 main phases of basin extension (broadly NE-SW and E-W) separated by basin shortening and inversion. Large thicknesses of sediment have been deposited since the Early Carboniferous with maximum burial depth likely to have been achieved in the Jurassic period.

3.3 The North Solway Fault

The North Solway fault marks the boundary between the Southern Uplands and the Solway Basin. The fault downthrows outliers of early Carboniferous (Dinantian) sediments against a basement of Silurian greywackes and Caledonian dykes (Lintern and Floyd 1988) with a maximum throw of at least 600m (Deegan 1973; Ord et al 1988). The fault can be traced for around 15km kilometres along strike (Figure 3-5) and trends between ENE-WSW and NE-SW. The fault is interpreted to have been active since Dinantian times due to the inferred age of syn-tectonic sediments (Deegan 1973; Ord et al 1988). The fault juxtaposes lithologies of the Lower and Upper Palaeozoic era (Lintern and Floyd 2000).

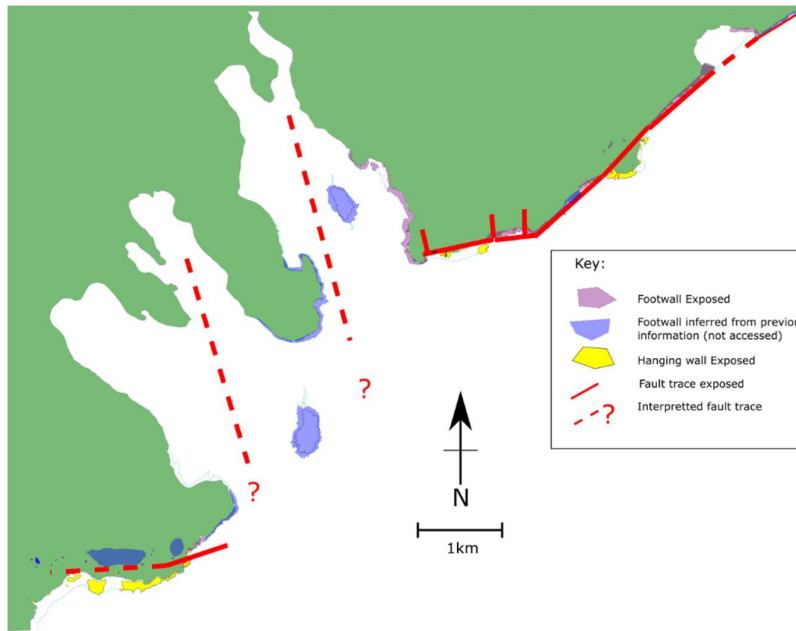


Figure 3-5 Map of the main fault trace. Includes observed and interpreted trends after Lintern and Floyd (2000), BGS 1:50,000 series (Sheet 5E and part 6W), Piper et al (2007) and the unpublished work of Alan Gibbs.

Synsedimentary faulting is evident (Ord et al 1988; Deegan 1973) where the depositional environments are interpreted as alluvial fan piedmont (Deegan 1973; Lintern and Floyd 2000).

Most publications concerning the area around the North Solway fault tend to focus on the Solway Basin (Brookfield 2004; Brookfield 2008; Newman 1999; Floodpage 2001), Devonian intrusions (ie. Piper et al 2007), deep crustal structures (Beamish and Smythe 1986; Chadwick and Halliday 1991) or regional scale faulting (Barrett 1988). Examples of studies which focus on the North Solway fault itself are less common. Deegan (1973) and Ord et al (1988) studied evidence relating to synsedimentary faulting to constrain the timing of basin onset at the NSF and interpreted fault activity during the Dinantian period. Evidence of fluid flow in the form of oil residues (U-Th dating: Parnell 1995) and Uraninite veins (U- Pb dating: Miller and Taylor 1996) related to the North Solway fault have been dated as Jurassic.

No prior studies discuss the internal structure of the North Solway fault or the interaction between the fault rocks and sedimentary rocks along this basin-bounding fault zone. However they do offer some indication as to what can be expected in the present day exposures. Ord et al (1988) describe multiple shear planes in a zone of brecciation 3m wide in the footwall at Castle Point, and that slickensides in cataclasite vary slightly but indicate a dominantly dip-slip motion. Lintern and Floyd (2000) report Carboniferous angular breccia stacked against a footwall of Silurian strata. The breccia is overlain by over-steepened conglomerates in a 10m wide zone adjacent to the fault (Lintern and Floyd 2000).

4. North Solway Fault Field Exposures

This chapter describes key aspects of the field site in order to explain the constraints on observations and data collection. The mapping methods, the field site layout, brief descriptions of the geology at key locations and the geometry of the main fault are then described. Although this is a common site for field visits, the observations in this chapter represent the first descriptions of the fault geometry, fault rocks and associated sediments at the individual sites. The detailed and quantitative results of the field work undertaken for this thesis are found in chapter 5.

4.1 General Description of fieldwork

Fieldwork was carried out during the summer months of 2012 – 2014. Base maps were freely available satellite images from Google maps™. The main features of the site were traced onto these base maps, including: main rock units, fault traces, zones of brecciation and mineralisation. Georeferenced dip and strike readings, field sketches and photographs were used to record the characteristics of the footwall units, hanging wall units and fault rocks. A mixture of clast counts to characterise breccia textures, vein data (dip/strike, crystal and fracture geometry) to quantify fluid flow conditions), hand samples and thin sections have further contributed to a detailed investigation of the fault zone. Unpublished field slips created by Dr Alan Gibbs were also used for initial planning of field work. These also provided information about areas of the site that were inaccessible during the present study (Hestan Island and East of Sandyhills Bay).

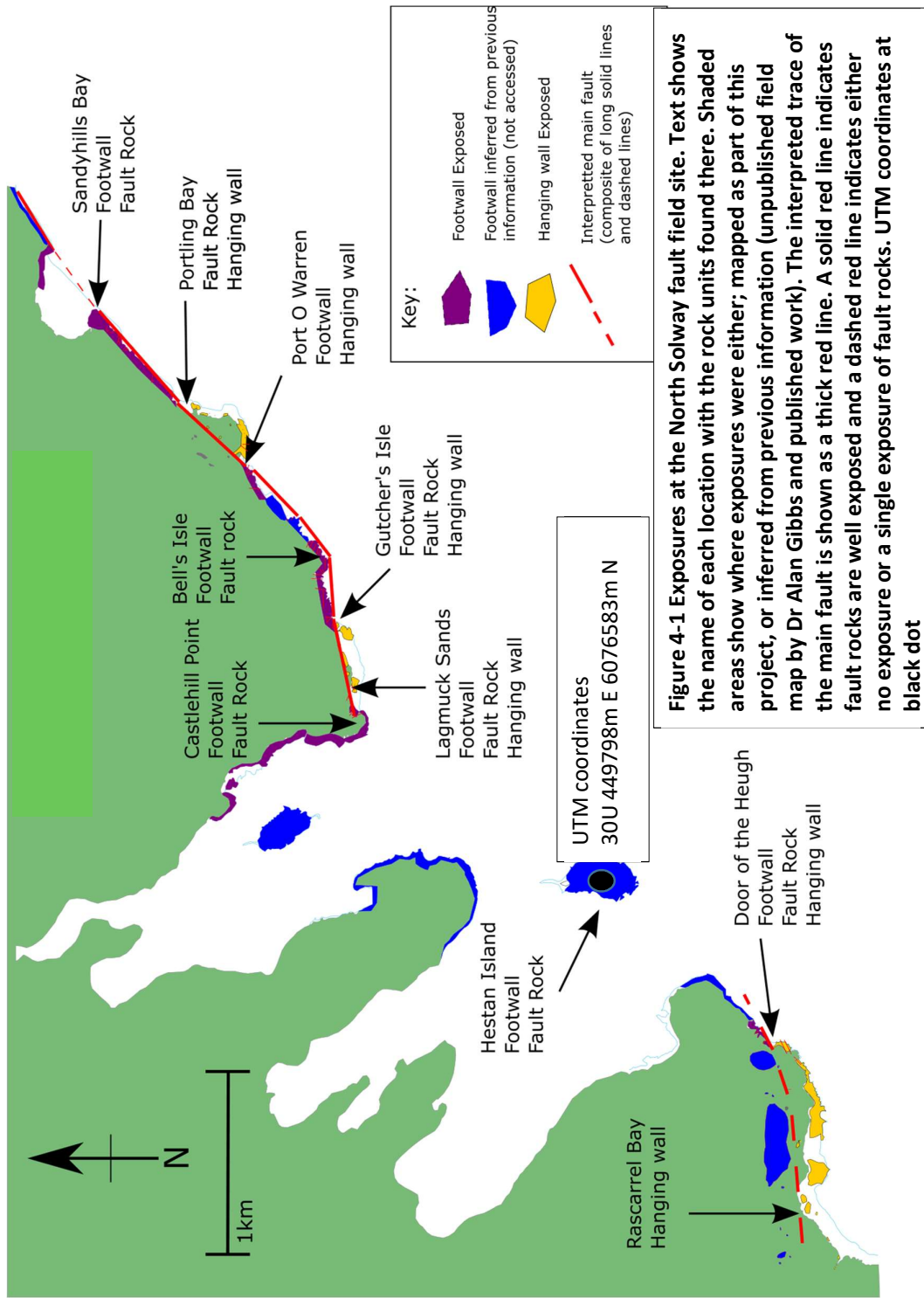


Figure 4-1 Exposures at the North Solway fault field site. Text shows the name of each location with the rock units found there. Shaded areas show where exposures were either; mapped as part of this project, or inferred from previous information (unpublished field map by Dr Alan Gibbs and published work). The interpreted trace of the main fault is shown as a thick red line. A solid red line indicates fault rocks are well exposed and a dashed red line indicates either no exposure or a single exposure of fault rocks. UTM coordinates at black dot

All locations mentioned in subsequent Chapters are shown in Figure 4-1, with text highlighting which fault components (footwall, hanging wall and fault rock) are exposed at each location.

Four locations along the strike of the North Solway fault were selected for more detailed baseline mapping: Door of the Heugh, Lagmuck Sands, Gutcher's Isle and Portling Bay. The locations were selected because they are the only locations where the internal fault zone structure is exposed and accessible on foot. These detailed maps are described in Section 4.6.

4.2 Site Topography

Most exposures at the site are at the foot of a high sea cliff which runs approximately along the line of the fault scarp. The exposed fault scarp reaches heights of up to c.30m and displays a variable strike. The rocks of the footwall are generally more resistant than the hanging wall rocks. However, the fault-related and palaeo-scarp-related breccias are variably resistant, resulting in a complex 3D exposure. The 3D geometry of the fault is shown in **Figure 4-2** where the main fault scarp is shown to be cut by cross faults.

Access to exposures is restricted by tide levels and some areas are only exposed for a few hours either side of low tide. Some exposures are accessible via public footpaths and beaches (Castlehill to Bell's Isle and Port O' Warren to Sandyhills) whilst others require scrambling over several metre-scale boulders (Door of the Heugh). Some areas are inaccessible due to soft tidal sediments (east of Sandyhills) or high sea cliffs (east of Door of the Heugh and west of Port o' Warren). Lithologies at or near the high tide mark were obscured by either barnacles and limpets or black algae and a few metres above this level

rocks are obscured by vegetation. Most of the data collected in this study is from exposures above the high tide mark and on the seaward side of vegetation.

The footwall and fault rocks of the North Solway fault are exposed in discontinuous segments which trend either parallel to, or at low angles to, the strike of the Solway basin. At the foot of the cliff there are frequent, isolated outliers of sedimentary basin sediments. These either protrude from beaches or are in contact with the footwall and fault rocks, though the latter is rare and the contact is usually obscured by vegetation or black algae.

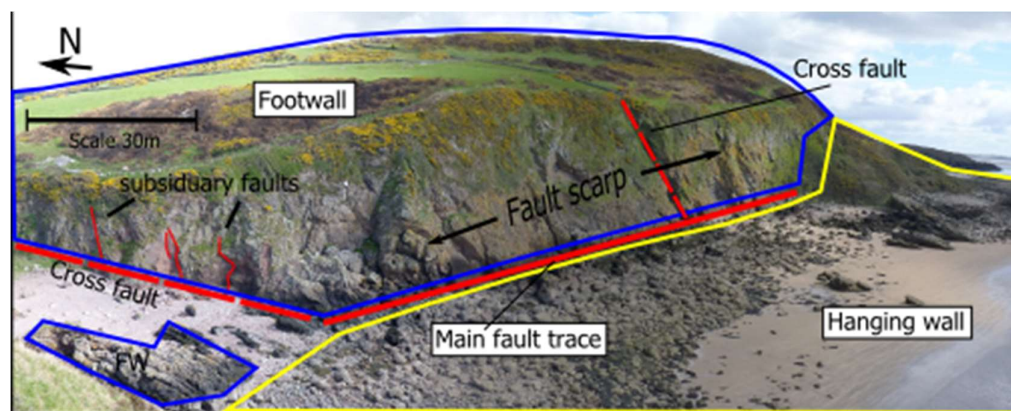


Figure 4-2 The North Solway fault basic elements (exposure from Castlehill Point to Lagmuck Sands). The scale bar in the top left represents approximate foreground scale. The main fault scarp is approximately 100m long and is oblique to the photograph. Isolated Hanging wall outliers are located just above the label “Hanging Wall”.

4.3 Footwall

The footwall of the North Solway fault comprises Silurian low-grade fine grained meta-sediments of the Ross Formation and Devonian Caledonian granodiorite and microdiorite intrusions (Lintern and Floyd 2000)

Meta sedimentary bed thicknesses range from thin to very thick. Lintern and Floyd (2000) characterised the mineralogy of the Silurian metasediments through point counting.

Summary histograms of modal distribution are shown in **Figure 4-3** A large proportion of

the meta-sediment is made of interstitial material and grains <0.01mm in diameter (Mx in Figure 4-3), with ~30% quartz and ~7% feldspar. Up to 10% of the modal composition was recorded as acidic igneous rock clasts (Ac) but these were not observed during this thesis.

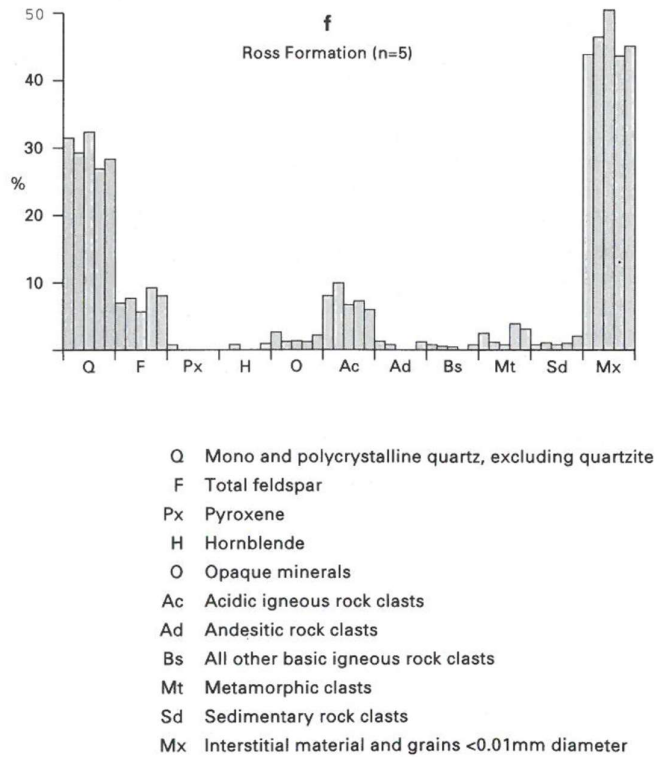


Figure 4-3 Summary histograms of modal composition data of five thin section of the Ross Formation from Lintern and Floyd (2000). 1000 points were counted in each thin section.

The meta-sediments are folded, fractured and faulted with some fractures infilled with vein minerals. Meta-sediment beds in the field dip mostly SE with some dipping to the NW at

angles between 38° and 70° (**Figure 4-4**). This trend is roughly parallel to the regional strike of the Silurian (NE-SW)

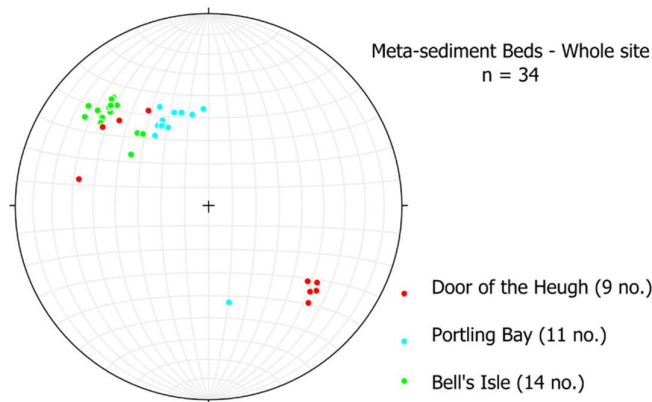


Figure 4-4 Poles to meta-sediment bedding exposed at the North Solway fault.

The meta-sediments are intruded by Devonian granodiorite and microdiorite dykes which have either planar geometry or more complex intrusive geometries (Figure 4-6). Many of the intrusions strike between NW-SE and ENE - WSW and are observed in the prominent cliffs.

The intrusions are medium to coarse grained. The mineralogy of the intrusions was studied by Lintern and Floyd (2000). They reported that they are commonly porphyritic, with phenocrysts of plagioclase, amphibole, biotite and quartz set in a feldspathic groundmass. Thin sections, examined as part of this thesis. taken from samples at Castlehill Point show varying degrees of chloritisation of both the ground mass and the phenocrysts (**Figure 4-5**). Rock strength was strong to extremely strong (BS 14689-1) with no observable variation in strength between intrusions with different levels of chloritisation.

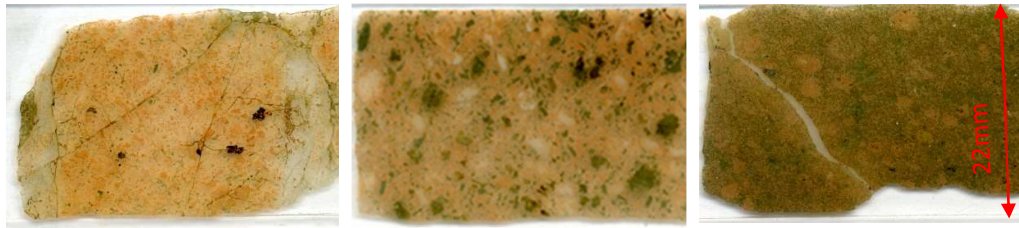


Figure 4-5 Scans of thin sections of intrusions from the Lagmuck Sands location showing increasing levels of chloritisation from left to right.

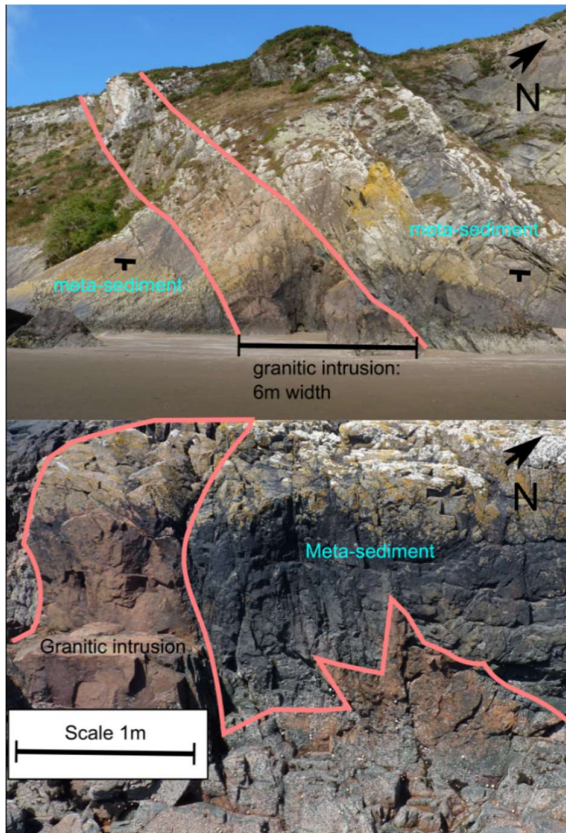


Figure 4-6 Intrusions of granitic dykes into meta-sediments (a) planar dyke near Sandyhills Bay, and (b) complex geometry dyke near Bell's Isle.

Both granitic and meta-sediment lithologies are fractured, veined and faulted implying later post-emplacement deformation. The granitic rock is structurally different to the meta-sediment with no observable directionally-dependant large-scale fabric. Strong cleavage is

not developed in the meta-sediments here but the meta-bedding is a large-scale fabric present at all locations.

4.4 Hanging wall

The hanging wall of the North Solway fault consists of interbedded coarse sandstones and conglomerates with occasional siltstones, mudstones and limestones. Bedding mostly dips towards the basin with deposits more than 20m from the fault zone displaying well-defined bedding, which typically dips between 10° and 30°. Sediments closer to the fault zone have a less well defined and more variably trending bedding and appear to be over-steepened (dipping up to 70° compared to colluvial slope angles which can be as steep as 56°; Blair and McPherson 1994).

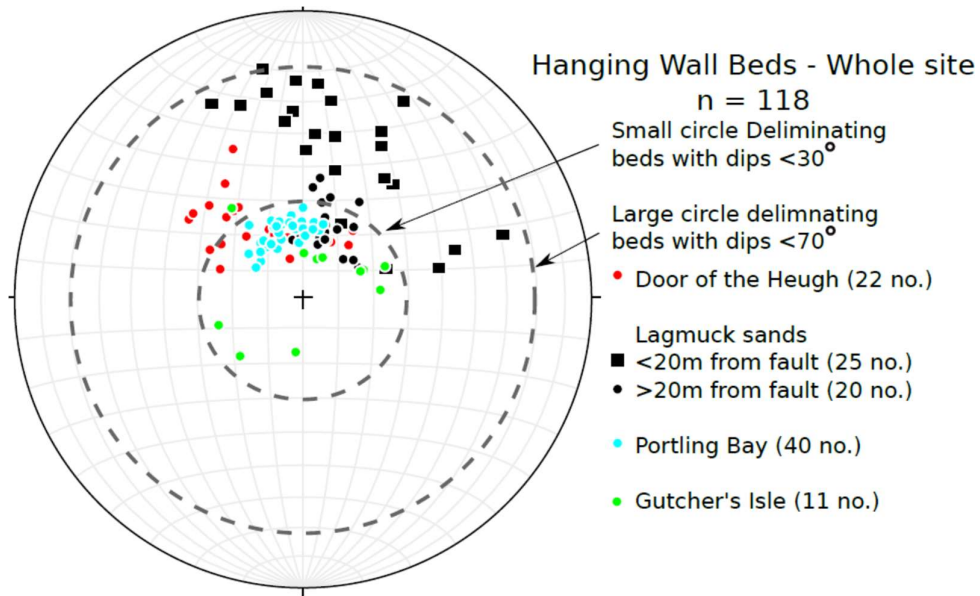


Figure 4-7 Poles to planes plot of hanging wall beds. Squares represent exposures close to the fault scarp. Dots represent exposure at a distance of 20m or more from the fault scarp.

Clasts within the conglomerates are of sedimentary, granitic and meta-sedimentary lithologies, and therefore appear to have been derived from both the footwall and hanging wall. The basin sediments of the hanging wall are cemented, fractured, veined and faulted.

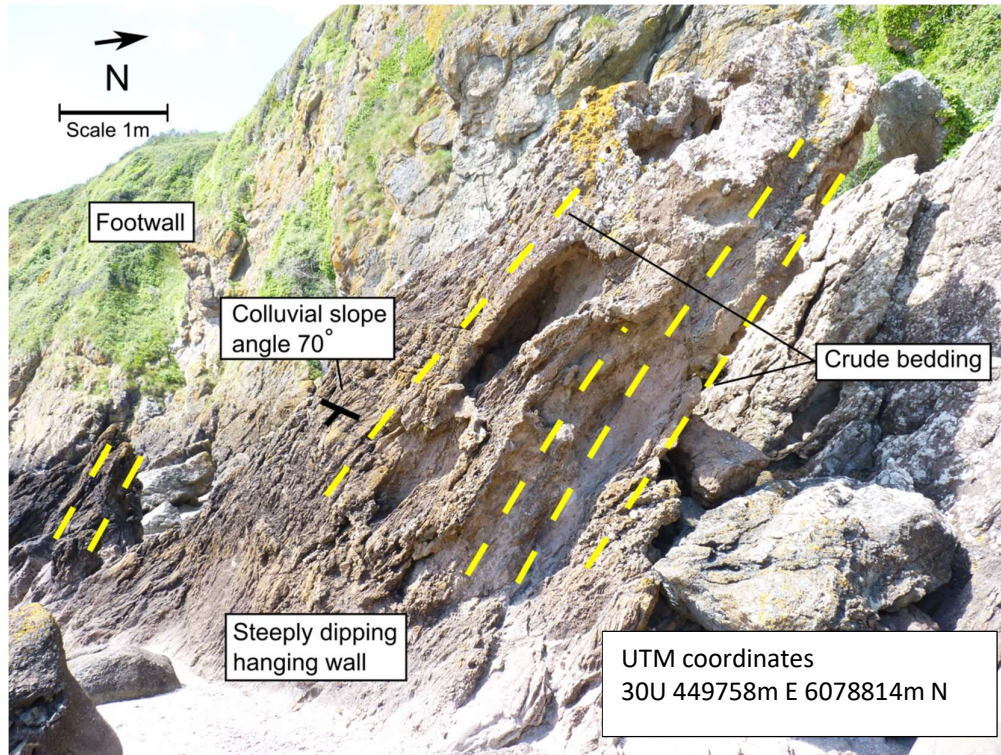


Figure 4-8 Steeply dipping hanging wall sediments

4.4.1 Distinguishing Between Tectonic and Sedimentary Breccia

In order to understand the development of the internal structure of the North Solway fault, it is necessary to develop a framework to distinguish between the rocks that are formed as a direct result of tectonic activity (tectonic breccias), and the rocks of the hanging wall that are primarily formed by sedimentary processes (sedimentary breccias). The following section describes the identifying features used to form a working definition for the purposes of the field work.

Sedimentary breccias and tectonic breccias can appear very similar in texture making it difficult to distinguish between them. This is confounded by the fact that some of the deposits are obviously re-worked and could represent tectonic breccias that have been re-mobilised by fault scarp degradation and sedimentation (re-sedimented breccias), or by repeated slip through sedimentary breccias by a fault active at the surface (re-faulted breccias).

In breccias more than 20m from the fault scarp, clast lithology is variable with sandstone, mudstone and coarser-grained igneous clasts observed alongside the metasedimentary and fine grained granitic clasts. These rocks are classified as conglomerates and coarse sandstones and as such are easily identifiable as basin sediments. Detailed logs of the hanging wall are found in Section 5-1.

Tectonic breccias and sedimentary breccias near the main fault trace share a number of characteristics; both types of breccias in these localities are formed almost exclusively of clasts of metasedimentary and granitic host lithologies in a fine-grained matrix. Clasts range from rounded to angular in both types of breccia and angular clasts are more commonly observed closer to the main fault than in the beds of conglomerates further from the fault. Both breccia types have a chaotic fabric.

There are locations where steep crude bedding is observed in close proximity to the fault zone (**Figure 4-8**). The crude bedding and proximity to a cliff face has led to an interpretation of lithified talus or colluvium and this deposit is therefore classified as a rotated sedimentary breccia.

Breccias directly in contact with the footwall show no bedding fabric. There may be an exception to this high up the cliff face at Lagmuck Sands, but these exposures are high

above any accessible outcrops (c.15m above ground level) and cannot be assessed safely.

The accessible breccias in contact with the fault scarp at Lagmuck Sands are arranged in pod-like geometries, similar to the tectonic breccia pods described by Caine et al (2010).

The pod like shape is also observed at Door of the Heugh at a distance of up to 15m from the main fault trace. Clasts within these breccias are observed to be in the process of fragmentation. Clast fragmentation within a body of breccia could be caused by any of the tectonic breccia-forming mechanisms discussed in Chapter 2.

Breccias were classified as either sedimentary or tectonic in origin by the following criteria:

- Proximity to the main fault scarp; breccias of tectonic origin are by definition within the fault. Breccias further from the fault are sedimentary.
- Breccia body shape; sedimentary breccia may be deposited in wedge shapes. Tectonic breccia could be arranged in pod-like geometries or in irregular shapes.
- Presence or absence of large scale fabric (bedding); sedimentary breccias may contain bedding. Bedding is unlikely to be present in tectonic breccias unless some sedimentation has taken place as a secondary process. (eg. Wright et al 2009 or Woodcock et al 2006).
- Clast lithology; Sedimentary breccias may contain clasts from a source lithology out-with the immediate surroundings. Tectonic breccias should be composed of clasts from the footwall and/or hanging wall, providing no sedimentary input into faults near the surface.

No single criteria definitively proves if a breccia body is either sedimentary or tectonic in origin. By considering all of the above criteria, inferences on the likely origin of breccias can be made. The terms sedimentary and tectonic breccias are used in this thesis to describe

both the characteristics of deposits based on the criteria above and to describe the inferred primary formation mechanism.

4.5 Deformation Elements

A number of faults have been observed that cut the footwall. The slip direction on these faults is difficult to infer as in most locations there are no marker beds to measure offset on. A rose plot of the strike of the footwall faults is shown in Figure 4-9. The plot shows that a significant number of faults strike NNW-SSE and broadly E-W.

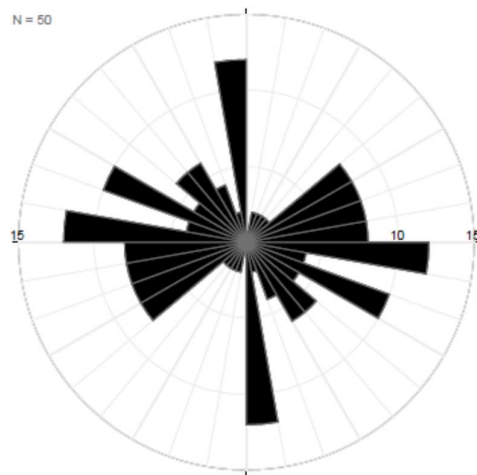


Figure 4-9 Rose diagram showing faults cutting footwall lithologies

Offset along these faults may account for some of the along strike variability in the footwall and fault scarp. Several subsidiary faults cut footwall lithologies and intersect the cross faults and fault scarp (e.g. **Figure 4-2**).

Tectonic breccias are predominantly composed of clasts of footwall lithologies and occur at several locations. These breccias range from mosaic and jigsaw textures to chaotic breccias. At Door of the Heugh and Lagmuck Sands chaotic breccias are arranged in pod-like structures (Figure 4-10 to 4-13). Chaotic breccia also occurs in breccia bodies that are cut by

fractures spaced c. 0.5m (Gutcher's Isle) and which do not resemble pods but display a blocky geometry (**Figure 4-14**). Chaotic breccia also occurs in smaller quantities in subsidiary faults and in places surround crackle and mosaic breccias. The tectonic breccias are described in more detail in section 4.8.







Two excellent exposures of fault gouge have been identified along the fault; Door of the Heugh and Portling Bay. At Door of the Heugh the fault gouge is around 400mm across and over the field seasons of this project has been variously covered by algae and uncovered by seawater. A larger gouge exposure is found at Portling Bay. This gouge is at least 10m wide, although no absolute widths can be measured as the contact between the gouge and other fault-related elements (ie. fault scarp or breccia) is not exposed. This exposure was covered by sands, gravels and boulders sporadically during the project. The fault gouges are described in greater detail in Section 4.9

4.6 Site locations (from south west to north east)

This section gives a description of each location along the main fault trace. A more detailed description of individual elements of the exposures is given for each of the four main locations within the relevant area of the site.

Detailed maps were created for the four locations by way of transects using a 30m measuring tape, graph paper and a compass. The features mapped are as follows; footwall (including lithology), hanging wall, fault rocks (including breccia texture and "donor" lithology where appropriate) and subsidiary faults. The maps were scanned and digitised using the same colour scheme for Figure 4-10, 4-12, 4.14 and 4.16. Each detailed map is accompanied by a cross section to provide indication of the fault zone structure in pseudo 3D. These cross sections were drawn by digitising a photograph of the main units with the

same colour scheme. The resulting cross sections are shown in Figure 4-11, 4-13 and 4-15, with an indication of the location and direction of the photograph. A description of what each mapped feature represents is given in Table 4-1, which acts as a detailed key to each figure.

Mapped unit	Lithology/structure
 Footwall meta-sediment	Meta-sediment of the footwall. Black lines within the blue areas are indicative of the trend of structures observed in the meta-sediment (bedding and folded bedding. Occasionally the meta-sediment is brecciated without a clear contact between unbrecciated and brecciated meta-sediments.
 Footwall granitic	Granitic rock of the footwall. Black lines within the pink areas are indicative of joints and fracture traces.
 Mixture of chaotic and mosaic breccia (granitic)	Breccia composed of clasts of only granitic rock. Chaotic and mosaic breccias were often mixed together and in places have been mapped as a single unit (indicated on the key of relevant figures).
 Chaotic breccia meta-sediment clasts	Chaotic and mosaic breccia of only meta-sediment clasts.
 Mixed clasts lithology chaotic breccia	Breccia containing clasts of multiple lithologies. By definition, this breccia has a chaotic texture as the clasts need to be entirely detached to mix with clasts of other lithologies.
 re-worked breccia clast	Representation of a single breccia clast composed of several re-worked




Mapped unit	Lithology/structure
	breccia clasts. These are described in detail in Section 4.8.2.
 Vein through clast	Veins that pass from surrounding matrix, through a clast of breccia. These are described in detail in Section 5.4.4
 Hangingwall sediments	Sedimentary rock of the hanging wall. In the areas selected for detailed mapping these comprised conglomerates and coarse sandstones.
 Gully with fault core exposures	At Door of the Heugh, fault gouge was observed in a narrow gully. This is described in detail in section 4.6.1.

Table 4-1 Detailed Key for units of detailed maps (Figure 4-10 to 4-16)

The descriptions in the following section are intended to as a guide to the reader, taking the reader through the entire field site. At the four locations where detailed mapping has been carried out, the descriptions are intended to supplement the map and cross section view.

4.6.1 Rascarrell Bay to Door of the Heugh

At Rascarrell Bay the hanging wall is composed of arkosic and conglomeratic sandstone, purple marl, siltstone, with thin mudstones and coals (Lintern and Floyd 2000). The footwall and fault rocks are not exposed at this section of the site except from Door of the Heugh.

The hanging wall at Door of the Heugh includes interbedded sandstones and conglomerates, with occasional turbidite layers. Figure 4-10 shows the detailed map resulting from the field work at Door of the Heugh and Figure 4-11 shows a cross section view of the same area. Only the very edge of the hanging wall exposures has been included

in the detailed mapping, purely to define the limit of the fault rock on the hanging wall side.

Tectonic breccia is exposed in large pods, each up to 4m across and several metres in height, consisting of chaotic breccia of mixed clasts lithology. Above a height of only a few metres the pods are obscured by vegetation but the columnar morphology of the vegetated surface suggests the pod shape may continue several metres above the level of exposure. The breccia pods are strong to extremely strong (terminology from BS 14689-1) and are separated by slip surfaces. The slip surfaces are identified by up to c.100mm wide zones of gouge which form the contact between separate pods. The slip surfaces are therefore considered to show evidence of grain size reduction between the pods as they move past each other within the fault.

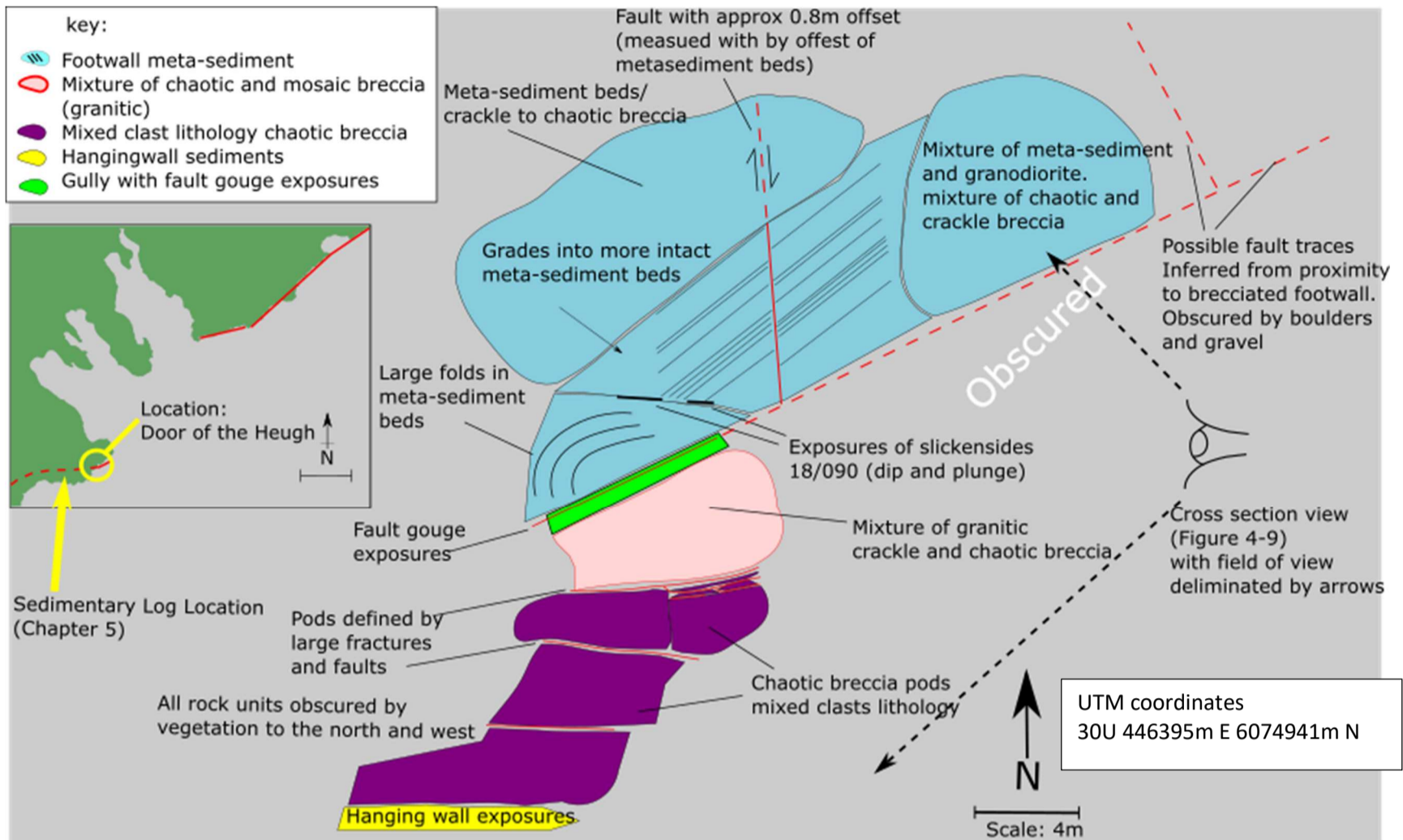


Figure 4-10 Detailed map of Door of the Heugh. Map colours are described in Table 1 and in the figure key. Grey areas are obscured by vegetation and boulders. Cross section view for Figure 4-9 is marked on the right hand side of the figure. The location of a sedimentary log described in Section 5.1 is shown.

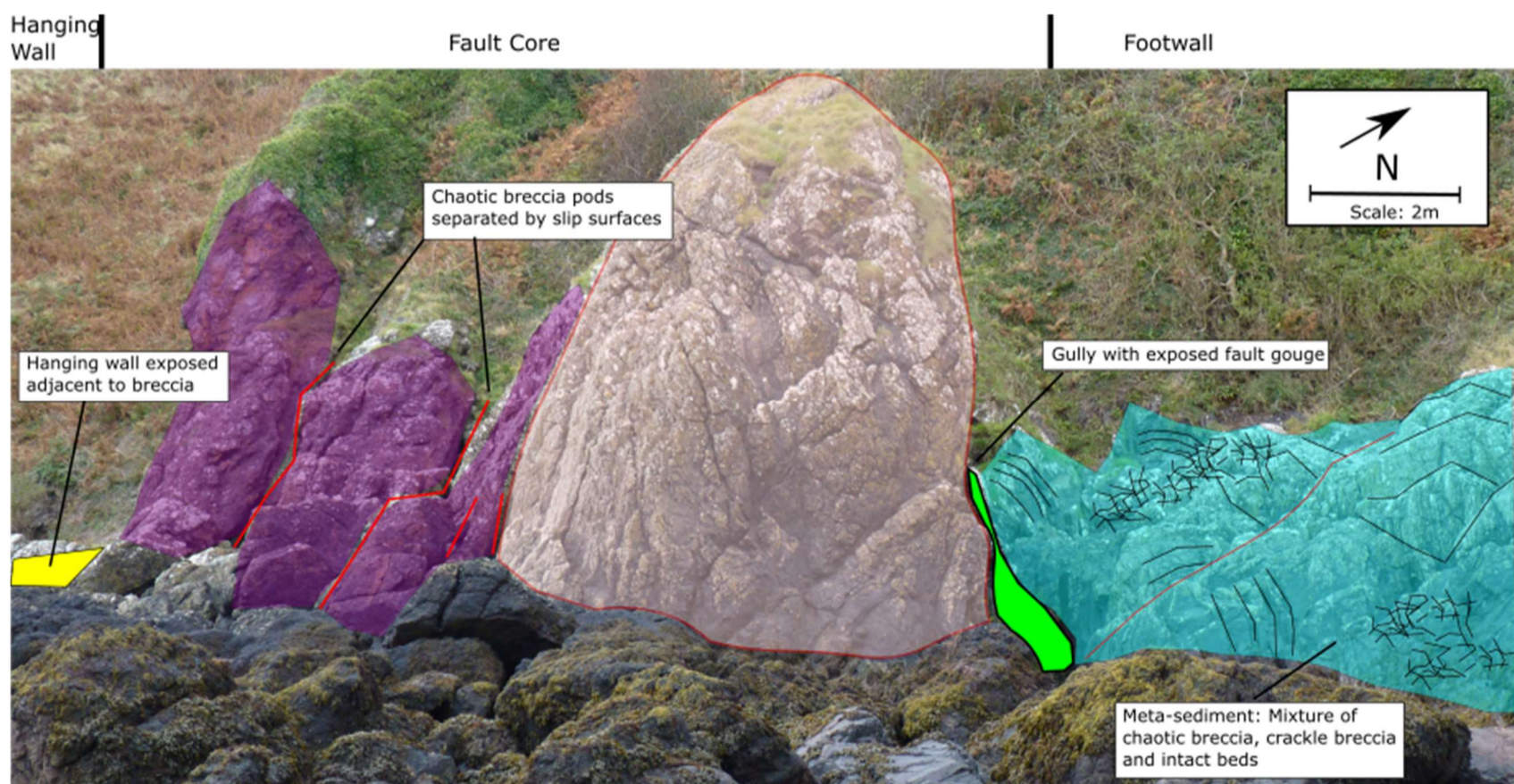


Figure 4-11 Cross-sectional view of the fault zone at Door of the Heugh. Photograph taken oblique to the main fault strike, main fault units digitised over the photograph. The key follows Table 1 and Figure 4-9.

On the footwall side of the breccia pods there is a large body of granitic breccia, consisting of chaotic and crackle/mosaic textures. This breccia body does not display the same degree of brecciation as the adjacent pods and contains no metasedimentary clasts.

A narrow "fault gully" (1m wide) is exposed between tectonic breccia and the footwall. At the base of the gully is an elongate gouge layer which is mostly obscured by algae, except for a few small patches which allowed occasional access to the gouge. The gouge will be described in detail in a separate section (Section 4.9) along with that seen at Portling Bay

The footwall at Door of the Heugh is predominantly composed of fractured, folded and faulted meta-sediments. An area of relatively intact meta-sediment beds are tilted to sub-vertical and cut by a single well-defined fault, which trends approximately N-S. The beds are offset by approximately 0.8m of apparent sinistral strike-slip. Immediately to the west of the relatively intact bed is a 1m² patch of slickenlines on a sub-vertical E-W face with trend and plunge of 18°/090°, which also suggests strike-slip movement at this location. However, there are no indicators of shear sense along this surface. It's therefore not possible to say if these are a pair of conjugate faults consistent with slip in a single stress regime or if they are formed from two independent events.

The exposures of footwall and fault rock at Door of the Heugh were only accessible during a few hours either side of low tide.

To the east of Door of the Heugh a high cliff face (>20m) comprises meta-sediments with rare granitic intrusions. These exposures were inaccessible due to the high cliffs and extreme tidal range.

4.6.2 Castlehill Point to Lagmuck Sands

The exposures east of Castlehill Point include a footwall predominantly composed of granitic intrusions with only occasional isolated exposures of meta-sediments. Both lithologies are highly fractured; granitic rocks have a fracture spacing of less than 100mm and the meta-sediments typically have a fracture spacing of less than 30mm. Castlehill point is a prominent headland which displays partially obscured breccias and footwall lithologies. A large cross fault immediately to the east of Castlehill point displays multiple shear surfaces in granitic footwall rocks (see **Figure 4-2**). Small subsidiary faults running parallel to the main NSF intersect the cross fault and contain small amounts of breccia (up to 30mm thick). Multiple shear surfaces are evident at every exposure of the footwall but it is not possible to tell the relative timing of these surfaces. The irregular surface of the cross fault makes it difficult to interpret the relative timing of these surfaces as it is not clear if these smaller slip surfaces are truncated by the large fault or if they offset the larger fault surface

To the west of Castlehill Point, hanging wall exposures of interbedded sandstones and conglomerates are steepened near the fault zone. In some areas the sedimentary rocks onlap the cliff face and are therefore interpreted to unconformably overly the footwall.

Figure 4-12 shows the detailed map at Lagmuck Sands and the corresponding cross section is shown in **Figure 4-13**. The hanging wall outcrops shown in the detailed map are weathered, have been rounded by wave action and show little structure. The location of these in close proximity to the footwall constrains the width of the fault zone to approximately 2m on the right hand side of the map and at least 8m on the left hand side of the map.

Chaotic mixed clast lithology breccias make up the majority of the fault zone.

Crackle/mosaic breccias are predominantly within the fault scarp with the exception of one large (approximately 4m across) body of granitic crackle breccia which grades into the chaotic breccia. Chaotic breccia, which is immediately adjacent to the fault zone and displays little or no textural fabric, is strong to extremely strong (engineering terminology - BS 14689-1). The chaotic breccia is often arranged in pods similar to Door of the Heugh but the pods are defined by fractures which show no evidence of offset.

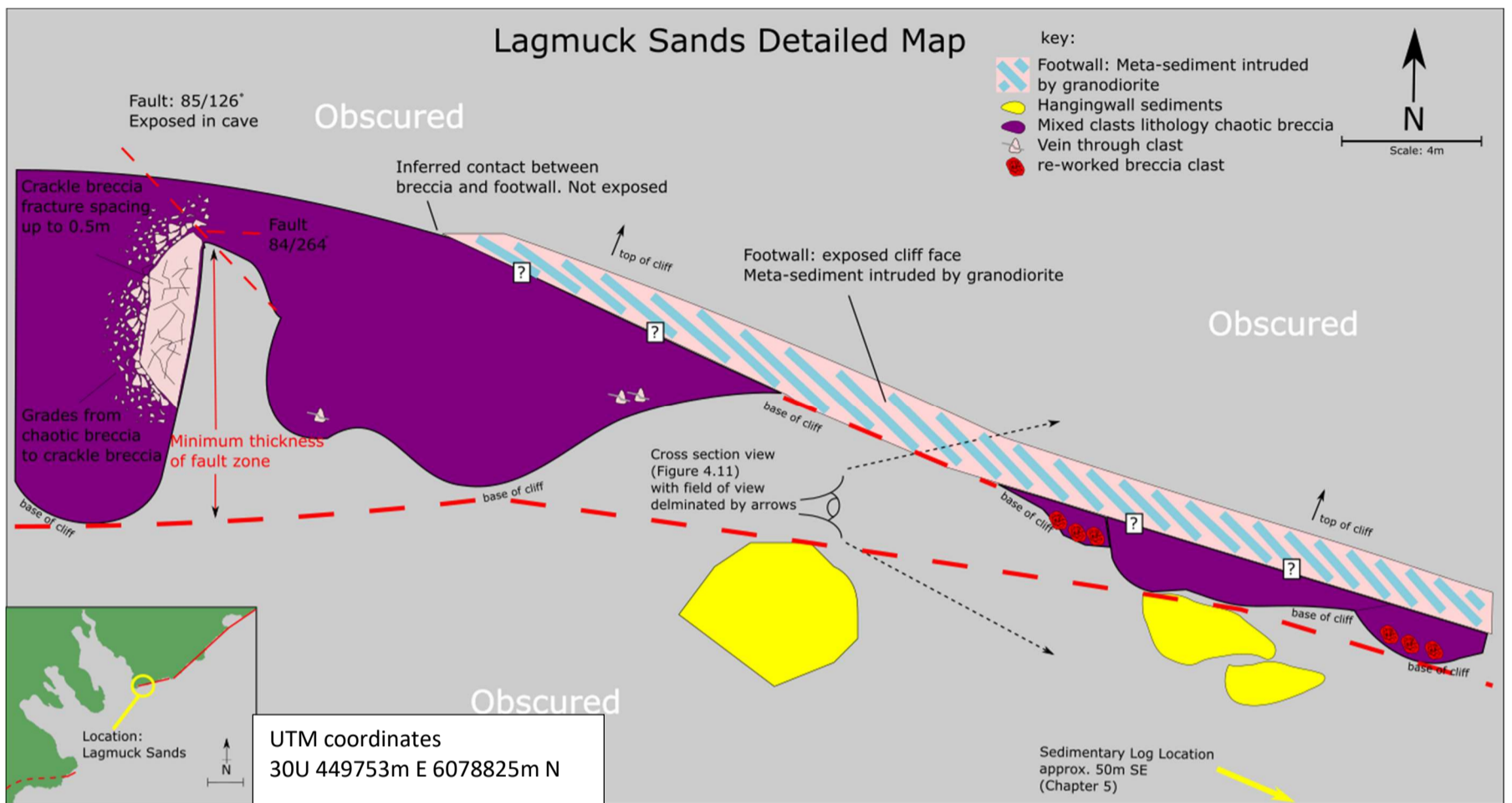


Figure 4-12 Detailed map of Lagmuck Sands. The footwall has been mapped as a single unit as distinguishing between lithologies became impractical due to frequent changes in lithology in plan view. The field of view for the cross section in Figure 4-11 is shown in the centre of the map. The location for a sedimentary log described in Section 5.1 is shown.

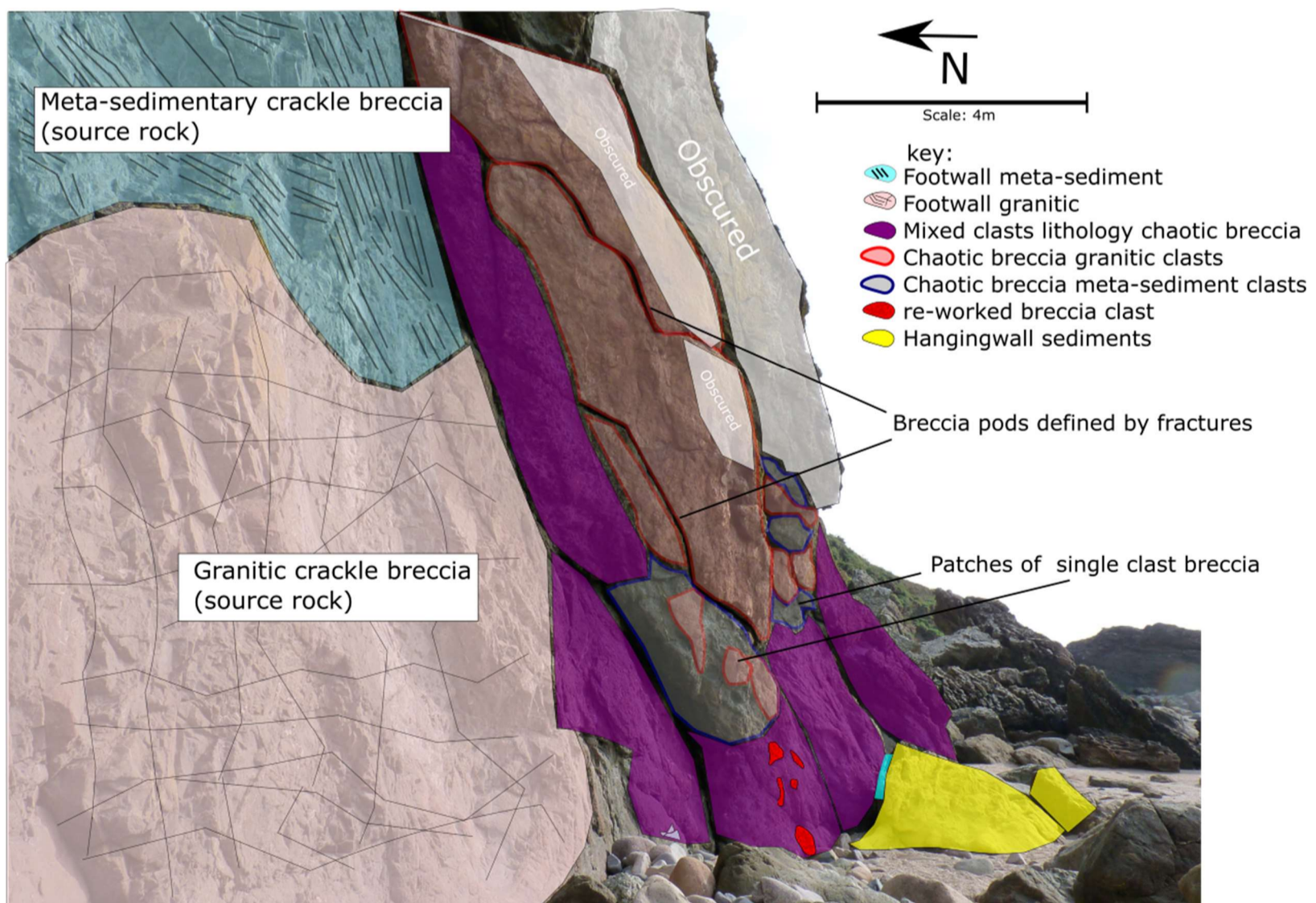


Figure 4-13 Cross section view of area shown in Figure 4-10. Photograph taken roughly fault parallel

Figure 4-13 shows mixed clast lithology breccia adjacent to footwall of a single lithology, suggesting that breccia clasts must travel through the fault zone in order to mix. There are also patches of single clast lithology breccias which suggest that clast mixing does not occur throughout the entire breccia body. Two other textures observed in the breccias will be discussed in detail in later sections; reworked breccia clasts (Section 4.8.2) and veins passing from surrounding matrix through clasts (Section 5.4.4).

4.6.3 East of Lagmuck Sands to Bells Isle

East of Lagmuck Sands the fault zone is obscured and hanging wall sediments of interbedded conglomerates and sandstones outcrop between large boulders containing similar coarse-grained sedimentary textures.

At Gutcher's Isle, detailed baseline mapping of the exposed fault elements was carried out and is shown in Figure 4-14 and Figure 4-15. The footwall is exposed in an irregular cliff up to 5m in height and has a mixture of granitic and meta-sedimentary lithologies. The footwall is cut by two steeply dipping slip surfaces; one at high angles to the main fault trace and the other oblique to the main fault trace. There are patches of chaotic granitic breccia within the footwall. The footwall is only exposed along a few metres of strike and is obscured elsewhere in the area by chaotic breccias, which also form a small cliff at the seaward edge. Chaotic breccias are present in large volumes (several m³) but are not arranged in pods. The breccia is arranged in a blocky geometry on the western side of Figure 4-15 defined by orthogonal fractures. On the eastern side of Figure 4-14 and shown on the cross sectional annotated photo in Figure 4-15 the fracture pattern is chaotic and the breccias are not in pods or blocks.

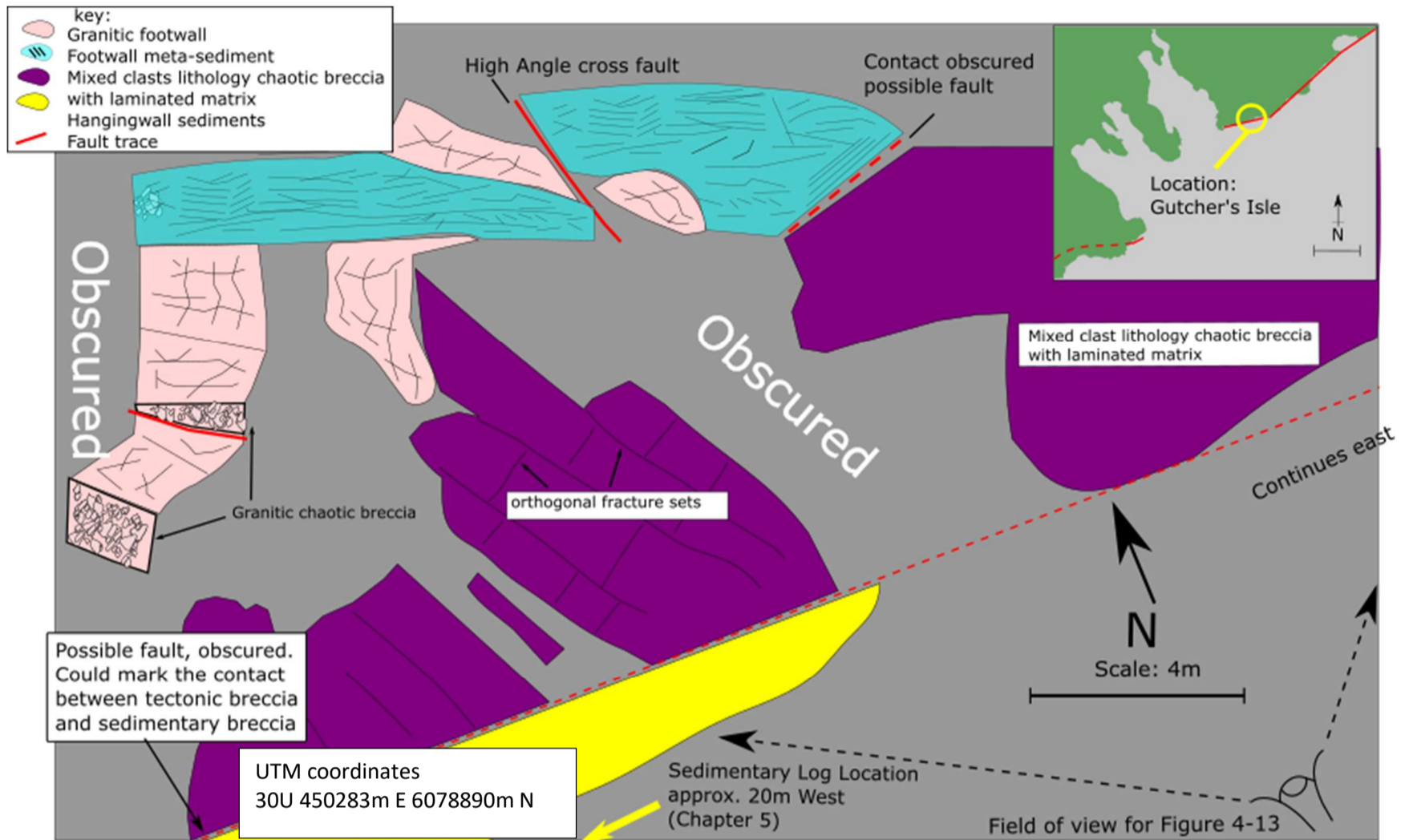


Figure 4-14 Detailed map of Gutcher's Isle. Much of the area is obscured by sand, boulders and vegetation. Location of sedimentary log is shown and described in Section 5.1.

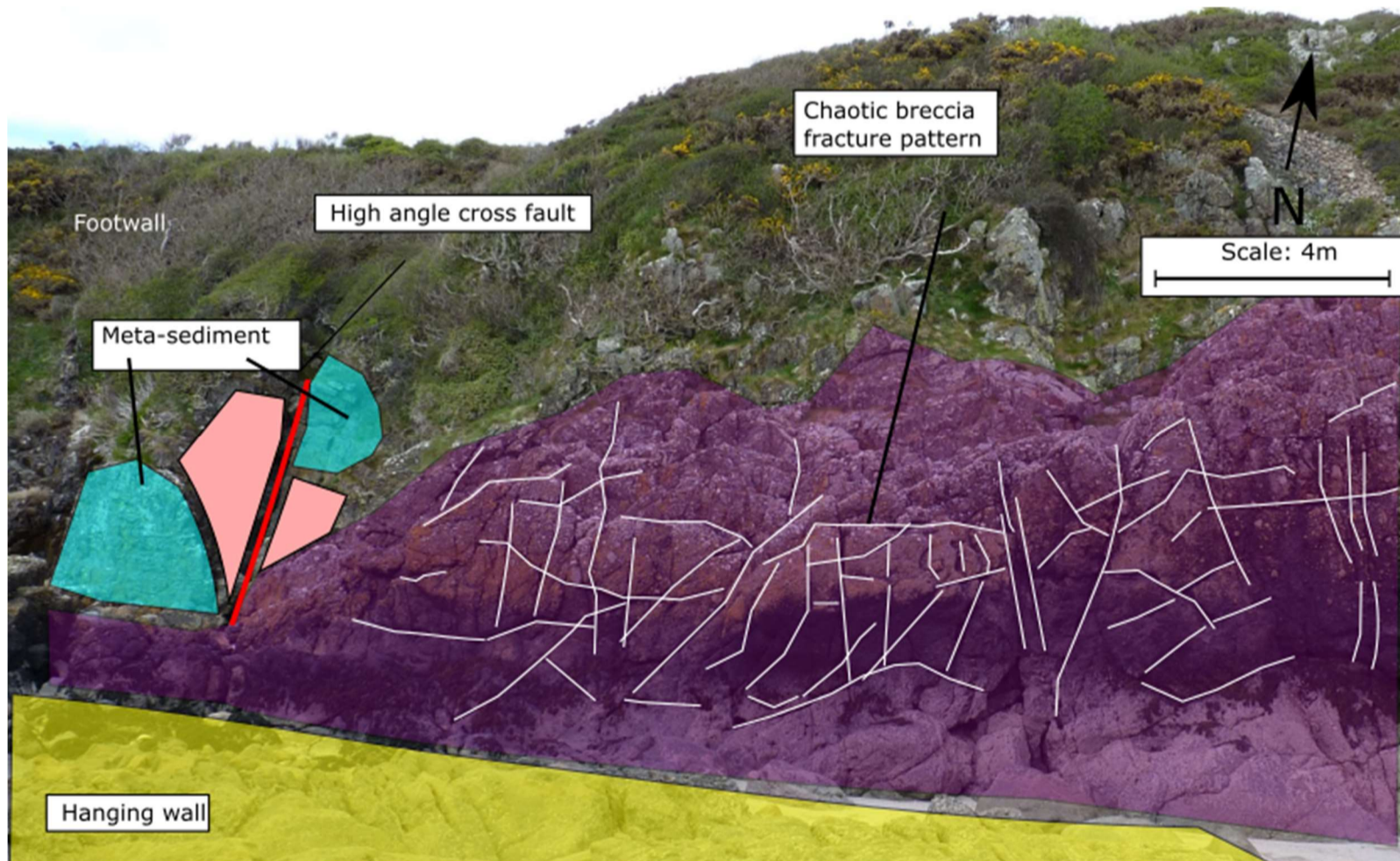


Figure 4-15 Cross Section view of Gutcher's Isle. Photograph is taken roughly perpendicular to the fault.

Crackle and mosaic breccia is exposed on the landward side of the chaotic breccia. Cutting both the chaotic breccia and the crackle/mosaic breccia is a fine grained fill with laminations. This will be described in detail in Section 4.8.3.1.

The hanging wall units crop out as isolated outliers of thick conglomerate beds dipping roughly basinward at 12° - 33°.

East of Gutcher's Isle towards Bell's Isle, the high cliff fault scarp and hanging wall exposures are absent. A mixture of faulted, fractured and veined footwall lithologies provide an undulating terrain which displays a number of cross faults and spectacular folds. At Bell's Isle, sheared footwall lithologies protrude basinwards and the partially obscured chaotic breccia suggests the southern edge of this headland has been subjected to significant faulting.

4.6.4 Bell's Isle to Sandyhills

Exposures of the main fault trace at this section are of a different character to other sections of the North Solway fault. A large cliff is composed of hornfels greywacke which appear to be largely intact with little or no brecciation present. In many places where the meta-sediments are intruded by granitic dykes, the cliff protrudes basinwards and these prominent features display brecciated, veined and discoloured fault rocks. The dykes strike roughly E-W and NW –SE and are in many cases offset by N-S and NW-SE trending cross faults. The resulting exposures contain small coves where meta-sediments are exposed at the base of high cliffs and small headlands where there is evidence of brecciation in the granitic rocks. The headlands appear to be more brecciated than the coves.

Between Port O Warren and Portling Bay, exposures of hanging wall sediments are composed of conglomeratic sandstones which fine upwards into grey siltstone, mudstone and limestone.

At Portling Bay, detailed baseline mapping was carried out and Figure 4-16(a) shows the resulting map and interpretive section. The SW edge of the map shows discontinuous sandstone beds which are adjacent to blocky sandstone. Closer towards the fault, the sandstone beds appear to grade into, and are entrained within, a fine-grained matrix. The sandstone is strong (BS14689-1), medium to fine-grained with a yellowish hue. This contrasts with the fine-grained matrix which is dark blueish grey and is typically weak. The sandstone is increasingly fragmented towards the fault and becomes isolated lenses entirely surrounded by matrix.

The lenses give way to large rounded boulders (Typically 2m across but up to approximately 5m) of coarse blueish grey sandstone (green on Figure 4-16(a)) which are also embedded in a dark blueish grey matrix. These boulders have the appearance of large survivor clasts within gouge (as described in Section 2.8). To the NE of the initial rounded boulders in matrix, the outcrop is obscured for c.10m by tidal sediments (approximately the centre of Figure 4-16(a)). Continuing to the NE the rounded sandstone boulders outcrop again but the matrix is obscured. The composition of the large survivor clasts changes to brecciated footwall lithologies and brecciated, rounded quartz (approx. 1m across). There are some rounded sandstone survivor clasts (between 0.2m and 5m) adjacent to rounded survivor grains of footwall lithology and some appear to be breaking down into the matrix as shown in **Figure 4-16(b)**. The survivor clasts are generally smaller (typically 0.5m across but up to 1.5m) closer to the fault.

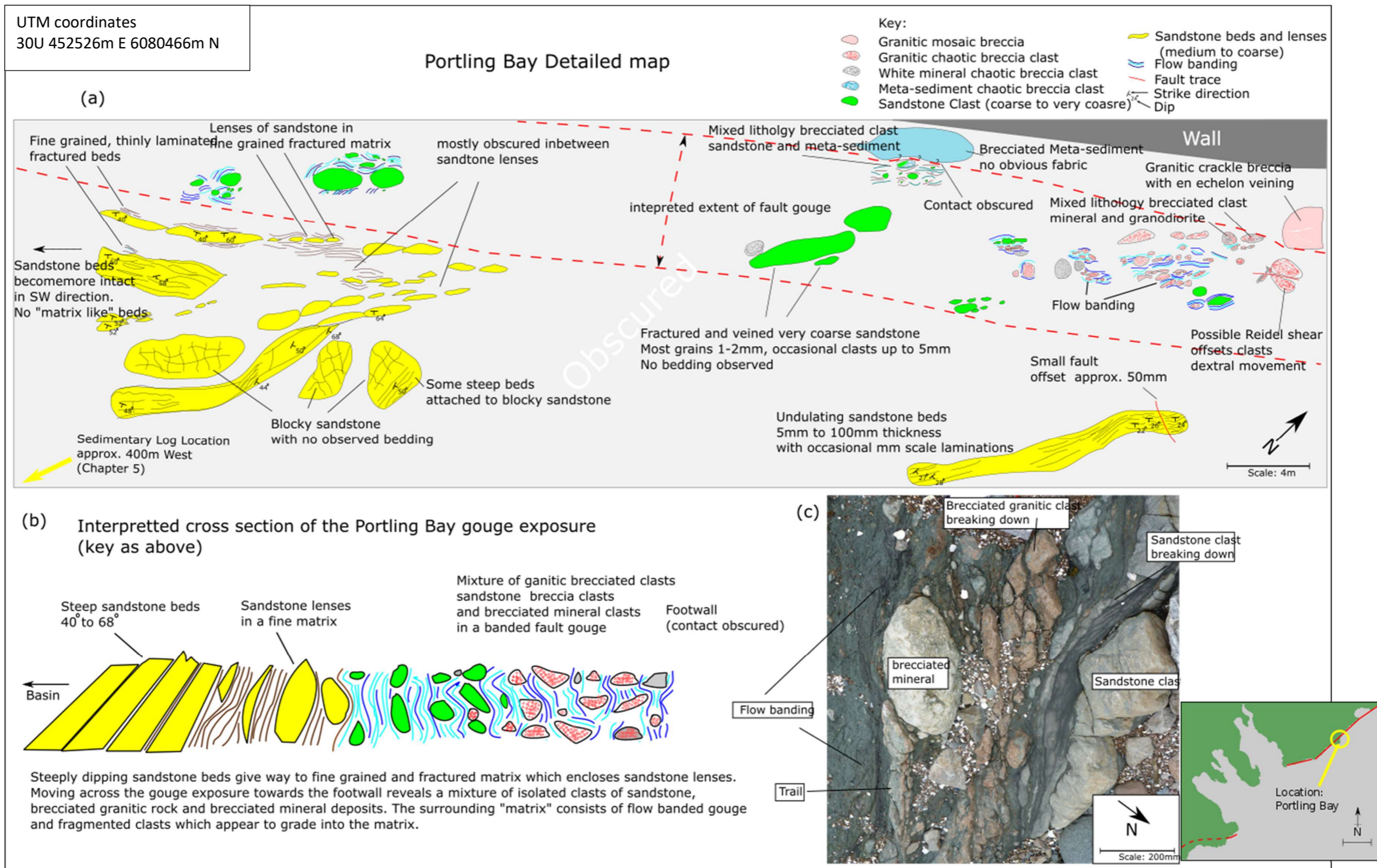


Figure 4-16 Portling Bay detailed map (a) map of gouge exposure. (b) interpreted cross section, and (c) photo of typical exposure showing clasts. The location for a sedimentary log is shown and is described in Section 5.1.

Figure 4-16(b) shows an interpreted cross section of the Portling Bay location. The section shows the gradational change from sandstone beds to isolated lenses and survivor grains before grading into survivor grains of breccia. The significance of this geometry is discussed in Section 6.2.6. The whole area has been interpreted as a large (>10m width) flat-lying exposure of gouge and around 20% of the gouge volume is survivor clasts. The textures observed during the detailed mapping are described in comparison to the gouge at Door of the Heugh in Section 4.9.

4.6.5 East of Sandyhills

During the field work carried out for the present study, numerous attempts were made to access outcrops east of Sandyhills. Extremely soft underfoot conditions made walking along this section dangerous. According to Lintern and Floyd (2000) and Miller and Taylor (1966), there are exposures of conglomerates and sandstones which are downthrown against Silurian basement intruded by porphyritic microdiorite. Brecciated rocks are exposed in cliffs and protruding from tidal flats (Lintern and Floyd 2000). Three cored boreholes were sited on tidal flats adjacent to the fault zone and are described below in Section 4.7.

4.7 Evidence for the geometry of the main fault trace

After mapping the locations of basic fault elements, the main fault location can be constrained at different segments along fault strike. In some sections, either the hanging wall sediments or the footwall host rocks are not exposed and so constraining the exact location of the main fault is not possible. However, there are a number of locations that the main fault trace can be tightly constrained by mapping the locations of footwall, hanging wall and fault rock exposures.

At Rascarrel Bay to Door of the Heugh, the footwall and fault rocks are not exposed. Some inland exposures of footwall lithologies coupled with the hanging wall exposures constrain the main fault trace location to within a few tens of metres. This is also the case at other sections of the site; Lagmuck Sands to Gutcher's Isle and Port O Warren to Portling Bay. At the Door of the Heugh, the location of the main fault trace is interpreted to lie where the fault gouge and chaotic breccia pods are exposed. From Castlehill point to Lagmuck sands and at Gutcher's Isle, the main fault trace is also located by the presence of all three main components of the fault zone (footwall, hanging wall and fault rocks).

The precise location of the fault between Door of the Heugh and Castlehill Point is obscured by modern tidal sediments c. 4.5km. There are faulted footwall rocks present on Hestan Island and the peninsula to the north of the island which may reflect either cross faults or the main fault trace. The prominent headlands at Castlehill Point and Bell's Isle are at locations where the main fault trace can be reasonably inferred to change location or orientation significantly. Exposures of fault rocks at both these locations are largely obscured by black algae and limpets. However, the position of Castlehill point protruding into the basin, the adjacent cross fault and the inferred trend of the main fault trace to the east, suggests the cross faults offset the main fault trace and could also affect the orientation of the main fault.

Moving east from Gutcher's Isle, there are no hanging wall exposures for c. 2km until Port O Warren. At Port O Warren and at Portling Bay, the main fault trace can be located accurately by mapping the exposures of footwall, hanging wall and gouge. East of Portling Bay to Sandyhills the main fault trace is defined by footwall and fault rocks only. As described in Section 4.6.4, the headlands which jut out basin-ward are more brecciated

than the coves. This suggests that the main fault trace is slightly south to SW of the cliff exposures and is possibly offset by the cross faults (Miller and Taylor 1966).

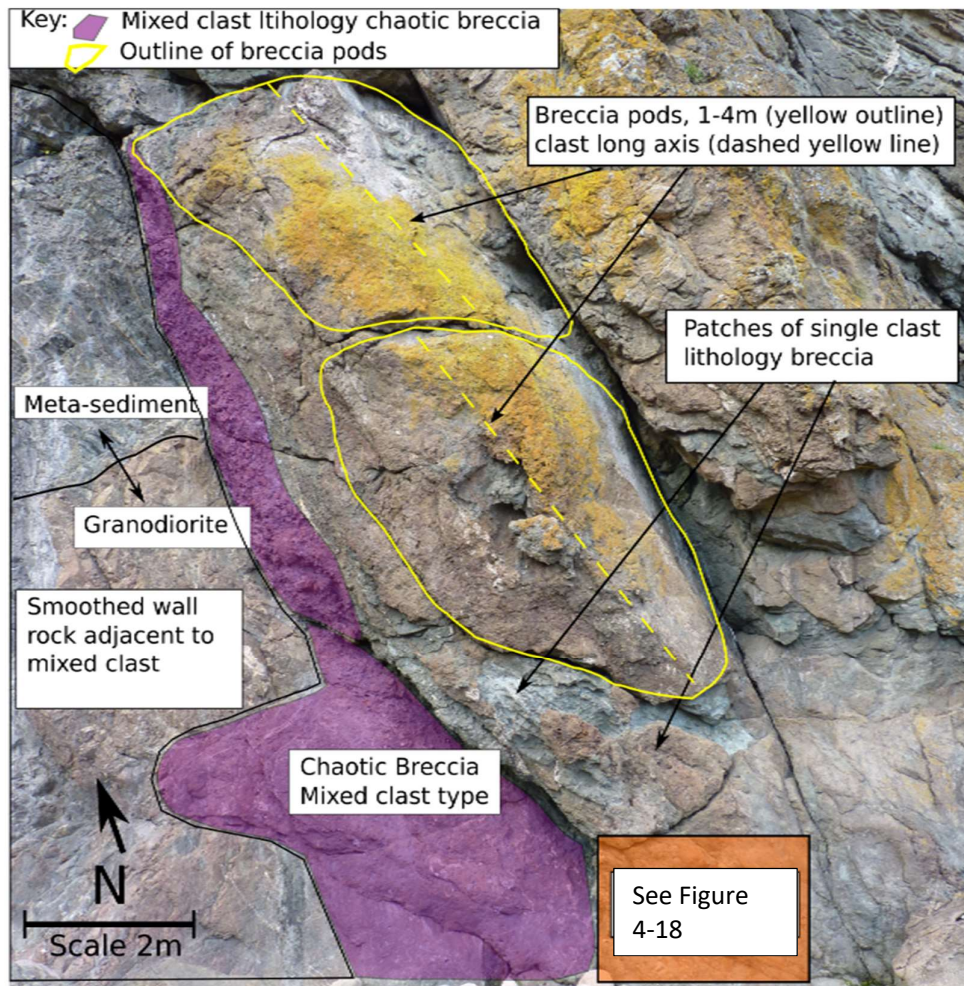
East of Sandyhills Bay, 3 boreholes were drilled pre-1966 (exact dates unknown). These boreholes pass through hanging wall strata of siltstone, sandstone and shales and intersect granitic and greywacke footwall lithologies. The locations of these boreholes are provided in 8 figure grid references, which only narrow locations to 10m squares, so the exact locations are unknown. However, the locations are accurate enough to infer that the fault has a relatively uniform strike to the east of Sandyhills Bay. Miller and Taylor (1966) used these logs to interpret a shear zone dipping at 50°.

The results of mapping show that the main fault trace is segmented and variably trends ENE- WSW and NE –SW (Figure 4-1). Segments which strike roughly NE-SW are found between Rascarrel Bay to Door of the Heugh and at Castlehill Point to Gutcher’s Isle. From Gutcher’s Isle to the NE the fault zone is clearly identifiable as striking NE-SW.

4.8 Tectonic Breccia

This section describes in detail the textures observed in the tectonic breccia at the North Solway fault.

Tectonic breccia is observed at several locations along on the North Solway fault. Where large volumes of tectonic breccia with a chaotic texture are present, the deposits are predominantly arranged in pod-like geometries. The breccia pods are well exposed at 2 locations; Door of the Heugh (Figure 4-10 and Figure 4-11) and Lagmuck Sands (Figure 4-12 and Figure 4-13, and Figure 4-17).



UTM coordinates
30U 449753m E 6078825m N

Figure 4-17 Breccia pods at Lagmuck Sands showing mixed clast lithology breccia adjacent to single lithology host rock. Breccia pods contain patches of single clast lithology breccia which appear to show little or no mixing of lithologies.

At both locations, the long axes of the pods vary from 2m to 4m and short axes vary from 1m to 2m and the axial ratios are fairly constant. The long axis of each pod is broadly

aligned down the dip of the fault and generally dips at high angles ($>70^\circ$). At Door of the Heugh, breccia pods are separated by slip surfaces where c.100mm wide zones of gouge form the contact between separate pods. At Lagmuck Sands, breccia pods are separated by fractures with no obvious evidence for shear displacement or gouge.

Breccias at Gutcher's Isle have a chaotic texture but are not arranged in similar pod-like structures. Chaotic breccias at this location are arranged in several block-like structures that are defined by fractures with a spacing of roughly 0.5m (Figure 4-14). This breccia could have originally formed as breccia pods that have subsequently been fractured or may have formed as something close to the present geometry. In other words, it is not clear if the variation in geometry of chaotic breccia could be caused by the formation process or by post-formation fault activity.

4.8.1 Along strike variability at the outcrop scale

The nature of the contact between breccias and footwall host rock is variable along strike. At Gutcher's Isle, some exposures show host rocks grading into tectonic breccias (decreasing fracture spacing and increasing fragmentation towards breccias), whereas in other exposures there is a sharp contact between host rocks and chaotic breccias. The contact between breccia pods and footwall host rocks at Lagmuck Sands is sharp. At Door of the Heugh a body of granitic clast breccia, which is a mixture of chaotic and crackle breccia, lies between the mixed lithology chaotic breccia pods and an exposure of gouge (Figure 4-10 and Figure 4-11).

Between Bell's Isle and Sandyhills, the only accessible exposures of chaotic breccia are smaller patches ($>2\text{m}^2$) that are surrounded by mosaic and crackle breccia textures. It is possible that chaotic breccias exist in the stretch of inaccessible fault zone east of Bell's Isle

(Figure 4-1) but from inspection at a distance with the naked eye (>30m), these exposures do not contain breccia pods.

The total width of chaotic breccia deposits varies along strike from c. 3m (Lagmuck Sands) to c. 15m (Door of the Heugh). The width of the chaotic breccia deposits at Lagmuck Sands varies within a few metres along strike from at least 8m to at least 3m, although the exact width is not always clear due to the contact with the footwall being obscured in places (see Figure 4-12).

Variation in the geometry of breccia deposits (width, structure and contact with host rock) could be evidence of deformation styles at the North Solway fault varying along strike. This will be discussed further in Chapter 6.

4.8.2 Re-worked breccias

Re-worked breccias refer to breccias which are observably subject to at least 2 distinctive phases of deformation. Phase 1 refers to the clasts in the original formation of breccia. Phase 2 refers to multiple phase 1 clasts that have behaved collectively as a distinct single clast in a later brecciation event.

Re-worked breccia clasts are observed at Lagmuck Sands and are restricted to a single pod of breccia. The re-worked breccia is composed of phase 1 granitic clasts which are identified by the contrasting texture with the surrounding breccia. Each phase 2 re-worked clast is very well rounded and they are lenticular to circular in shape with long axes roughly parallel to dip (Figure 4-18) similar to the long axes of the breccia pods. Striking the phase 2 breccia clasts and the surrounding breccia with a geological hammer reveals that both breccias have similar strengths of very strong to extremely strong (BS14689-1).

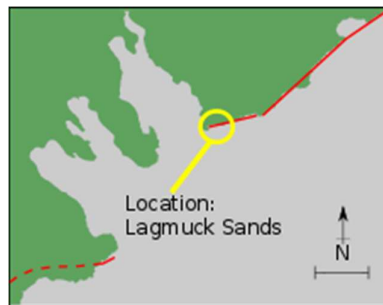
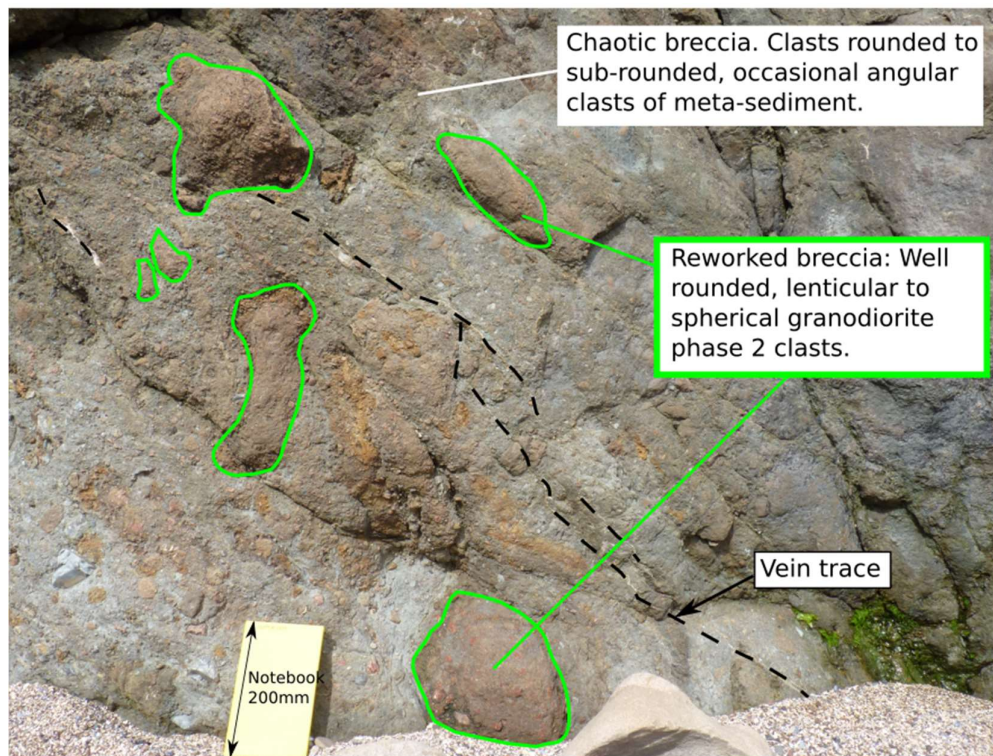


Figure 4-18 Re-worked breccia clasts at Lagmuck Sands

The shape of the phase 2 breccia clasts suggests that significant energy has caused rounding, possibly resulting from multiple deformation events that have abraded the clasts. An alternative explanation could be dissolved breccia, however there are no obvious solution boundaries. The possibility of intrusions into existing tectonic breccia is ruled out due to the matrix appearing granular. It should be noted that this conclusion is only based on observations made by eye in the field and not on detailed studies of thin sections. The contrast in texture between the re-worked clasts and the surrounding breccia suggests that

during the phase 2 brecciation, the phase 1 clasts have behaved as a cohesive unit with little interaction with the surrounding material (apart from attrition of re-worked phase 2 clast edges). The phase 2 breccias could have had different mechanical properties to the surrounding breccia. The cohesive strength of the phase 2 breccias may have come from cementation by fluids or by lithification through burial. The surrounding breccias could either have behaved as a granular (incohesive) material or have some cohesion but less cohesive strength than the re-worked clasts.

Alternatively, the re-worked breccia clasts could have formed by collapse of breccias into a fault void. Collapse into void space is described in Section 2.4.6. The void itself could be formed with cemented breccia on the walls. Cemented breccia could then fall into a fault void and come to rest in contact with breccia of contrasting composition. Subsequent re-working after this event could then cause rounding of the edges of the phase 2 fault void clasts.

4.8.3 Matrix

The matrix in tectonic breccias consists of broken down fragments of footwall lithologies. As described in section 2.7, a 2mm cut-off between grains and clasts follows the breccia classification system of Woodcock and Mort (2008). Objects with a long axis smaller than 2mm are classified as grains in the system and are therefore are part of the matrix. The matrix in almost all breccias shows little or no distinctive fabric with the exception of 2 locations described below

4.8.3.1 Laminated matrix

There are two locations (Lagmuck Sands and Gutcher's Isle) where there are laminations in the matrix. At Lagmuck Sands, two small exposures (up to c. 200mm across) of coarse to medium lithified sand grains show layers which are defined by contrasts in grain size (**Figure 4-19**). The laminated matrix is surrounded by breccia with no discernible fabric, similar to the rest of the chaotic breccia at Lagmuck Sands.

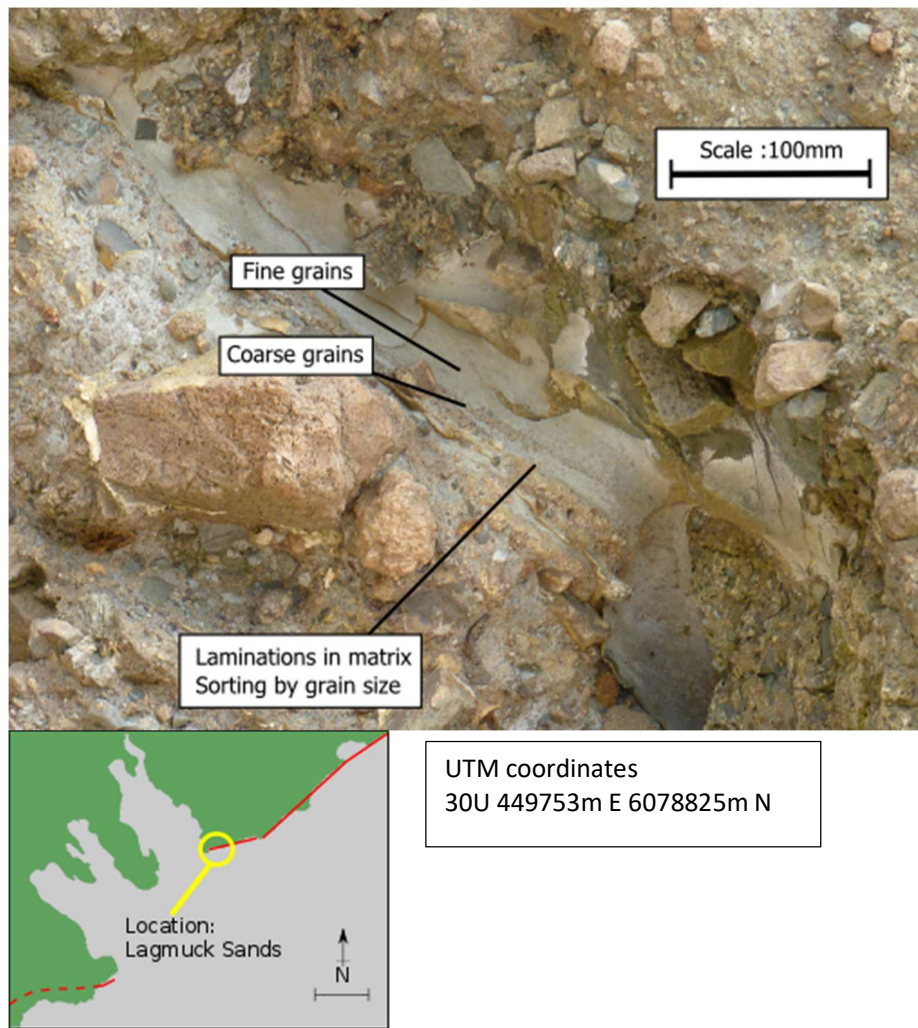


Figure 4-19 Laminated matrix in tectonic breccias at Lagmuck Sands. Note the tilting of the laminations which is towards the basin (dipping to the SW). The dip was estimate to be 20° by eye as the laminations are difficult to reach (above head height on the underside of a breccia pod).

At Gutcher's Isle, the laminated matrix contrasts with that found at Lagmuck Sands in a number of ways. The laminations at Gutcher's Isle are more common and the most abundant grain size is much smaller than at Lagmuck Sands (**Figure 4-20** and Figure 4-21). The laminated matrix at Gutcher's Isle contains rare granitic grains which, although typically less than 1mm across are still larger than the rest of the matrix.

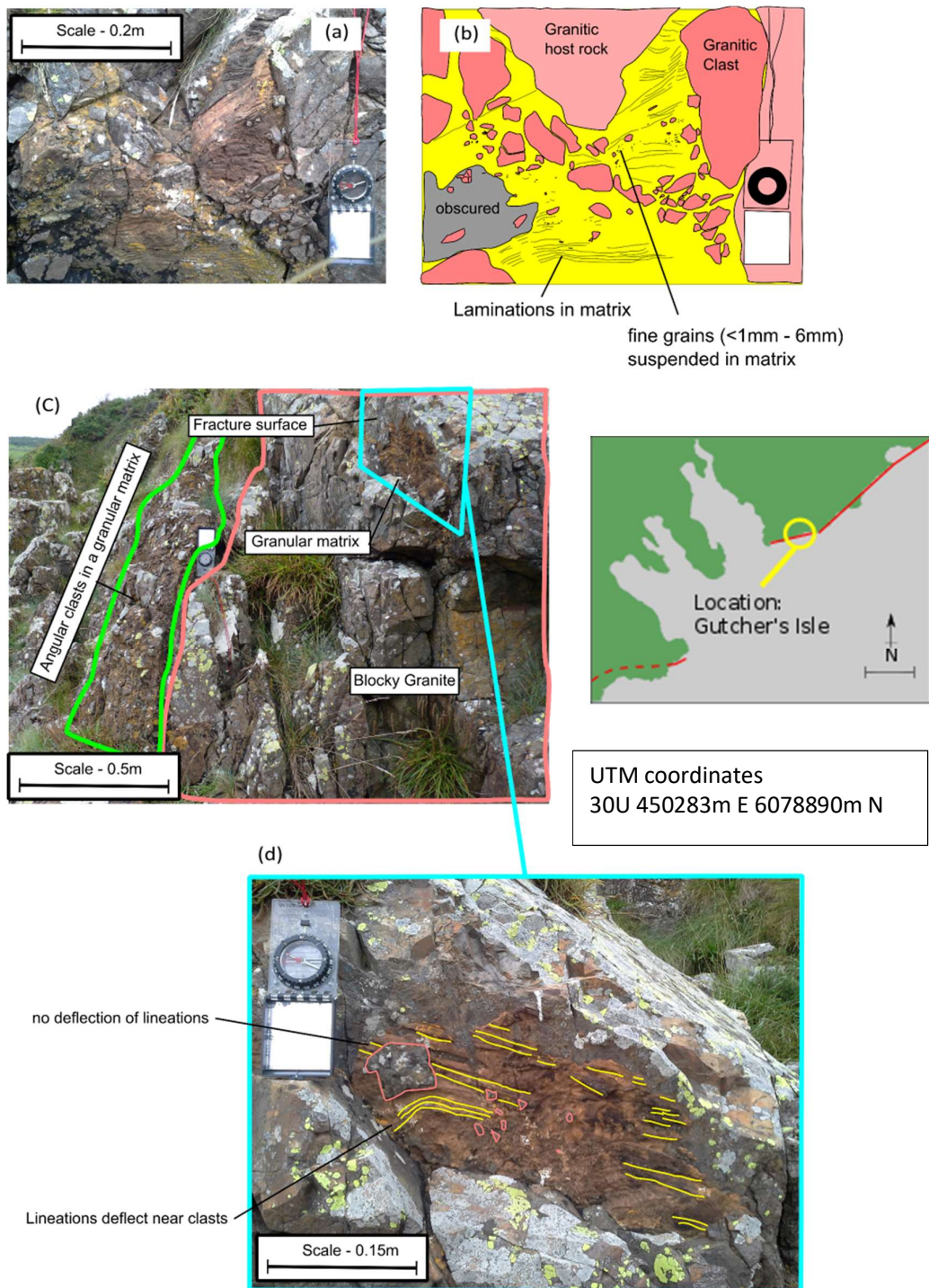


Figure 4-20 Laminations in matrix at Gutcher's Isle (a) field photograph and (b) digitised field sketch of the same exposure. (c) Photograph of exposure showing blocky, fractured granitic host rock with planar fractures. Fracture is filled with laminated granular matrix. (d) Close up of planar fracture with laminated granular matrix. Lineations either deflect near clast boundaries or remain in the same orientation adjacent to clasts.

The composition of the surrounding matrix is not possible to identify under optical microscope due to the small size of the grains. The matrix that fills planar fractures separating blocks of granitic footwall rock also contains laminations (Figure 4-20). This suggests that the fractures in the granitic footwall had significant aperture prior to deposition of the matrix. The matrix is distinct from the surrounding granitic rocks and suggests that either; matrix grains have travelled from remote host rocks and have been deposited at a later time than the fracture and brecciation of the granitic rocks, or that the matrix is composed of host rock subjected to processes of intense grain size reduction which has not affected the existing blocks of granitic rock. There is no evidence for shear of this matrix, such as shear fabrics, at the macro or (optical) microscopic scale.

At Gutcher's Isle, layers of fine grained matrix material (c. <0.1mm) are sorted by grain size. Coarse fragments (>0.1mm generally, as big as 1.5mm locally) of granitic lithologies are present in a few layers but not all. The laminations occur in cycles which coarsen upwards (**Figure 4-21**). Several fragments of granitic lithologies (c. 0.1mm-1.5mm) are deposited in isolated layers and are absent in adjacent layers, suggesting that several larger fragments are deposited in a short space of time, followed by periods where only finer grains are deposited. Some lineations deflect around clasts which may represent disturbance in the topographic consistency of layers caused by the introduction of coarser grains (c. 0.1mm – 1.5mm) into a very low strength fine grained matrix (<0.1mm).

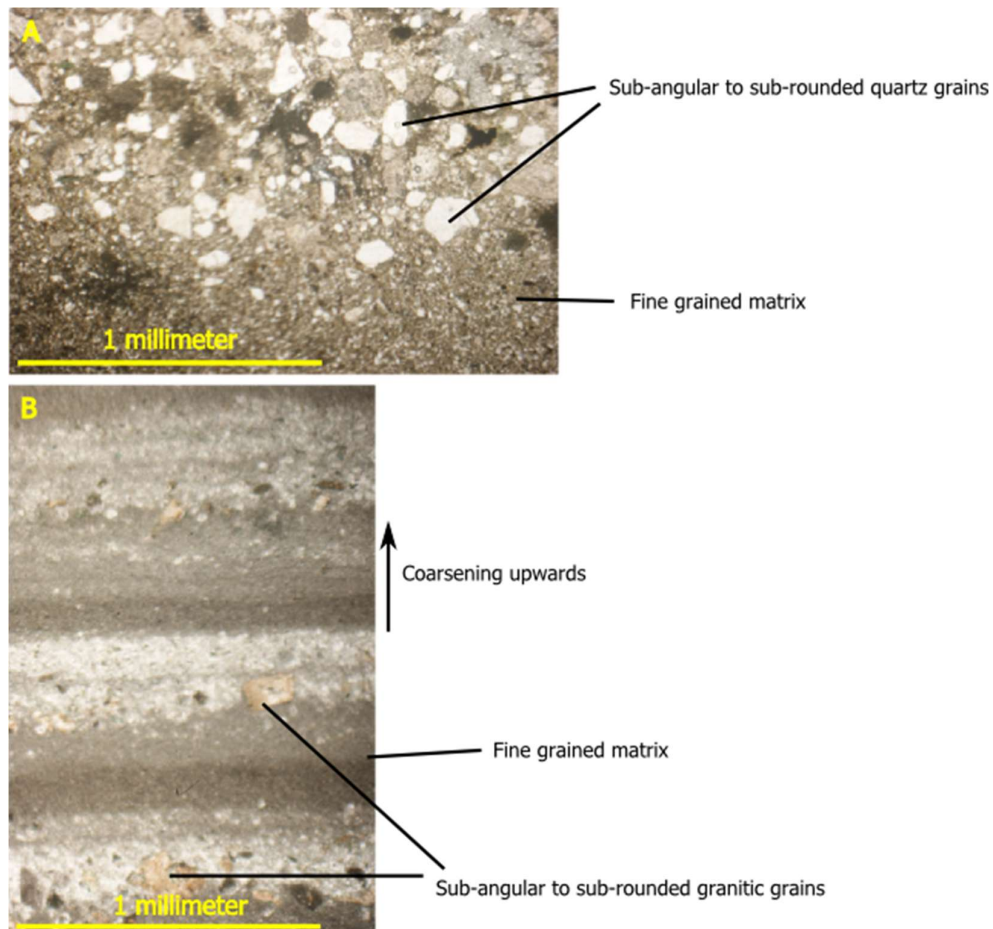


Figure 4-21 Thin Section photographs of laminations in breccia at A) Lagmuck Sands and B) Gutcher's Isle. Thin section in plane polarised light showing sub-angular to sub-rounded quartz grains in a fine grained matrix. Note the graded contact between layers of fine and coarse grained material. B) Thin section in plane polarized light showing grains with a granitic texture in a fine grained matrix. Section is approximately vertical and strikes NW-SE. Layers show coarsening upwards with a complete succession from coarse to fine grain size approximately 0.7mm thick. Transitions from coarse to fine grained layers are abrupt when compared with section A.

There are several possible mechanisms for the formation of laminations in granular material in and around fault zones as described in section 2.4.6. Laminations may have formed at the surface by sedimentation in open fractures (Wright et al 2009) or in sub-surface voids (Woodcock et al 2006; 2014; Walker et al 2011). Laminations may either be formed by gravity (i.e. during deposition) or by remobilisation and re-sedimentation of grains by fluidisation.

The coarsening upwards in the laminations at Gutcher's Isle are suggestive of dry mass movements in grain flow events as described in Bertran and Taxier (1999), rather than sedimentation by gravity processes from fluid saturated mass movements, which could be expected to produce a fining upwards texture (Jaeger et al 1996).

The laminations within the matrix at Lagmuck sands are coarser grained than at Gutcher's Isle. The coarsest layers in thin section are composed of sub-angular to sub-rounded quartz grains of approximately 0.1mm diameter, with the finer grained layers composed of sub-rounded to rounded quartz grains less than 0.1mm. The rounded grains and absence of angularity are interpreted as a mature sedimentary texture. The maturity of the grains precludes rapid sedimentation from the immediate vicinity and points to either significant transport, or significant re-working. The laminations described above and their possible sedimentary origin cast doubt on the interpretation of the breccias with laminated matrix as tectonic derived. Bedding has been described in tectonic settings by Wright et al (2009) and Woodcock et al (2006). Alternatively, the sedimentary matrix is a fill which is emplaced into the tectonic breccia at a later date. This is discussed in Section 6.2.4.

4.8.4 Summary of Tectonic Breccia

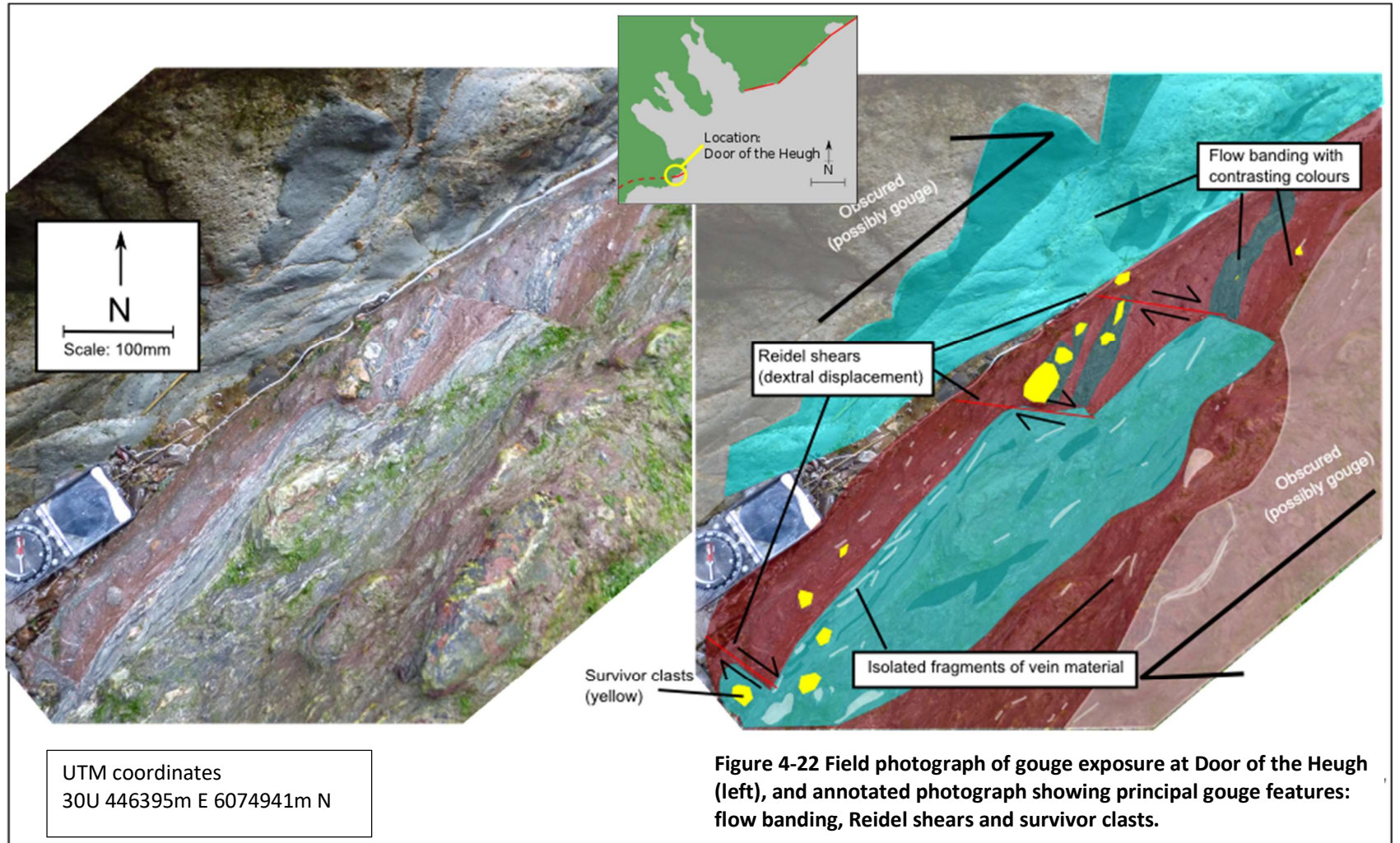
Breccia texture and geometry varies along fault strike, as does the contact between breccia and the fault walls. Tectonic breccias with a chaotic texture are found in pod-like and blocky geometries. Some pods are defined by fracture surfaces, others by thin slip surfaces. Tectonic breccias are predominantly footwall derived. Re-worked breccia textures (multi-phase breccias) were observed at Lagmuck Sands. There are two locations where laminations delineated by changes in grain size are found within breccias. The sedimentary textures are possibly emplaced later than the formation of the breccias.

4.9 Fault Gouge

There are two exposures of fault gouge along the main fault trace; Door of the Heugh and Portling Bay. Both exposures display several features common to fault gouges as described in section 2.8. The Door of the Heugh gouge is estimated to be c. 5m² in plan view, with less than 1m² exposed as most of the outcrop is covered by seaweed and algae. Survivor clasts within the Door of the Heugh gouge are well rounded, with the largest survivor clasts around 100mm diameter with c. 20 survivor grains around 10 – 20mm (Figure 4-22).

The Portling Bay exposure is much larger at around 400m² in plan view and much of the area is obscured by shell fragments and sand. The observations here are made from detailed mapping of exposures which were only available when the debris were removed by wave action. Attempts to clean areas of both outcrops were unsuccessful as fragments of gouge tended to be scraped off along with the debris, obscuring the texture of the gouge.

At Door of the Heugh, Reidel shears, trails and flow banding are interpreted as resulting from right lateral deformation (Figure 4-22). The pervasive Reidel shears and rounded survivor clasts suggest that the gouge is well developed. Such well-developed shear fabrics have been shown experimentally to develop at higher slip (Haines et al 2013). At Door of the Heugh the gouge is exposed between tectonic breccia and footwall, meaning the footwall is the likely source of the material that was entrained into the gouge. Contact between the units appears sharp although this contact is not well exposed.



At Portling Bay, clasts reach up to 5m in width and approximately 20 clasts are around 500mm. These clasts make up around 20% of the rock volume. All clasts are rounded suggesting that the clasts were abraded. Several clasts at Portling Bay show fracturing and the development of fragment trails which suggests that clasts were broken down and entrained into the gouge material (Figure 4-23).

Some survivor clasts are composed of brecciated quartz (see Figure 4-23) and reach up to 1.5m in diameter. The clasts are rounded and have a chaotic breccia texture. Large survivor clasts of brecciated quartz must have been quartz deposits which were at least as big as, and possibly much bigger than the current clast. This strongly suggests that mineralisation into large voids occurred at the NSF. There were no such large deposits found during the present study.

Offset along Reidel shears in the Portling Bay gouge shows right lateral deformation but within a few metres there are trails and flow banding that indicate left lateral deformation (Figure 4-23). The close proximity of contrasting strike slip component of shear could suggest a dip slip (normal) fault motion. This would mean that the dominant shear direction is not possible to observe from the near horizontal exposure and the observed shear directions are secondary or minor shears as described in section 2.8. The lack of observed dominant shearing direction could also signify that the gouge has not fully developed the pervasive Reidel shears and particle alignment which can be expected in well-developed gouge (Haines et al 2013). In other words, the dominant shearing direction is yet to be fully established across the entire gouge zone and deformation may be heterogeneous.

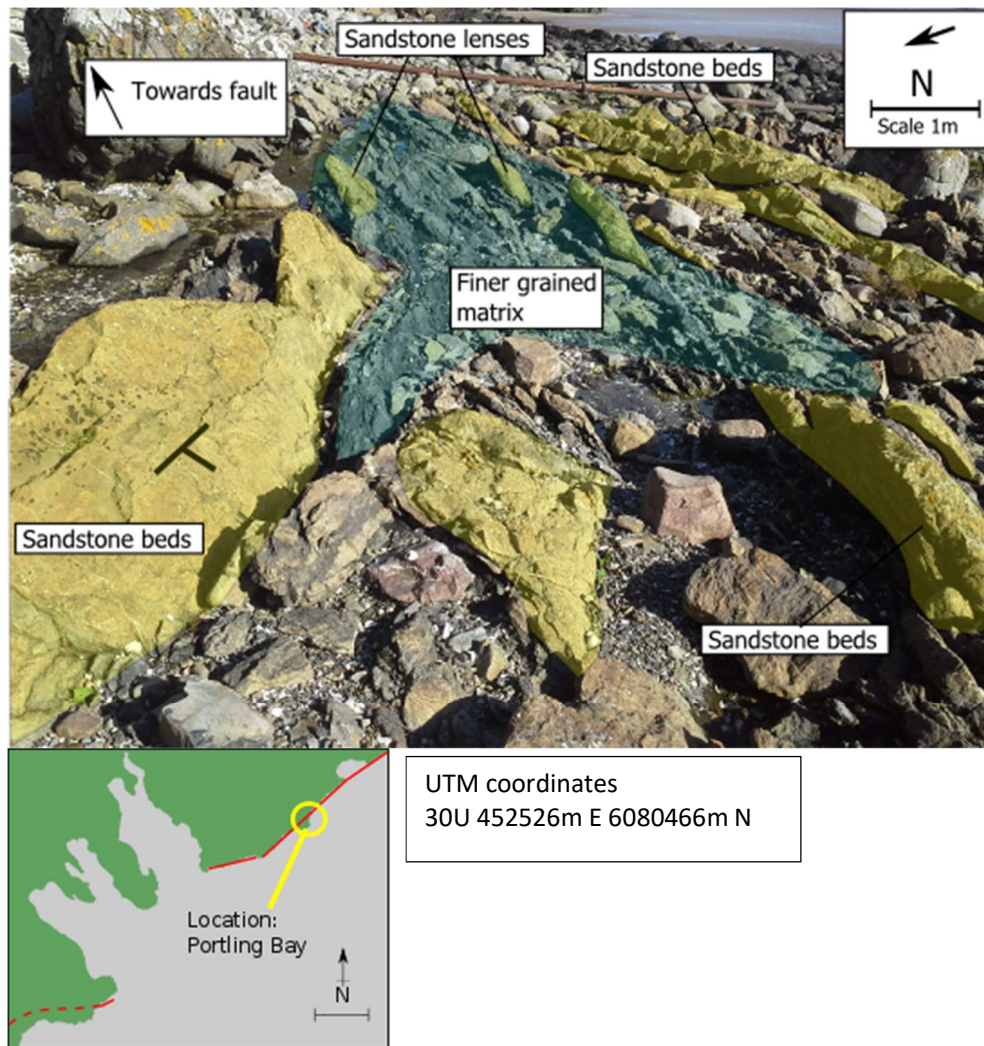


Figure 4-25 Sandstone beds adjacent to the gouge exposure at Portling Bay. Deformation of sandstone beds increases towards the fault (right to left). Sandstone beds become isolated lenses in a fine grained matrix closer to the fault zone.

4.9.1 Fault Gouge Summary

The gouge at Door of the Heugh and Portling Bay has some contrasting features. The position of the gouge within the fault zone is different at Door of the Heugh and Portling Bay. At Portling Bay, the gouge layer is adjacent to hanging wall exposures. Contact with either the footwall or fault rocks is obscured. The hanging wall appears to grade into the gouge layer, with steep sedimentary beds (40° - 60°) of fine to coarse sandstone interbedded with a finer thinly laminated deposit. The sandstone layers appear relatively

intact at the furthest edge away from the gouge layer passing to a more irregular bedding surface and eventually isolated sandstone lenses in a matrix of finer grained sediments (**Figure 4-25**). This suggests that the gouge at Portling bay is hanging wall-derived. The fine-grained matrix amongst relatively intact sandstone lenses could be interpreted as preferential deformation of fine grained facies derived from the hanging wall.

The features described above could be evidence of bed parallel extension resulting from tilting of a monocline. The Ferrill model was described in Section 2.11 and will be discussed further in Section 6.2.4.

5. Data from Multiple Sites at the North Solway Fault.

This chapter describes the detailed and quantitative work carried out to characterise the internal architectures of the North Solway fault (NSF). The chapter describes data collected at several locations along strike, augmenting the detailed mapping and descriptive work described in Chapter 4. Other studies are mentioned to provide context for the observations and will be expanded upon in the discussion (Chapter 6).

5.1 Hanging Wall

The following section describes the sedimentary succession in the hanging wall at the North Solway fault. The descriptions below are intended to build on previous Chapters by quantifying some notable characteristics of the hanging wall sediments.

5.1.1 Sedimentary Logs

Sedimentary logs have been carried out to quantify the grain size, facies variations and clast to matrix ratios for the hanging wall deposits at 4 locations; Door of the Heugh (location shown on Figure 4-10), Lagmuck Sands (location shown on Figure 4-12), Gutcher's Isle (location shown on Figure 4-14) and Portling Bay (location shown on Figure 4-16).

At Door of the Heugh the succession logged is a c. 17m succession of coarse sandstone, fine sandstone and conglomerates and is c.100m from the fault. **Figure 5-1** shows that the majority of the logged succession consists of coarse sandstone. Two conglomerate beds of subangular to angular and subangular to rounded clasts have a clast content of 80% and 90%. The largest clast size of 700mm is found in the conglomerate bed between c.8.6m – 10.3m. The coarse sandstones typically consist of 10 - 35% clasts with matrix of 2mm diameter. The largest clast in the coarse sandstone is 300mm in diameter. Beds of fine and

medium grained sandstone typically display laminations of between 3 and 20mm thickness.

Clasts are infrequent in these layers and the largest clast is 50mm in diameter.

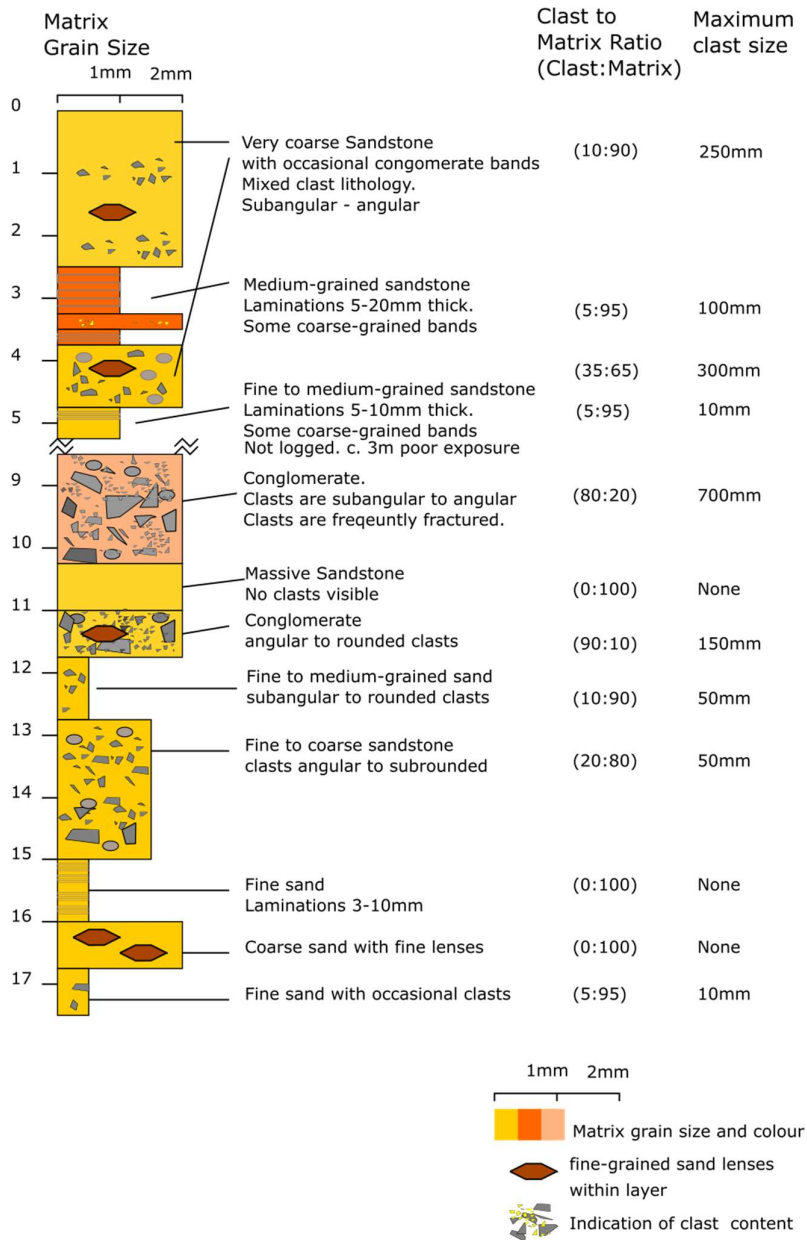


Figure 5-1 Sedimentary log for Door of the Heugh. Sediments c. 100m from the main fault.

At Lagmuck Sands, 4m of the hanging wall has been logged at c. 40m from the fault (**Figure 5-2**). At this location the succession is dominated by coarse sandstone with clast contents of 0 – 20%. The largest clast is 120mm in diameter. Coarse sandstone layers where the clast content is up to 10% contain lenses which are interbedded with laminated mudstones and fine sandstone. There are also lenses of fine sandstone within the coarse sandstone layers.

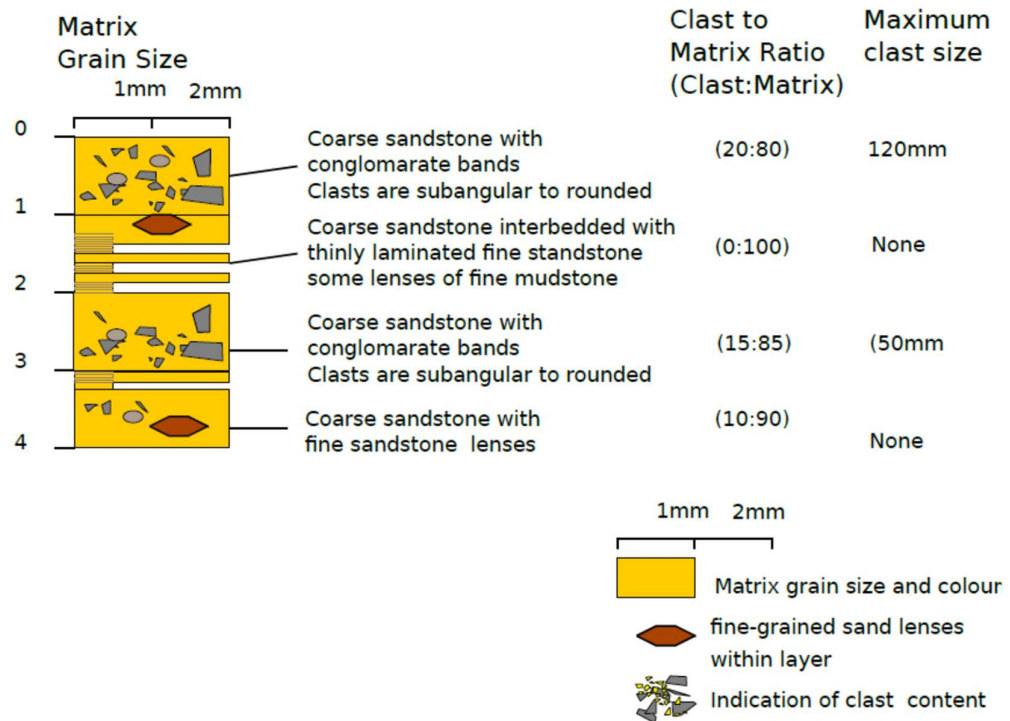


Figure 5-2 Sedimentary Log for Lagmuck Sands. Sediments c. 40m from the main fault.

At Gutcher's Isle a 7.2m interrupted succession was logged at c.20m from the fault (**Figure 5-3**). There are two sections of no exposure at around 2m and 3.8m apparent thickness along the log but these are estimated to make up less than 0.5m apparent thickness of the succession each. Most of the succession consists of coarse sandstone and conglomerate. Two thin beds of medium grained sandstone with low clast content (5-10%) have a maximum clast size of 40mm. Clasts typically make up 0 – 20% of the sandstone beds and

65 – 90% of the conglomerate beds. Clasts are subangular to rounded in both the sandstone and conglomerate beds with maximum clast size of 300mm in the sandstone and 400mm in the conglomerate beds.

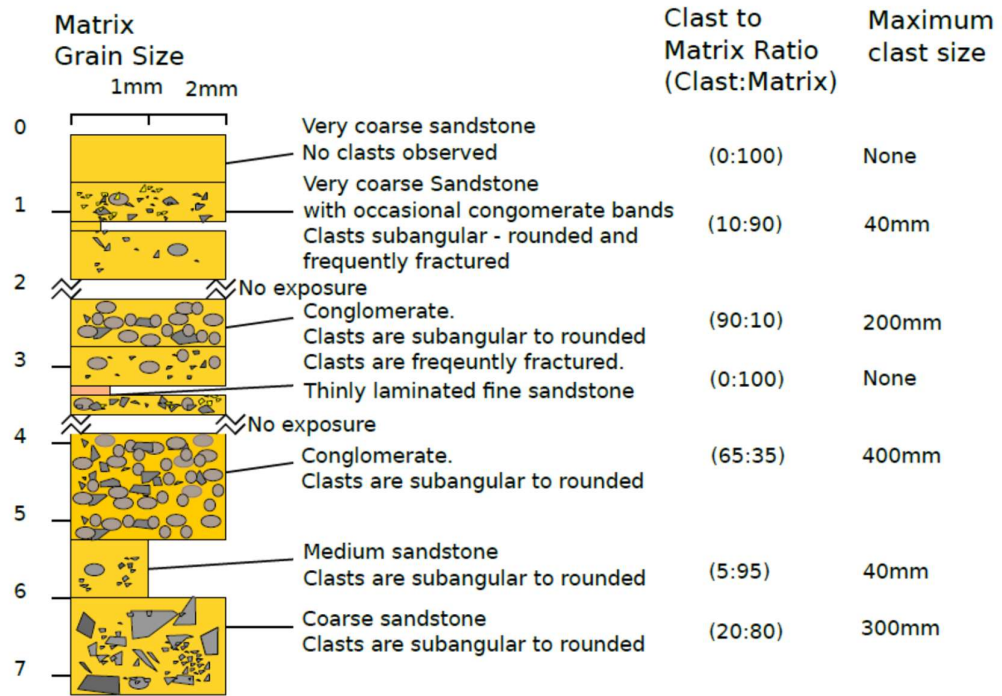


Figure 5-3 Sedimentary Log for Gutcher's Isle. Key is the same as that used for figures 5-1 and 5-2. Sediments c. 20m from the main fault.

At Portling Bay, 7.6m of the hanging wall was logged (**Figure 5-4**) and the textures here contrast with the other three sites. The succession logged is c.100m from the fault and is dominated by laminated mudstone and medium grained sandstone. Clast content is low, with most layers having no clasts and only two layers with 5% clasts. The largest clast size is 40mm. Irregular bedding surfaces are visible in a layer with laminated sandstone between 1.2m and 1.8m, these have been interpreted as ripple marks and are shown in **Figure 5-5** (b).

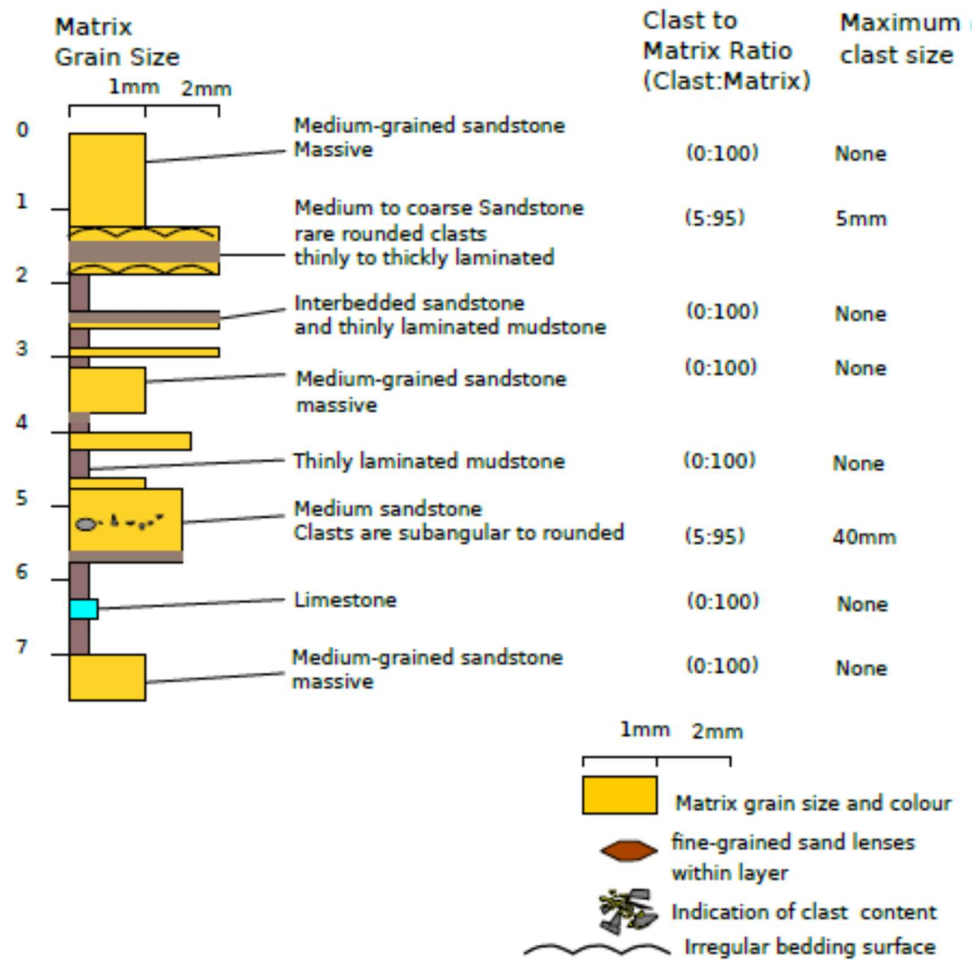


Figure 5-4 Sedimentary Log for Portling Bay. Key is in the bottom right corner of the figure. Sediments c. 100m from the main fault.

5.1.2 Fine-grained Hanging Wall Sediments

As described above, the sediments at Portling Bay are finer grained sandstones, siltstones and mudstones (Figure 5-5a) and contain almost no clasts. Symmetrical ripple marks were observed in fine sandstone at Portling Bay (Figure 5-5b) indicating the sediments were laid down in shallow sea or near-coastal environments.

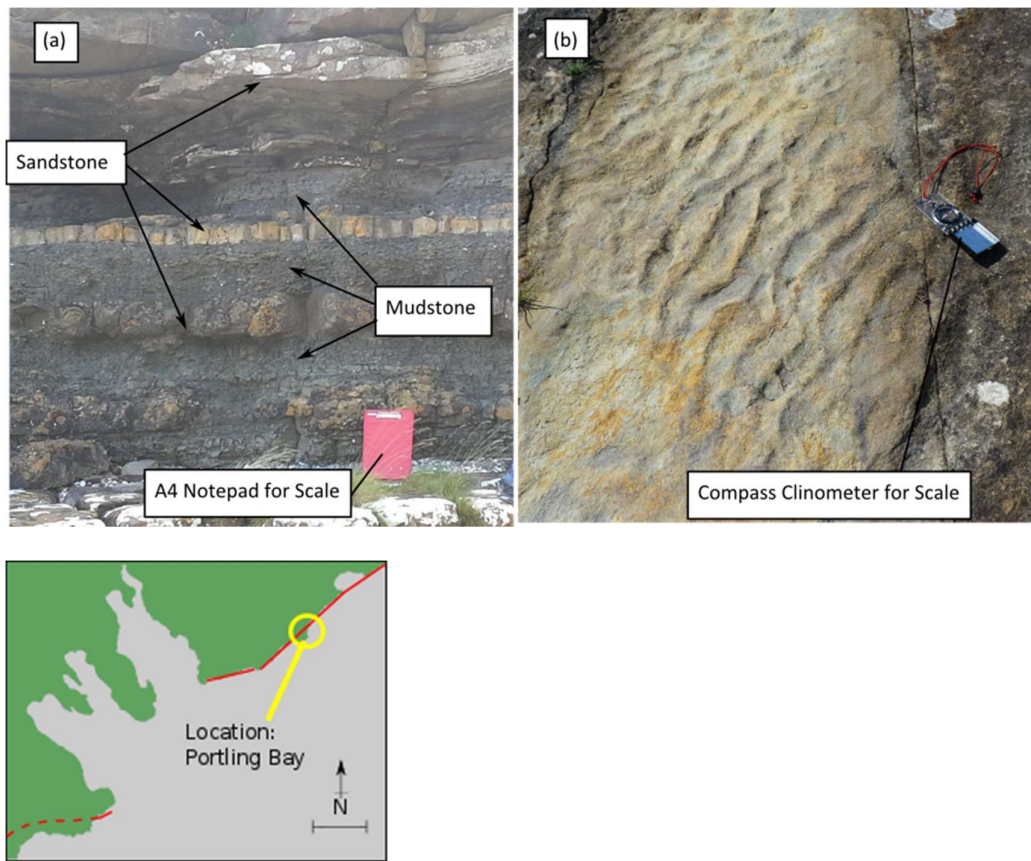


Figure 5-5 Sedimentary rocks at Portling Bay c. 100m from the NSF. The distance to the fault is estimated at this location based on a projected fault geometry from adjacent exposures because the fault scarp is obscured by vegetation. (a) Beds of mudstone and sandstone, and (b) ripple marks in the same location.

5.1.3 Summary of Hanging Wall Textures

Hanging wall sediments observed along the NSF are mostly coarse grained. Bed thicknesses vary from mm-scale laminations (fine sandstones and mudstones) to metre-scale boulder beds (conglomerates). Clast to matrix ratios vary within a few metres within the succession and also vary with location along the fault. As described in Chapter 4, sedimentary breccias near the main fault have poorly defined steep beds and are coarse grained. By contrast, basin sediments further from the main fault zone have well defined shallow dipping beds.

Sediments at Portling Bay are different to the rest of the field locations as they are composed of fine grained sediments with rare clasts.

5.2 Clast Lithology and Shape

Tectonic and sedimentary breccias have been compared in terms of outcrop scale features (Chapter 4 and Section 5.1) but the textures are difficult to quantify. In order to examine the textures of the sedimentary and tectonic breccia, methods have been employed to quantify; proportion of clasts and grains, shape and size of clasts, source lithology of clasts. Clasts were assessed using two methods described below for the tectonic breccias; clast count scanlines (Section 5.2.1) and image analysis. Sedimentary breccias were assessed using only clast count scanlines. Image analysis of sedimentary breccias was not carried out as a relative lack of clasts in the sedimentary breccias meant the number of clasts in each image taken would be very low (typically less than 10 per image).

Following the Woodcock and Mort (2008) classification of matrix and grains, a 2mm diameter was used as a cut off between clasts and matrix. The following results are then discussed in terms of proportions of “clasts” and “grains”.

Due to processes of grain size reduction, it could be expected that large volumes of entrained sedimentary breccia would cause a greater proportion of grains (ie. smaller, broken down clasts) than the sedimentary breccias outside the fault core. The tectonised sedimentary breccia should then have a smaller grain size than the sedimentary breccia. If the opposite is the case, it indicates that large amounts of sedimentary breccias have not been entrained into the fault zone.

5.2.1 Clast Composition Count Scanlines

In order to investigate and quantify the textural differences between the tectonic breccia and hanging wall breccia deposits, clast counts (identifying clast lithology and size) were carried out for all 3 locations where chaotic breccia exists in large quantities. Using scanlines (shown in Figure 5-6) eliminates selection bias as clasts are identified and recorded at regular intervals along an arbitrary line, objectively quantifying which clasts are encountered in the direction of measurement. Ideally clast count scanlines would be carried out in 3 perpendicular lines. This is however not possible due to the outcrop geometry. Scanlines were carried out in sets of 2 perpendicular lines on exposed faces with as varied orientation as possible in an attempt to characterise the composition of breccias in 3D and to minimise any directional bias.

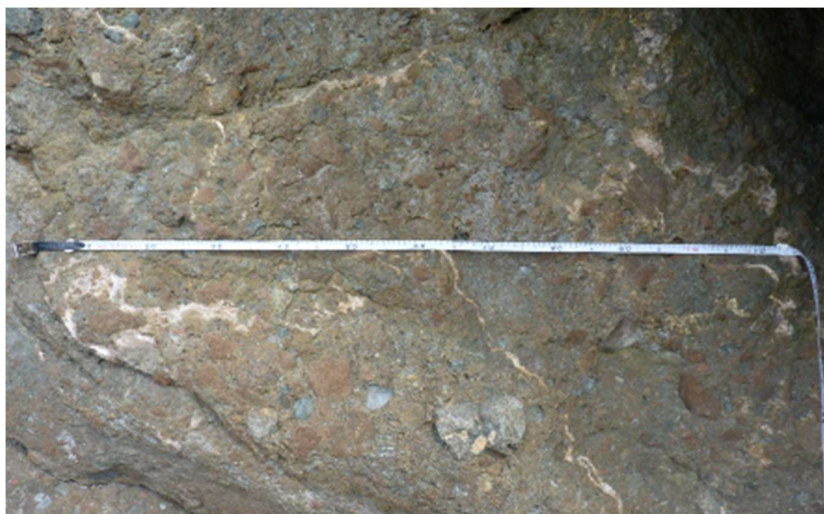


Figure 5-6 Scanline count tape on tectonic breccia

5.2.2 Results of Clast Composition Scanlines

Following the Woodcock and Mort (2008) classification of matrix and grains, a 2mm diameter was used as a cut off between clasts and matrix. **Table 5-1** shows the proportion of clasts and grains at each location.

Location	Fault Component (total length of scanlines)	Grains (diameter <2mm): number [%]	Clasts (diameter >2mm): number [%]
Door of the Heugh	Hanging wall (6m)	222 [50%]	220 [50%]
	Tectonic Breccia (6m)	202 [39%]	314 [61%]
Lagmuck Sands	Hanging wall (6m)	391 [75%]	130 [25%]
	Tectonic Breccia (6m)	318 [58%]	232 [42%]
Gutcher's Isle	Hanging wall (6m)	311 [69%]	135 [31%]
	Tectonic Breccia (4m)	107 [44%]	134 [56%]

Table 5-1 Proportion of clasts to grains in clast count scanlines. The total length of scanline at each location is also shown. Clast or grain counted every 10mm of scan length.

At all three sites, the proportion of total point counts that are grains (less than 2mm) is higher in the hanging wall than in the tectonic breccia. This result will be discussed in Section 5.3.5.

Figure 5-7 shows histograms of clast long axis length derived from clast composition scanlines in the hanging wall breccias. The histograms are positioned on a map to show the field location where the scanlines were carried out.

The relative proportions of the three host lithologies varies slightly between the three sites. At Door of the Heugh granitic clasts are the least frequent, compared to Lagmuck sands where they are the most frequent. This may partially reflect the fact that no granodiorite is observed in the footwall at the Door of the Heugh. At Gutcher's Isle, sedimentary clasts were encountered more frequently than footwall-derived clasts, suggesting significant volumes of extra-basinal sediments were deposited into the margins of the Solway basin.

The size-frequency distributions are also different at each site. At Door of the Heugh, the majority of clasts of all lithologies are less than 10mm in diameter. Clasts of

metasedimentary and sedimentary rocks have a similar grain size distribution, whereas granite clasts are more dominated by smaller grain sizes. In contrast at Lagmuck sands and Gutcher's Isle the slope of the grain size distribution is roughly equivalent for all three clast lithologies.

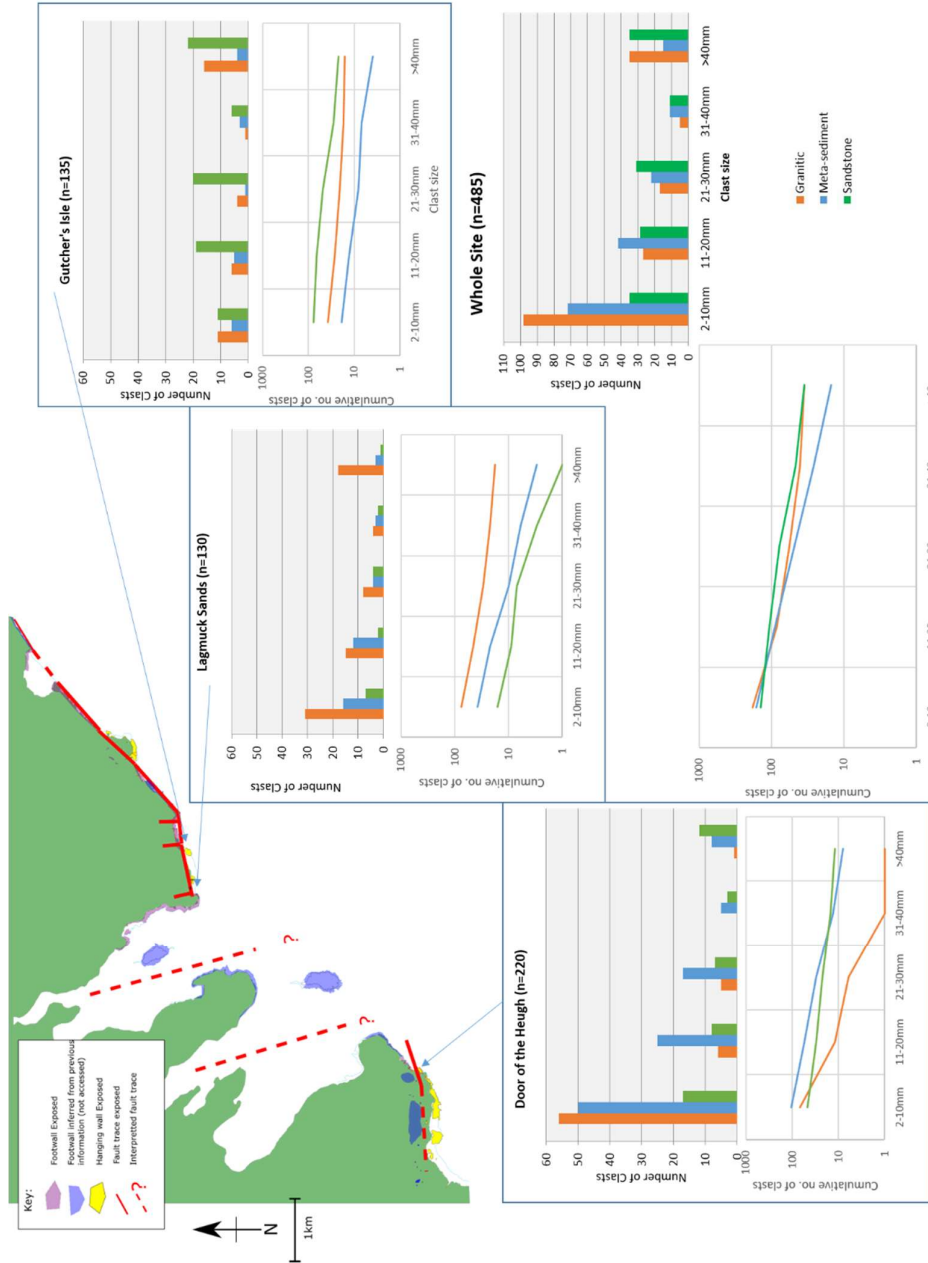


Figure 5-7. Clast count scanlines in sedimentary breccia. Histograms of number of clasts by lithology and location with cumulative line graphs of the same data below.

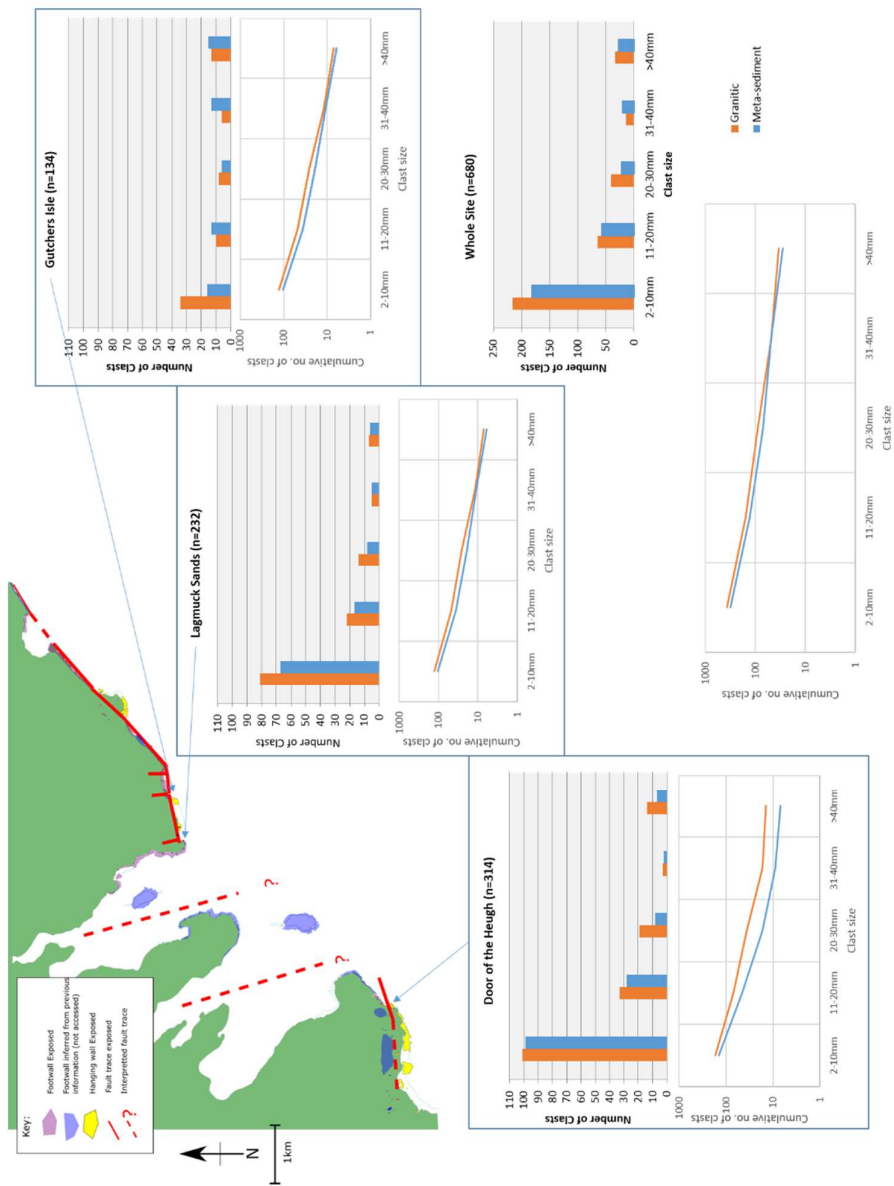


Figure 5-8. Clast count scanlines in tectonic breccia. Histograms of number of clasts by lithology and location with cumulative line graphs of the same data below.

Figure 5-8 shows the histograms and cumulative line graphs for clast count scanlines for tectonic breccia. At all three sites no sedimentary clasts were observed along any of the scanlines. However, sedimentary clasts were observed both at Door of the Heugh and Lagmuck sands (less than 10 in total). The data back up the relative scarcity of sedimentary clasts in the tectonic breccias.

The granitic and metasediment clasts at Lagmuck sands and Gutcher's Isle have almost identical clast size frequency distributions. At Door of the Heugh, the granitic clast size frequency distribution is similar to the other two sites, but the metasediments clasts are slightly less frequent and skewed towards smaller grain sizes.

Comparing the clast size distribution for tectonic and sedimentary breccias shows that sedimentary breccias are slightly finer grained than the tectonic breccias.

5.3 Image Analysis

To investigate if clast lithology affects breccia size and shape image analysis was carried out. It could be expected that the metasediment would behave differently during brecciation. The metasediments appear to be more isotropic compared to the granitic intrusions and it is reasonable to expect each lithology to break down in a different way. Bjork et al (2009) used image analysis of fault gouge and granodiorite dykes to quantify deformation processes. Exponent power law "D values" similar to those calculated by Blenkinsop (1991) can be used to infer the process of fragmentation of breccias and gouges.

Image analysis is a technique of quantifying images to extract data. The technique used is built on that used by Karatson et al (2002) for volcanoclastic flows, Smith et al (2008) for tectonic breccia and Bjork et al (2009) for fault gouge and intrusions. Often, the method uses digitised photos as carried out by Smith et al (2008). The main difference between the method used here and the Smith et al method is that photographs of outcrops were used in this study and Smith et al used photographs of polished breccia samples.

The method involves marking out a square on an exposed face of breccia (**Figure 5-9**). A photograph of the square is taken using a digital camera and printed using a portable field

printer. Clasts are then marked on the print out with an indication of lithology at the outcrop. This is done in the field to make identification easier during digitisation and to avoid confusion with potential visual artefacts. Automatic digitisation of clasts using image processing techniques proved unreliable due to artefacts in the digital photographs resulting from shadows, algae and weathering of the exposed surface. For this reason, the image was digitised manually by tracing the outline of each clast using a graphics package. The outlines of the clasts were uploaded to the Fiji software package where the image is further processed to ortho-rectify the image using the square set out in the field. Clasts were analysed using the imageJ *Analyze Particles* function. The function projects a best fit ellipse over each particle and quantifies the clast's size, shape and orientation. The function also summarises this data by providing maximum, minimum, mean and standard deviation for each parameter for all the clasts in the analysed image.

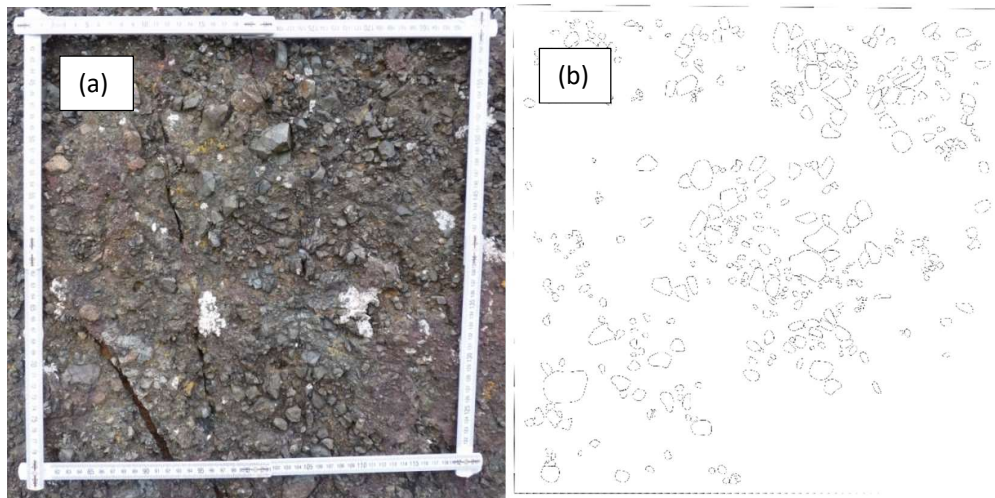


Figure 5-9 (a) Square marked out for field photograph for image analysis. (b) metasediment clast outlines digitised and ortho-rectified.

A total of 4 images were analysed; 2 each at Door of the Heugh and Lagmuck Sands respectively. An attempt was made to select faces that were orthogonal to each other to

investigate clast composition in 3D; this was not possible due to available exposures. Locations for analysis were selected based on the quality of exposure and exposure orientation. Another issue in finding locations for analysis was the variable topography of breccias, ideally perfectly flat faces should be used.

Of a total of 2352 clasts digitised, 48 had a long axis less than 2mm. Although these clasts fall outside the grain to clast cut off as described in Section 2.5, they are included here for completeness. Because the grain size was generally smaller in the sedimentary breccias, image analysis could not be carried out for the sedimentary breccias.

5.3.1 Clast Size Image Analysis Results

Figure 5-10 shows the histograms of clast long axis length for each site separately, along with both sites plotted together. In agreement with the scanline observations there are more granitic clasts than metasedimentary clasts at Door of the Heugh. The scanline data at Lagmuck Sands showed roughly equal proportions of granite and breccia clasts, whereas the image analysis data show more metasedimentary than granite. This is likely to be a function of the very limited samples area of the image analysis.

In general, the slope of the grain size distribution is similar for both sets of lithologies at both sites. This suggests that both lithologies are breaking down within the tectonic breccias in the same way – i.e. that there is no strength difference or fabric anisotropy in either lithology that causes them to break down to different clasts size populations.

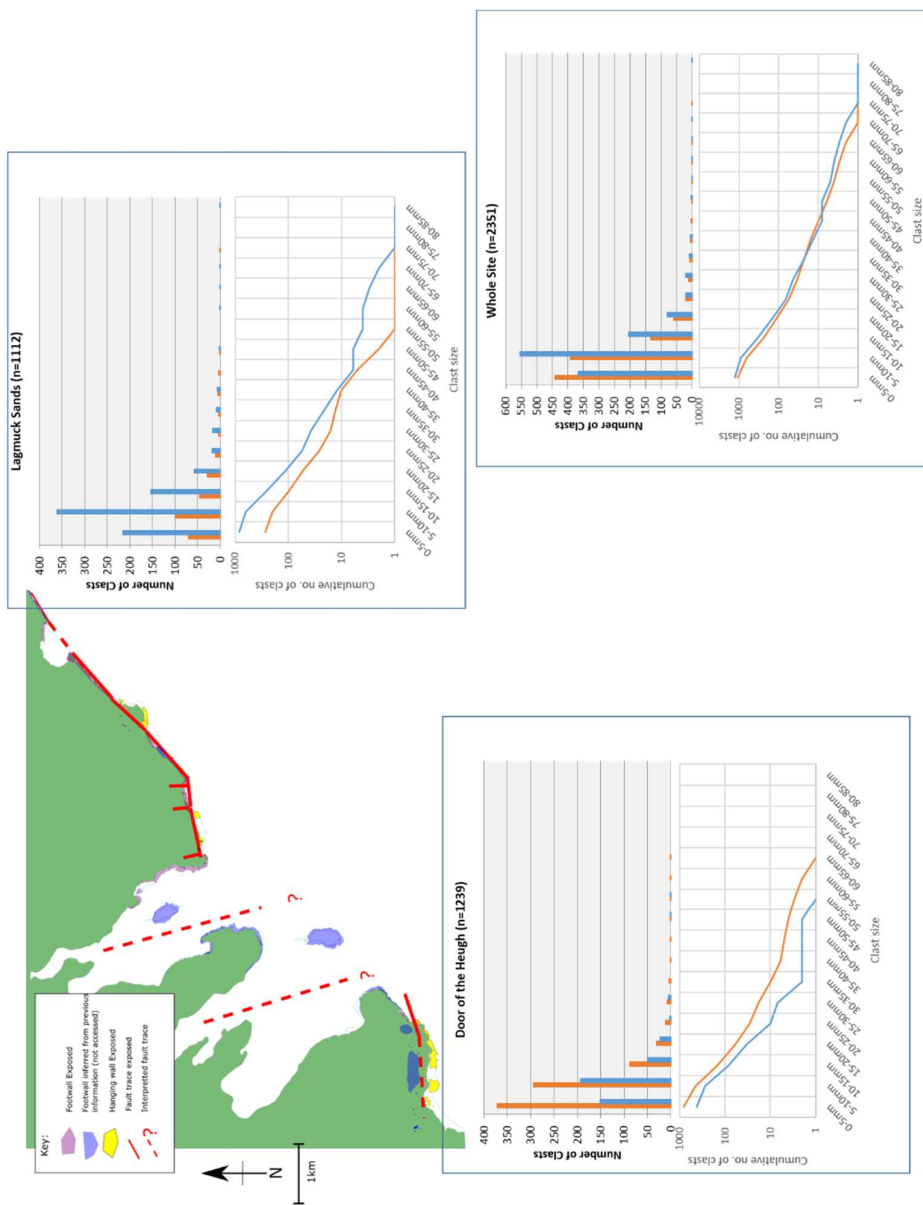


Figure 5-10. Image analysis clast long axis length in tectonic breccia. Histograms of number of clasts by lithology and location with cumulative line graphs of the same data below.

5.3.2 Clast Size and Shape All Data

Table 5-2 shows the results of image analysis for all four measured faces relating to clast size and shape. The minimum, maximum, mean and standard deviation of each of the parameters in the analysis are listed for clasts of both lithologies. A description of each parameter is given below:

- Area – area of clast calculated by counting number of pixels within each clast outline.
- Major and Minor axis – Long and short axis of clast best fit ellipse.
- Circularity – 1.0 = perfect circle, values closer to 0 represents an elongated shape.
- Aspect Ratio = Major axis/Minor Axis.
- Solidity – area/convex area, a value of 1.0 indicates no convexity to the clast shape

Lithology		Area (mm ²)	Major axis (mm)	Minor axis (mm)	Circularity	Aspect Ratio	Solidity
Msed	Mean	60.3	8.797	5.663	0.772	1.586	0.931
Granitic	Mean	59.5	7.905	5.300	0.803	1.526	0.939
t-score		-0.11	-3.05	-1.90	7.10	-3.44	2.68
P value		0.91	0.002	0.057	0.0000	0.0005	0.007
Msed	SD	157.6	6.952	4.267	0.117	0.435	0.091
Granitic	SD	179.8	7.176	5.001	0.088	0.395	0.037
Msed	Min	1.6	1.582	1.158	0.007	1.011	0.042
Granitic	Min	0.9	1.267	0.870	0.005	1.006	0.029
Msed	Max	3820.9	83.344	58.372	0.969	4.691	0.989
Granitic	Max	3224.7	73.621	55.771	1.000	4.899	0.987

Table 5-2 Clast size and shape results for image analysis of all clasts. Values of mean, standard deviation (SD), minimum (min) and maximum (max) for the parameters for each clast lithology

T-tests have been carried out to investigate the significance of the results against a null hypothesis (eg. no difference between the two lithologies) at 95% confidence level.

5.3.2.1 Clast size

The mean area of clasts is similar for each lithology as is the standard deviation for mean area. The high standard deviation confirms that both lithologies have a lot of variability in clast size and the low t score shows that each lithology has a similar variability in clast size.

Minimum and maximum values for areas of clasts are similar for both lithologies. The mean of major axis lengths is slightly higher in the granitic clasts as is the standard deviation for granitic clasts.

5.3.2.2 Clast Shape

The values of mean, maximum and minimum circularity, aspect ratio and solidity are similar for each lithology. The only notable difference between the two lithologies are the standard deviations for circularity and solidity which are higher in the meta-sediment clasts compared to the granitic clasts. T tests suggest that any differences in the areas of the granite and meta-sedimentary clasts are not statistically significant but for circularity, aspect ratio, solidity and major axis the differences are all significant at the 95% confidence level. Clast shapes are therefore variable depending on lithology.

An explanation for the greater variability in meta-sediment shapes may come from the non-isotropic fabric of this lithology. The macro scale structure of the meta-sediment is non isotropic as meta-bedding is observed wherever the meta-sediment is reasonably intact.

This result suggests that deformation of both lithologies creates similar breccia clasts, with the exception of slight variations of clast shape depending on lithology.. It could be therefore suggested that the clasts of both lithologies have reacted in a similar way to processes within the fault zone. The processes of initial formation and re-working of breccia clasts of both lithologies are likely to be similar given the predominance of mixed clast lithology breccias (assuming adjacent clasts experience the same deformation events).

5.3.3 Clast Orientation

The angle of the clast long axis angle to horizontal was plotted on rose diagrams to explore if any shape preferred orientation (SPO) is present in the chaotic breccias. The rose

diagrams were analysed by both visual inspection and by the mean direction method used by Smith et al (2008). Because only nonspheroidal clasts can show a preferred orientation, only clasts with an aspect ratio greater than 1.4 are considered (after Cladouhos 1999b). To investigate if the original lithology played a role in the defining the clast shape the granitic and meta-sedimentary clast long-axis orientations were plotted separately (Figure 5-11 and Figure 5-12) .

In order to quantify the SPO of breccia clasts and investigate if there is any relationship between clast size and/or aspect ratio (AR) and SPO, the mean vector method was used. The method involves the addition of unit vectors (orientations of clasts in this case) and calculating the resultant vector angle which represents the mean angle (M). The length of the resultant vector is calculated and represents a measure of the strength of particle alignment (R). R values closer to 1 represent stronger SPO.

In Figure 5-11 and Figure 5-12 black arrows represent the resultant mean direction graphically with the M and R values written beside each face.

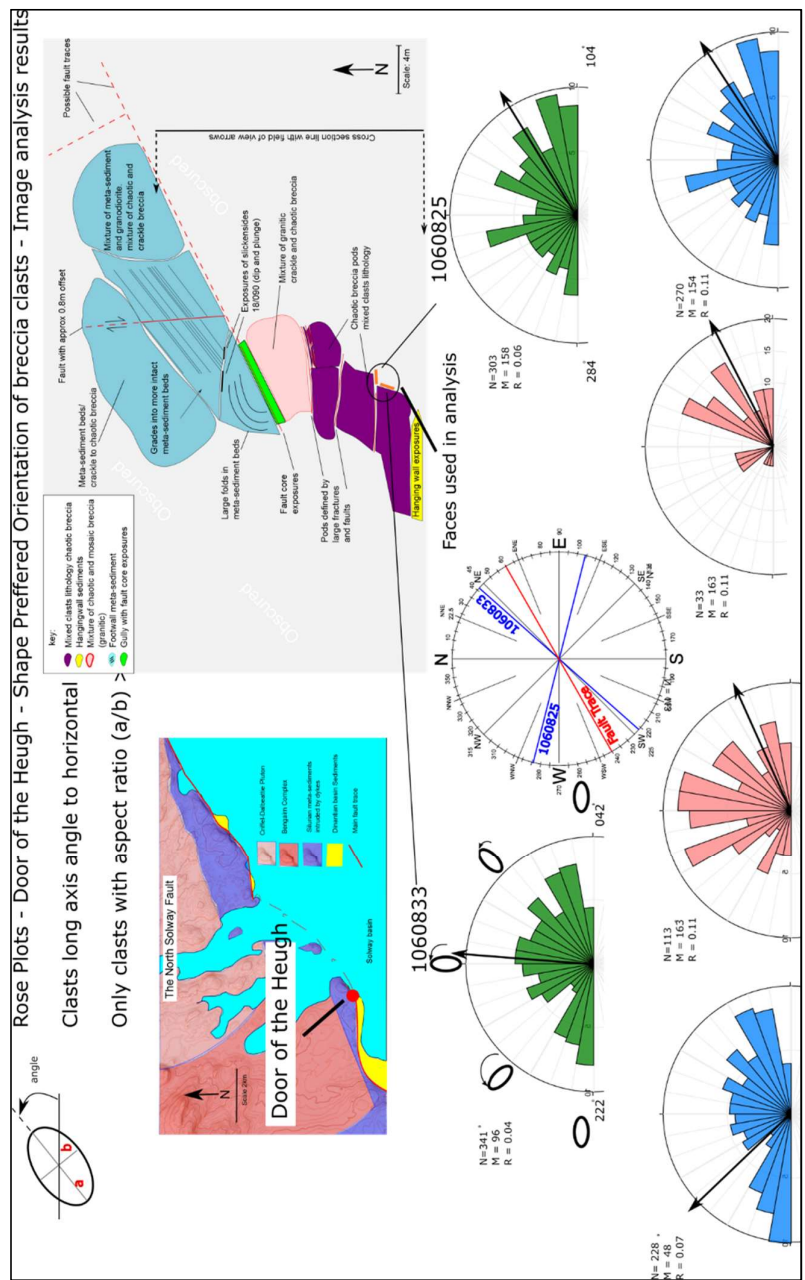


Figure 5-11 Clast long axis orientation from image analysis of 2 breccia photographs at Door of the Heugh. The location of each field site along the whole fault is shown as is the location of the breccia faces analysed on the detailed maps at Door of the Heugh and Laggmuck Sands. The strike of the analysed faces are plotted onto a compass symbol along with the main fault trace at each location to show the relationship between the orientation of the faces analysed to the orientation of the main fault trace. Rose plots are used to present the number of clasts orientated in 10° bins to the horizontal. Rose plot colours as follows; Blue – metasediment clasts, pink – granitic clasts, and green Both lithologies plotted together.

At Door of the Heugh, image 1060833 is taken on a breccia face which strikes 20° obliquely to the main fault trace. A total of 341 clasts were analysed in this image of which, 228 were meta-sedimentary and 113 were granitic. SPO vectors are variable in orientation between the two lithologies but the low R values (0.07 and 0.11) suggest that strong SPO is not developed in either lithology.

Also at Door of the Heugh, image 1060825 is taken on a breccia face which strikes 44° obliquely to the main fault trace. A total of 303 clasts were analysed in this image of which, 270 were meta-sedimentary and only 33 were granitic. SPO vectors are separated by only 9° (163° granitic and 154° meta-sedimentary), however when both lithologies are plotted together the R value is low (0.06) and is does not represent strong SPO.

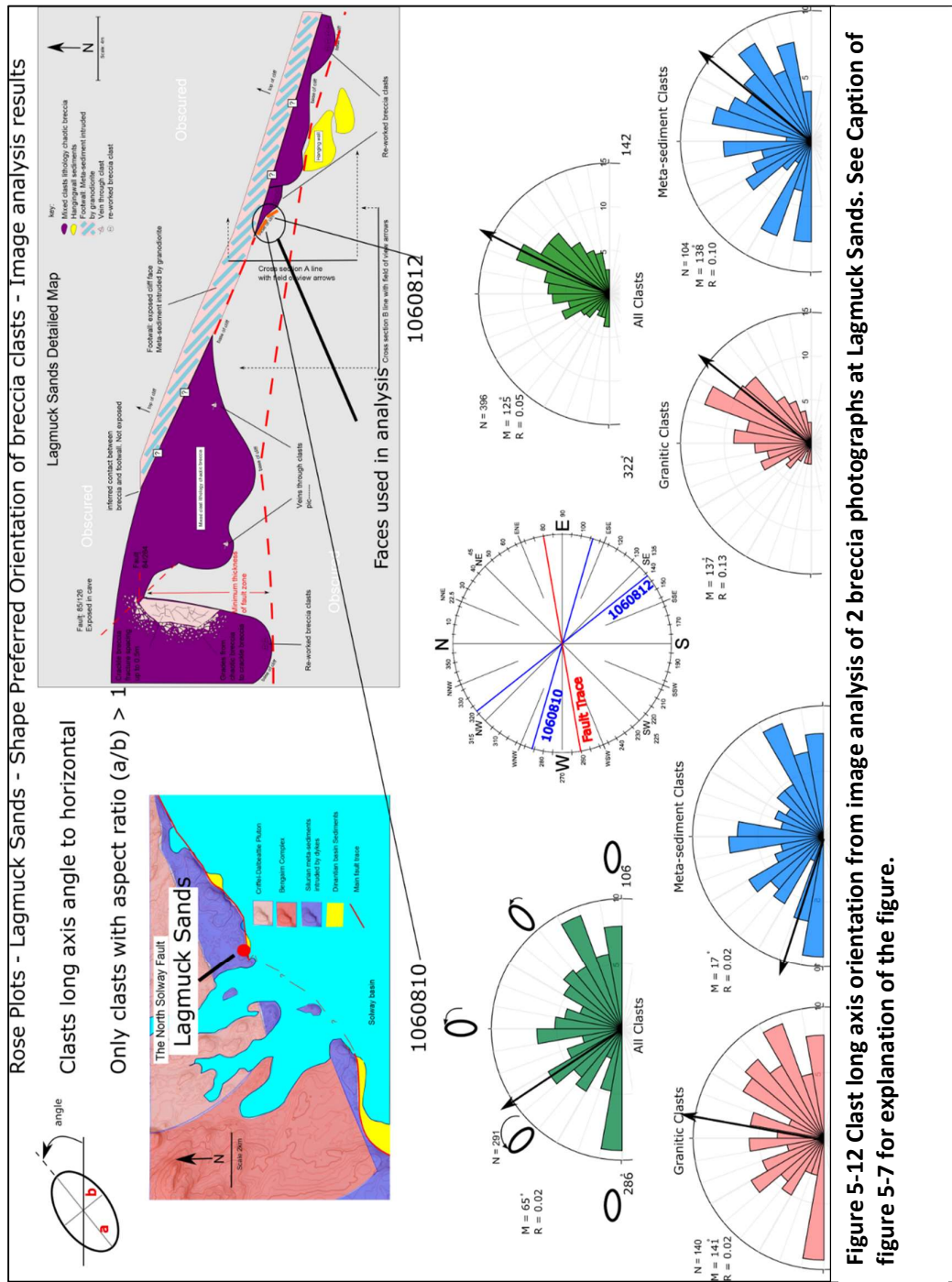


Figure 5-12 Clast long axis orientation from image analysis of 2 breccia photographs at Lagmuck Sands. See Caption of figure 5-7 for explanation of the figure.

At Lagmuck Sands, image 1060810 is taken on a breccia face which strikes 25° obliquely to the main fault trace. A total of 292 clasts were analysed in this image of which, 152 were meta-sedimentary and 140 were granitic. SPO vectors are variable in orientation between

the two lithologies but the low R values (0.02) suggest that strong SPO is not developed in either lithology.

Also at Lagmuck Sands, image 1060812 is taken on a breccia face which strikes 62° obliquely to the main fault trace. A total of 396 no clasts were analysed in this image of which, 104 were meta-sedimentary and 292 were granitic. There appears to be strong SPO developed in the granitic clasts when the rose plot is inspected visually. The mean vector strength is the highest for all the data (13%). The granitic clasts dominate the plot of both lithologies together.

One of the four faces shows a strong SPO and that face is predominantly composed of granitic clasts (74% of clasts are granitic). This could suggest that where granitic clasts are dominant, SPO of breccia clasts occurs at the North Solway fault. The limited number of faces analysed makes this inference hard to justify. The orientation of the faces are not orthogonal so the data set doesn't give a true reflection of the clast orientation with respect to the main fault trace.

There appears to be no relationship between clast SPO and orientation to the main fault zone. However, the faces analysed (4 no.) only represent 2 locations where SPO with respect to fault trace has been investigated for the present study. Also, the exposures of breccia do not offer faces which are orthogonal to each other and the analysed faces are not parallel and perpendicular to the fault trace. For these reasons, this negative result is not considered conclusive.

5.3.4 Image Analysis Limitations

The method of image analysis of clasts is time consuming both in the field and during the digitisation process. The method also requires very clean exposures so that individual clasts

can be identified. There are therefore limits to the amount of suitable exposure and the amount of data it is possible to collect.

Whilst the data gives an approximation of clast size distribution in the breccias, data produced using image analysis of field photographs is limited to 2 orders of magnitude of particle sizes (c. 1mm to 100mm). For a thorough investigation of clast size, grain size distributions are typically over several orders of magnitude and plotted on a particle size distribution chart (PSD). This chart is often created by using a series of sieves for coarse particles (0.063mm diameter and above) and using pipette sedimentation for silt and clay particles (0.063mm diameter and below). These methods were not possible for the breccias at the NSF as the breccia particles are tightly bonded together. Separation of particles may cause destruction of some particles and therefore artificially produce a fraction of small grain sizes, skewing the grain size distribution.

An attempt was made to calculate the power law exponent “D values” for the particle size distributions resulting from the image analysis, similar to that calculated by Bjork et al (2009). D values were not possible to calculate over a wide enough range of clasts sizes (typically at least an order of magnitude) to be representative. This is a product of the image analysis being carried out on the range of clast sizes identifiable by eye. Expanding the method to smaller particle sizes could also be done by thorough analysis of thin sections. Due to time constraints it was not possible to carry out image analysis of polished sections for this thesis.

5.3.5 Source of Clasts

Clasts counted in the tectonic breccias are entirely derived from the two footwall lithologies; meta-sediment and granitic rocks. Breccia with clasts of both meta-sediment

and granitic origin) can be found adjacent to wall rock of a single lithology. This suggests that clasts travel within the fault and also suggests that clast mixing occurs within the fault. This will be discussed in Section 6.2.7.

Clasts of sedimentary rock are very rare, and none were picked up on the scanlines or the image analysis squares which were as randomly placed as possible. Sedimentary clasts are only observed at only 2 locations (Door of the Heugh and Lagmuck Sands) and are absent from the majority of “pods” and blocks of breccia exposed on site. The sedimentary clasts in tectonic breccia (less than 10no. observed in total) were not sampled and were identified by eye in the field.

It is clear from the results of clast count scanlines (see Table 5-1) that grain size is not generally smaller in the tectonic breccias compared to the sedimentary breccia. In fact, the opposite appears to be true and the sedimentary breccias are shown to be slightly finer grained. This shows that large volumes of hanging wall sediments are not entrained in the fault where chaotic breccias are found.

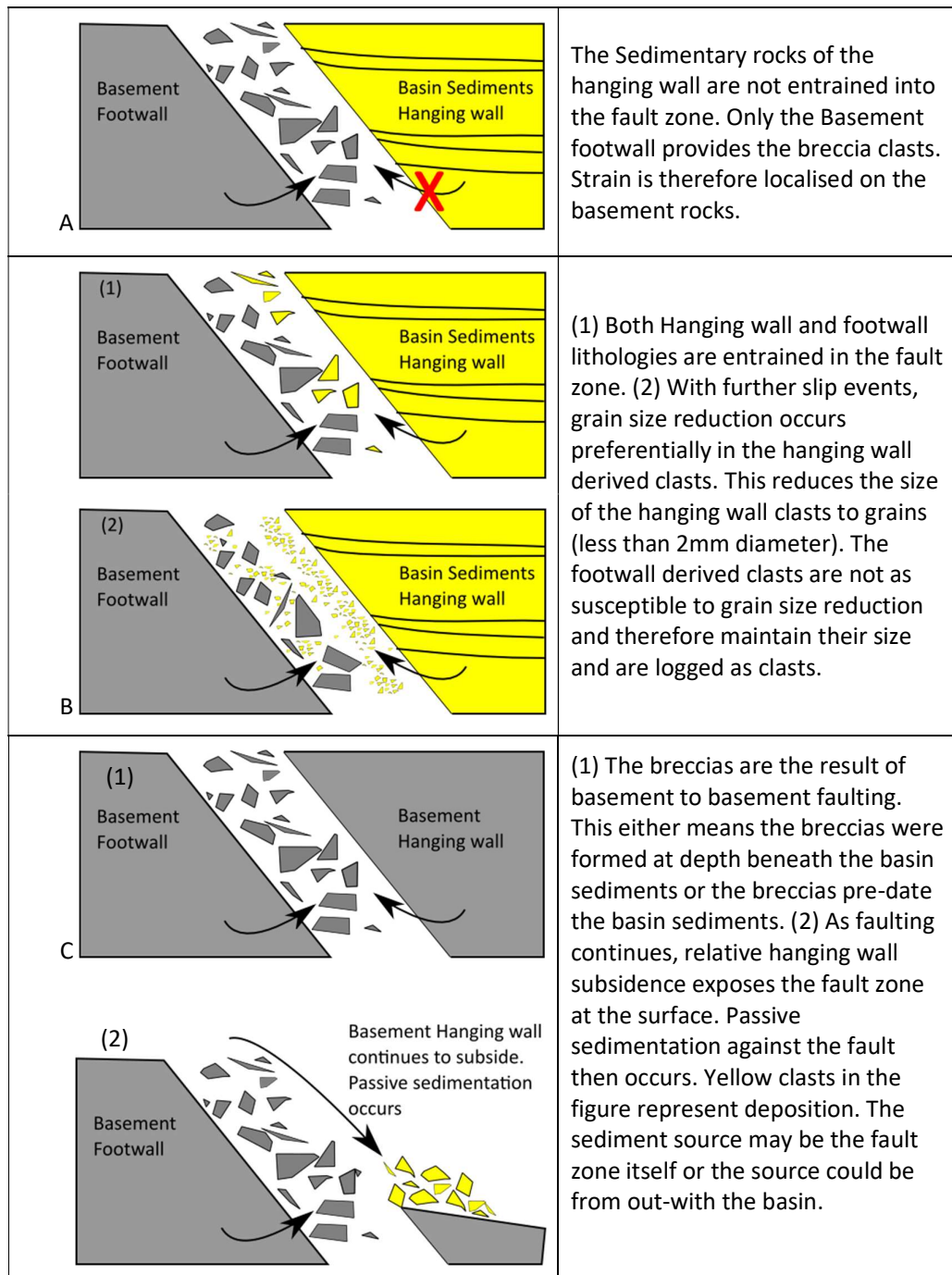


Figure 5-13 Three hypotheses for the lack of clasts derived from sedimentary lithologies within tectonic breccia deposits. A - hanging wall lithologies are not entrained in the fault zone. B - preferential grain size reduction in the hanging wall derived clasts. C – breccias are the result of basement against basement faulting.

There are three possibilities for the lack of sedimentary input in tectonic breccias (illustrated in **Figure 5-13**): the first is that strain is accommodated within the footwall, with only minor strain accommodation in the hanging wall. This would result in only minor volumes of hanging wall being entrained into the fault zone. The second possibility is that strain accommodation between the footwall and hanging wall is roughly equal, but hanging wall lithology clasts are broken down more readily than footwall lithology clasts. The clasts of hanging wall lithology would then be more likely to be identified as matrix due to grain size reduction processes in the breccias. A third possibility is that the breccias are formed at depth where the fault is basement against basement and therefore sedimentary lithologies are not present to mix with the breccia. Passive sedimentation against an exhumed fault zone would then explain the presently exposed configuration.

I consider the most likely explanation is that the breccias are the result of basement-basement faulting. Clasts in the breccia are almost entirely footwall derived, with very few sedimentary clasts identified. Where the fault is clearly the result of basement to sediment faulting at Portling Bay, the fault zone is composed of a wide gouge zone with sediments grading into the fault (see Figure 4-16). This will be discussed further in Section 6.2.6.

5.4 Discontinuities and Veins

Discontinuities and mineral veins were studied in the field to investigate and quantify the mechanical and fluid flow history of the fault. Fracture and vein data were collected using a compass clinometer. Fractures were selected to characterise the dominant joint sets and dip and strike was recorded along with location relative to the fault. Fractures were randomly selected in order to characterise a large area/exposure rather than collect fracture frequency data over small transects. This method of data collection doesn't include

information about the intensity of fractures but it does characterise dominant sets over large areas. A further limitation of this data set is that the selection of fractures randomly will probably be biased towards fractures with a significant aperture and excludes tight or incipient fractures. Vein data included location, dip and strike and observations of vein fill and fill texture.

Carbonate veins were identified in the field using acid. The majority of the veins studied were not carbonate. Hand samples of basin sediments containing veins were not taken in the field due to difficulties taking representative samples. When attempting to sample with a geological hammer, the vein material and surrounding rock would disintegrate and any structure in the veins was lost. Small veins (0.5 to 2mm width) in the breccia and footwall were studied in thin section with an optical microscope and predominantly consisted of quartz.

5.4.1 Hanging wall

Poles to planes plots of discontinuities in the hanging wall deposits are plotted by location in Figure 5-14. At Portling Bay, a cluster of steeply dipping fractures are oriented NW-SE. A minor cluster of steeply dipping fractures are oriented roughly NE-SW. At Gutcher's Isle, almost all of the fractures are steeply dipping. The orientation of fractures is variable with a cluster at WNW-ESE. At Lagmuck Sands a dominant cluster of fractures dipping between 50°-70° trend NW-SE. At Door of the Heugh, a spread of fracture orientation are predominantly steeply dipping with a cluster oriented broadly NW-SE.

When all locations are plotted together, discontinuities in the hanging wall mostly dip at steep angles (greater than 60°) and vary in orientation, clustering around NW-SE (Figure 5-14). The cluster of fractures in a NW-SE direction are at high angles to the fault and only

26 of 131 of the measured fractures are close to fault parallel (broadly NE-SW). The variability in orientation is not location specific, with all four locations along strike showing similar variations in fracture orientation.

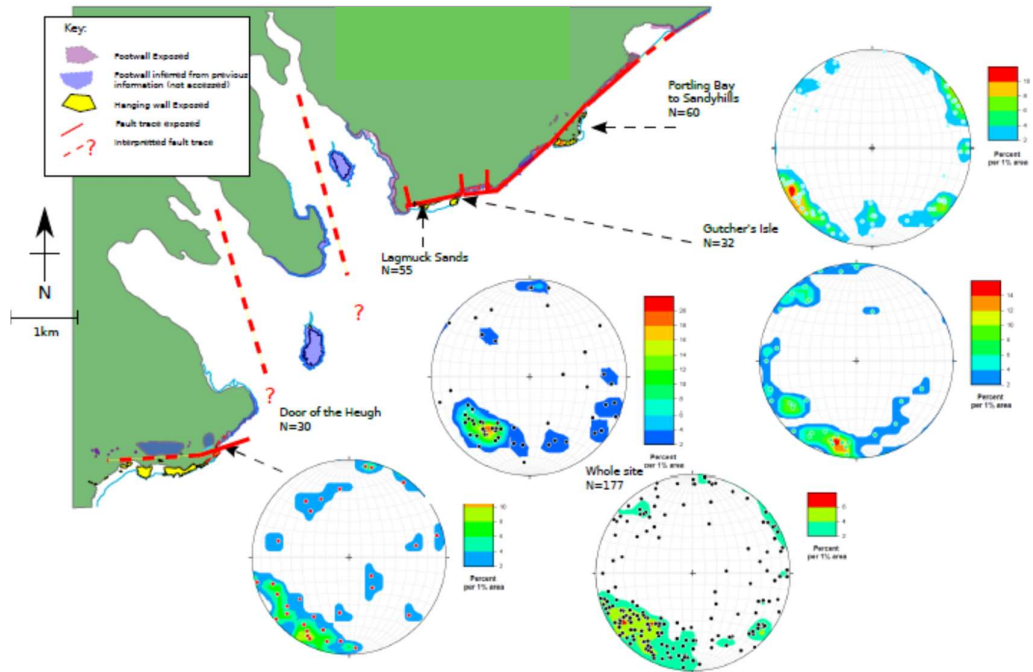


Figure 5-14 Stereographic projection of poles to planes of hanging wall fractures, plotted by location along the fault.

If the fractures are directly associated with normal faulting, a cluster of fractures parallel to fault strike could be expected (ENE-WSW and NE-SW). A simple model of hanging wall distortion due to extensional activity is therefore unlikely to apply here. However, fractures have been shown to form at high angles to, and in close proximity to normal faults (Katternhorn et al 2000).

At a larger scale, regional scale processes may have caused the formation of steeply dipping fractures in the sedimentary deposits. Regional extensional movement of basin sediments

or can result in vertical principal stresses and horizontal minimum stresses and are therefore likely to cause the formation of fractures with steep dip angles.

The variability of strike could result from changes in the regional stress field (direction of minimum stresses through geological time). The cluster of fractures measured in NW-SE direction could have formed in response to the regional extensional movement that formed the roughly NNW-SSE half-graben Permo-Triassic basins of the Southern Uplands described in Section 3.2.3.

Poles to planes veins in the hanging wall are shown in **Figure 5-15**. At Porting Bay there is a set of steeply dipping veins which are oriented NNW-SSE. At Gutcher's Isle there are two clusters of steeply dipping veins trending roughly N-S and E-W. At Lagmuck Sands the majority of fractures trend broadly NW-SE but have a range of dips from shallow angles (c. 10°) to sub vertical, this could represent two separate antithetic clusters; one steeply dipping, one shallow dipping. Veins in the hanging wall at Door of the Heugh were not measured as there were few accessible examples in the field at that location.

When veins from all locations are plotted together, a dominant orientation of NNW – SSE can be seen (Figure 5-15). Comparing veins (Figure 5-15) and fractures without fill (Figure

5-14), the veins have a narrower spread of orientation than the unfilled fractures but the dominant orientations are the same.

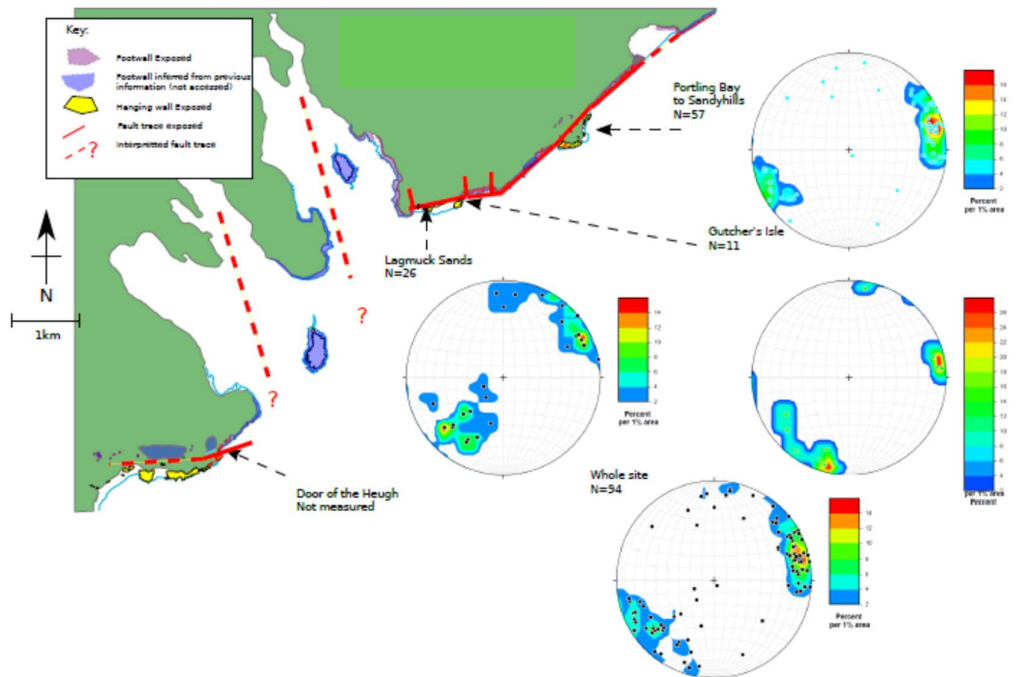


Figure 5-15 Stereographic projection of poles to planes of hanging wall veins

The dominant vein orientation must represent structures that were open at some time in the past that provided pathways for mineral rich fluids. Mineral deposition may take place concurrently with fracture opening or after fractures are opened. The relative lack of veins in other orientations could be due to fluids depositing minerals in a single geological event and under a single stress regime, in other words if regional stresses remained relatively constant during fluid flow and mineral precipitation. Alternatively, fluid flow could have occurred episodically when stress conditions temporarily permitted flow in a particular orientation (eg. during fault slip events) when the local stress regime changed intermittently.

Various textures observed in the vein fill at the site give clues to the relationship and relative timing between the mineral rich fluid flow events and the opening of fractures. There were 94 veins measured in the hanging wall. Of these, only 9 were observed to have partial fill or vugs within them and only 16 had any observable direction of crystal growth, perpendicular to vein walls. All the other veins in the hanging wall had solid veins with no observable crystal growth direction observed with either the naked eye or a 10X magnification hand lens. This suggests that the veins of the hanging wall have not grown incrementally as fractures propagate. The lack of observable textures also precludes constant mineral rich fluid, supplied into open voids which would create conditions for large crystal growth as described in Bons et al (2012).

Contrasting mineral types were rarely observed in the same vein, though one example is shown in Figure 5-16. The contrasting vein fills were identified by colour and reaction to acid with quartz lining the fracture walls followed by a band of carbonate and the remainder of the fracture being filled with quartz. This suggests that fluid composition changed at least twice. Changes in the composition of fluids in basin bounding faults has been shown to occur on timescales of c 100,000 years by Boles et al (2004). Crack seal mechanisms on much shorter timescales may be related to individual rupture events (Petit et al 1999). A lack of vein texture could represent sudden changes in conditions, such as a rapid stress drop during rupture events, which cause minerals to come out of solution and form crystals rapidly.

It is possible that the lack of observable crystals or mineral fibres is a function of the generally small scale crystals (less than 1mm) observed during the field work. Examining veins in thin section under an optical microscope could show parallel crystal quartz

textures. However, where crystals were large enough to be observed in the field, preferred orientation of crystals was rare.

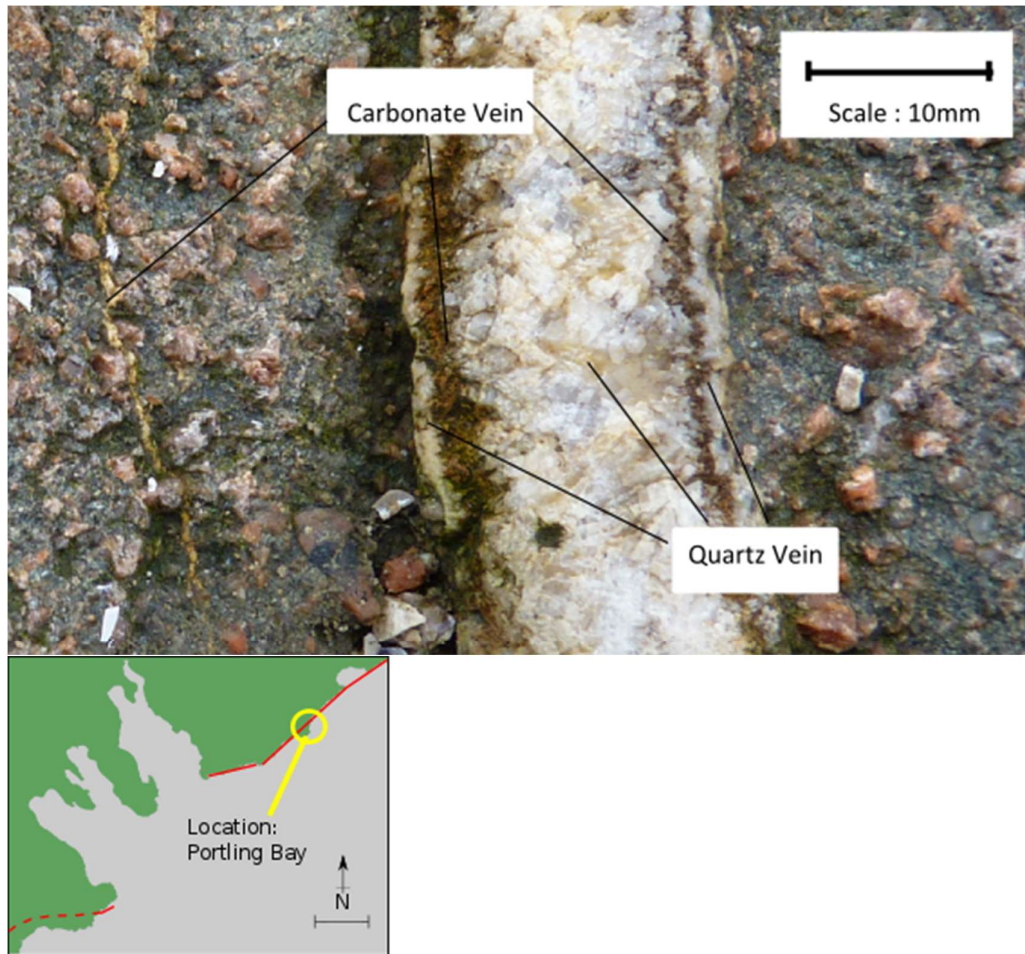


Figure 5-16 Quartz and carbonate minerals occupying the same vein in the hanging wall.

5.4.2 Tectonic Breccia

Poles to planes of fractures in tectonic breccia are shown in Figure 5-17. At Portling Bay there is a spread of orientations with a cluster of steeply dipping fractures oriented WNW-ESE. At Gutcher's Isle there is a spread of orientations and dips with a number of steeply dipping fractures with varying orientation. At Lagmuck Sands a cluster of N-S oriented fractures dip between 20° and sub vertical. Another cluster is oriented NW-SE with dips

between 30° and 60°. At Door of the Heugh, a cluster of steeply dipping fractures are broadly oriented NW-SE.

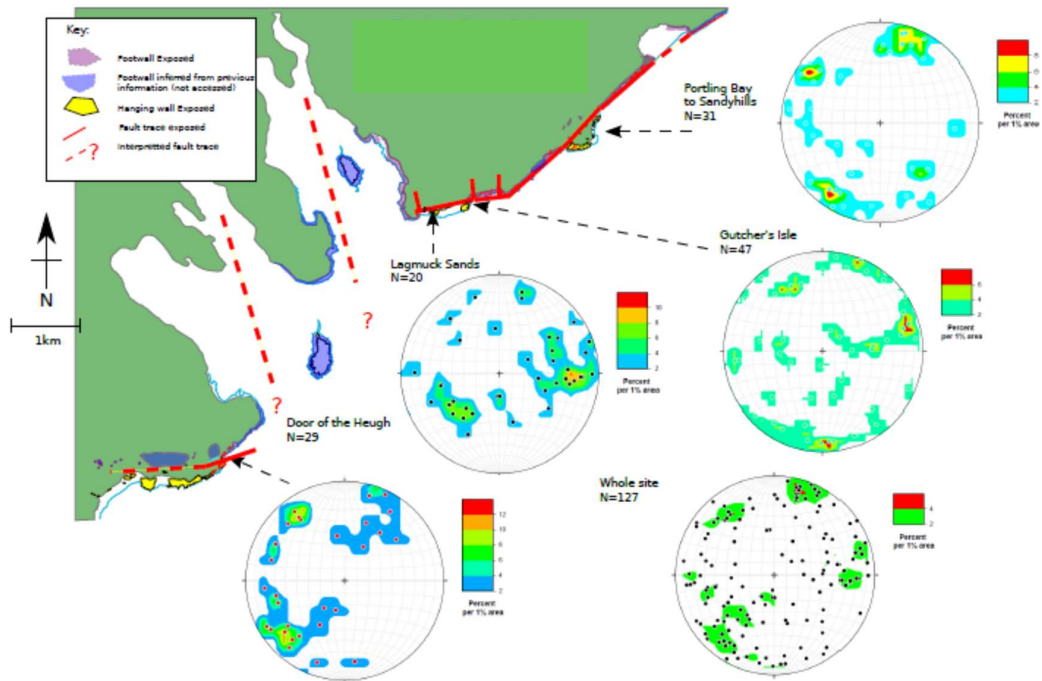


Figure 5-17 Stereographic projection of poles to planes of breccia fractures

When all locations are plotted together there is a spread of orientations and dips. There are two weak clusters - a steeply dipping cluster oriented WNW-ESE and another less steeply dipping cluster broadly oriented NW-SE, but the variability in dip and orientation is most notable.

The strike and dip of fractures in tectonic breccia are highly variable and show only weakly dominant sets. The broad NW-SE and WNW-ESE orientations (perpendicular to the main fault and cross faults) are most notable and one or both of these sets occur at each location. The lower concentration when all locations are plotted together suggests that fracture orientation in the breccia is influenced by the location along the fault, but generally fractures oriented NW-SE and WNW-ESE are found at each location.

The absence of any strongly dominant orientation of fractures within the breccias could be due to frequent changes in dominant stresses within the fault zone.

The variability in orientation of fractures in the breccia could be explained by the breccias forming in the fault core and reactivation of the fault through geological time. Changes in the mode of faulting through time, due to depth of faulting (dilation/shear) has been shown to result in an increasingly complex fracture system (Soden et al 2014). Additionally, mechanical heterogeneities associated with variations in lithology have been shown to exert a first order control on fracture and fault evolution (eg. Moir et al 2013).

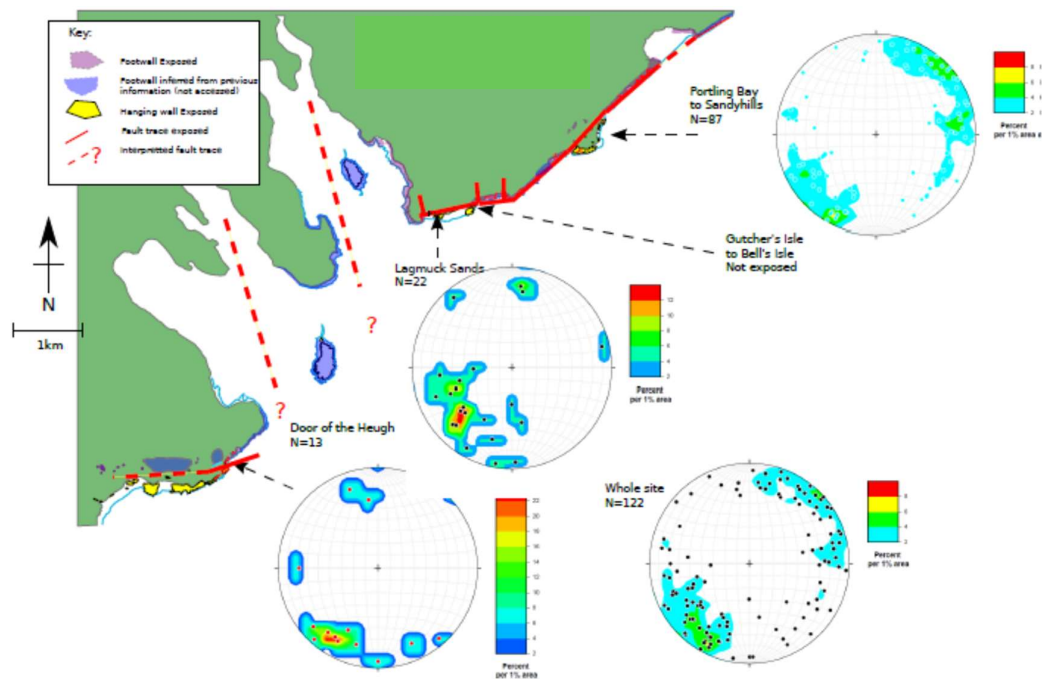


Figure 5-18 Stereographic projection of poles to planes of veins in breccia

Poles to planes of veins in tectonic breccia are shown in Figure 5-18. At Portling Bay there is a cluster of broadly NW-SE steeply dipping veins. At Lagmuck Sands there is a broad orientation of NW-SE veins which dip at varying angles to the NE. At door of the Heugh there is a cluster of steeply dipping NE-SW veins which dip to the NE.

When all locations are plotted together, the broad NW-SE orientation dipping at predominantly steep angles is notable.

The mostly steep dip angle of veins broadly clustered into a NW-SE orientation is similar to the hanging wall (Figure 5-18 and Figure 5-15).

5.4.3 Footwall

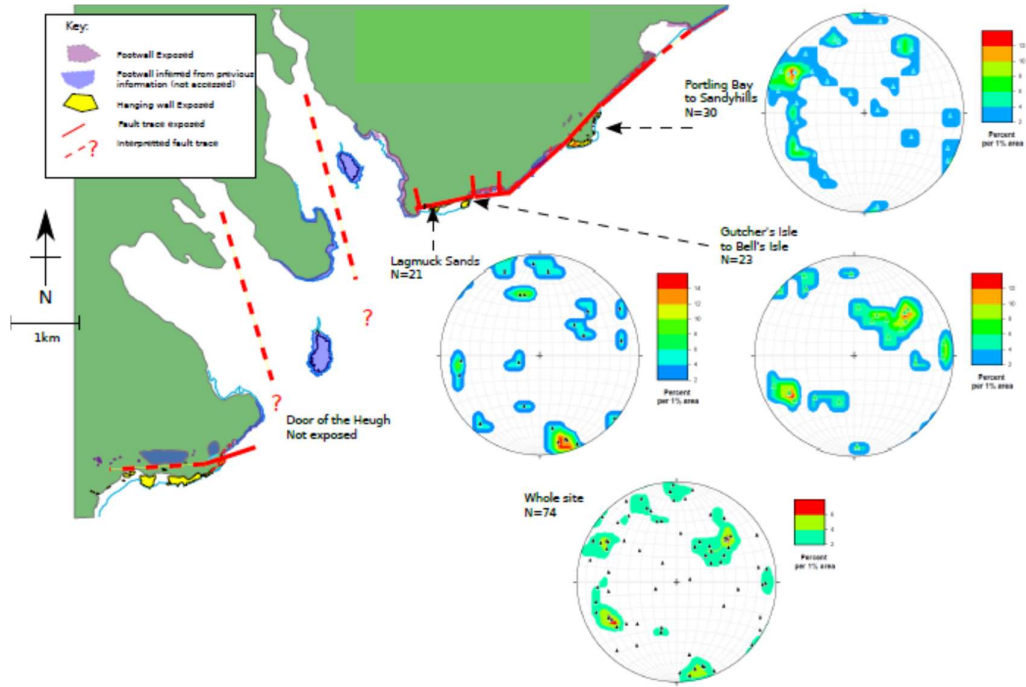


Figure 5-19 Stereographic projection of poles to planes of fractures in granitic footwall

Poles to planes plots of fractures in granitic footwall (Figure 5-19), metasediment (Figure 5-20) and both footwall lithologies (Figure 5-21) have been plotted.

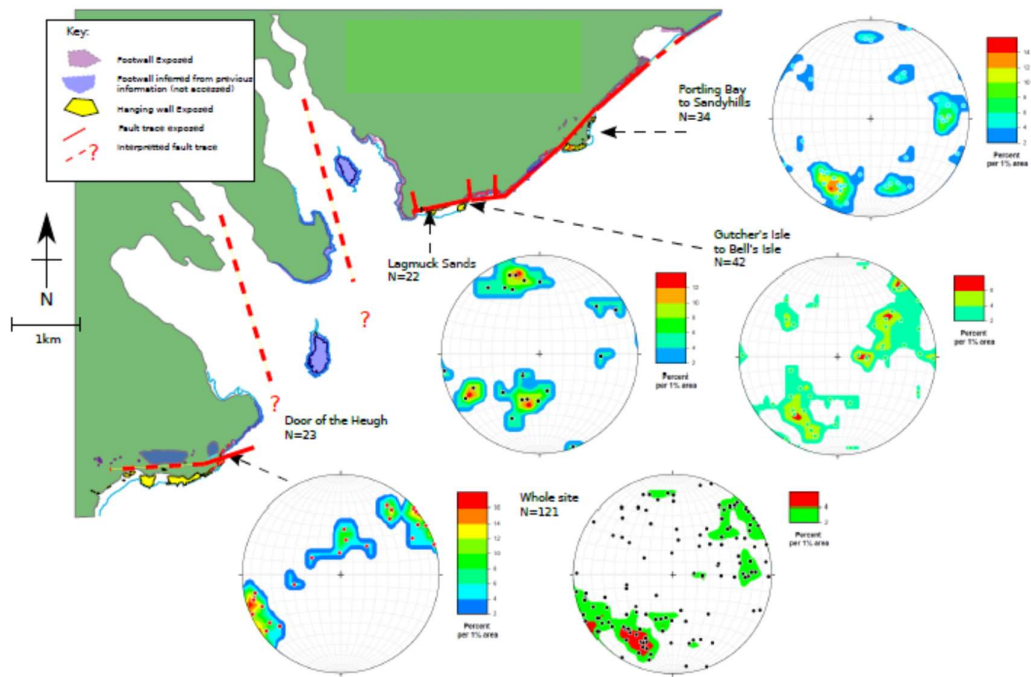


Figure 5-20 Stereographic projection of poles to planes of fractures in metasedimentary footwall

At Portling Bay, fractures in the meta-sediments cluster NNW-SSE with a smaller cluster oriented N-S. The granitic fractures at this location cluster NNE-SSW but there is also a lot of variation of orientation for the remaining fractures.

At Gutcher's Isle, the meta-sediment fractures have a varied dip but are generally oriented NW-SE. This is similar to the granitic fractures. At Lagmuck Sands, there is a cluster of fractures oriented ENE-WSW which have steep dips. There is also a cluster of fractures with shallower dips oriented NW-SE. The granitic fractures also contain a cluster around ENE-WSW which are steeply dipping. This is roughly fault parallel at Lagmuck Sands. At Door of the Heugh, granitic footwall is not exposed.

When the whole site is plotted together for each footwall lithology, a general NW-SE trend is seen in both plots. In the meta-sediment the fractures oriented NW-SE are generally

steeply dipping. In the Granitic fractures the NW-SE cluster are generally shallower dipping.

Another cluster is evident with steep dips which are oriented roughly E-W.

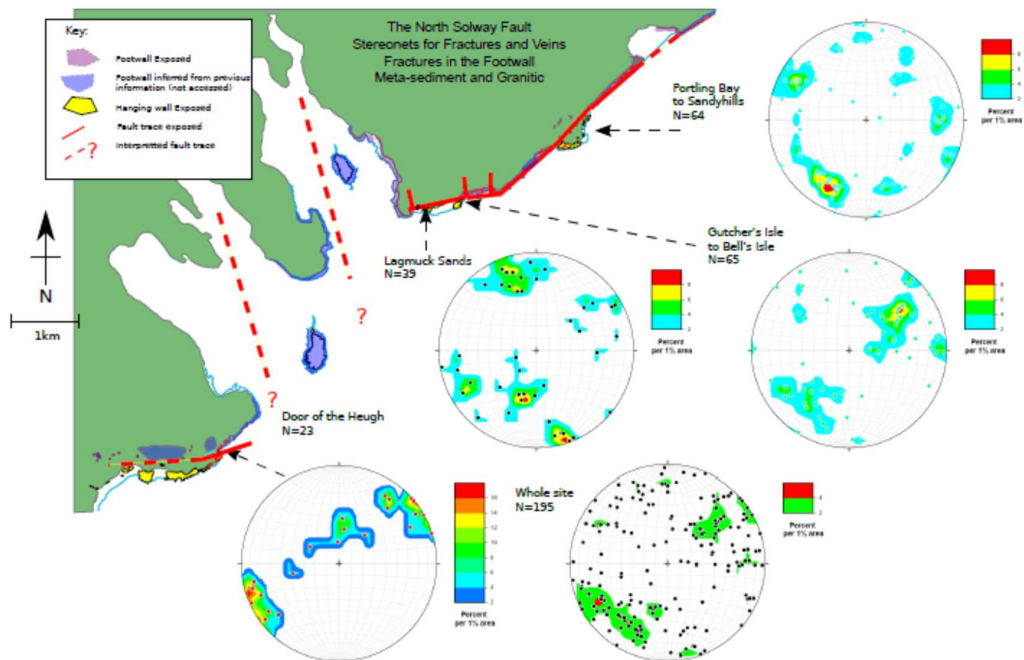


Figure 5-21 Stereographic projection of poles to planes of fractures in the footwall

Both footwall lithologies have been plotted together (Figure 5-21). At Portling Bay to Sandyhills, there is a spread of fracture orientation with a cluster around ENE-WSW (approximately fault perpendicular), dipping approximately 70° . Two smaller clusters are oriented NNW – SSE and N-S.

At Gutcher's Isle, two antithetic clusters are oriented roughly NE-SW. The cluster which strikes to the SW (right hand rule) have variable dips from $>20^\circ$ to sub vertical but have a narrow spread of strike. The dips of the cluster which strike to the NE are less variable (c. 30° to 70°) and the strike is spread between NNW and WNW. These two clusters are approximately perpendicular to the main fault trace and roughly parallel to the small cross faults which were are marked on the map.

At Lagmuck Sands, a cluster of fault parallel steeply dipping fractures are oriented ENE-WSW. The cluster contains fractures which are both synthetic and antithetic to the fault zone. A shallower dipping cluster also strikes roughly parallel to the main fault trace at this location. A weaker concentration of fractures antithetic to each other strike fault NNE-SSW which perpendicular to the main fault trace and parallel to the cross faults marked on the map.

At Door of the Heugh, the fractures measured are cutting meta-sediment only as granitic footwall is not exposed at this location. The fractures are predominantly steeply dipping and oriented NNW – SSE with a shallower dipping cluster striking approximately E-W. These could represent fractures which are perpendicular to the meta-bedding at this location.

When all locations are plotted together, the variability of fracture orientation is notable with only a weak cluster of roughly NW-SE fractures. The cluster is predominantly steeply dipping with a lower concentration of shallower dipping fractures evident.

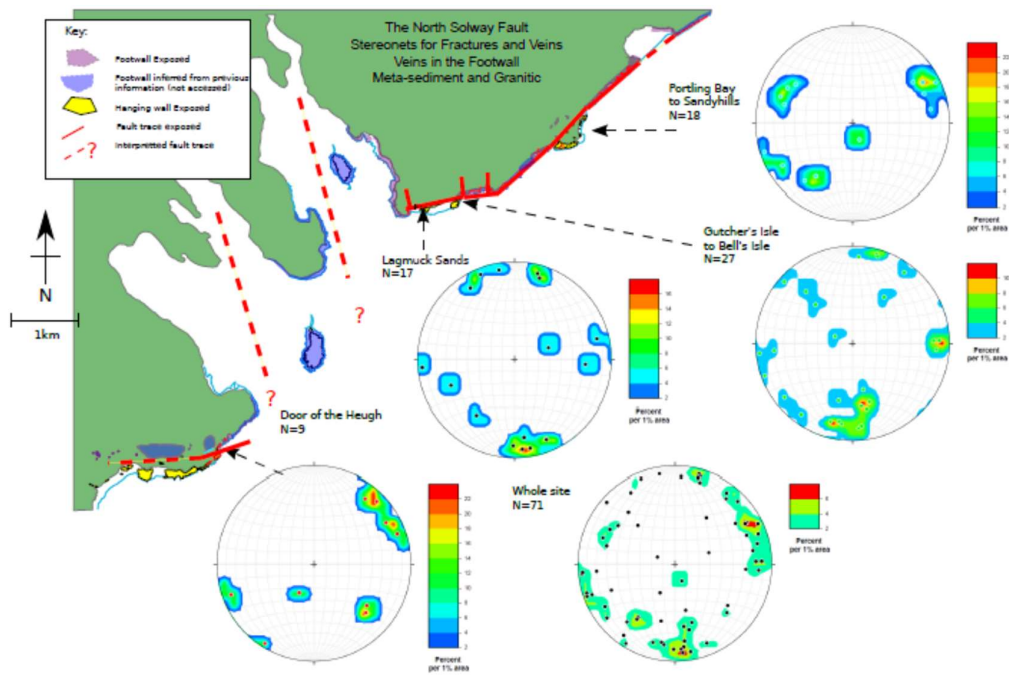


Figure 5-22 Stereographic projection of poles to planes of veins in the footwall

The plots of poles to planes of foot wall veins (Figure 5-22) shows that at Portling Bay, there is a cluster of steeply dipping NNE-SSW veins. There is also a cluster of NNW – SSE veins, dipping approximately 60°. At Gutcher’s Isle there is a cluster of veins which strike E-W with dips ranging from around 40° to sub vertical. A smaller cluster of steeply dipping veins strike N-S. At Legmuck Sands, there is a cluster of steeply dipping E-W oriented veins. At Door of the Heugh, a steeply dipping cluster of veins strike roughly NW-SE.

When all veins in the footwall are plotted together, there is a cluster of E-W oriented veins which are steeply dipping. There is also a steeply dipping cluster of NNW-SSE veins. Compared to the veins in the hanging wall and breccia, the orientation of veins in the footwall appears to be more varied.

5.4.4 Veins through clasts

Veins in both the hanging wall and the breccias are typically hosted in matrix. However, at 3 separate locations veins were observed to cross from the surrounding matrix through clasts. This was observed in both the hanging wall breccia (all 3 locations) and the tectonic breccia (Lagmuck Sands only). The veins which cut through clasts are all oriented roughly NW-SE similar to the dominant trend of veins in the hanging wall (Figure 5-23). There were 20 separate veins found to cut clasts suggesting that although the veins cut clasts relatively infrequently, they occur along the whole fault and not just locally.

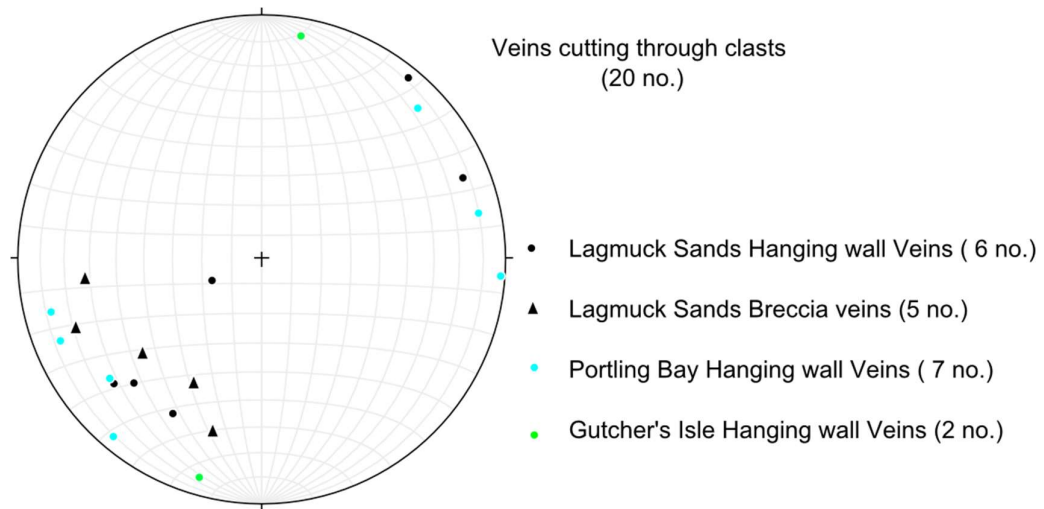


Figure 5-23 Poles to planes stereographic projection of Veins which cut through clasts

The veins cutting clasts, as shown in Figure 5-24, suggests that clasts are broken down through bulk crushing as described in section 2.4.3, rather than, or as well as attrition. Attrition would be expected to affect the outer edges of clasts rather than break through the centre. Implosion or dilation of a breccia would be less likely to fracture through a clast as this could only happen if the bond between matrix and clast was stronger than the clast material.

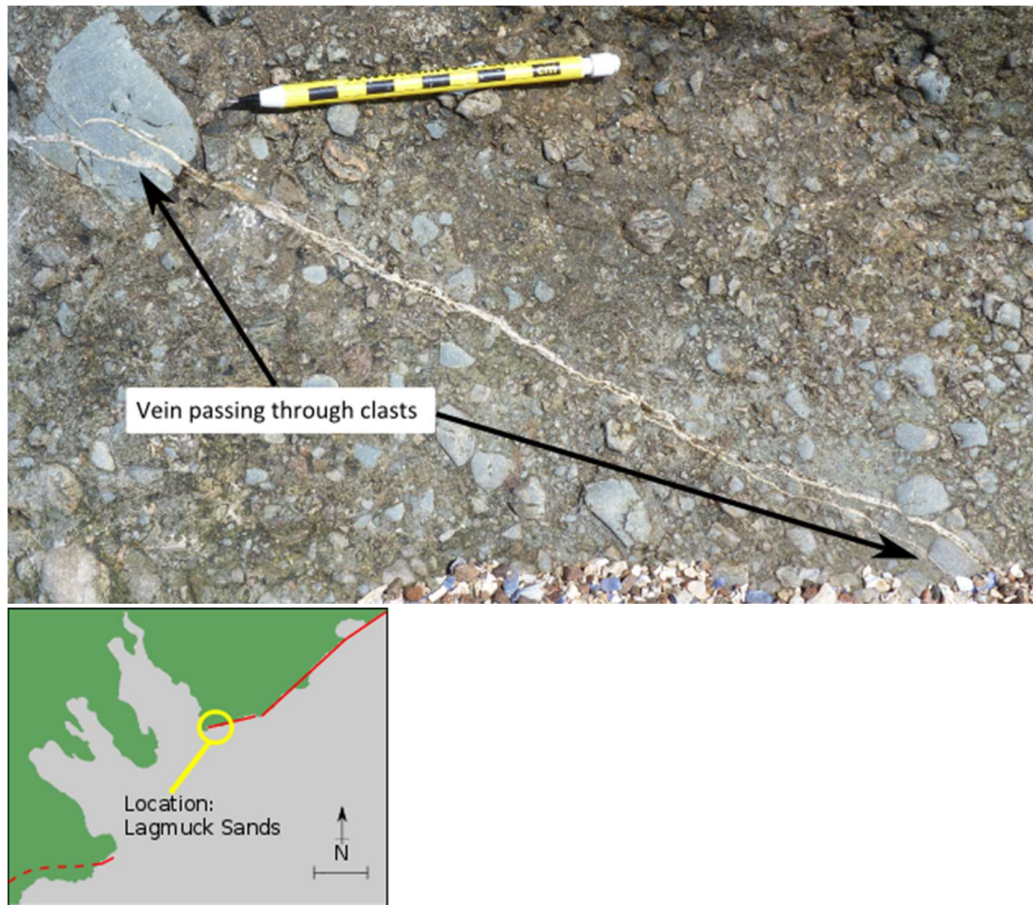


Figure 5-24 Vein in tectonic breccia passing through clasts. The scale showing on the yellow pencil is 10mm intervals

5.4.5 Interpretation of Fracture and vein Data

Fracture strike and dip vary with lithology in the footwall. The two lithologies which make up the basement rocks along the north Solway fault have contrasting macro structures which may go some way towards explaining the variable fracture orientations. The meta-sediments have retained the meta-bed structures and these former bedding planes themselves are significant discontinuities.

The meta-bedding planes are roughly oriented NE-SW. The two clusters dip antithetically and represent opposing fold limbs (Figure 4-3). The tight clusters of fold limbs suggest that the majority of the meta-sediment folds are similarly oriented.

Fractures forming in the meta-beds may be heavily influenced by the macro-scale fabric of the beds. The dominant orientation of meta-sediment fractures at all locations of the site is roughly NW-SE, perpendicular to the meta-bedding.

A more variable orientation of fractures is shown in the stereonet of granitic (Figure 5-19) than metasedimentary rocks (Figure 5-20). The dyke-like morphology of the granitic intrusions produce less pervasive and less regular discontinuities than the meta-bedding, and do not seem to have controlled fracture spacing. The fracturing occurring after the intrusion of the dykes could then be expected to form in more variable orientations in the response to the macro-scale fabric.

At most locations along the fault, fractures in the footwall lithologies display a rough NW-SE cluster (Figure 5-21). This is generally perpendicular to the structural trend of the region and the orientation of the North Solway fault. A similar trend is observed in the near-fault basin sediments (Figure 5-14) and within the breccia of the fault zone (Figure 5-17). The trend is matched in the veins cutting all 3 components of the fault and the veins which passed through clasts. This single dominant orientation cutting all lithologies may represent deformation which occurred after the formation of the youngest hanging wall Carboniferous rocks. The pervasive NW-SE trend is roughly similar to the regional phase of extension which formed the NNW-SSE Permo-Triassic basins (described in Chapter 3).

5.4.6 Summary of discontinuities and veins

In summary, observations of the veins and fractures show:

- A persistent broad NW-SE orientation of fractures and veins are found in all units of the NSF.
- The dominant strike of fractures and veins is at high angles to the fault.
- Fault parallel fractures are rare, including within the hanging wall suggesting simple hanging wall distortion during extension is not the dominant cause of fractures.
- Veins in all lithologies tend to be steeply dipping. Footwall veins are more variably oriented than the veins in the hanging wall and breccia.
- Fractures which strike at high angles to the fault cut all lithologies. Some of these fractures have remained open for long enough periods to allow mineral rich fluids to flow through them.
- The fact these fractures are present in the hanging wall indicates these sediments were lithified.

6. The North Solway fault Geometry

This Chapter discusses the geometry and throw of the North Solway fault (NSF) at the whole-fault scale. The NSF downthrows a hanging wall of predominantly coarse clastic sediments against a footwall of igneous and metasedimentary basement.

6.1 Fault Plan View Geometry

In plan view geometry the NSF displays a variable strike between ENE-WSW and NE-SW (Figure 6-1). As described in Chapter 4, the NSF is exposed in extensive strike direction (several km) but from Door of the Heugh to Lagmuck sands there is no exposure due to tidal sediments and to my knowledge, no publicly available seismic surveys in that location. Two large bays along the trend of large NNW-trending faults at this location could be part of the fault system (See Figure 3-3 and Figure 6-1).

There are three competing models in the literature which could be applied to the geometry of the NSF:

1. The NSF may be a multi-segment fault similar to that described in a review by Fossen and Rotevatn (2016) and references therein
2. The NSF may be offset by major NNW-trending transfer faults similar to that proposed by Gibbs (1984). Gibbs's model was applied to the Solway basin by Barret (1988).
3. The segments represent non-coaxial extension similar to the model of Henstra et al (2015).

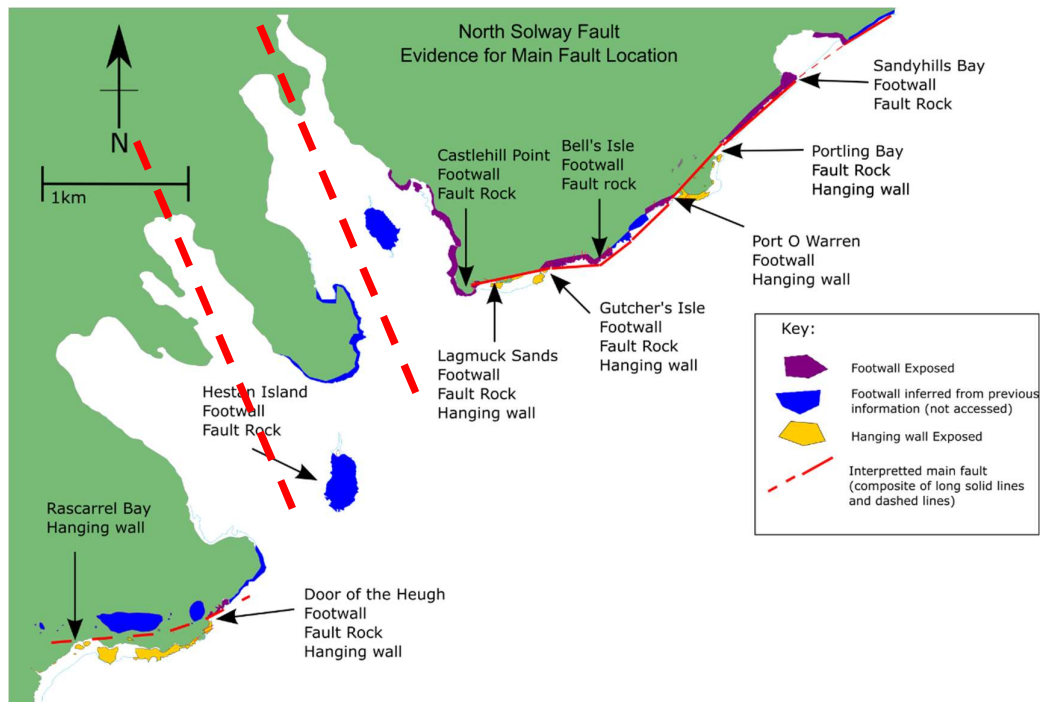


Figure 6-1 Reproduction of Figure 4.1 showing the evidence of the main fault trace of the North Solway, with the addition of indicative cross faults in the large bays.

1. The multi-segment model (Figure 6-2 a)

The development of large segmented faults has been split into 2 separate mechanisms by Fossen and Roetvatn (2016); isolated fault segments which coalesce to form large through-going faults, and coherent faults which form as a continuous fault above a buried structural lineament (Figure 6-3).

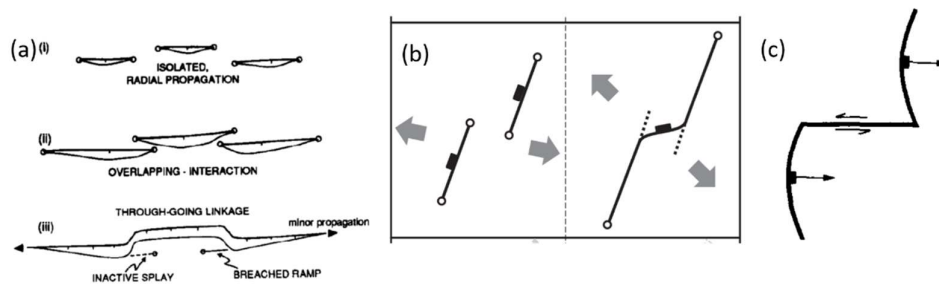


Figure 6-2 Three models for the formation of zig-zag plan view geometry. (a) Cartwright et al (1995) model of isolated segments which link kinematically and form a large fault as the segments become soft linked. (b) from Henstra et al (2015) where non coaxial extension results in fault segments being linked by later, oblique faults. (c) Gibbs (1984) model of transfer strike-slip faults forming at the same time as the normal fault segments.

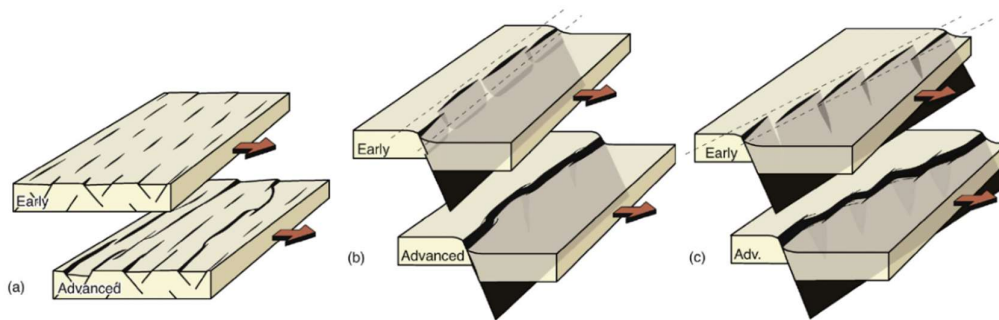


Figure 6-3 Mechanisms for forming large segmented faults. (a) Isolated segments model, (b) coherent fault from segments parallel to an underlying structure, (c) variation of (b) where fault segments form oblique to an underlying structure. Red arrows show the direction of extension and the dashed lines in (b) and (c) represent the trend of the underlying structure. Figure from Fossen and Rotevatn (2016).

The basement rocks of the NSF are not homogenous because the meta-sediments were later intruded by Caledonian intrusions, and the NSF seems to have formed at the margins of these intrusions. Large granitic intrusions such as the Alston Block and the Lake District Block are often flanked by normal faults as is shown in Figure 6-4. This is thought to be due to the relative buoyancy of the crystalline granitic rock compared to the surrounding basement.

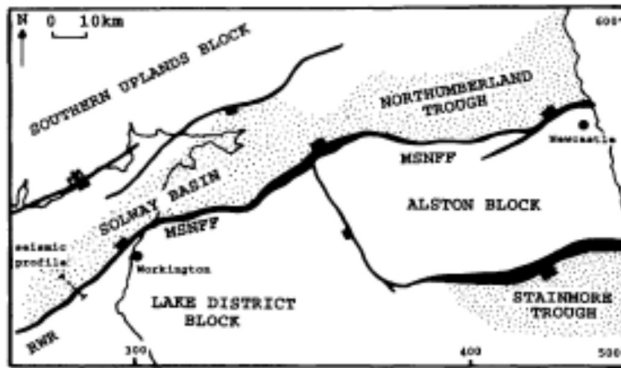


Figure 6-4 Map view of the Northumberland - Solway system showing normal faulting at the flanks of the Alston Block and Lake District Block. The North Solway fault is represented by straight line on the left hand side of the figure. From Chadwick et al (1993).

Figure 6-3 (b) and (c) show the coherent fault mechanism whereby an underlying basement structure exerts control on fault development in the strata above. When a large structure is reactivated, faults form perpendicular to the contemporary direction of least compressive stress and form a series of parallel segments. Figure 6-3 (b) shows the formation of segments parallel to the underlying structure in response to a direction of least compressive stress that is perpendicular to the underlying structure. When the direction of least compressive stress occurs oblique to the strike of the underlying structure the trend of the fault segments form perpendicular to the least compressive stress direction but the whole fault zone is in line with the underlying structure and the segments from oblique to the rest of the fault (Fossen and Rotevatn 2016) as shown in Figure 6-3 (c). The key point for this thesis is that Figure 6-3 (b) and (c) shows either mechanism of initiation for large faults results in a zig-zag geometry in plan view; this is discussed further in Section 6.1.1. As described in Section 3.3, the NSF follows the trend of the earlier subduction zone, so is likely to have been influenced by a deeper fault zone.

2. Transfer faults (Figure 6-2 b)

Gibbs (1984) presented a model for fault growth at basin margins where transfer faults form coevally with the main fault (Figure 6-5). Transfer faults form in response to normal

fault slip on two parallel faults. To accommodate slip on both faults at the same time an oblique transfer fault forms between the two surfaces. This is in contrast to the other models presented here which require transfer faults to form later than the initial faults.

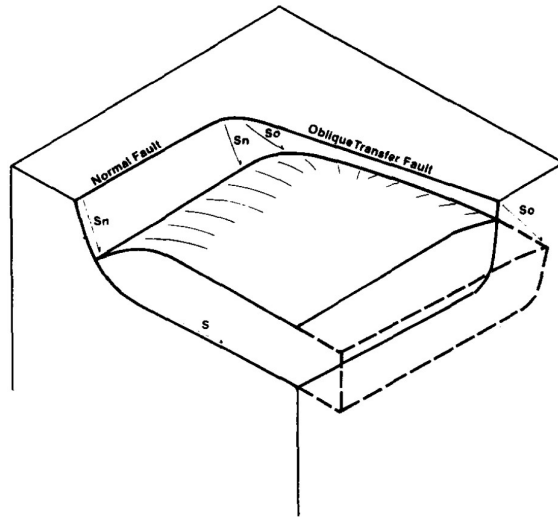


Figure 6-5 Isometric sketch of normal fault slip (S_n) and oblique fault slip (S_o) on a listric fault surface, connected to a shallow dipping sole detachment (S), from Gibbs (1984).

Listric normal faults connect to a “*sole detachment*” along which extension is accommodated. For faults synthetic to the underlying detachment hanging wall rollover is towards the fault, for faults that are antithetic to the underlying detachment, sediments are tipped towards the basin (Figure 6-6). As described in Section 4.4 bedding in the hanging wall broadly dips towards the basin. Beamish and Smythe (1986) estimate the Iapetus suture to be broadly northward dipping, this implies that the NSF is likely to be antithetic and the Maryport fault is likely to be synthetic to the Iapetus structure. The Gibbs model is therefore compatible with the dip of the hanging wall beds at the NSF and the estimated dip of the Iapetus suture.

Fossen and Rotevatn (2016) expressed doubt about the listric geometry with deep linkage to a sole detachment as being an artefact introduced by the strong focus within structural geology on such geometries at the time. They argue that basin bounding faults and transfer

zones which accommodate syn-sedimentary faulting at opposite sides of the basin do not have to be listric in order to be geometrically viable.

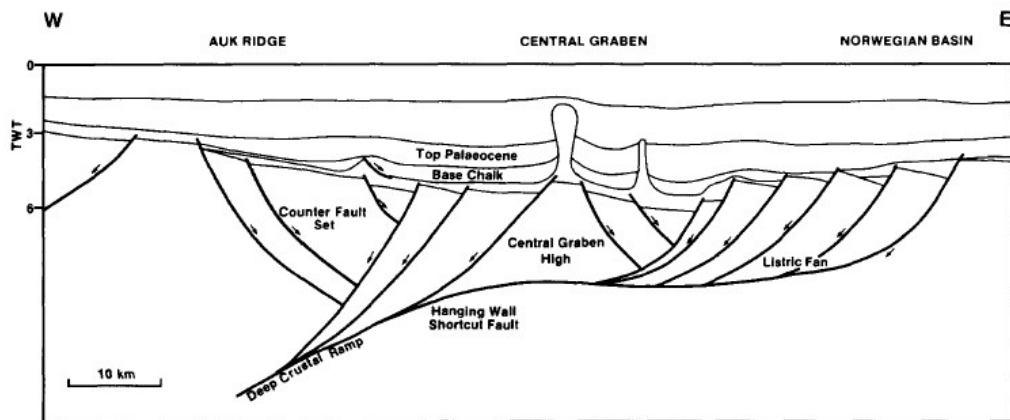


Figure 6-6 Gibbs (1984) cross section showing listric fault geometry in the North Sea. The hanging wall beds adjacent to synthetic faults dip away from the basin. The hanging wall beds adjacent to the anithetic faults dip towards the basin, similar to that at the NSF.

3. Non-coaxial Extension (Figure 6-2 c)

A third model is the coaxial extension model of Henstra et al (2015). In a study of seismic data crossing the Vesterdjupet fault zone at the margin of the North Traena basin in Norway, Hentra et al suggested that a zig-zag plan view geometry of a basin margin fault zone can be caused by a rotation of the stress field. Early segments which may be widely spaced, are subsequently linked by new segments that are oblique to the first set due to the rotation of the stress field. Henstra et al argue that a rotation of the stress field of 30-

50° between the Early Triassic and the Late Jurassic to Early Cretaceous resulted in new faults forming between the initial segments as is shown in Figure 6-7.

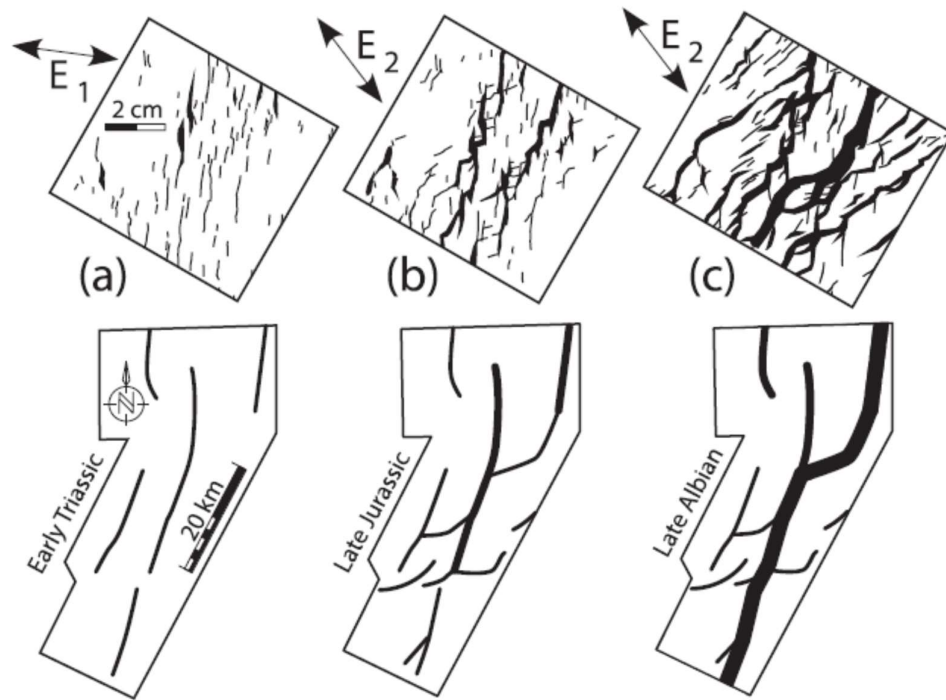


Figure 6-7 Formation of zig-zag plan view geometry at the North Traena Basin margin, Norway. The initial faults created in the stress field E1 are linked by subsequent faulting in the direction E2. From Henstra et al (2015).

This mechanism for the development of overlapping may explain segmented faults which appear too far apart to interact. The inference from the Henstra et al model is that stress field rotation forms new faults which develop later than the initial segments. Faulting on the original segments may continue if the orientation to the stress field is favourable or these segments may be arrested if the stress field orientation is unfavourable (i.e. if the rotation is high enough).

6.1.1 Interpretation of the North Solway fault plan-view geometry

A deep shear zone has been interpreted from seismic surveys to underlie the Solway – Northumberland basin complex, which is thought to represent the Iapetus Suture (Beamish and Smythe 1986; Chadwick and Holliday 1991). The exact trend of the Iapetus suture is unknown but is approximately in line with the regional structural trend which is between E-W and NE-SW. Segmented faulting along the NSF could be in response to extensional reactivation along the line of the Iapetus suture which is thought to be in a broadly N-S direction (Chadwick et al 1995).

The extension direction at the time of basin onset or the trend of the underlying structure itself are not well constrained. What can be done is to sketch out possible fault segments and linkage to determine if segment linkage in the sense of Fossen and Roetvatn's (2016) isolated segments mechanism is viable. Figure 6-8 shows speculative segments sketched where the fault is obscured in an attempt to link the two separate sections of the fault. Segments are drawn parallel to either the NE-SW or the ENE-WSW observed segments.

In Figure 6-8 two scenarios are shown that link the map view geometry of the NSF using segments that are parallel to the mapped segments. Extending a single segment oriented NE-SW from Door of the Heugh results in overlapping segments at Castlehill point. The inclusion of an ENE-WSW segment also results in overlapping of the segments. Linking the mapped segments by parallel speculative segments does not result in a simple linked segmented fault with zig-zag plan-view geometry. The multi-segment models described above do not provide a satisfactory explanation for the present geometry of the NSF. Therefore, multi-segment linkage models alone do not adequately explain the current geometry.

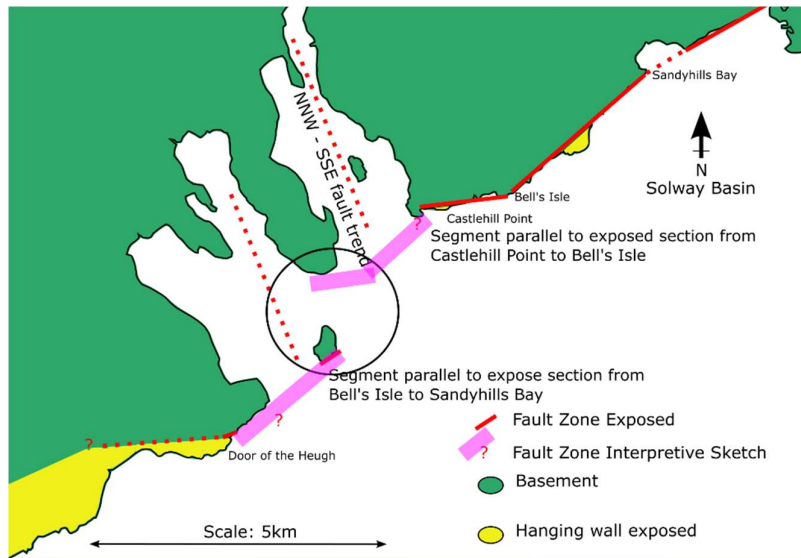
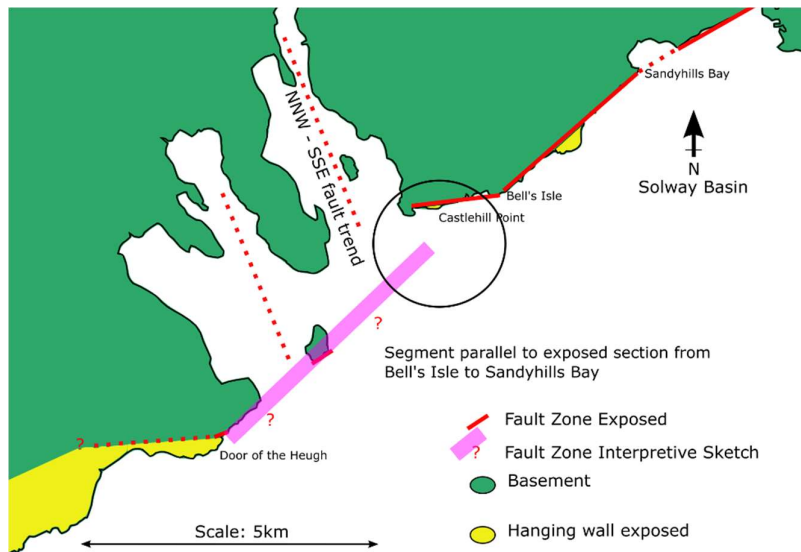


Figure 6-8 Sketches of potential fault geometries in the obscured section of fault zone between Door of the Heugh and Castlehill Point. A thicker pink line is used to show interpretive fault segments to make it clear which segments speculative and which are mapped. The black circles highlight the locations where segments overlap when segments are drawn parallel to the mapped segments.

The NSF may have been influenced by another set of structures. One possibility is that transfer faults may have formed at the same time as the main segments. R.A Chadwick (*pers comm.* 2018) has reported that the NNW-SSE structures in the Northumberland-Solway region (the Pennine fault shown on Figure 6-11 and the Lake District Boundary fault

off the page to the left of Figure 6-11) offset the base of the Permo-Triassic sediments. This gives confidence that these structures were active after base Permian and it is likely that activity continued beyond the Triassic.

The large NNW-SSE trending bays may be indicative of such faults. Figure 6-8 shows that without some strike-slip offset along such transfer faults the mapped and projected segments don't meet. This suggests that, at least to some degree, the Gibbs model or the Henstra et al model is necessary to account for the NSF segment geometries. There are minor faults in this orientation that cut the footwall but offset along these faults is difficult to infer as no marker beds exist except at Door of the Heugh, where left lateral offset is less than 1m in one fault only. Due to lack of appropriate markers, for the vast majority of cross faults in this orientation exposed in the footwall there are no mappable indications of direction or magnitude of offset.

Without knowing the magnitude and direction of offset in the major cross faults at the NSF, either of the Gibbs or Henstra et al models could apply. The distinction in timing between the two models is that the cross faults form at a later date in the Henstra et al model (normal faults) rather than coevally with the first generation of normal faults in the Gibbs model (transfer faults). The Gibbs model would likely form oblique faults which are predominantly strike-slip and the Henstra et al model would likely form dip-slip faults (with a minor oblique component). No kinematic indicators on the cross-faults were found in the present study, which would be conclusive evidence for the direction of offset. However, the offset direction required to create the overlap shown in Figure 6-8 is compatible with the Gibbs model. The Henstra et al model cannot be ruled out on this basis alone.

Barret (1988) produced a model for the growth of the Northumberland-Solway basin complex that constituted stable margins (sediments pinch out at the edge of the basin),

faulted margins (sedimentation along normal faults) and a series of half-grabens separated by large transfer faults striking perpendicular to the basin margin as shown in Figure 6-9. Active faulting can occur at opposing margins of the basin during extension as transfer faults accommodate strike-slip deformation. Fault activity on opposite margins of the basins controlled sedimentation across the Northumberland-Solway basin system.

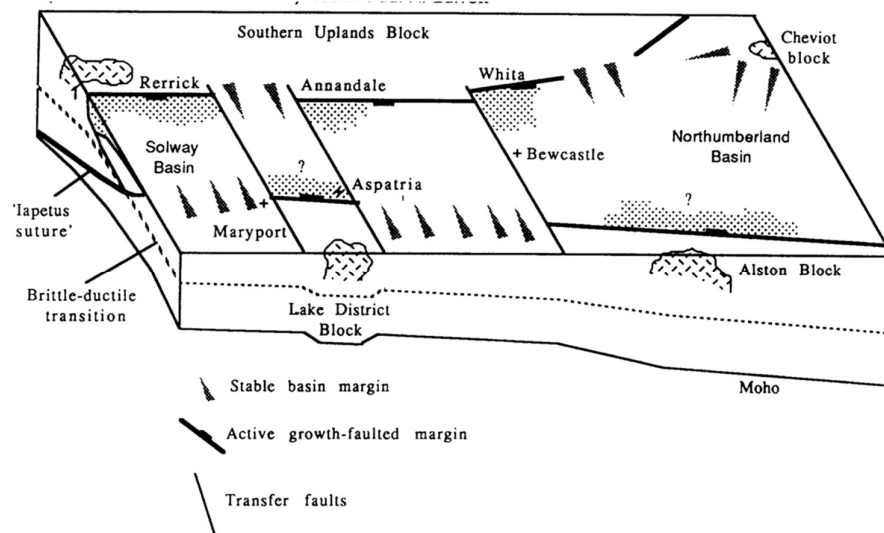


Figure 6-9 Model for reverse polarity of basin sedimentation which includes large transfer faults which cross the basin. After Barret (1988)

The Floodpage et al (2001) seismic lines in Figure 6-10 include a basin-parallel line from the SW edge of the Solway basin just to the east of the NSF. At the NE end of this seismic line a large fault zone dipping approximately 70° SW cuts the basin sediments as well as possibly extending into the basement. Parallel to this fault, another fault is contained within the Carboniferous sediments and the basement, but not in the post-Variscan sediments above. It is possible these faults represent major transfer faults which cut the basin sediments and the basement rocks. Faults at high angles to the basin margins, as predicted by the Gibbs

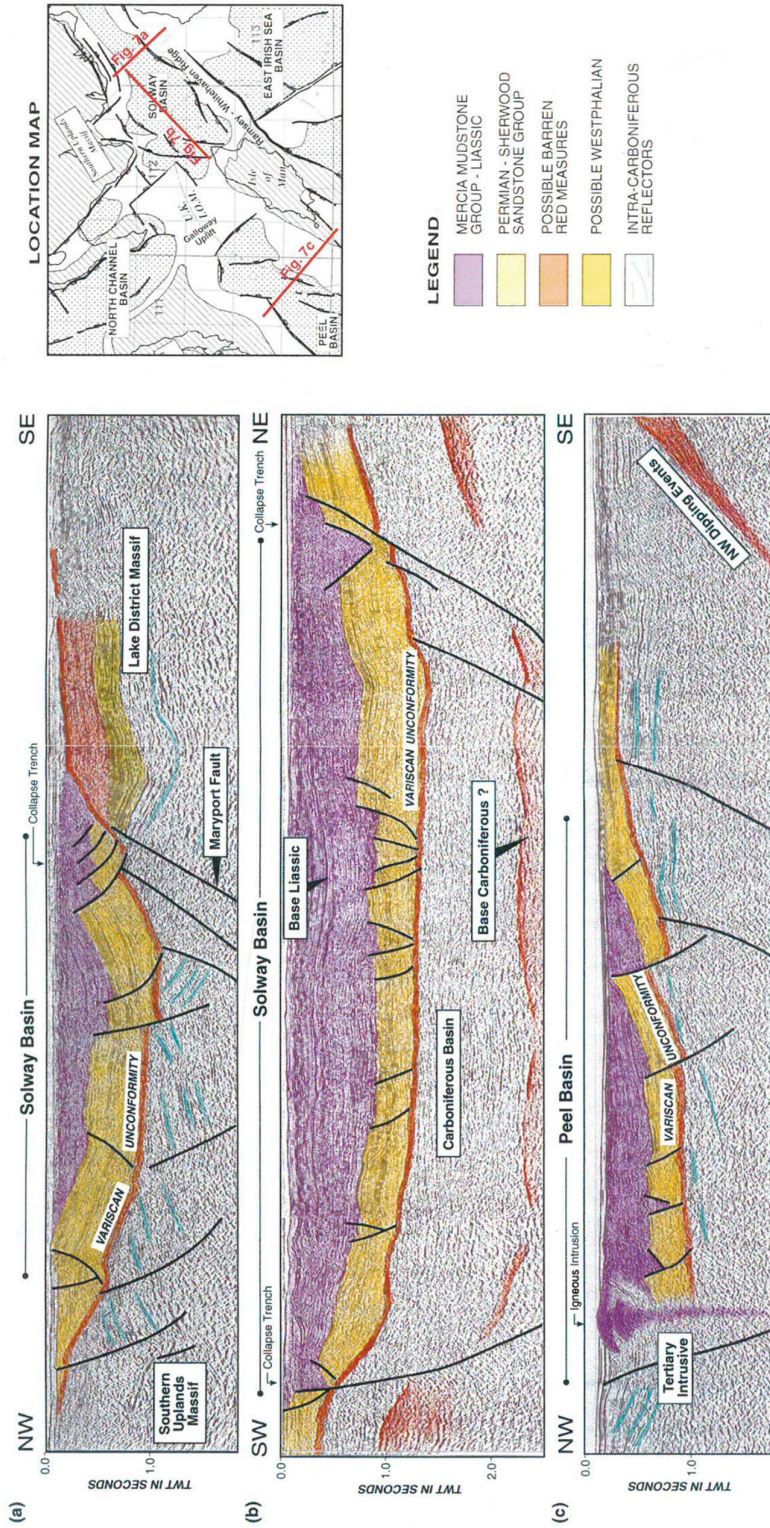
(1984) model could therefore be present across the whole basin, not just at the margins.

The Barret (1988) model could also be valid if these structures are strike-slip transfer faults.

Chadwick et al (1995) report that no evidence in support of the Barret model was found in their study. Their study was wholly focussed to the east of the NSF and didn't include seismic lines parallel to the basin margins. Evidence of major cross basin transfer faults is less likely to be encountered in a study which doesn't include seismic sections oriented parallel to the basin margins. Sediments adjacent to the NSF dip toward basin, consistent with the Gibbs model as the NSF which is antithetic to the underlying Iapetus suture. The basin-ward dipping faults that trend parallel to the NSF are required to link to the NSF and for this geometry to be valid, these faults need to be listric. The seismic interpretation in Chadwick et al (1995) and Floodpage et al (2001) show faults with a curved down dip geometry but they do not link towards a "sole detachment" as required geometrically by the Gibbs model although it should be noted that the detachment may be deeper than the sections.

In summary, fault segment mechanisms alone are not viable at the NSF. Strike-slip offset along structures at high angle to the main fault trend are required to explain the current geometry of the NSF.

Figure 6-10 reproduction of Figure 3-4. Interpretation of seismic lines in the Peel and Solway basins, from Floodpage et al (2001).



6.1.2 Fault Throw

Basement lithologies in the footwall of the NSF means that there are no exposed marker beds with which to estimate throw. Scarp heights of 10s of metres along the exposed fault provide minimum values for throw, but as will be discussed below, throw along the NSF is likely to be much greater than the modern-day scarp heights.

Along-strike from the Solway basin, the Northumberland Trough is thought to have formed due to subsidence which was principally facilitated by faulting along the Maryport-Stublick-Ninety Fathom system (MSN). The MSN fault system (Described in Section 3.2. and shown on Figure 3-3) is a major through-going structure at the southern margin of the Northumberland basin extending for c. 120km along-strike, and with a maximum throw of up to 5000m (Chadwick et al 1995). The Northern Margin of the Northumberland Solway basin complex consists of shorter discontinuous faults with throws up to 1000m (Chadwick et al (1995). Deegan (1973) reported an estimated maximum throw of c.600m at Door of the Heugh based on the cumulative thickness of sedimentary succession in the vicinity of the fault.

Figure 6-11 shows interpreted seismic lines from the Northumberland Trough and the eastern section of the Solway basin, from Chadwick et al (1995). East of the North Solway fault, the northern margin of the Solway basin is thought to onlap the Southern Uplands. A fault may exist below the onlapping sediments. There are normal faults along strike of the NSF that downthrow basin sediments to the south, however some of the oldest sediments in the basin (Lower Border Group, pink with white dots in Figure 6-11 Seismic line B-B') pinch out to the north of these faults. The implication of the Chadwick et al (1995) study for the NSF is that the fault is not part of a continuous large through-going fault defining the northern margin of the Northumberland-Solway Basin complex.

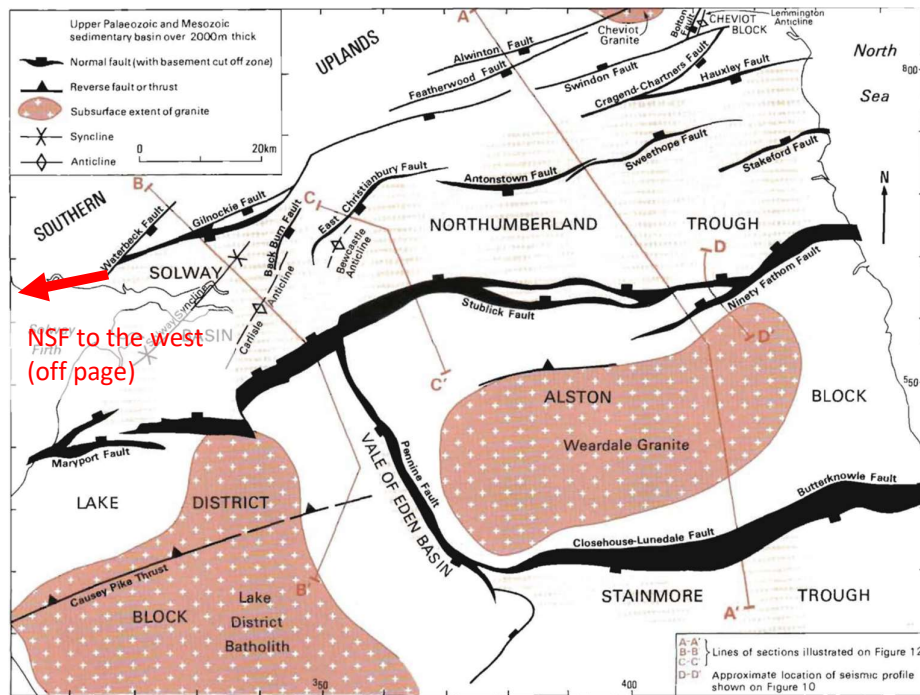
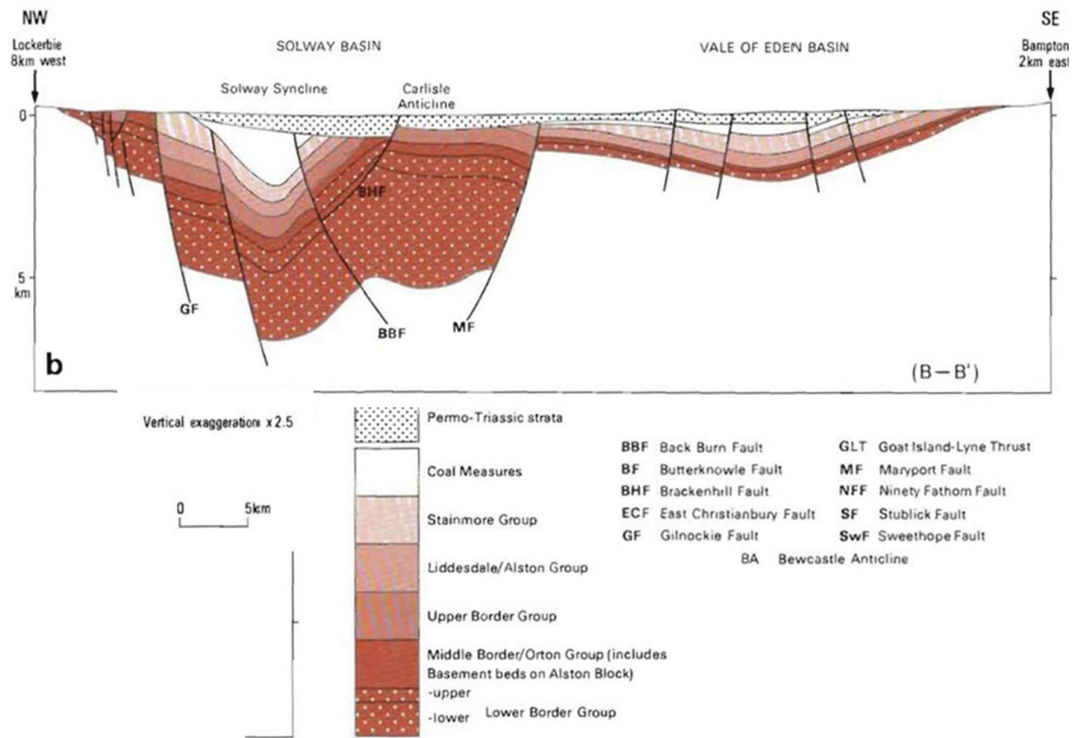


Figure 6-11 Cross sections and structural map of the Solway Basin (to the east of the NSF) and Northumberland Trough from Chadwick et al (1995).

The seismic sections shown in Figure 6-10 after Floodpage et al (2001) do not cross the basin boundary but do show that a number of synthetic parallel normal faults in sedimentary sequences to the south east of the NSF field exposures. Both Floodpage et al (2001) and Chadwick et al (1995) show that there are sub-parallel synthetic normal faults within the Solway-Northumberland basin complex. Total throw is distributed across several structures and not entirely accommodated at the basin margin. If a basin margin fault is a single controlling element on basin growth, the throw could be estimated by the thickness of the sedimentary deposits in the basin. However, throw on the NSF is likely to be less than the total sediment thickness as some space for the basin sediments must be accommodated within the parallel faults that are synthetic to the NSF.

A key parameter for limiting the maximum throw on a fault is fault length. Constraining the total length of the NSF is in itself a difficult task as the fault is only exposed for c. 10km along strike but various authors (Deegan 1973; Ord et al 1988; Lintern and Floyd 2000; Chadwick et al 1995) have estimated the length of the fault to be greater than that currently exposed. In those studies, the presence or absence of the NSF is interpreted from hanging wall sediments. Coarse angular clast dominated beds are interpreted as resulting from sedimentation at the foot of a fault scarp and the disturbance of soft sediments are interpreted as occurring adjacent to an active fault. All authors agree that there is little evidence for the fault west of Rascarrel Bay and east of Kirkbean (to the west of Sandyhills Bay). This constrains the maximum fault length of the NSF to be approximately 20km.

Figure 6-12 shows the extent of the exposures of the NSF against the extent of the NSF mapped by Newman et al (1999). The exposed section is short, perhaps half the estimated along-strike length of the NSF. Within the exposed length shown on Figure 6-12 there are

sections of the fault with limited or no exposure, such as the large bays interpreted as cross faults (dashed red lines in Figure 6-12).

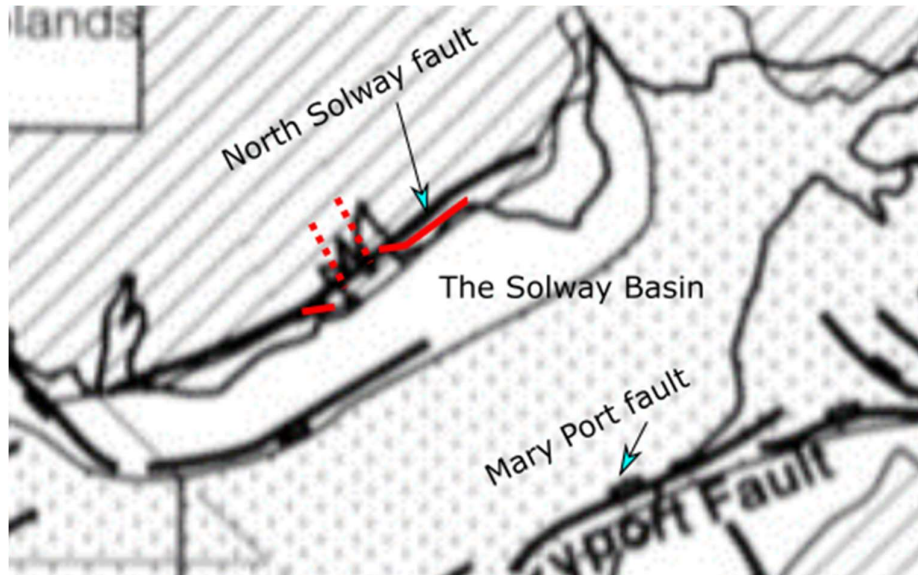


Figure 6-12 the extents of the NSF from the present study (in red) superimposed on a close-up of a map of the Solway basin in Newman et al (1999). The NSF in the Newman et al map is shown as a straight black line.

Schlische et al (1996) plot fault length and displacement for several faults in different tectonic settings and rock types (Figure 6-13). For faults with a length of order of 10-20km in length, maximum throw can be expected to be between 100m and 1500m. This is a simplification of a complex process of fault growth by slip accumulation and yields a throw value which varies by more than an order of magnitude.

The accumulation of fault slip on the scale of a fault such as the NSF requires multiple earthquakes or slip events (Cowie and Shipton 1998). Even the largest single fault rupture events are unlikely to add more than several meters of slip (McCalpin 1996), thus to accumulate the order of magnitude of throw at the NSF requires multiple slip events. This

has important implications for the architecture of the fault as slip must have occurred several times on the same fault. This will be discussed in Section 7.

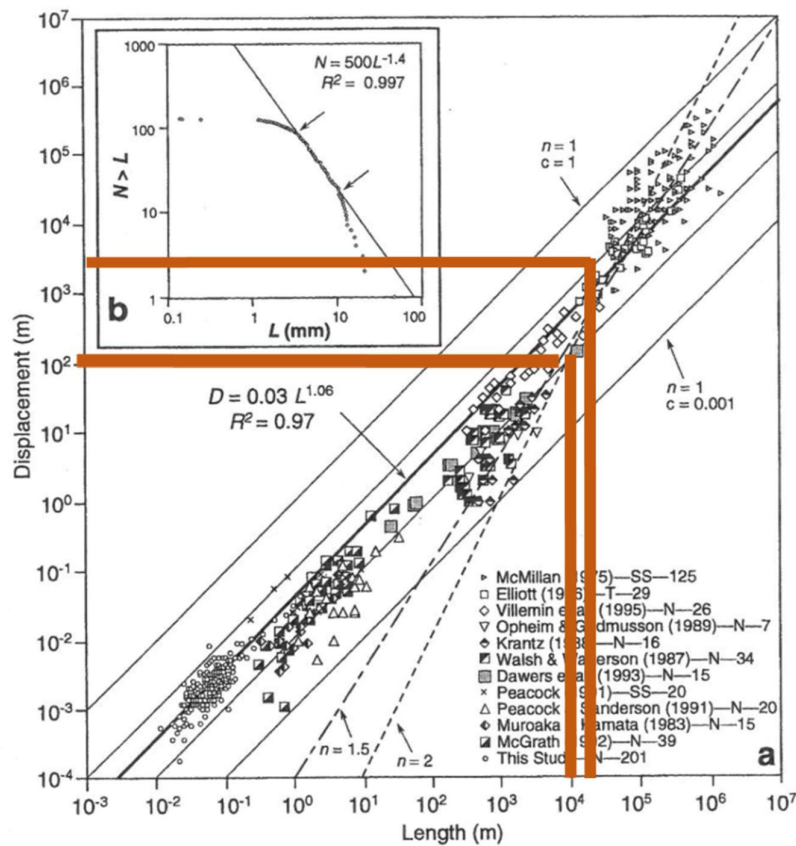


Figure 6-13 Fault length v displacement plot from Schlische et al (1996) annotated (brown lines) to highlight the values used in the present study. Maximum and minimum values for the length of the NSF (brown lines) are projected to estimate the possible range of throw for the NSF.

the throw on the NSF was estimated by setting upper and lower bound values for along strike fault length and comparing those values to the global data set in Schlische et al (1996). The resulting throw estimation varies between 100m and 1500m, demonstrating that large faults in general are not well constrained even when part of a fault is exposed at the surface. Global data sets can provide a very crude estimation on which to base an estimation of throw upon. The issue with using global data sets is that the many variables which have contributed to the development of individual faults are masked and the

estimates are therefore imprecise. Without indications of absolute throw such as marker beds, comparisons with global data sets are the best estimate possible.

Using subsurface data such as seismic surveys and interpretations shown in Figure 6-11 provides some degree of information, for example the structures parallel and synthetic to the NSF must have accommodated some throw to create the space for basin growth. We therefore know that throw on the NSF is less than the total thickness of basin sediments.

Large faults are however poorly understood and there is not enough data to compare individual faults to.

6.1.3 Summary of fault scale geometry

Normal faulting along the northern margin of the Northumberland-Solway basin complex is discontinuous and is not as through-going as the southern margin. Parallel faults within the basin means the throw on individual faults is smaller than the total thickness of the sediments. For fault segment models to be valid at the NSF some offset along major transfer faults is inevitable. The NSF has a limited throw compared to the total basin sediment thickness because the basin is accommodated on multiple fault strands.

From the above discussion it is evident that reconstructing the initiation and development of the internal architecture large km-scale faults is problematic. There are a number of reasons for this difficulty. Successive fault slip episodes occur within the same rock volume and cause evidence of earlier geometries to be lost. Exposures of large fault zones tend to be discontinuous which obscures many of the important structure (eg. the length of the NSF can only be estimated), and due to the relative sparseness of exposures with respect to fault zone variability, it is often difficult to develop any systematics between fault architectures and larger-scale fault geometry.

7. The North Solway Fault Internal Architecture

This Chapter will summarise the observations made in previous Chapters and place those observations into the context of the development of fault internal structure and flow properties of faults at basin margins. The 3D exposures of the internal structure of the NSF provide an opportunity to study a basin margin fault several kilometres in length which has undergone synsedimentary deformation. Only two previous studies of basin margin faults describe the internal structure of basin margin faults with crystalline footwalls and sedimentary hanging walls (Caine et al 2010; Kristensen 2016). As described in Chapter 4, detailed mapping of the internal structure of the NSF has revealed a complex 3D architecture which varies along strike between the 4 key field sites (Door of the Heugh, Lagmuck Sands, Gutcher's Isle and Portling Bay). This Chapter summarises and discusses the deformation elements that make up the NSF internal structure.

7.1 Breccia Formation

Most of the breccias at the NSF have a chaotic texture and are composed of clasts of both footwall lithologies (meta-sedimentary and granitic). There are some patches of single clast lithology breccias, for instance Figure 4-12, but the majority of chaotic texture breccias are mixed lithologies. Chaotic breccias consist of clasts which are completely detached from the host rock and have been rotated and translated to such a degree that it is not possible to fit them back together.

One possible mechanism for the formation of breccias at the NSF is brecciation into voids that form along the fault zone. Several authors have described dilation breccias forming in voids from wall rock implosion which result in a *jigsaw* texture breccia or *fitted fabric* texture, rather than chaotic textures. Sibson (1986) and Melosh et al (2014) describe a

fitted fabric or jigsaw breccia that would likely occur in breccias formed by wall rock implosion. Tarasewicz et al (2005) and Woodcock et al (2007) describe a similar jigsaw breccia at the Dent fault. Wright et al (2009) recognised crackle or mosaic breccia textures at the Gower faults, SW Wales. Caine et al (2010) described jigsaw texture breccia pods with a similar geometry to those encountered at the North Solway fault and attributed the formation of the pods to decompression boiling and rapid silica cementation in voids created by a corrugated fault surface.

All the reported examples of breccia due to wall rock implosion have crackle or mosaic textures because the mechanism requires a large pressure drop, which can cause minerals to come out of solution resulting in rapid cementation of the clasts. Conversely, as described in Section 2.6.4, Woodcock et al (2006) and Woodcock et al (2014) interpreted chaotic breccias to have formed by gravity collapse into a fault-related void, in part due to the observation of crude bedding within the breccias. This is a potential mechanism for the chaotic texture observed in the breccias at the NSF although no such bedding on a relevant scale was observed in this study. The principal differences between the Woodcock et al gravity collapse model and the Sibson (1986) implosion model are the length of time the void space is open and the mechanism of failure of fault void walls.

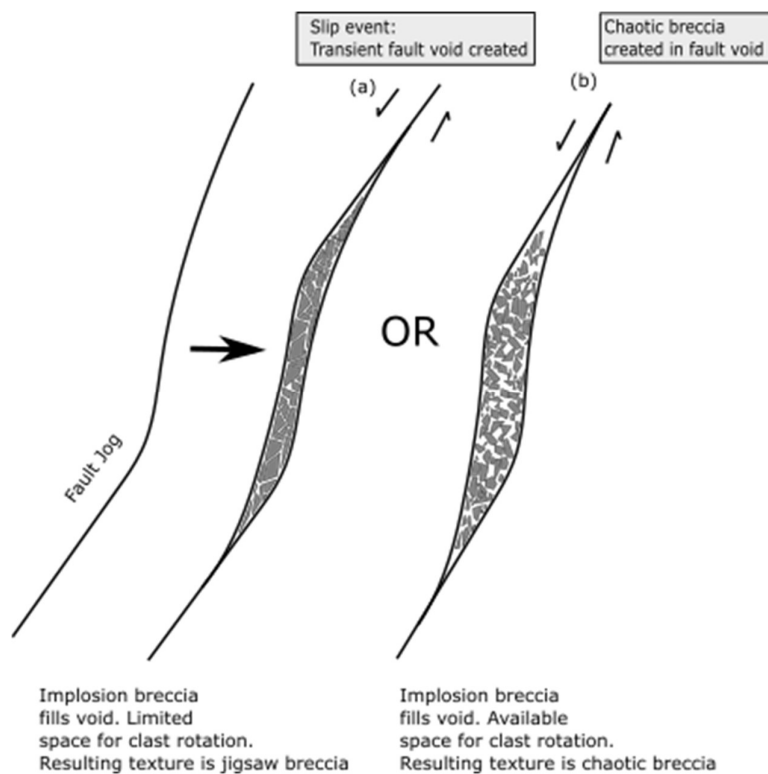


Figure 7-1 Formation of dilation breccias (a) with a fitted fabric and (b) with a chaotic texture.

I am proposing that the fabric that develops within such an open void depends not only on the length of time the fault void is open but also on the size of the void into which the breccia is formed. Figure 7-1 shows a possible mechanism for brecciation into voids which creates a chaotic texture (b) rather than a jigsaw texture (a). If a relatively small void is formed and the differential pressures supported by the wall rocks are high enough, the breccia will dilate into a jigsaw texture. This is because there is little space for clasts to rotate in when the breccia is formed. I am proposing that if a larger void is formed, the volume of breccia formed due to implosion may be relatively small compared to the volume of the void. This behaviour is analogous to rock bursts in underground construction (e.g. Mazaira and Konicek 2015) where small amounts of material can rapidly eject into relatively large voids. The implication is that implosion could create a chaotic texture instantaneously

if there is space for the clasts to rotate when free of the wall rock (Figure 7-1b). This mechanism would provide a chaotic texture breccia without the crude bedding that results from gravitational collapse. Dilation breccias are therefore not necessarily jigsaw textured and a possible mechanism for the breccia pods at the NSF is wall rock implosion.

7.1.1 Breccia pods

At Door of the Heugh and Lagmuck Sands, there are thick breccia deposits in the form of pods of chaotic breccia. The chaotic breccia is strong to extremely strong (strength description from BS 14689-1) and arranged in pods, which are separated by slip surfaces at Door of the Heugh and fractures with no appreciable offset at Lagmuck Sands. This requires an explanation as to why the deformation style is different at Lagmuck Sands and Door of the Heugh.

The slip surfaces at Door of the Heugh are characterised by a reduction in grain size likely due to cataclasis, accompanied by shear fabrics. This contrasts with the texture of the majority of the breccia volume which displays no evidence of shear. There are two possibilities for the development of shear surfaces in breccia described below:

1. Breccias are cemented or lithified

Fault slip event(s) creates a large body of breccia, several metres wide, possibly with a chaotic texture. Cementation of breccias occurs, either by mineral deposition from fluids (which may occur rapidly during the initial fault slip event or over longer timescales) and/or by lithification of breccias due to increased burial depth. This would increase the shear strength of the breccia. During further fault slip events, the breccias may deform along discrete surfaces accompanied by grain size reduction between two relatively competent surfaces.

2. Breccia remains in a granular state but is deformed at high confining pressures.

Strain localisation and grain size reduction has been shown to occur in 3D numerical simulation of granular materials by Mair and Abe (2008). This has also been proven laboratory experiments. Bolton (1986) and references there-in, describe how granular soils in laboratory shear tests fail by particle crushing when test pressures are sufficiently high to limit dilation of the sample. This causes shear stresses to overcome the strength of particles before the particles can move past each other. Gupta (2016) and references therein describe particle breakage in large-scale triaxial tests of rock fill material (particle sizes up to 100mm). The relevance to fault breccias is that shear stresses occurring under high enough confining pressures (eg. at depth) can cause the crushing of grains and grain size reduction within granular materials. The discrete slip surfaces are not therefore conclusive proof that cementation of breccia pods caused them to act as competent units. An alternative explanation is that granular breccia under large enough confining pressure deformed in a similar manner to coarse grained soils in shear box tests. Pod-like bodies of breccia described by Caine et al (2010) at the Stillwater fault, Nevada share similar characteristics with the breccia pods at the North Solway fault. Caine et al reports that matrix and clasts have been cemented to form a cohesive body of rock. At the NSF and at the Stillwater fault there are pods defined by slip surfaces and others are defined by fractures. The direction of pod long axis is oriented to down the dip of the fault at both sites.

A key interpretation made by Caine et al (2010) is that the pods at the Stillwater fault are formed by hydro-brecciation and decompression boiling. This indicates rapid cementation of breccias immediately after formation and is demonstrated by a matrix of crystalline mineral. The breccia at NSF is high strength and therefore must have been cemented or

lithified. However, there is little evidence to suggest extensive rapid mineralisation of the chaotic breccia at the NSF. There are some discrete veins within the breccia at the NSF but there is no indication that the matrix predominantly consists of quartz cement as is the case at the Stillwater fault. Figure 7-2 shows the contrast in texture between the Caine et al (2010) breccias (a) and the breccias at the NSF (b). The quartz mineralisation is clear in the Dixie Valley breccias whereas the NSF breccia do not display any mineral matrix visible with the naked eye. The rapid cementation of breccias from deep mineral rich fluids at the Stillwater fault interpreted by Caine et al (2010) is therefore not an appropriate model for the breccia at the NSF.

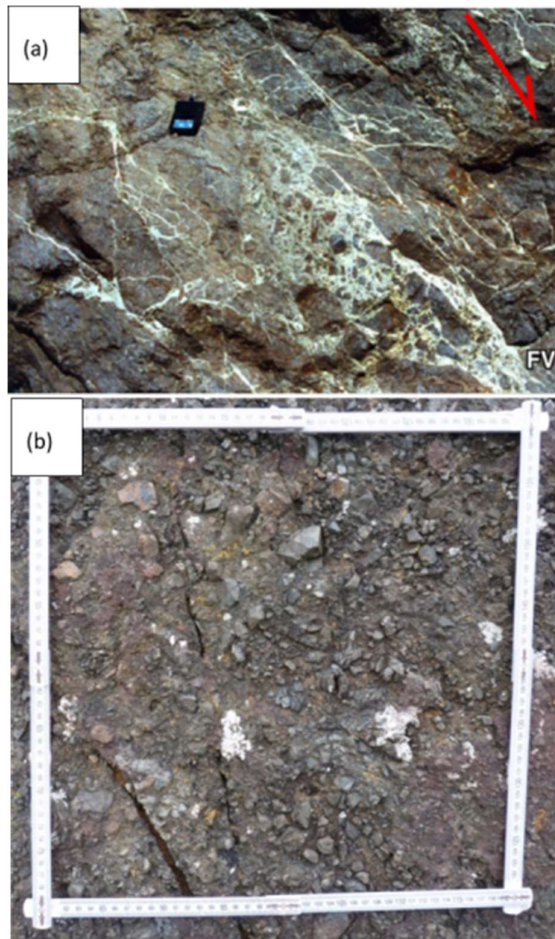


Figure 7-2 Breccia textures at (a) Dixie Valley, Nevada (from Caine et al 2010) showing quartz dominated matrix; and (b) the NSF showing a granular matrix.

Figure 7-3 shows a model for the relative depths of deformation occurring at Door of the Heugh and Lagmuck Sands. The initial formation of the pods at both sites may be the same, I am proposing that the relative depths of the subsequent deformation processes are different. The lack of shear texture at Lagmuck Sands is interpreted as evidence of relatively shallow brittle deformation. The reworked breccia texture is also evidence of brittle deformation (Section 7.1.2). The shear textures at Door of the Heugh are interpreted to be due to the depth of post- breccia formation slip on the NSF, including intense grain size reduction evidenced by the gouge layer (discussed in Section 7.1.4). The relative depths of all sites will be discussed in Section 7.2.

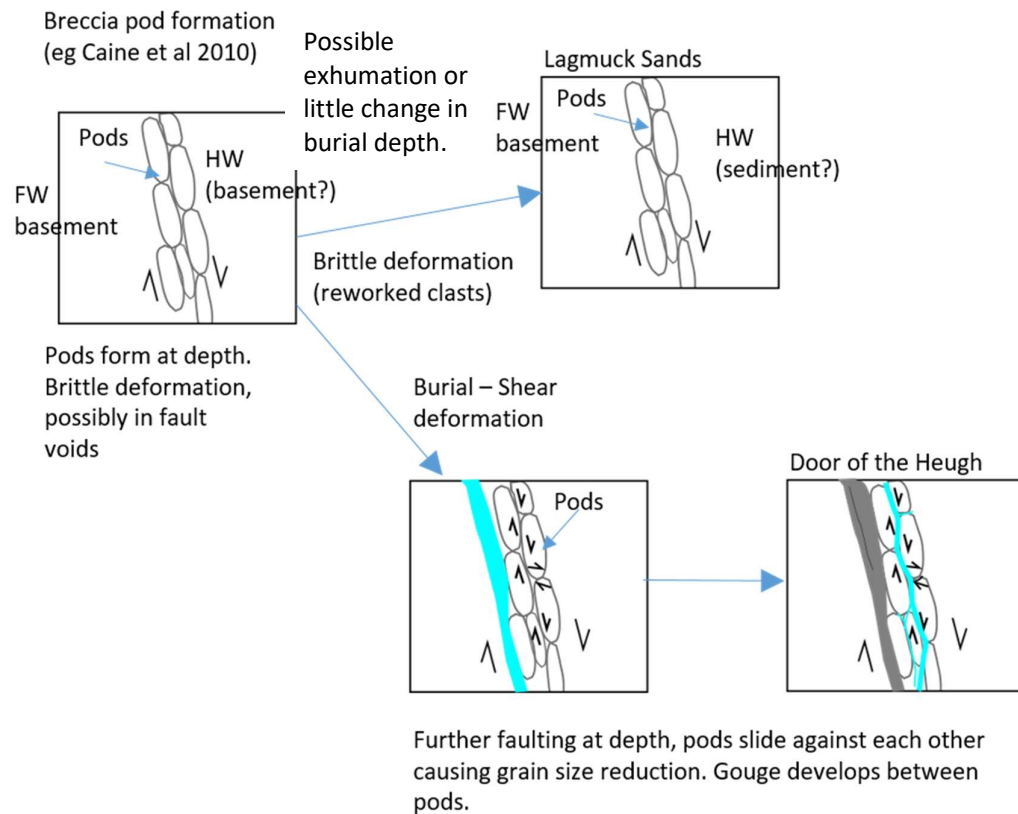


Figure 7-3 Model for the development of breccia pods at Lagmuck Sands and Door of the Heugh. Slip indicators shown with black arrows. Light blue indicates gouge formation.

7.1.2 Re-worked breccia textures

The re-worked breccia clast texture at Lagmuck Sands (Section 4.8.2) suggests a bulk brittle and granular behaviour during subsequent slip events. Re-worked breccia textures are reported in several studies (Tarasewicz et al 2005; Woodcock et al 2006; Woodcock et al 2007; Wright et al 2009; Caine et al 2010). All authors ascribe this texture to cementation of breccia which binds the clasts and matrix, followed by further fault slip events which cause the formation of the re-worked clasts. What is not clear is how a breccia becomes cemented and subsequently deforms as a clast within a surrounding granular (at the time of formation) material. The reworked clasts must be stiff enough to retain the textures of an earlier breccia.

There are three possible models for the formation of these textures; large clasts of footwall lithologies are entrained and gradually broken down by slip events and interaction with the surrounding breccia, breccia cementation followed by progressive attrition or, breccia cementation followed by collapse into a new void.

A large clast of footwall which is relatively intact internally could be rounded by attrition of at the clast edges. At the time of incorporation into the fault, this block would not have a brecciated texture initially. This is similar to the dolomite lenses incorporated into the Carboneras fault, Spain (Faulkner et al 2008). During continued deformation, pervasive fracturing through a clast could brecciate the clast internally whilst attrition occurs at the edges. I consider this to be less plausible at Lagmuck Sands as the clasts would likely break down, fragmenting into the surrounding breccia during subsequent slip events.

In the progressive attrition model, breccia is formed and cemented. During further slip events a body of breccia becomes detached from the original breccia. This body is made of

multiple clasts but behaves as a single cohesive unit during further slip events. Attrition of the edges clasts then occurs progressively until the reworked breccia clasts become rounded to lenticular.

For the void collapse model, a generalised sequence is shown in Figure 7-4. A volume of cemented breccia is subjected to further slip adjacent to a newly-formed void. The fault void wall collapses (either by implosion or by gravity collapse) and the reworked clasts are remobilised as discrete bodies of breccia. Further slip events cause brecciation of the surrounding rock volume and the original breccia clasts become entrained in a younger generation of breccia. Continued slip caused rounding of the remobilised breccia clasts.

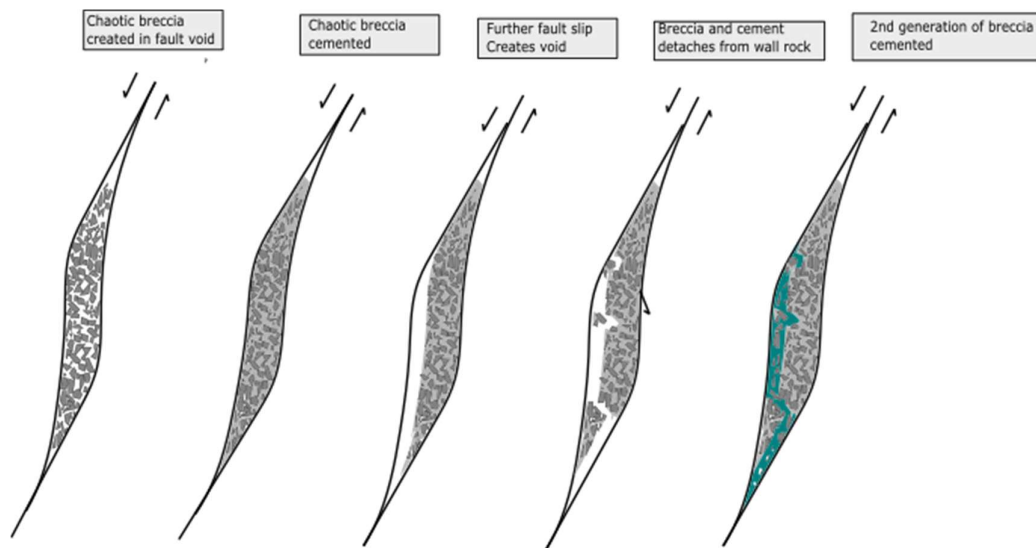


Figure 7-4 model for the generation of reworked breccia textures in fault voids

Whatever the mechanism for the formation of the reworked clasts, the texture of these clasts suggest that breccias have formed in multiple phases and also indicate that breccia (which must be granular immediately after formation) can behave both in a bulk brittle and a granular way. The granular behaviour of the phases of deformation after the initial formation is demonstrated by entrainment of this re-worked clast and subsequent

rounding within the breccia. The bulk brittle behaviour of breccia is demonstrated by the formation of the large clast as the reworked breccia texture implies that an earlier generation of breccia has been cemented, followed by incorporation into a younger breccia deposit. Steeply dipping discrete veins cutting the breccias also indicates bulk brittle behaviour because the breccias are fractured as a cohesive body of rock.

Bulk brittle behaviour in breccias is also evident from the minor slip surfaces that bound breccia pods, described in Section 7.1.1. Granular behaviour may dominate the initial breccia formation but bulk brittle behaviour occurs as the breccia deforms as a cohesive block.

7.1.3 Tectonic Breccias Cut by Sedimentary Textures

At Gutcher's Isle there are chaotic breccia deposits that are extensively cut by thinly laminated fine-grained sediments with occasional coarse granitic grains (Figure 7-5 a). These fill fractures that cut the breccia and which must have had a significant aperture at the time of formation. One of the breccia pods at Lagmuck Sands contains a small volume of bedded grains, indicating grading processes have occurred within the tectonic breccia (Figure 7-5 b).

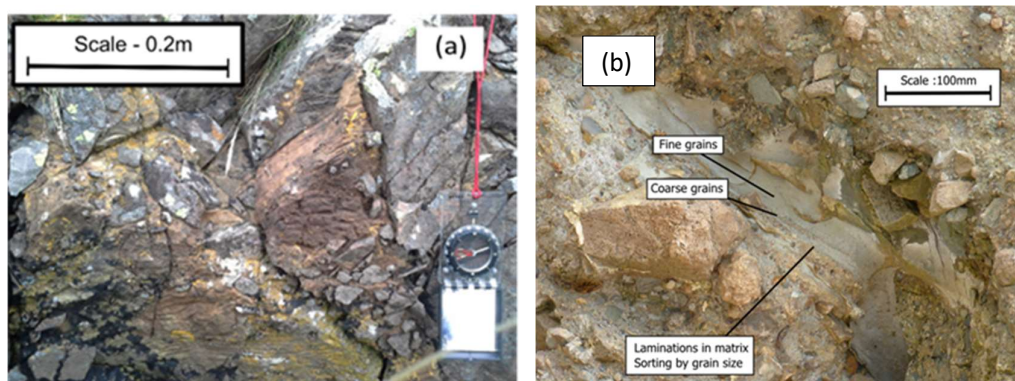


Figure 7-5 Sedimentary textures within tectonic breccia at (a) Lagmuck Sands, and (b) Gutcher's Isle.

There are two possible mechanisms for sedimentary infill within tectonic environments.

One such mechanism is sedimentation into voids via connection with the land surface but at relatively shallow depths. Woodcock et al (2014) interpreted laminations in extensional fractures as having formed from sand and mud infiltrating from the surface. Wright et al (2009) observed quartz grains within the sediment which had no obvious source within the fault and interpreted this as suggestive of a connection with the land surface, filling the void with exotic material.

A second possible mechanism is re-sedimentation of clastic material within fault zones with no connection to the land surface. Wright et al (2009) studied fissures in a limestone dominated Dinantian sedimentary succession which were filled during active faulting and remained open after faulting. Fine sediments (<2mm in diameter) made of grains of haematite were deposited from minerals in voids. The haematite then detached from the void walls and fell to the bottom. Walker et al (2011) described clastic intrusion due to fluid over-pressure which forces sediments to mobilise within a fault. This can be caused by fault-related fluid pressures or compression of sediments due to collapsing cavity roofs.

The sedimentary textures within breccias at Gutcher's Isle could be the result of breccias being exposed at the surface, with fine grained sediments filling fractures. The coarsening up texture may represent small scale mass flow events (eg. Bertran and Taxier 1999) with predominantly very fine sediments. This may also explain the isolated granitic grains, which could have been detached from the host rock in a sedimentary setting and deposited locally during these events. Coarse grained sediments in the hanging wall at Gutcher's Isle (Section 5.1) could indicate that the fault scarp has been exposed at the surface.

Sedimentation at the surface seems the most likely explanation for the sediments in the Gutcher's Isle breccias. Walker et al (2011) described tabular intrusions into existing

sediments that drag the existing sediments upward. As described in Section 4.8.3, some of the laminated sediments are relatively planar at Gutcher's Isle and lineations deflect around clasts of wall rock lithology. This could be as a results of sediments intruding open fractures in the granitic host rock, but does not explain the coarsening upwards texture, which is much more reminiscent of the deposition of dry granular sediment.

The rounded texture of the sediment grains within the Lagmuck Sands tectonic breccias suggest significant transport. We can rule out with some confidence these grains being deposited through rapid sedimentation from a local source, followed by rapid lithification. It is possible that rounding of the grains is the result of attrition within the fault. For this mechanism to be viable the sediments would have to remain in a granular state over several slip events. It is also possible that the grains originated outside the breccias and filled a void via connection with the land surface. This would mean that significant rounding could have taken place at the surface before the grains were deposited in the fault. The bedded grains were observed on the underside of a pod. The position of the clastic grains within the pod does not fit with direct sedimentation at the surface. At Lagmuck Sands either sedimentation via connection to the land surface or re-sedimentation within the breccias at depth are considered the most likely explanations.

Figure 7-6 shows a model for formation of the sedimentary textures in clasts at Gutcher's Isle. Fractures and breccia are formed within the fault zone, possibly at depth. The fault is then exhumed and exposed at the surface. Sedimentation then takes place with the exposed fractures from two sources; fine sediments from a source not identified and coarse clasts from the immediate footwall.

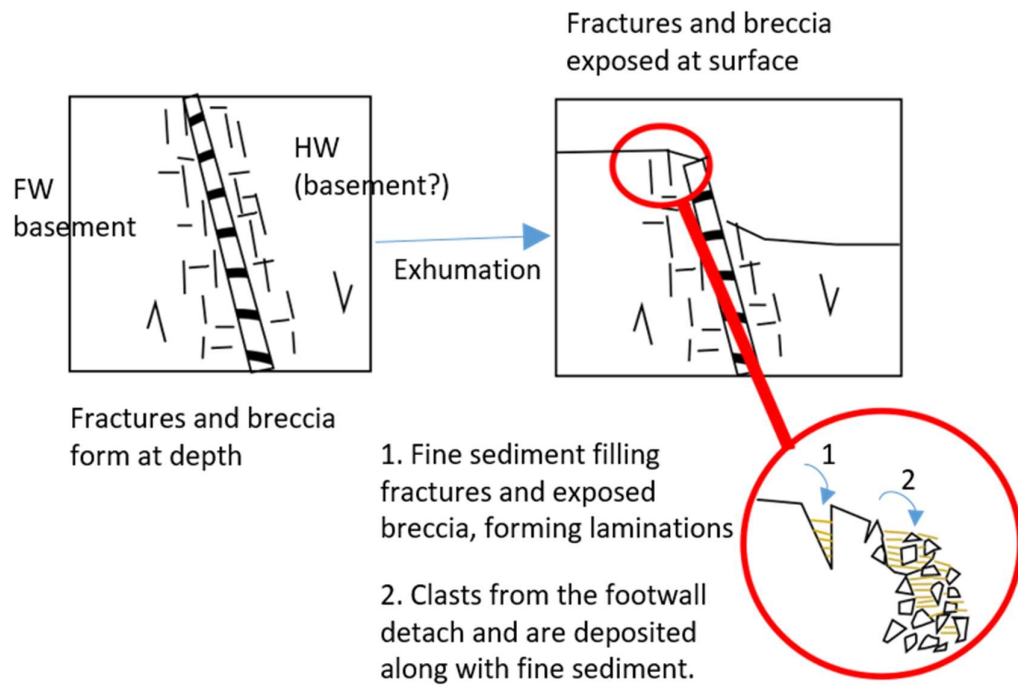


Figure 7-6 Model for sedimentation in breccias at Gutchers Isle

The initial breccia formation could have taken place at depth or near the surface. The lithification of the fine-grained sediments indicates that the breccias and their sedimentary infill have been buried or cemented since the infilling took place. This was followed by exhumation. This could be further constrained through petrological studies, but this was outwith the scope of this thesis.

It is difficult to determine the source of the graded sediments in the tectonic breccia as there is a lack of direct evidence of emplacement processes. Fault zones provide a potential setting (voids) for sedimentary processes to occur at depth. Other processes such as mobilisation of sediments which are not driven by gravity (over-pressure of fluids for example) could also be operating at depth within faults. When tectonic breccias are exposed at the surface the interaction between fault rocks and sedimentation is clear. The graded sediments at Lagmuck Sands demonstrate that gravity-driven processes do not

exclusively operate at the surface. Subsurface voids also experience gravity driven deposition (eg. Woodcock et al 2007).

7.1.4 Gouge at Door of the Heugh

The fault zone at Door of the Heugh consists of a narrow gouge zone (c. 400mm wide). The gouge contains Reidel shears, flow banding, grain fracturing and trails. The gouge is positioned between the footwall and the crackle/mosaic granitic breccia suggesting the gouge is sourced from footwall lithologies. The slip surfaces between pods contain up to 100mm wide slip surfaces which can be classified as gouge.

Haines et al (2013) demonstrated experimentally that Reidel shears and flow banding develop in gouge as slip progresses. The textures described in section 4.9 are therefore indicative of continued deformation in the same rock volume (strain weakening). Some deformation has been accommodated by the breccia pods as shown by the development of slip surfaces between the pods. The gouge between the breccia pods does not show any of the features associated with well-developed gouge and which implies that the majority of slip at the Door of the Heugh locality is accommodated by the main gouge.

The discussion on fault throw in Section 6.1.2 demonstrates the difficulty in predicting the amount of slip on the whole fault scale. Kristensen et al (2016) estimated that gouge up to 500mm thick at the Dombjerg fault, Greenland demonstrates slip magnitudes of tens or hundreds of meters. The Door of the Heugh locality doesn't offer any direct evidence as to the magnitude of offset (e.g. markers) but does suggest that a large proportion of the offset could be accommodated within a relatively narrow zone compared to the width of the fault zone.

Shipton et al (2006) showed that although fault thickness shows a generally positive correlation with fault displacement, for a single value of displacement fault thickness can vary by 3 orders of magnitude. At Door of the Heugh, the fault zone is several metres in width but the textures within the fault zone suggest slip is accommodated in a few discrete slip surfaces at pod boundaries and the main gouge layer. Fault zone thickness therefore does not necessarily increase with displacement in order to accommodate slip. Discrete elements within the fault can accommodate slip without incorporating the wider rock volume.

Strain weakening is a recognised process whereby deformation causes weakening within the rock volume (eg. Copley and Woodcock 2016). Subsequent slip events are more likely to be focussed on these zones of weakened rocks, resulting in a strength contrast between relatively undeformed rocks and adjacent fault rocks (eg. gouge). Slip is therefore repeatedly accommodated on the weaker rocks meaning the same structures are reactivated. The contrast between the textures within the gouge and the rock volume outside of the gouge suggests that strain weakening has occurred at the Door of the Heugh.

7.1.5 Portling Bay

At Portling Bay the fault zone is characterised by an c. 8m wide gouge (shown in figure 4-16) consisting of clasts of hanging wall, brecciated footwall and brecciated mineral deposits. The hanging wall grades into a gouge where initially steeply dipping sandstone beds give way to boudinaged sandstone lenses in a fine-grained matrix. Moving towards the fault the sandstone lenses become more rounded and resemble large clasts rather than lenses. Closer to the footwall there are large clasts (c. 0.5m in diameter) of brecciated footwall lithologies. Shear fabrics are poorly developed in comparison to Door of the Heugh.

Sediments at the tip of an upward propagating fault have been studied by Sharp et al (2000), Ferrill et al (2012) and reviewed by Ferrill et al (2017). Ferrill et al (2012) described mechanically contrasting sediments ruptured by an upward propagating fault. Pre-rupture, the sediments are tilted into a syncline above the fault tip and the fault propagates through this syncline forming a tilted monocline adjacent to the fault. During continued shear, mechanically contrasting layers begin to behave differently – layer parallel shear is accommodated in the weaker mudstone layers whilst the stronger, less ductile layers (competent limestone in Ferrill et al 2012) cannot extend continuously in the same manner. These stronger layers undergo brittle deformation and become boudinaged in the steepening monoclonal limb and the previous continuous bed becomes a series of discontinuous boudins surrounded by fine grained mudstone.

The mapping carried out in this thesis has shown that on the hanging wall side of the fault zone steepened sandstone beds become discontinuous and grade into boudins and isolated clasts within a fine matrix as predicted by Ferrill et al (2012). The boudinaged sandstone beds suggest that the sediments were lithified at the time of faulting as they are required to be mechanically strong compared to the mudstone in order to deform in a brittle way. If the sediments at Portling Bay were lithified above the tip of an upward propagating fault, they must have been deposited and subsequently buried before the NSF propagated through them. This suggests a relatively long period of time where the NSF was not active. Other evidence in support of a period of lower fault displacement is the textures of the sediments at Portling Bay which will be discussed in Section 7.1.7.

Figure 7-7 shows a model for the formation of the gouge at Portling Bay based on the Ferrill et al (2012) model. The sediments accumulate and are buried and lithified. This is followed by propagation of the fault zone through the sediments resulting in layer parallel shear. As

deformation continues the stronger sandstone becomes detached lenses which are gradually incorporated into the fault zone during subsequent slip events.

The Portling Bay exposures are not entirely explained by the Ferrill et al (2012) model. Large clasts of reworked brecciated footwall lithologies make up a high proportion of the exposed fault zone (c.20% of the volume) towards the footwall. This suggests that the fault zone either; widened to incorporate previously formed breccia, or blocks of breccia were “sedimented” into the fault zone from a fault scarp which became incorporated into the gouge as faulting continued. There is no evidence (such as the talus seen at Lagmuck sands) to suggest sedimentation at the base of a fault scarp has taken place at Portling Bay. It therefore seems more likely for the fault to incorporate previously formed breccias at depth rather than through sedimentary processes.

The spatial distribution of clasts of footwall derived breccia as shown in Figure 4-16 could be explained by reworking of earlier breccias as they incorporated into the gouge. However, the clasts are several meters from the interpreted boundary of the gouge. This means either that the footwall-derived breccia clasts have mixed with the sediments and travelled several metres from the edge of the fault gouge, or that the gouge boundary has extended (by abrasion?) several meters into the footwall-derived breccias and the clasts are close to their original location.

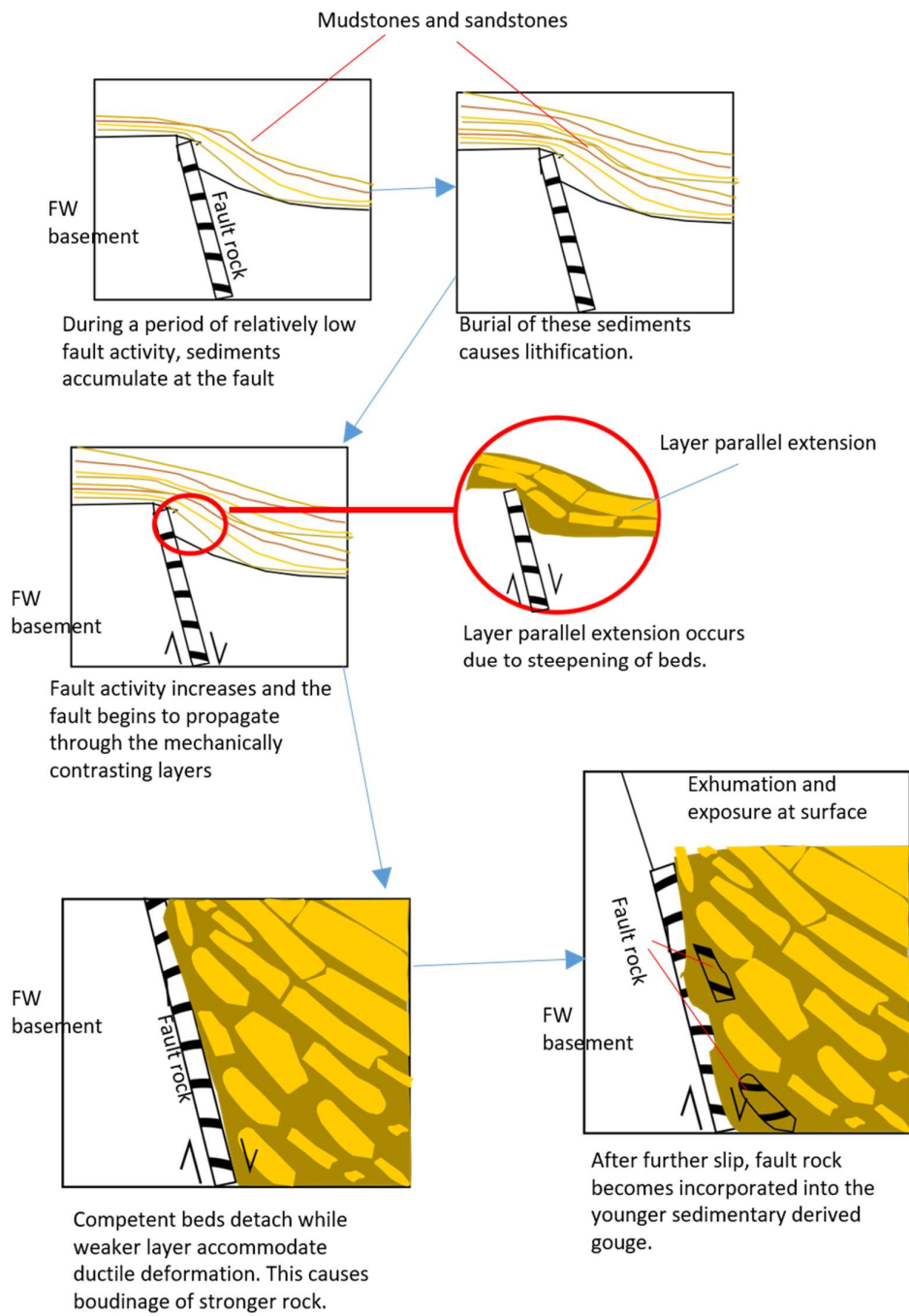


Figure 7-7 Model for the development of layer parallel shear at Portling Bay

The Portling Bay “gouge” (Figure 7-7) demonstrates the interaction between sedimentary and tectonic breccias. The “mixing” of clasts of tectonic breccia and sedimentary breccia in the Portling Bay gouge feature suggests that continued faulting of a mechanically stratified succession causes earlier generations of fault breccias to be incorporated within the gouge. The fault zone must have widened at this locality in order to incorporate the tectonic breccias.

The thickness of the fault at the Portling Bay gouge appears to have been strongly influenced by the properties of the mechanically contrasting layers and the availability of fine grained material to be incorporated into the fault zone, as predicted by Ferrill et al (2017) and references therein. As such, the interaction between sedimentary deposits and tectonic breccias have strongly influenced the fault zone and a simple model of direct sedimentation from a fault scarp does not apply. It is more appropriate to think of the basin margin sediments as coupled with the fault zone in a feedback relationship where the fault zone influences sedimentary processes and the sedimentary succession influences the architecture of the fault zone.

Deformation at Portling Bay is distributed across the fault zone of several metres width. The shearing textures at Door of the Heugh are concentrated on a much narrower gouge zone are evidence of strain weakening (Section 7.1.4). The wider, more distributed deformation evident at Portling Bay suggests that strain weakening is not such a dominant mechanism at Portling Bay. This could be due to the lower contrast between the host rocks on the hanging wall side (interbedded sandstones and mudstones) and the fault rocks. The weaker host lithologies are likely to be more readily incorporated into the fault zone at Portling Bay than the stronger footwall lithologies of Door of the Heugh. This enables deformation to be distributed over a wider area.

The Door of the Heugh gouge is flanked by basement lithologies whereas the gouge at Portling Bay gouge is the result of basement to sedimentary faulting. The contrast between the two locations is therefore evidence of the different architecture that can occur on the same fault depending on the strength of the host lithologies. Stronger basement rocks result in narrow zones of strain weakening whereas weaker lithologies result in wider distribution of the deformation. This could be due to the lower strength contrast between host lithology and deformation elements.

7.1.6 Evidence of Granular Behaviour in Faults

The North Solway fault provides an opportunity to study clast mixing and clast origin (ie. footwall or hanging wall). The footwall consists of two contrasting lithologies which can be identified in clasts and used to determine the closest possible source of clasts. The same can be said of the contrasting footwall and hanging wall lithologies. As described in Section 7.1.1, textures which demonstrate granular behaviour with the fault suggest that rapid cementation of breccias did not closely follow the initial formation event.

There are volumes of breccia which are of a single clast lithology and volumes of breccia which contain clasts of both footwall lithologies. There is mixed clast lithology breccia adjacent to footwall of a single lithology, as shown in Figure 4-13, indicating that clasts have travelled through the fault zone for at least 3m as that is the distance to the nearest matching footwall unit up-dip. For breccias clasts to travel, the breccia must be behaving as a granular body.

The dominance of the chaotic mixed breccia texture could also indicate that the breccias remain in a granular state over several slip events meaning breccia clasts are able to mix during slip events. Processes which cause clast mixing after breccia formation but before

the breccia is cemented/lithified are possible. As described in section 7.1.1, this thesis proposes that chaotic breccias could form due to collapse/implosion in voids and this could cause mixing during formation. The degree of mixing possible by this mechanism is difficult to quantify.

As described in Section 7.1.5, large clasts consisting of reworked footwall-derived breccia have been mapped at Portling Bay. The entrainment of these clasts within the gouge layer at Portling Bay indicates that the fault zone has incorporated earlier generations of breccia. The breccia entrained here displays clast trails, which form when survivor clasts are progressively broken down in gouge (Rutter 1986). The trails indicate there is interaction between the surrounding matrix and the clast itself.

Evidence of grain-scale mixing was described by Caine et al (2010) as clasts of exotic lithologies (not derived from the footwall or hanging wall) were found in breccia pods. Clasts derived from outside of the local footwall and hanging wall lithologies demonstrate input of clasts into the fault rock volume and also the mixing and transport of those clasts within breccias. If clasts did not mix, then exotic lithologies would be expected only to contact with the outer limits of the pods and not be found within the pods themselves.

There are numerous examples in the literature demonstrating that grain-scale mixing appears to be rare in faults. Chester and Chester (1998) mapped a clear boundary between two ultracataclasites derived from contrasting lithologies at the Punch Bowl fault, California which has a displacement of over 40km. Few structures in the Punchbowl fault that cut this boundary and as a result there is little to no grain-scale mixing of the two lithologies in the fault rocks.

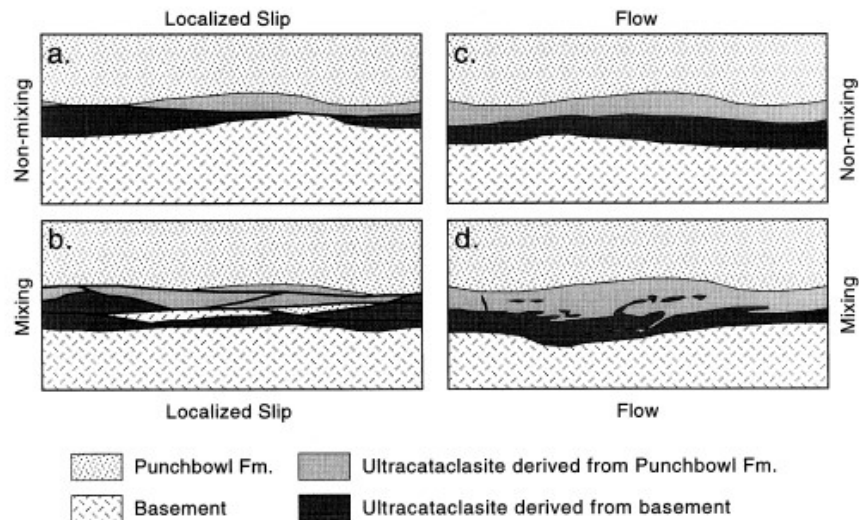


Figure 7-8 Four end member models for degree of mixing in ultracataclasite from Chester and Chester (1998). (a) single slip surface controls deformation – no mixing. (b) slip on multiple anastomosing surfaces leads to mixing. (c) laminar or streamlined flow occurs in the ultracataclasite but is distributed and the units remain juxtaposed. and (d) turbulent flow causes mixing of the fault rocks.

The NSF has a much lower displacement than the Punchbowl and is a normal fault rather than strike slip. The principal slip surface of the Punchbowl fault is sinuous at the several kilometre scale, whereas the NSF has a segmented plan view structure, this may be due to the exposure orientation with respect to the slip vector. Chester and Chester interpret slip dominated by relatively distributed laminar flow which has accommodated all the slip. Granular mixing within the Punchbowl fault is therefore not necessary to accommodate slip as interaction with the surrounding rock mass is rare. This is an example of strain weakening as described in Section 7.1.4.

Cowan et al (2003) showed that for relatively high displacement faults there is only limited mixing within fault zones. The Copper Canyon fault, Death Valley USA is a detachment fault of several km throw. Displacement along the fault was accommodated by a mixture of

localised slip on discrete surfaces (Principal Slip Plane; PSP in Figure 7-9) and distributed flow within gouge and foliated breccia (zones I and II in Figure 7-9).

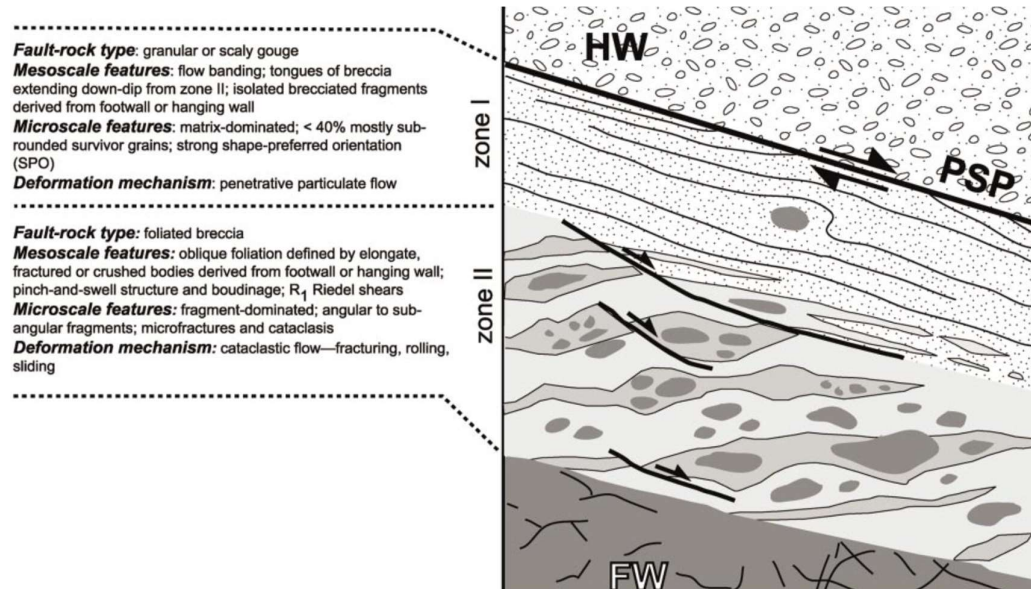


Figure 7-9 Fault rock units at the Copper Canyon fault. The thickness of zones I and II vary between 100mm and 1m. Note the descriptions of each zone mentioning footwall and hanging wall clasts are found in each. From Cowan et al (2003).

Mixing of footwall and hanging wall lithologies occurred in zones I and II as distributed flow accommodated some displacement. Each zone was predominantly derived from the adjacent wall rock but some clasts of breccia derived from the opposite side of the fault were found (see the descriptions of each zone in Figure 7-9).

Some mixing of lithologies was shown at the Copper Canyon fault where gouge was described as having “cut” the hanging wall in some locations. A diagram of this is shown in Figure 7-10 from Cowan et al (2003). The previous principal slip plane (labelled 1 in Figure 7-10) is the oldest slip surface in the figure and is cut and offset by faults (labelled 2 in Figure 7-10) which do not cross the gouge layer. Penetrative flow then caused gouge to intrude into the hanging wall (labelled 3 in Figure 7-10). Another well-defined slip plane was

formed (labelled 4 in Figure 7-10) which was finally cut and offset by the latest faulting (labelled 5 in Figure 7-10).

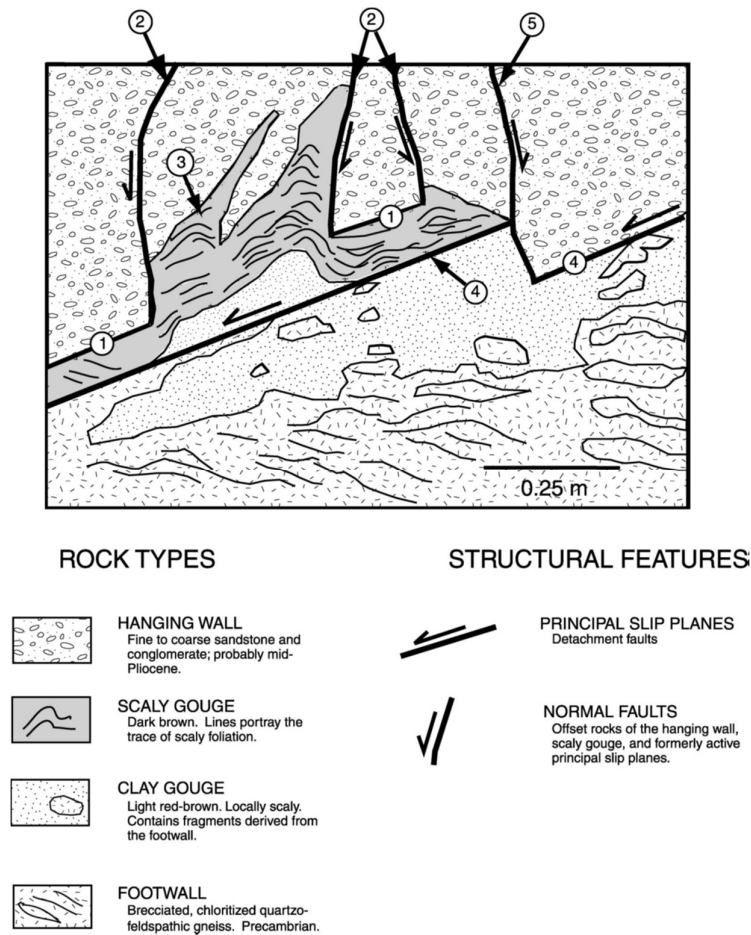


Figure 7-10 Entrainment of wall rock lithologies into gouge at the Copper Canyon fault in Death Valley, USA. From Cowan et al (2003)

The Cowan et al model contrasts with the Chester and Chester model of localisation on a single slip plane or distributed laminar flow. The Cowan et al model includes a switch of the mode of deformation with increasing displacement; slip on a single principal slip surface is disrupted by cross-cutting slip planes and distributed flow. This allows the incorporation of wall rock in to the fault zone and also provides a mechanism for grain flow and mixing in foliated breccia and gouge.

The Cowan et al model offers a possible mechanism for the entrainment of footwall or hanging wall lithologies at the NSF. It is likely that the complex 3D architecture of the NSF is less likely to produce distributed shear or a single principle slip plane because mechanical asperities in the host rock and the fault zone affect the type of deformation.

The heterogeneous geometry and internal architecture of the NSF is likely evidence for more turbulent flow in the fault rocks than at the Punchbowl fault. If deformation within the fault zones is not concentrated on a single slip surface then mixing of the fault rocks is more likely. Distributed deformation or heterogeneous deformation concentrated on several slip surfaces could form the textures observed at Portling Bay where large clasts of footwall-derived breccias are mixed with hanging wall derived clasts. In the Cowan et al model, incorporation of wall rocks into the fault gouge occurs when slip surfaces cross the boundary between gouge and wall rock. If this occurred on the footwall side of the NSF at Portling Bay, blocks of footwall or previous generations of breccias would be incorporated into the gouge. As the sandstone and mudstone layers are interbedded on the hanging wall side of the fault, the sandstone boudins are likely to be incorporated into the gouge as slip progresses. This means that a “boundary” is not defined because the hanging wall sediments grade into the gouge (Section 4.9). Distributed deformation of the hanging wall enables incorporation of the wall rock into the gouge whereas discrete slip surfaces crossing the gouge boundary are required on the footwall side.

Further deformation events are required to mix the footwall derived and hanging wall derived blocks with the fault and slip events must have occurred several times to produce the well-rounded survivor clasts at Portling Bay.

7.1.7 Sedimentation at Active Faults

The hanging wall deposits near the fault zone display poorly defined steep bedding (up to 70° at Lagmuck Sands) and dip towards the basin. These sediments are coarse conglomerates with angular clasts and are interpreted as talus deposits. The hanging wall sediments further from the fault typically have shallower dips (c. 20°) and dip towards the basin. These sediments are typically a succession of coarse sandstones with conglomerate interbeds. At Lagmuck Sands some sedimentary rocks onlap the fault scarp as described in Section 4.7.2.

The sedimentary logs at the 4 key sites show variation in hanging wall textures along strike at the NSF. The 3 sites that have predominantly coarse grained facies contrast to the finer grained sedimentary beds at Portling Bay. The hanging wall sediments at Portling Bay are situated approximately 100m from the fault scarp, are relatively fine grained compared to the rest of the sites and contain ripple textures suggesting that they may have been deposited in shallow water environments. Sediments exposed at Door of the Heugh are also around 100m from the fault but the sedimentary succession is dominated by coarse grained beds, the coarse grained facies could indicate a high topographic relief, such as at the foot of a fault scarp. At Lagmuck sands and Gutchers Isle, the distance to the fault scarp (<50m) is much less than at Door of the Heugh and Portling Bay (c. 100m) and the larger grain size and angular clasts could be expected in such close proximity to the fault.

The grain size in the Portling Bay sediments indicates a different depositional environment perhaps due to the absence of a large fault scarp. Coarse grained facies such as talus deposits and conglomerates are absent from the Portling bay locality, even directly adjacent to the fault.

It is possible that this is due to the sediments being of different ages between the 4 key sites. Previous work at the NSF has estimated a younging to the east in the sediments adjacent to the fault (eg. Deegan 1973). The NSF may therefore have breached the surface and have formed a significant fault scarp during deposition of the sediments at Door of the Heugh, Lagmuck Sands and Gutcher's Isle. The presumably younger sediments furthest to the east at Portling Bay may have been deposited at a time when the NSF did not display a large fault scarp at the surface, implying slowing down or cessation of slip at this point in the stratigraphy.

Linking the sediment textures to scarp height is essentially linking geomorphology and tectonics. Blair and Macpherson (1994) realised that preserved alluvial fans in the rock record can yield information about previous tectonic environments. They recognised that alluvial fans formed by debris flows tend to have higher coarse grain content than those formed by sheet floods. The implication of this is that fans forming in settings with a high topographic relief will have higher proportions of large grain sizes than those formed in settings with lower topographic relief. Sediment input is dominated by debris flows in the former and by water-laden sediments in the latter.

The scale of the fans discussed in Blair and Macpherson are typically several kilometres in length (Figure 7-11). This is significantly further from the fault surface than the sedimentary facies in this study (between 0m and 100m from the fault). The relevance of their study to the NSF is that the primary formation processes of alluvial fans are rock avalanches and colluvial slope failure. The alluvial fans listed as examples in the Blair and Macpherson study are in tectonic settings of Death Valley and Owens Valley, California where the topographic relief is generated through tectonic action. The scale of those fans is significantly largely than the NSF deposits of talus and conglomerate where grain size is by definition higher

than the sandstones further from the fault. The variation in size between the Death Valley fans the deposits could be due to two factors; scarp relief and the length of time the scarp is exposed. The length of time the scarp is exposed depends on the uplift rate of the fault scarp or on the rate of deposition.

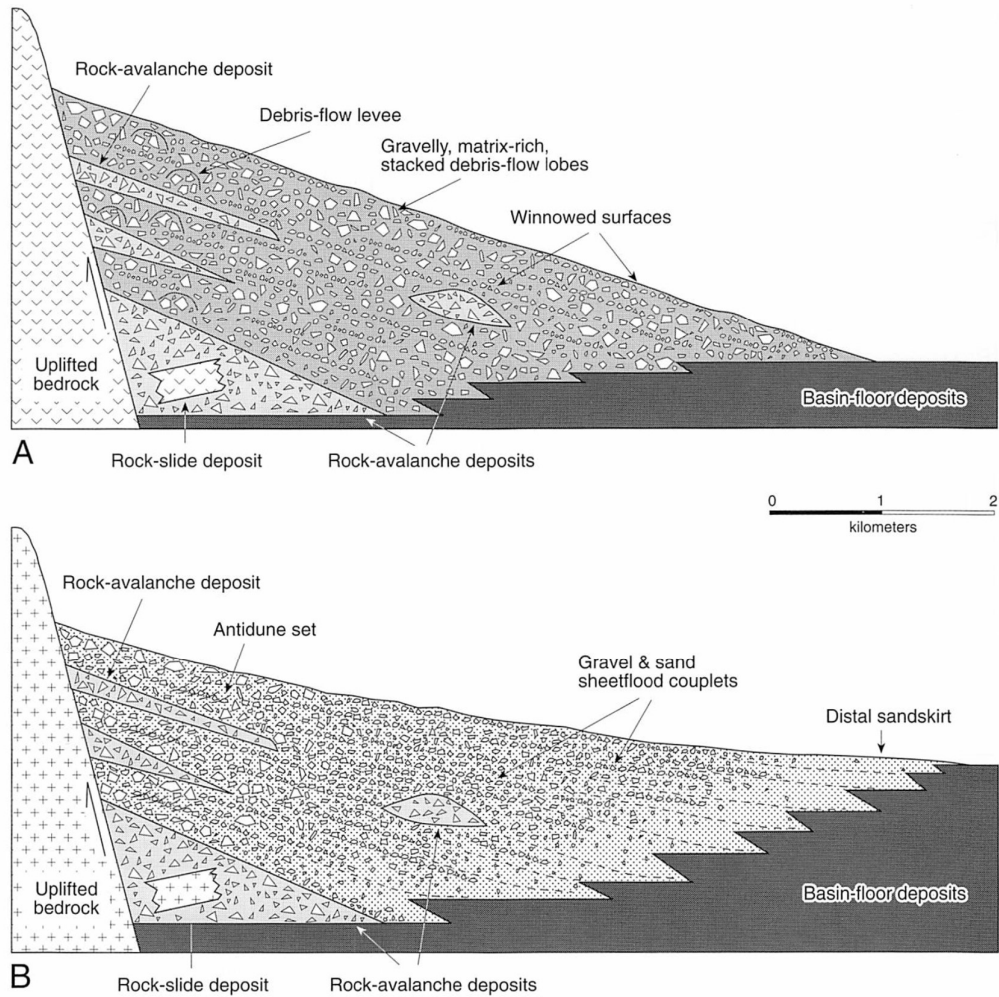


Figure 7-11 Schematic cross section of typical alluvial fan structures and textures from Blair and McPherson (1994). A) Debris flow dominated fan, and B) Sheet flood dominated fan. Vertical exaggeration is 2x.

McCalpin (1996) derived a schematic diagram to understand how sediment erosion/deposition rates relate to fault scarp height and the diagram is shown in Figure 7-12.

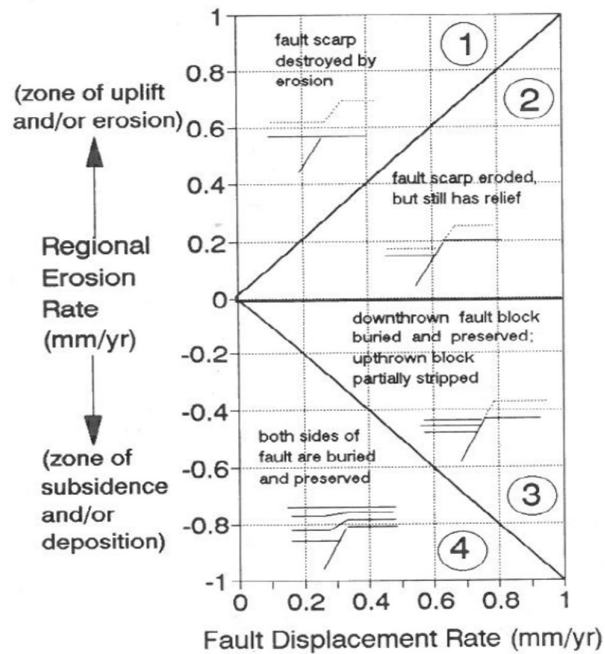


Figure 7-12 Schematic diagram of relative rates of fault scarp uplift versus geomorphic processes. From McCalpin (1996)

In quadrant 1, the erosion rate is high enough that the fault scarp is eroded before displacement can renew the fault scarp. In quadrant 2 displacement rates are high enough that some fault scarp relief is maintained despite the erosion. In quadrant 3, the fault outcrops on a landscape undergoing subsidence and deposition but fault displacement rate is higher than the deposition rate. In quadrant 4, the fault is buried by sediments as displacement rates do not keep pace with deposition rates therefore the fault scarp is not exposed.

At the NSF the evidence of a palaeo-fault scarp is preserved in sediments at some locations (Door of the Heugh, Lagmuck Sands and Gutcher's Isle) and evidence of a lack of palaeo fault scarp is preserved at Portling Bay. The grain size of the hanging wall sediments (as described above) is one key piece of evidence. At Portling Bay, the lack of exposed fault scarp at the surface is also evident in the textures of the fault gouge-entrained hanging wall beds. The Ferril model of fault propagation folding with layer parallel extension in mechanically contrasting beds was described in relation to the Portling Bay exposures in Section 7.1.5. For this model to be valid, the NSF would have to propagate through the sediments. Sedimentary beds must have been laid down above the buried NSF and breaching the surface is not possible until after propagation through those layers. Portling Bay would therefore fit into the 4th quadrant of the McCalpin model. Multiple quadrants in the McCalpin model in Figure 7-12 are represented along strike of a single fault.

The variability of hanging wall textures at the NSF are interpreted as evidence of variable surface breaching on the same fault. The Portling Bay sediments could have formed at a different time to the other (older?) sediments, when deposition rates were higher than fault displacement rates. The other three sites were formed when erosion rates were less than fault displacement rates meaning a scarp was maintained.

7.1.8 Fault Proximal Sediments and Deformation Characteristics

The detailed description of sediments at the NSF allows the interpretation that they formed adjacent to fault scarp and above a buried fault. This is key to the timing of the sediments with respect to fault displacement. Figure 7-13 shows the model of Kristensen et al (2016) for basin margin faults with basement footwall and sedimentary hanging wall. The hanging wall is split into three phases; pre-rift, syn-rift and post-rift. The pre-rift hanging wall is not exposed at the NSF. There are exposures of syn-rift sediments (Door of the Heugh, Lagmuck

Sands and Gutcher's Isle) and exposures of 'post'-rift sediments (Portling Bay) which have been subsequently ruptured by the upward propagating NSF.

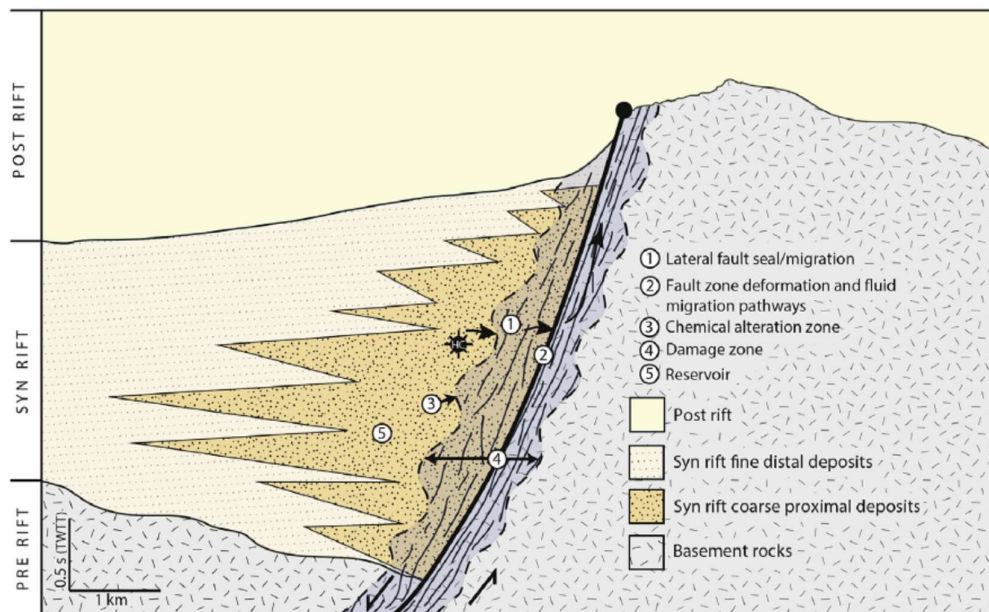


Figure 7-13 Schematic cross section of a basin bounding fault with syn-rift sediments. From Kristensen et al (2016).

A key observation in the Kristensen et al model is the Chemical Alteration Zone (CAZ). The CAZ is a zone of calcite cementation in the pore space of syn-rift clastics and is identified by contrasting colour and deformation features when compared with the generally non-cemented sediments from outside the CAZ. Jointing, fracturing and minor faults were observed within the relatively high strength low porosity sediments of the CAZ. Outwith this zone where the sediments are predominantly sandstones and conglomerates the deformation features include disaggregation deformation bands (Kristensen et al 2016). The extent of the CAZ varies along strike but reaches as much as 1km into the basin from the Dombjerg fault.

The hanging wall sediments studied at the NSF are all within c. 100 metres of the fault zone. Ord et al (1988) described soft sediment deformation features at the NSF such as slumps, folds and liquefaction features, but not deformation bands. The sediments adjacent to the NSF have been lithified and this is likely to have happened during burial either during the Carboniferous or Jurassic period. Discrete calcite veins were observed in hanging wall at the NSF but there is no evidence to suggest extensive mineralisation of the hanging wall which would change deformation behaviour of the sediments. The lack of an extensive chemical alteration zone suggests that large amounts of mineral saturated fluids have not been present at the NSF or that mineral saturated fluids were present but precipitation of minerals did not occur.

7.2 Relative deformation depths of the NSF field sites

The above discussion of each site has shown that the NSF internal structure varies along strike. Door of the Heugh has deformation styles that suggest brecciation and subsequent faulting occurred at depth. Lagmuck Sands has deformation styles that suggest brecciation at depth but also evidence for bulk brittle behaviour which may have occurred at shallower depths than Door of the Heugh. Gutcher's Isle has textures which suggest at least one phase of exposure at or near the surface (sedimentation into breccias), followed by burial which lithified the sediments and another phase of exhumation to the present day configuration. Portling Bay has evidence for sedimentation above a fault (possibly due to a period where fault activity was lower) followed by rupture and continued deformation of the sediments until parts of the fault zone from earlier deformation were incorporated into fault.

With the exception of Portling Bay, the field sites all show evidence that basement-on-basement faulting is the most likely juxtaposition at the time of breccia formation as little or no hanging wall is entrained in the fault (see Section 5.3.9). This implies that the breccias at Door of the Heugh, Lagmuck Sands and Gutcher's Isle are older than the fault rocks at Portling Bay which are the result of basement to sedimentary hanging wall faulting.

The breccia pods at Door of the Heugh and Lagmuck Sands show two different deformation styles as described in Section 7.1.1. The Door of the Heugh pods have been sheared whereas the Lagmuck Sands pods do not appear to have been sheared. Contrasting deformation styles can also be found within the pods themselves; reworked breccias and sedimentary fabric within the breccia at Lagmuck Sands have not been observed at Door of the Heugh. The strength of the breccias at Lagmuck Sands and Door of the Heugh is currently roughly equal. The contrasting deformation styles could be due to that different depths at which an additional phase of deformation occurred.

Changes in deformation intensity with depth have been interpreted at a basin margin by Kristensen et al (2016). The basement footwall of the Djomberg fault is more intensely jointed than the sedimentary hanging wall. This is attributed to the multiple phases of deformation experienced by the older footwall at greater depths compared with the relatively young hanging wall, which will have undergone only the most recent deformation during Jurassic-Cretaceous rifting.

The mechanical behaviour in faults is recognised to evolve through time. One possible cause of the variation in deformation styles is depth. Figure 7-14 shows the field sites and the relative depth of each field site at the time of formation. The diagram is conceptual and does not represent additional phases of burial and exhumation that may have occurred at each site after formation of the fault rock. From the above discussion it is clear that none of

the locations show a simple single brecciation event followed by exhumation. All the sites have experience additional processes after the initial phase of brecciation. The diagram is an illustration of the varied deformation styles at the NSF and demonstrates that a basin bounding fault zone will display many different deformations styles along strike.

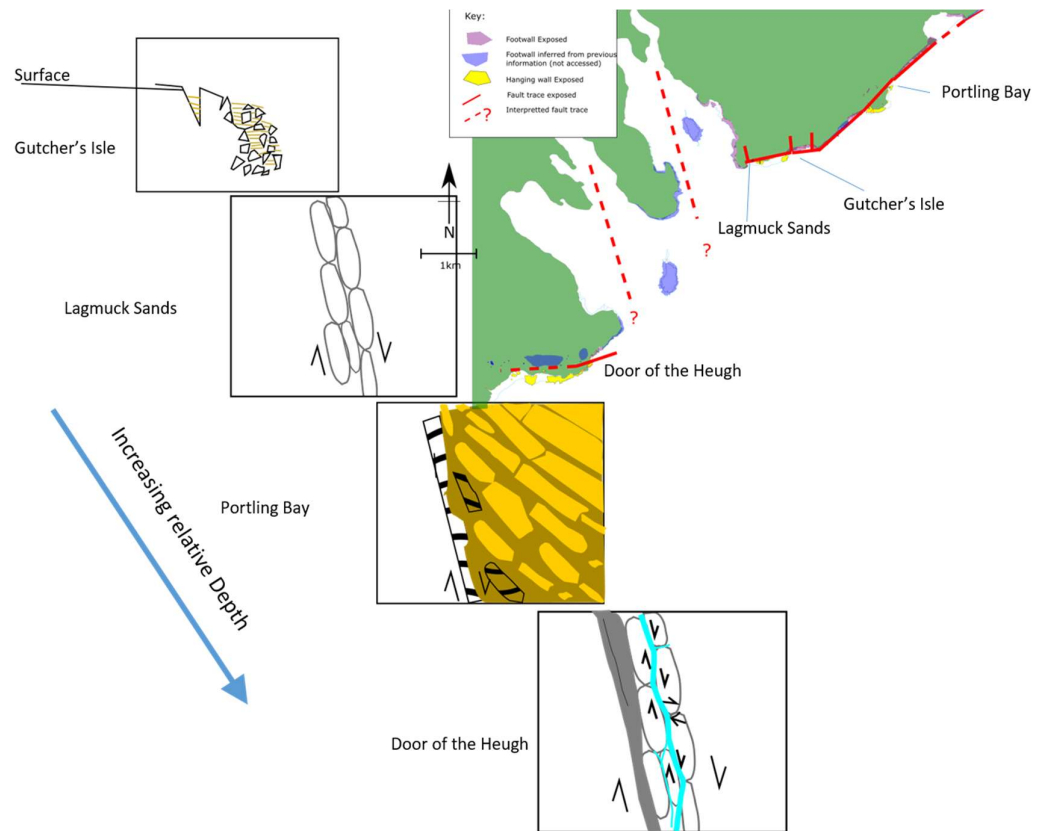


Figure 7-14 Model for the variations in relative depth of faulting at the NSF, with a map to show the 4 key locations.

The absolute values of depth of deformation for the NSF are not known. As described in Chapter 3, Parnell (1995) estimated the whole Solway basin to be several kilometres deep. It is not clear what the magnitude of burial was of the basin margin NSF. The importance of placing the field sites in the context of relative depth is that it demonstrates how large fault zones will display varying modes of deformation under changing structural conditions. A

fault zone undergoing a long history of burial and exhumation will therefore vary in deformation style through time. This has important implications for predicting fault architecture at depth. Studies of fault architecture are limited by the available data which is typically constrained to present day exposure at the surface. Large faults such as the NSF may expose fault architectures from different depths and therefore different times in the evolution of the fault. Studies of fault architecture therefore need to consider the limitations of the available exposures and how representative those exposures are of the whole fault.

7.3 Fault Zone Fractures and Veins

Fractures in the footwall and hanging wall are predominantly oriented at high angles to the fault whereas in the tectonic breccia, there is a more varied spread of orientations. This is interpreted to be a result of the breccia fractures forming in a spatially complex, and evolving stress field within the fault. The veins-through-clast texture was observed in the hanging wall and tectonic breccia. The dominant orientation of the veins that cut clasts is at high angles to the main fault (Section 5.4.4).

As described in section 5.4, discrete veins are evident in all fault components; footwall, fault rocks and hanging wall. The dominant orientation of veins in the hanging wall and breccia is at high angles to the fault zone. In the footwall there is a more varied spread of orientation of veins than the hanging wall and tectonic breccia. Steeply dipping discrete veins cut the breccias suggesting that breccias were fractured as a cohesive body of rock and those fractures provided a pathway for fluids. Vein textures were typically small blocky crystals with little observable structure in veins (eg. direction of growth).

A number of authors have recognised a seismic cycle of faulting and fluid flow (eg. Byerlee 1993; Sibson 2000). One aspect of this cycle is fault rock sealing that affects the mechanics of faulting (eg. Woodcock et al 2007, and Caine et al 2010, Soden et al 2014, Kristensen et al 2016). Fault rocks are sealed by mineral-saturated fluids and the flow regime switches from granular media based flow to focussed flow in fractures. Soden et al (2014), recognised that the fluid conducting elements within a fault can become sealed, switching flow from within the fault core and damage zone to fractures up to several hundreds of metres from the edge of an annealed damage zone.

Tarasewicz et al (2005) and Woodcock et al (2007) recognised that fault rock sealing by mineral-saturated fluids may occur in a single seismic cycle. This means that fault rock sealing does not need to occur over several seismic events and may occur within a single inter-seismic period. The granular nature of breccias immediately after formation could be expected to provide a relatively high permeability pathway for fluid flow through the pore space compared to the low permeability of the footwall rocks and lithified sedimentary hanging wall rocks. For discrete veins to be found in chaotic breccia there must be limited interaction with the intergranular pore space meaning flow is concentrated in fractures rather than through the pore space of the breccia. This suggests that breccias are cemented and behave as a brittle body of rock which is then fractured. The dominant flow mechanism changes from diffuse flow through the breccia as a permeable medium to discrete fracture-based pathways (Woodcock et al 2007; Caine et al 2010; Indrevaer et al 2014). If breccias remained in a granular state (ie. not lithified nor cemented) discrete fractures would be less likely to remain open without fluids interacting with the surrounding pore space.

The lack of observable structure in the veins at the NSF is suggestive of a low number of “crack-seal” events as described by Bons et al (2012) (Figure 7-15). It is possible that after

cementation of the breccia matrix, a single fracturing and fluid flow event created individual veins.

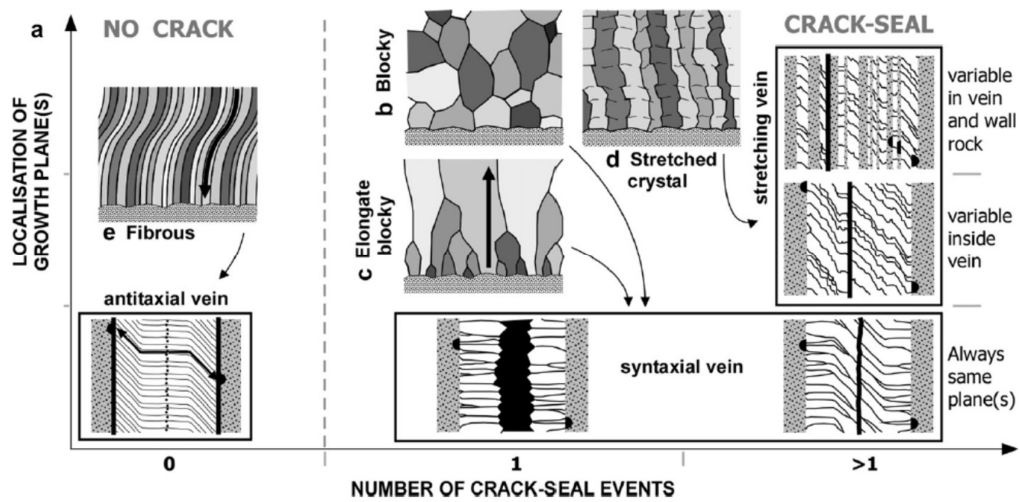


Figure 7-15 Basic scheme linking vein type and crystal morphology. After Bons et al (2012)

Rapid cementation could produce the lack of observable texture in the veins. Minerals can come out of solution rapidly if there are large changes in pressure. This was suggested by Caine et al (2010) at the Stillwater fault as described in Section 7.1.1, where rapid decompression boiling caused the cementation of breccias. A key difference between the NSF and the Stillwater fault is that there is more intense mineralisation of the breccia volume (See Figure 7-2) at the Stillwater fault. The discrete veins in the breccia of the NSF could have formed by a similar process, but the breccia must have already been lithified or cemented at the time of vein formation.

The veins of the fault breccia and hanging wall show a predominant near-vertical orientation as described in section 5.4. The predominance of steeply dipping veins in the breccias could represent a pathway for deep sourced, mineral rich fluids to flow up the fault. The same could be true of the near-fault hanging wall veins, although this

interpretation is without comparable results from further into the basin (i.e. further from the fault).

Woodcock et al (2006;2007), found that veins cut through clasts (termed pervasive veins) in carbonate derived breccias of the Dent fault in the damage zone where dilational jigsaw breccias dominate. These veins pass through the matrix and veins and therefore formed after brecciation. For dilational breccias to have fractures through clasts, the breccias must be stronger than the country rock due to cementation (as postulated by Woodcock et al (2006; 2007).

Another model which is a possible explanation for the veins-through-clasts texture is bulk crushing of clasts as described in Section 2.4.5. Figure 7-16 shows the model of bulk crushing postulated by Billi et al (2005) whereby contact between clasts in compression or shear causes clasts to fracture. Bulk crushing provides a mechanism for veins to occur in a granular material without the need for cementation. In Section 7.1.1 the formation of a plane of shearing in granular material subjected to a shear box test was described. The breaking of clasts in shear box tests was described as a possible mechanism for grain size reduction between the breccia pods at Door of the Heugh without the need for cementation.

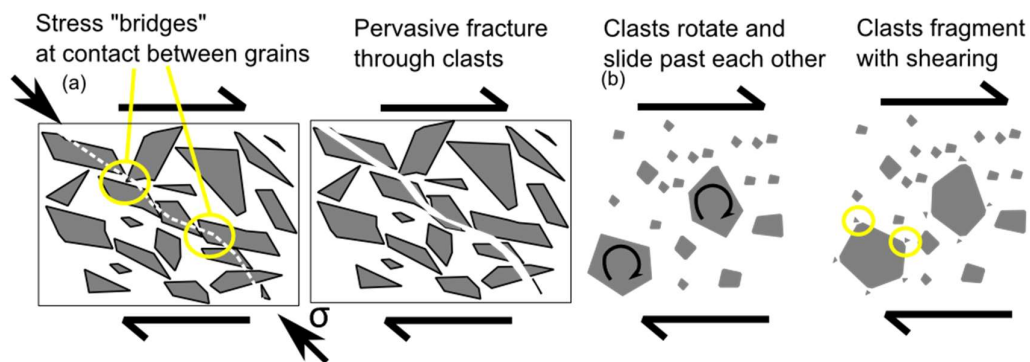


Figure 7-16 Reproduction of Figure 2-2. Processes of attrition of breccia clasts. (a) Bulk crushing by compressive stress and (b) abrasion by clast rotation and fragmentation. After Billi (2005)

For bulk crushing to occur, a granular material must experience compression. This may come from a global compressive stress field. Another source of compression is a confined granular material under shear (eg inside a fault) where clast contacts “bridge” and a localised compressive stress is created between clasts that cannot slide past each other (Figure 7-16 a).

The key requirement for bulk crushing is confinement of the breccia. If the breccia can dilate such as into voids, then bulk crushing is not possible. The NSF displays some shear textures at Door of the Heugh and Portling Bay. The only location where vein-through-clasts were identified in tectonic breccia was Lagmuck Sands, where no shearing textures in the breccia were observed. In both the sedimentary and tectonic breccias there is little evidence to indicate shear, with the exception that the clasts have clearly been fractured. Bulk crushing in shear is therefore less likely an explanation for the vein-through-clast texture. A compressive stress field is a possible explanation however there is no other suggestion that the NSF has deformed in compression.

Defining a single process that has caused the vein-through-clast texture is problematic at the NSF. It is possible that the breccia was cemented before further deformation caused

fracturing through clasts. As described above, discrete veins could form in uncemented breccias as could discrete veins passing through clasts. The NSF is thought to be a broadly normal fault and the breccias display textures which suggest formation in voids (7.1) and this could be caused by dilational faulting. I am also proposing that the breccias were cemented at the time of vein emplacement, suggesting this occurred after either lithification through burial or after cementation in a previous fluid flow event. I am also proposing that the discrete vein-through-clasts texture is the result of cementation and subsequent fracturing, rather than fracturing of confined granular uncemented breccias.

The breccias at the North Solway fault are therefore interpreted as evidence of fault rock cementation which restricts flow and forces the flow regime to switch from granular media flow (through breccias) to fracture-hosted flow.

Figure 7-17 shows the processes of faulting and sedimentation, coupled with cementation at basin margins. The green and red flow charts follow processes of brecciation at the NSF. The photographs at the top of the figure indicate where the features were identified (tectonic or sedimentary breccias). The photographs at the bottom of the figure show the textures that have led to the interpretation of the brecciation processes. From top to bottom of the figure: The breccia formation processes are either tectonic or sedimentary, lithification is by burial or cementation. Cementation is shown as occurring at depth, based on the lack of evidence for surface based cementation (eg, travertine deposits). The next step in the evolution of the breccias at the NSF is deformation which can result in re-worked breccia clasts or veins through clasts texture. These two end member textures are the result of the relative strength of the clast compared to the surrounding cement. If the cement is weaker than the clasts fracturing will not pass through fractures and the breccia

will deform as a granular material. If the cement is stronger than the clast, fracturing can pass through the clast.

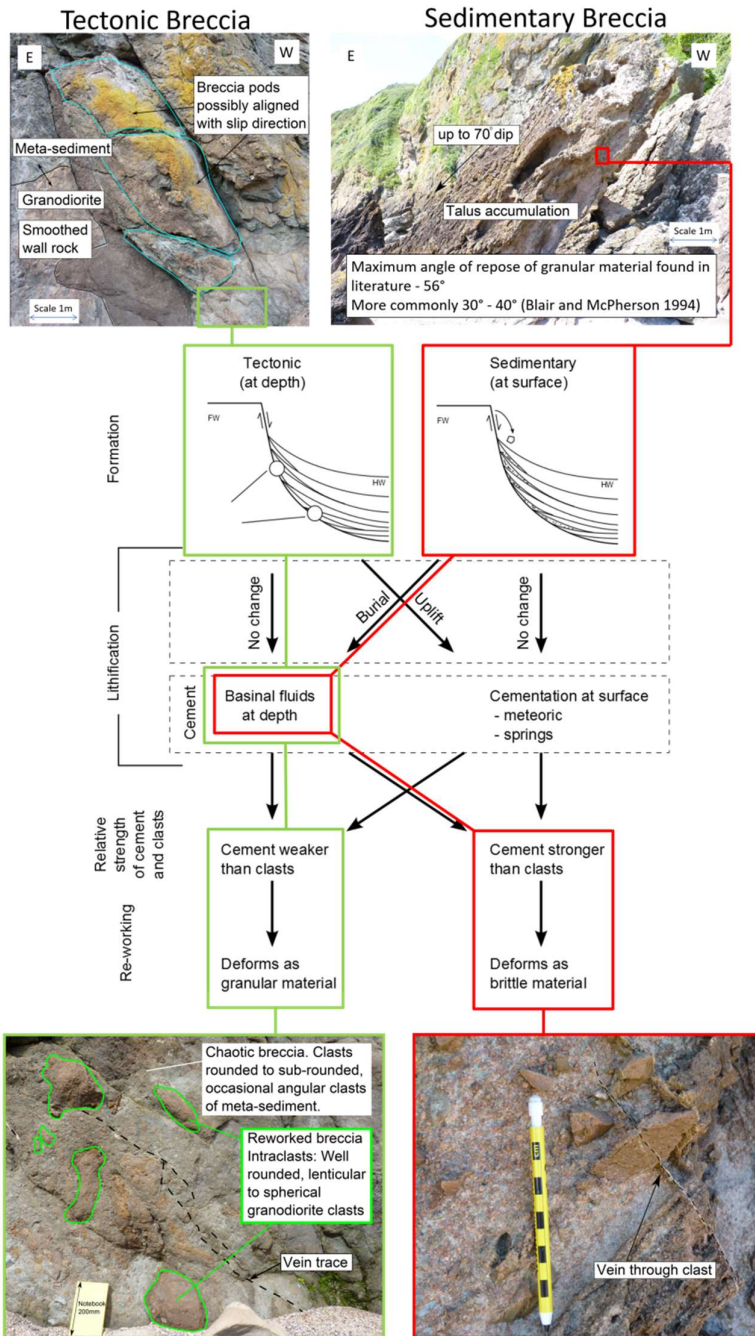


Figure 7-17 Processes at basin margin faults.

8. Conclusions and Further Work

- The NSF internal structure varies along strike. Door of the Heugh has deformation styles that suggest brecciation and subsequent faulting occurred at depth. Lagmuck Sands has deformation styles that suggest brecciation at depth but also evidence for bulk brittle behaviour which may have occurred at shallower depths than Door of the Heugh. Gutcher's Isle has textures which suggest at least one phase of exposure at or near the surface (sedimentation into breccias), followed by burial which lithified the sediments and another phase of exhumation to the present day configuration. Portling Bay has evidence for sedimentation above a fault (possibly due to a period where fault activity or slip rate was lower) followed by rupture and continued deformation of the sediments until parts of the fault zone from earlier deformation were incorporated into fault.
- Breccia textures give an indication of the mechanical state of the rock when brecciation happened. Breccias can behave mechanically as either a granular material (clasts travel through fault) or as a single brittle body of rock (shear surfaces between breccia pods). Breccias collapsing into voids may display chaotic textures given enough space for clasts to rotate. Analogous to this behaviour in faults is rock bursts in tunnels.
- Breccias can form in voids without a classic implosion texture, this is analogous to rock bursts in tunnels where the volume of material collapsing into a void is small enough to allow rotation of clasts.
- The km-scale plan-view geometry of the NSF is complex and cannot be explained by simple conceptual models for fault segment linkage. The plan view geometry is zig-zag but the segments cannot be connected using segment parallel to the current

geometry. Strike-slip offset along structures at high angle to the main fault trend are required to explain the current geometry of the NSF. Literature data, field observations and discussions with local geological experts (R.A. Chadwick pers com) suggest that this is a likely mechanism.

- The Door of the Heugh gouge is flanked by basement lithologies whereas the gouge at Portling Bay gouge is the result of basement to sedimentary faulting. The contrast between the two locations is therefore evidence of the different architecture that can occur on the same fault depending on the strength of the host lithologies. Stronger basement rocks result in narrow zones of strain weakening whereas weaker lithologies result in wider distribution of the deformation.
- The NSF demonstrates the coupling of sedimentary and tectonic processes at basin margins. The detailed description of sediments at the NSF leads to the interpretation that they formed adjacent to fault scarp and above a buried fault. This is key to the timing of the sediments with respect to fault displacement. The Portling Bay sediments have been interpreted as being incorporated into the fault zone with layer parallel extension caused by the tilting of the beds due to fault propagation. The style of layer parallel extension was influenced by contrasting mechanical properties of layer which in turn affects the propagation of the fault. Faulting and sedimentation are therefore closely coupled at the basin margin.
- Predictive algorithms for fault zone composition and properties exist for intra-basinal faults, but have not been applied, and indeed would not be applicable, where the footwall contains hard rock basement lithologies. These intra-basinal fault algorithms are based on host rock properties and throw. The complex along-strike variations in fault architecture at the NSF, show that internal architecture at this fault is additionally affected by 1) complex ongoing deformation and

reactivation (leading to differences in likely throw that could not be resolved by this thesis), 2) the superposition of breccia processes related to tectonic slip and sedimentation, sometimes over multiple cycles, 3) varied depth of exhumation resulting in overprinting of multiple processes that affect the fault rocks, 4) potentially fluid flow can affect fault mechanics, though this is not well constrained at this site. The challenge is to understand which simplifications adversely affect the usefulness of models and which are appropriate for the applicability of models.

- This study highlights a challenge for studying large faults in general. Only a portion of the fault is exposed along-strike and typically an even smaller portion of the down dip extents of faults are exposed (10's of metres at the most). Even the best exposed large-scale faults are largely hidden from view, with subsurface data consisting of seismic data and well logs in a best-case scenario. Characterising the fundamental values of throw and fault length is problematic when using such data at basin margin faults, due to lack of offset markers in the footwall. Relating large-scale features to the internal architecture of the fault is therefore challenging as good exposures and extensive subsurface data sets will not provide a complete picture.

8.1 Further work

The conclusions reached in this study were largely based on field scale observations of a single fault. To address the issues raised by this work would require:

- Petrological studies on the NSF breccias to look for evidence of deformation mechanisms (e.g. cracking and annealing) at depth. This would constrain the

evolution of the whole fault zone, removing some of the uncertainty about depth control on fault texture

- Petrological studies on the vein fill and cement of NSF breccias. Mineral fill could help to constrain what fluids were transported through the breccias, again bracketing ages. If it was possible to gain enough samples, fluid inclusions, isotopes and other geochemical analyses would be useful. However, the volume of vein material observed was very low and a detailed paragenesis would be required to make such analyses meaningful.
- Unsurprisingly, none of the seismic lines reviewed in this thesis cross the basin boundaries in the Northumberland-Solway basin. Carrying out seismic surveys that cross into the footwall would complement the present study by allowing comparison of subsurface data with the present day outcrops. Better characterisation of the along-strike fault extent and throw could be a product of this data, similar to Mcleod et al (2000). Orthogonal seismic lines would allow detection of the large cross fault structures which form the bays between Door of the Heugh and Lagmuck Sands.
- Similar studies of the architecture at other basin margin faults in the Solway-Northumberland basin system would also compliment the present study. It is difficult to relate fault architecture to basin-scale fault processes. This may be achievable with a basin wide study of fault architecture at for example the Maryport fault, 90 fathom fault. However, the ability to conduct such studies is highly dependent on exposure, and it is likely that a meaningful dataset that allows statistically-constrained prediction of internal fault architecture, and hence petrophysical properties, of basin margin faults requires pooling of data from

multiple faulted sites. This would require a campaign of field studies at well exposed faults globally.

References

- Agosta, F. and Aydin, A. (2006) Architecture and deformation mechanism of a basin-bounding normal fault in Mesozoic platform carbonates, central Italy. *Journal of Structural Geology*. **28** pp. 1445-1467
- Agosta, F. (2008) Fluid flow properties of basin-bounding normal faults in platform carbonates, Fucino Basin, central Italy. In: Wibberley, C.A.J. Kurz, W. Imber J. Holdsworth, R.E. and Collettini, C. (eds) Structure of fault zones: Implications for mechanical and fluid flow properties. *Geological Society of London Special Publication*. **299** pp. 277-291
- Allen, P.A. and Densmore, A.L. (2000) Sediment flux from an uplifting fault block. *Basin Research*. **12** pp. 367-380
- Balsamo, F. Storti, F. Piovano, B. Salvini, F. Cifelli, F. and Lima, C. (2008) Time dependent structural architecture of subsidiary fracturing and stress pattern in the tip region of an extensional growth fault system, Tarquinia basin, Italy. *Tectonophysics*. **454** pp. 54-69
- Barnhoorn, A. Cox, S.F. Robinson, D.J. and Sended, T. (2010) Stress and Fluid-driven failure during fracture array growth: Implications for coupled deformation and fluid flow in the crust. *Geology*. **38** pp. 779-782.
- Barrett, P. A. (1988) Early Carboniferous of the Solway Basin: A tectonostratigraphic model and its bearing on hydrocarbon potential. *Marine and Petroleum Geology*. **5** pp. 271-281
- Beamish, D. and Smythe, D.K., (1986) Geophysical images of the deep crust: the Iapetus suture. *Journal of the Geological Society* **143** pp. 489-497
- Bell, R.E. McNeill, L.C. Bull, J.M. Henstock, T.J. Collier, R.E.L. and Leeder, M.R. (2009) Fault architecture, basin structure and evolution of the Gulf of Corinth Rift, central Greece. *Basin Research*. **21** pp. 824-855
- Benedicto, A. Plagnes, V. Vergely, P. Flotté, N. and Schutlz, R.A. (2008) Fault and fluid interaction in a rifted margin: integrated study of calcite-sealed fault-related structures (southern Corinth margin). In: Wibberley, C.A.J. Kurz, W. Imber J. Holdsworth, R.E. and Collettini, C. (eds) Structure of fault zones: Implications for mechanical and fluid flow properties. *Geological Society of London Special Publication*. **299** pp. 257-275.
- Bense, V.F. Gleeson, T. Loveless, S.E. Bour, O. and Scibek, J. (2013) Fault zone hydrogeology. *Earth-Science Reviews*. **127** pp. 171-192
- Bertran, P. and Texier, J.P. Facies and microfacies of slope deposits. *Catena*. **35** pp. 99-121
- Billi, A. (2005) Grain size distribution and thickness of breccia and gouge zones from thin (<1m) strike-slip fault cores in limestone. *Journal of Structural Geology*. **27** pp. 1823-1837
- Bjork, T. E. Mair, K. and Austrheim (2009) Quantifying granular material and deformation: Advantages of combining grain size, shape, and mineral phase recognition analysis. *Journal of Structural Geology*. **31** pp. 637-653

- Blair, T.C. and McPherson, J.G. (1994) Alluvial fans and their natural distinction from rivers based on morphology, hydraulic processes, sedimentary processes, and facies assemblages. *Journal of Sedimentary Research*. **64** pp. 450-489
- Blenkinsop, T.G. (1991) Cataclasis and processes of particle size reduction. *Pure and Applied Geophysics*. **136** pp. 59-86
- Boles, J.R. Eichubli, P. Garven, G. and Chen, J. (2004) Evolution of a hydrocarbon migration pathway along basin-bounding faults: evidence from fault cement. *AAPG Bulletin*. **88** pp. 947-970.
- Bolton, M.D. (1986) The strength and dilatancy of sands. *Geotechnique*. **36** pp. 65-78
- Bons, P.D. Elburg, M.A. and Gomez-Rivas, E. (2012) A review of the formation of tectonic veins and their microstructures. *Journal of Structural Geology*. **43** pp. 33-62
- Borzsonyi, T. and Stannarius, R. (2013) Granular materials composed of shape-anisotropic grains. *Soft Matter*. **9** pp. 7401-7418
- Brookfield, M.E. (2008) Palaeoenvironments and palaeotectonics of the arid to hyperarid intracontinental latest Permian – late Triassic Solway basin (UK). *Sedimentary Geology*. **210** pp. 27-47
- Brookfield, M.E. (2004) The enigma of fine-grained alluvial basin fills: the Permo-Triassic (Cumbrian Coastal and Sherwood Sandstone Groups) of the Solway Basin, NW England and SW Scotland. *International Journal of Earth Sciences*. **93** pp. 282-296
- BS EN ISO 14689-1:2017 British Standard: Geotechnical Investigation and testing – identification and classification of rock: Part 1 Identification and description.
- Byerlee, J. (1993) Model for episodic flow of high-pressure water in fault zones before earthquakes. *Geology*. **21** pp. 303-306
- Caine, S.C. Evans, J.P. and Forster, C.B. (1996) Fault zone architecture and permeability structure. *Geology*. **24** (11) pp. 1025-1028
- Caine, S.C. Bruhn, R.L. and Forester, C.B. (2010) Internal structure, fault rocks, and inferences regarding deformation, fluid flow, and mineralisation in the seismogenic Stillwater normal fault, Dixie Valley, Nevada. *Journal of Structural Geology*. **32** pp. 1576-1589.
- Carthwright, J.A. Trudgill, B.D. and Mansfield, C.S. (1995) Fault growth by segment linkage: an explanation for scatter in maximum displacement and trace length data from the Canyonlands Grabens of SE Utah. *Journal of Structural Geology*. **29** pp. 1319-1326
- Cartwright, J. Huuse, M. and Aplin, A. (2007) Seal bypass systems. *AAPG Bulletin*. **91** (8) pp. 1141-1166.
- Chadwick, R.A. and Holliday, D.W. (1991) Depp crustal structure and Carboniferous basin development within the lapetus convergence zone, northern England. **148** pp. 41-53

- Chadwick, R.A. Evans, D.J. and Holliday, D.W. (1993) The Maryport fault: the post-Caledonian tectonic history of southern Britain in microcosm. *Journal of the Geological Society, London*. **150** pp. 247-250
- Chadwick, R.A. Holliday, D.W. Holloway, S. and Hulbert, A.G. (1995) The structure and evolution of the Northumberland-Solway Basin and adjacent areas. British Geological Survey. Subsurface memoir
- Chester, F.M. and Chester, J.S. Ultracataclastite structure and friction processes of the Punchbowl fault, San Andreas system, California. *Tectonophysics*. **295** pp. 199-221
- Cladouhos, T.T. (1999a) Shape preferred orientation of survivor grains in fault gouge. *Journal of Structural Geology*. **21** pp. 419-436
- Cladouhos, T.T. (1999b) A kinematic model for deformation within brittle shear zones. *Journal of Structural Geology*. **21** pp. 437-448
- Copley, A. and Woodcock, N. (2016) Estimates of fault strength from the Variscan foreland of the Northern UK. *Earth and Planetary Science Letter*. **451** pp. 108-113
- Cowan, D.S. Cladouhos, T.T. and Morgan, J.K. (2003) Structural geology and kinematic history of rocks formed along low-angle normal faults, Death Valley, California. *GSA Bulletin*. **115** pp. 1230-1248
- Cowie, P.A and Shipton, Z.K. Fault tip displacement gradients and process zone dimensions. *Journal of Structural Geology*. **20** pp. 983-997
- Cowie, P.A. Attal, M. Tucker, G.E. Whittaker, A.C. Naylor, M. Ganas, A and Roberts, G.P. (2006) Investigating the surface process response to fault interaction and linkage using a numerical modelling approach. *Basin Research*. **18** pp. 231-266
- Deegan, C.E. (1973) Tectonic control of sedimentation at the margin of a Carboniferous depositional basin in Kirkcudbrightshire. *Scottish Journal of Geology*. **9** (1) pp. 1-28
- Densmore, A.L. Dawers, N.H. Gupta, s. Guidon, R. Goldin, T. (2004) Footwall topographic development during continental extension. *Journal of Geophysical Research*. **109** F3, F03001
- De Paola, N. Holdsworth, R.E. McCaffrey, K.J.W. and Barchi, M.R. Partitioned Transtension: an alternative to basin inversion models.
- Dockrill, B. and Shipton, Z.K. (2010) Structural controls on leakage from a natural CO₂ geologic storage site: Central Utah, U.S.A. *Journal of Structural geology*. **32** pp. 1768-1782.
- Eichubl, P. Davatzes, N. C. and Becker, S. P. (2009) Structural and diagenetic control of fluid migration and cementation along the Moab fault, Utah. *AAPG Bulletin*. **93** (5) pp. 653-681
- Elliott, G.M. Wilson, P. Jackson, C.A.L. Gawthorpe, R.L. Michelsen, L. Sharp, I.R. (2012) The Linkage between fault throw and footwall scarp erosion patterns: an example from the Bremstein fault complex, offshore Norway. *Basin Research*. **24** pp. 180-197
- Faereth, R.B. Johnsen, E. and Sperrivk, S. (2007) Methodology for risking fault seal capacity: Implications of fault zone architecture. *AAPG Bulletin*. **91** (9) pp.1231-1246

- Faulkner, D.R. Mitchell, T.M. Rutter, E.H and Cembrano (2008) On the structure of large strike-slip faults. In: Wibberley, C.A.J. Kurz, W. Imber J. Holdsworth, R.E. and Collettini, C. (eds) Structure of fault zones: Implications for mechanical and fluid flow properties. *Geological Society of London Special Publication*. **299** pp. 139-150
- Faulkner, D.R. Jackson, C.A.L. Lunn, R.J. Schlische, R.W. Shipton, Z.K. Wibberley, C.A.J. Withjack, M.O. (2010) A review of recent developments concerning the structure, mechanics and fluid flow properties of fault zones. *Journal of Structural Geology*. **32** pp. 1557-1575.
- Ferrill, D. A. Morris, A. P. McGinnis, R. N. (2012) Extensional fault-propagation folding in mechanically layered rocks: the case against the frictional drag mechanism. *Tectonophysics*. **576-577** pp. 78-85
- Ferrill, D. A. Morris, A. P. McGinnis, R. N. Smart, K.J. Wigginton, S.S. and Hill, N.J. (2017) Mechanical stratigraphy and normal faulting. *Journal of Structural geology*. **94** pp. 275-302
- Fisher, R.V. (1960) Classification of volcanic rocks. *Bulletin of the Geological Society of America*. **71** pp. 973-982
- Floodpage, J., Newman, P., and White, J. (2001) Hydrocarbon prospectivity in the Irish Sea area: insights from recent exploration of the Central Irish Sea, Peel and Solway basins. In; Shannon, P.M., Haughton, P.D.W., and Corcoran, D.V. (eds) *The Petroleum Exploration of Ireland's Offshore Basins*. Geological Society, London, Special Publications, **188**, pp. 107-134
- Ford, M. Rohais, S. Williams, E.A. Bourlange, S. Jousselin, D. Backert, N. Malarte, F. (2013) Tectono-sedimentary evolution of the western Corinth rift (Central Greece). *Basin Research*. **25** pp. 3-25
- Fossen, H. and Rotevatn, A. (2016) Fault linkage and relay structures in extensional settings – A review. *Earth Science Reviews*. **154** pp. 14-28
- Gawthorpe, R. L. and Leeder, M. R. (2000) Tectono-sedimentary evolution of active extensional basins. *Basin Research*. **12** pp. 195-218
- Gibbs, A.D. (1984) Structural evolution of extensional basin margins. *Journal of the Geological Society of London*. **141** pp. 609-620
- Glennie, K.W. (2002) Permian and Triassic. In: Trewin, N. H. (ed) *The Geology of Scotland* (4th edition). The Geological Society, London
- Gupta, A.K. (2016) Effects of particle size and confining pressure on breakage factor of rockfill materials using medium triaxial test. *Journal of Rock Mechanics and Geotechnical Engineering*. **8** pp. 378-388
- Haines, S.H. Kaproth, B. Marone, C. Saffer, D. and der Pluijm, B. (2013) Shear zones in clay-rich fault gouge: A laboratory study of fabric development and evolution. *Journal of Structural Geology*. **51** pp. 206-225

- Hausegger, S. Kurz, W. Rabitsch, R. Kiechle, E. and Brosch, F-J (2010) Analysis of the internal structure of a carbonate damage zone: Implications for the mechanisms of fault breccia formation and fluid flow. *Journal of Structural Geology*. **32** pp. 1349-1362.
- Henstra, G.A. Rotevatn, A. Gawthorpe, R.L. and Ravenas, R. (2015) Evolution of a major segmented normal fault during multiphase rifting: The origin of plan-view zigzag geometry. *Journal of Structural Geology*. **74** pp. 45-63
- Indrevaer, K. Stunitz, H. and Gergh, S. G. (2014) On Palaeozoic-Mesozoic brittle normal faults along the SW Barents Sea Margin: fault processes and implications for basement permeability and margin evolution. *Journal of the Geological Society* **171** pp. 831-846
- Jaeger, H.M. Nagel, A.R. and Behringer, R.P. (1996) The physics of granular materials. *Physics Today*. **49** pp. 32-38
- Jebrak, M. (1997) Hydrothermal breccias in vein-type ore deposits: A review of mechanisms, morphology and size distribution. *Ore Geology Reviews*. **12** pp. 111-134
- Kudrolli, A. (2004) Size separation in vibrated granular matter. *Reports on Progress in Physics*. **67** pp. 209-247
- Kim, S.B. Chough, S.K. and Chun, S.S. (2003) Tectonic controls on spatio-temporal development of depositional systems and generation of fining-upward basin fills in a strike-slip setting: Kyokpori formation (Cretaceous), south-west Korea. *Sedimentology*. **50** pp. 638-655
- Knipe, R.J. Jones, G. and Fisher, Q.J. (1998) Faulting, fault sealing and fluid flow in hydrocarbon reservoirs: an introduction. In: Jones, G. Fisher, Q.J. and Knipe (1998) Faulting, fault sealing and fluid flow in hydrocarbon reservoirs: an introduction. *Geological Society of London Special Publications*. **147** vii-xxi
- Kristensen, T.B. Rotevatn, A. Peacock, D.C.P. Henstra, A. Midtkandal, I. and Grundvag, S.A. (2016) Structure and flow properties of syn-rift border faults: The interplay between fault damage and fault-related chemical alteration (Dombjerg Fault, Wollaston Forland NE Greenland). *Journal of Structural Geology*. **92** pp. 99-115
- Leeder, M.R. Seger, M.J. and Stark, C.P. (1991) Sedimentation and tectonic geomorphology adjacent to major active and inactive normal faults, southern Greece. *Journal of the Geological Society of London*. **148** pp. 331-343
- Lintern, B.C. and Floyd, J.D. (2000) Geology of the Kirkcudbright-Dalbeattie district. *Memoir of the British Geological Survey*, sheets 5W, 5E and part of 6W (Scotland).
- Lopez, D.L. and Smith, L. (1995) Fluid flow in fault zones: Analysis of the interplay of convective circulation and topographically driven groundwater flow. *Water Resources Research*. **31** (6) pp. 1489-1503.
- Lopez, D.L. and Smith, L. (1996) Fluid flow in fault zones: Influence of hydraulic anisotropy and heterogeneity on the fluid flow and heat transfer regime. *Water Resources Research*. **32** (10) pp. 3227-3235.

- Loveless, S. Bense, V. and Truner, J. (2011) Fault architecture and deformation processes within poorly lithified rift sediments, Central Greece. *Journal of Structural Geology*. **33** pp. 1554-1568
- Lunn, R.J. Shipton, Z.K. and Bright, A.M. (2008) How can we improve estimates of bulk fault zone hydraulic properties. In: Wibberley, C.A.J. Kurz, W. Imber J. Holdsworth, R.E. and Colletini, C. (eds) Structure of fault zones: Implications for mechanical and fluid flow properties. *Geological Society of London Special Publication*. **299** pp. 231-237.
- Luther, A. Axen, G. and Selverstone, J. (2013) Particle-size distributions of low-angle normal fault breccias: Implications for slip mechanisms on weak faults. *Journal of Structural Geology*. **55** pp. 50-61
- Mair, K. and Abe, S. (2008) 3D numerical simulations of fault gouge evolution during shear: Grain size reduction and strain localisation. *Earth and Planetary Science Letters*. **274** pp. 72-81
- Manzocchi, T. Walsh, J.J. Nell, P. and Yielding, G. (1999) Fault transmissibility multipliers for flow simulation models. *Petroleum Geoscience*. **5** pp. 53-63
- Manzocchi, T. Childs, C. and Walsh, J.J. (2010) Faults and fault properties in hydrocarbon flow models. *Geofluids*. **10**, pp. 94-113
- Mazaira, A. and Konicek, P. Intense rockburst impacts in deep underground construction and their prevention. *Canadian Geotechnical Journal*. **52** pp. 1426-1439
- McArthur, A.D. Hartley, A.J. and Jolley, D.W. (2013) Stratigraphic development of an Upper Jurassic deep marine syn-rift succession, Inner Moray Firth Basin, Scotland. *Basin Research*. **25** pp.285-309
- McCalpin, J. P. (1996) Paleoseismology. Academic Press, London
- McLeod, A.E. Dawers, N.H. and Underhill, J.R. (2000) The propagation and linkage of normal faults: insights from the Strathspey-Bren-Statfjord fault array, northern North Sea. *Basin Research*. **12** pp. 263-284
- Melosh, H.J. (1979) Acoustic fluidization: A new geologic process? *Journal of Geophysical Research – Solid Earth*. **84** pp. 7513-7520
- Melosh, B. L. Rowe, C. D. Smit, L. Groenewald, C. Lambert, C. W. and Macey, P. (2014) Snap, Crackle, Pop: Dilational fault breccias record seismic slip below the brittle-plastic transition. *Earth and Planetary Science Letters* **403** pp. 432-445
- Miller, J.M and Taylor, K. (1966) Uranium mineralisation near Dalbeattie, Kirkcudbrightshire. *Bulletin of the Geological Society of Great Britain*. **25** 1-18
- Monzawa, N. and Otsuki, K (2003) Comminution and fluidization of granular fault materials: implications for fault slip behaviour. *Tectonophysics*. **357** pp. 127-143
- Mort, K. and Woodcock, N.H (2008) Quantifying fault breccia geometry: Dent Fault, NW England. *Journal of Structural Geology*. **30** pp. 701-709

- Mortimer, E. Gupta, S. and Cowie, P. (2005) Clinoform nucleation and growth in coarse-grained deltas, Loreto basin, Baja California, Mexico: a response to episodic accelerations in fault displacement. *Basin Research* **17** pp. 337 - 359
- Motoki, A. Vargas, T. Iwanuch, W. Sichel, S.E. Balmant, A. and Aires, J.R. (2011) Tectonic breccia of the Cabo Frid area, Satae of Rio de Janeiro, Brazil, intruded by Early Cretaceous mafic dyke: evidence of the Pan-African brittle tectonism? *Geosciences*. **64** pp. 25-36
- Newman, P.J. (1999) The geology and hydrocarbon potential of the peel and Solway Basins, East Irish Sea. *Journal of Petroleum geology*. **22** (3), pp. 305-324
- Ord, D.M. Clemmey, H. and Leeder, M.R. (1988) Interaction between faulting and sedimentation during Dinantian extension of the Solway basin, SW Scotland. *Journal of the Geological Society*. **145** pp. 249-259
- Parnell, J. (1995) Hydrocarbon migration in the Solway basin. *Geological Journal*. **30** pp. 25-38.
- Peacock, D. C. P. Nixon, C. W. Rotevatn, A. Sanderson, D. J. and Zuluaga, L. F. (2016) Glossary of fault and other fracture networks. *Journal of Structural Geology*. **92** pp. 12-29
- Petit, J.P. Wibberley, C.A.J. and Ruiz, G. (1999) 'Crack-seal', slip: a new fault valve mechanism? *Journal of Structural Geology*. **21** pp. 1199-1207
- Piper, J.D.A. McArdle, N.J. and Almaskeri, Y. (2007) Palaeomagnetic study of the Cairnsmoor fleet of granite and Criffel-Dalbeattie granodiorite contact aureoles: Caledonian tectonics of the Southern Uplands of Scotland and Devonian palaeogeography. *Geological magazine*. **144** (5) pp. 811-835
- Rawling, G. C. and Goodwin, L.B. (2003) Cataclasis and particulate flow in faulted, poorly lithified sediments. *Journal of Structural Geology*. **25** pp. 317-331
- Reimold, W.U. (1995) Pseudotachylite in impact structures – generation by friction melting and shock brecciation?: A review and discussion. *Earth Science Reviews*. **39** pp. 247-265
- Rutter, E.H. Maddock, R.H. Hall, S.H. and White, S.H. (1986) Comparative microstructures of natural and experimentally produced clay-bearing fault gouges. *Pure and Applied Geophysics*. **124**
- Schlische, R.W. Young, S.S. Ackerman, R.V and Gupta, A. (1996) Geometry and scaling relations of a population of very small rift-related normal faults. *Geology*. **24** pp. 683-686
- Sharp, I.R. Gawthrope, R.L. Underhill, J.R. and Gupta, S. (2000) Fault-propagation folding in extensional settings: Examples of structural style and synrift sedimentary response from the Suez rift, Sinai, Egypt. **112** (12) pp. 1877-1899.
- Shipton, Z.K. Soden, A.M. Kirkpatrick, J.D. Bright, A.M. Lunn, R.J. (2006) How thick is a fault? Fault Displacement-Thickness scaling revisited. In: Abercrombie, R. (ed.) Earthquakes: Radiated Energy and the Physics of Faulting. *Geophysical Monograph Series*. **170** pp. 195-198
- Sibson, R.H. (2000) Fluid involvement in normal faulting. *Journal of Geodynamics*. **29** pp. 469-499

- Sibson, R.H. (1977) Fault rocks and fault mechanisms. *Journal of the Geological Society of London*. **133** pp. 191-213.
- Sibson, R.H. (1986) Brecciation processes in fault zones: Inferences from earthquake rupturing. *Pure and Applied Geophysics*. **124** pp.159-175
- Smith, S.A.F. Colletini, C and Holdsworth, R.E. (2008) Recognizing the seismic cycle along ancient faults: CO₂-induced fluidization of breccias in the footwall of a sealing low-angle normal fault. *Journal of Structural Geology*. **30** pp. 1034-1046
- Soden, A.M. and Shipton, Z.K. (2013) Dilational fault zone architecture in a welded ignimbrite: The importance of mechanical stratigraphy. *Journal of Structural Geology*. **51** pp.156-166
- Soden, A.M. Shipton, Z.K. Lunn, R.J. Pytharouli, S.I. Kirkpatrick, J.D. Nascimento, A.F.D and Bezerra, F.H.R. (2014) Brittle structures focused on subtle crustal heterogeneities: implications for flow in fractured rocks. *Journal of the Geological Society, London*. **171** pp. 509-524
- Solum, J.G. van der Pluijm, B.A. and Peacor, D.R. (2005) Neocrystallization, fabrics and age of clay minerals from an exposure of the Moab Fault, Utah. *Journal of Structural Geology*. **27** pp. 1563-1576
- Tarasewicz, J. P. T. Woodcock, N. H. and Dickson, J. A. (2006) Carbonate dilation breccias: Examples from the damage zone to the Dent fault, northwest England. *GSA Bulletin*. **117** pp. 736-745
- Tenthorey, E. Cox, S.F. and Todd, H.F. (2003) Evolution of strength recovery and permeability during fluid-rock reaction in experimental fault zones. *Earth and Planetary Science Letters*. **206** pp. 161-172
- Trewin, N. H. and Rollin, K.E. (2002) Geological history and structure of Scotland. In: Trewin, N. H. (ed) *The Geology of Scotland* (4th edition). The Geological Society, London
- Walker, R.J. Holdsworth, R.E. Imber, J. and Ellis, D. (2011) The development of cavities and clastic infills along fault-related fractures in Tertiary basalts on the NE Atlantic margin. *Journal of Structural Geology*. **33** pp. 92-106
- Wall, G.R.T. and Jenkyns, H.C. (2004) The age, origin and tectonic significance of Mesozoic sediment-filled fissures in the Mendip Hills (SW England): implications for extension models and Jurassic sea-level curves. *Geological Magazine*. **141** pp. 471-504
- Wibberley, C.A.J. Yielding, G. and Di Toro, G. (2008) Recent advances in the understanding of fault zone internal structure; a review. In: Wibberley, C.A.J. Kurz, W. Imber J. Holdsworth, R.E. and Colletini, C. (eds) *Structure of fault zones: Implications for mechanical and fluid flow properties*. *Geological Society of London Special Publication*. **299** pp. 5-33.
- Wignall, P.B. and Pickering, K.T. (1993) Palaeoecology and sedimentology across a Jurassic fault scarp. *Journal of the Geological Society of London*. **150** pp. 323-340
- Woodcock, N.H. Dickson, J.A.D. Tarasewicz, J.P.T. (2007) Transient permeability and reseal hardening in fault zones; evidence from dilation breccia textures. In: Lonergan, L. Jolly, R.J.H. Rawnsley, K. Sanderson, D.J. (Eds.), *Fractured reservoirs*. *Geological Society of London Special Publications*. **270** pp. 43-53

Woodcock, N.H. Omma, J.E. and Dickson, J.A.D. (2006) Chaotic breccia along the Dent Fault, NW England: implosion or collapse of a fault void? *Journal of the Geological Society of London*. **163** pp. 431-466.

Woodcock, N.H. and Mort, K. (2008) Classification of fault breccias and related fault rocks. *Geological Magazine*. **145** (3) pp. 435-440

Woodcock, N.H. Miller, A.V.M. and Woodhouse, C.D. (2014) Chaotic breccia zones on the Pembroke Peninsula, south Wales: Evidence for collapse into voids along dilational faults. *Journal of Structural Geology*. **69** pp. 91-107

Wright, V. Woodcock, N.H. and Dickson, J.A.D. (2009) Fissure fills along faults: Variscan examples from Gower, South Wales. *Geological Magazine*. **146** pp. 890-902

Zhang, L. Xianorong, L. Vasseur, G. Changua, Y. Yang, W. Yuhong, L. Chengpeng, S. Lang, Y. and Jianzhao, Y. (2011) Evaluation of geological factors in characterizing fault connectivity during hydrocarbon migration: Application to the Bohai Bay basin. *Marine and Petroleum Geology*. **28** pp. 1634-1647.